IAEA-TECDOC-357

# STABLE AND RADIOACTIVE ISOTOPES IN THE STUDY OF THE UNSATURATED SOIL ZONE

PROCEEDINGS OF THE FINAL MEETING
OF THE JOINT IAEA/GSF CO-ORDINATED RESEARCH PROGRAMME
FOR STUDYING THE PHYSICAL AND ISOTOPIC BEHAVIOUR
OF SOIL MOISTURE IN THE ZONE OF AERATION,
ORGANIZED BY THE
INTERNATIONAL ATOMIC ENERGY AGENCY
AND HELD IN VIENNA, 10–14 SEPTEMBER 1984

A TECHNICAL DOCUMENT ISSUED BY THE
INTERNATIONAL ATOMIC ENERGY AGENCY, VIENNA, 1985

STABLE AND RADIOACTIVE ISOTOPES
IN THE STUDY OF THE UNSATURATED SOIL ZONE
IAEA, VIENNA, 1985
IAEA-TECDOC-357

Printed by the IAEA in Austria
November 1985

PLEASE BE AWARE THAT
ALL OF THE MISSING PAGES IN THIS DOCUMENT
WERE ORIGINALLY BLANK

The IAEA does not maintain stocks of reports in this series. However, microfiche copies of these reports can be obtained from

INIS Clearinghouse
International Atomic Energy Agency
Wagramerstrasse 5
P.O. Box 100
A-1400 Vienna, Austria

Orders should be accompanied by prepayment of Austrian Schillings 80.00 in the form of a cheque or in the form of IAEA microfiche service coupons which may be ordered separately from the INIS Clearinghouse.

# FOREWORD

At the beginning of 1980 the International Atomic Energy Agency and the German Gesellschaft für Strahlen und Umweltforschung m.b.H. signed an agreement to support a joint programme of coordinated research for "Studying the physical and isotopic behaviour of soil moisture in the zone of aeration".

The aim of this programme was to apply and develop isotope techniques in the study of the unsaturated zone in order to get a better understanding of water movement between the soil surface and the phreatic water table.

Ten Research Contracts were granted to different hydrological and isotope hydrological institutes in developped and developping countries with a special focus on arid and semi arid areas where the estimation of groundwater recharge and actual evaporation rate is of prime importance in the assessment and utilization of groundwater resources.

Besides the use of classical methods to study the flux of moisture, the isotopic investigations promoted in the programme were oriented towards:

- Development of technology of field sampling methods, with special attention to non-cohesive soils for obtaining representative soil samples.
- Improvement of laboratory methods for soil water extraction and analysis.
- Interpretation of stable isotopes and chemical profiles for water balance and molecular exchange processes with atmospheric moisture.
- Use of artificial tracer techniques; injection of labelled water to follow the complex process of infiltration and evaporation.
- Influence of the geomorphological and geological features on the infiltration process.
- Determination of mixing and dispersion processes and mathematical simulation.

The results of the different investigations carried out within this framework were presented and discussed during the final coordination meeting held in Vienna at the IAEA Headquarters in September 1984. The present publication brings together the main results with conclusions and recommendations on the usefulness of studies of the $^{18}O$, $^{2}H$ and $^{3}H$ isotopes in water in the unsaturated zone.

The manuscript of this Technical document received no editorial treatment by the Agency.

# CONTENTS

# DISPERSION AND MOVEMENT OF WATER IN THE UNSATURATED ZONE OF SANDS AND GRAVELS

D. BAKER, D. KLOTZ, K.-P. SEILER
GSF-Institut für Radiohydrometrie,
Neuherberg,
Federal Republic of Germany

**Abstract**

In sands with high water content dispersion is stronger than at saturated state; however it decreases with the lowering of the water content. The same results are found for percolation velocities. At high saturation obviously the change in permeability is not as strong as the change in effective porosity.

Percolation velocities in gravels are in the range of 25 m/a at infiltration rates of about 25 mm/d and rise with the infiltration rate. Bedding in the unsaturated zone has a pronounced influence on lateral flow; to a certain extent it increases with the infiltration rate. A mathematical model was used to study both of these influences; the results are in good agreement with field observations

## 1. Introduction

The GSF-Institut für Radiohydrometrie carried out laboratory and field experiments to get a better understanding of water movement, mixing and dispersion processes in the zone of aeration. Special emphasis in the field experiments was given to the question of why percolation velocities determined by means of environmental isotopes differ in some cases from those determined by means of hydraulic and of tracer tests.

The boundary conditions of these experiments were adapted to geological, hydrogeological and meteorological conditions in arid to semiarid zones.

Because of technical problems in performing the field experiments and for the sake of reproducebility of the results, we did not stress non-steady state hydrodynamic boundary conditions as they prevail in nature. All experiments were carried out with steady state boundary conditions. These conditions result in maximum values of percolation and of dispersion.

In an attempt to better understand and interpret the experimental results, a mathematical model of flow in unsaturated ground was developed. It was used to examine the effects of changes in permeability on the lateral propagation of percolation water.

## 2. The sediments and the determination of its hydraulic parameters

Laboratory experiments were carried out with three different quarz sands of the grain sizes given in fig. 1 A. These sands are typical for eolian transport, because their grain sizes are lower than 0,6 mm, they are well sorted and well rounded.

The grain size distributions of the field sediments under investigation are shown in fig. 1 B; it is bimodal, which is typical for the quick and discontinuous sediment transport occuring, for example, in wadis.

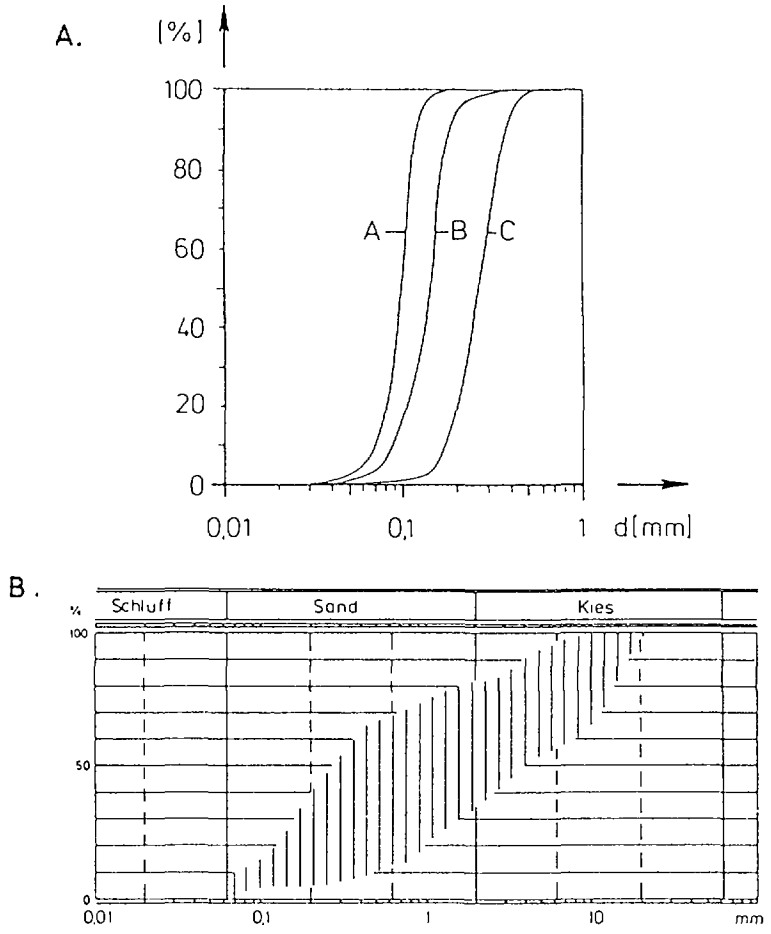


Fig. 1: Grain size distribution of sands (A) from laboratory tests and from gravels (B) in the field

Saturated permeability has been determined according to the Darcy law by means of laboratory experiments or by pumping test; the longitudinal dispersivity has been obtained from the concentration-time graph of the injected tracer; the effective porosity was calculated from the ratio of filter to distance velocity (Table 1).

Tab. 1: Saturated permeability and porosity of sediments under research; n.d. = not determined

| Sediment | saturated permeability (m/s) determined by means of | | effective porosities (vol.%) determined by means of | | total porosity vol. % |
|---|---|---|---|---|---|
| | columns | pumping test | columns | pumping test | |
| Sand A | 3,1 E-5 | - | 48 | - | 48 |
| Sand B | 3,5 E-5 | - | 50 | - | 50 |
| Sand C | 2,0 E-4 | - | 39 | - | 39 |
| Gravels of Dornach | 4,5 E-3 | 4,5 E-3 | 8,5 | 9,0 | 25 |
| Gungolding | 1,2 E-3 | 8,0 E-3 | 15,6 | - | 23 |
| Farchant | 1,2 E-2 | 2,5 E-2 | 16,5 | 16,5 | 25 |
| Talham | n.d. | n.d. | n.d. | n.d. | n.d. |

The concentration-time curves were recorded by sampling or by continuous registration in laboratory experiments; in field tests they were recorded only by sampling.

The unsaturated state has been obtained in laboratory by draining off the columns either by means of gravity or by generating a pressure drop with a suction plate.

Tensiometer experiments [7] were carried out to determine unsaturated permeability of sandy gravels and sands (Fig. 2). These measurements were made while draining the sample. Hysteresis due to draining or wetting of the sample exists and may have a strong influence on the results. Fig. 3 shows this hysteresis for one experiment with sandy gravels, in which a difference in permeability of one order of magnitude arises, de-

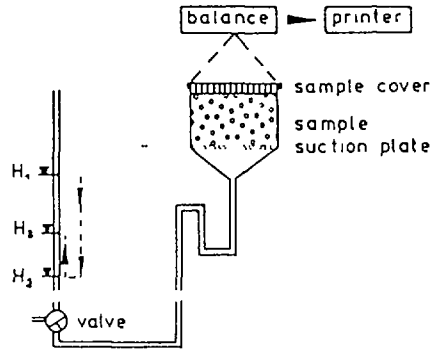


Fig. 2: Tensiometer for measuring unsaturated permeability and suction - water content relation. The experiment proceeds from $H_1$ to $H_3$

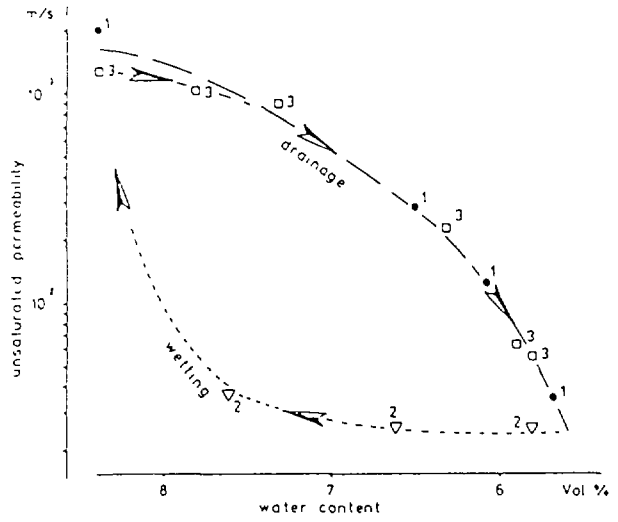


Fig. 3: Hysteresis in the relation between water content and unsaturated permeability due to wetting or drying the sample

pending on whether the measurements are taken during draining (cases 1 and 3 in Fig. 3) or wetting of the sample (case 2 in Fig. 3). This hysteresis is more pronounced in bimodal grain size distributions due to their strongly varying pore size distribution; it is less pronounced in well sorted sands.

Tensiometer experiments are time consuming; therefore we determined only draining permeabilities. The calculation of distance velocities by means of these data may result in too high values. However the comparison of laboratory and field results [1] demonstrates a fairly good agreement of both (see chapter 5.4).

## 3. Tracers in use

The dye tracers fluorescein, eosin and the radioactive tracers $^{82}Br$, $^{51}Cr$-EDTA and $^{3}H$ were used.

Batch experiments, executed during one week, were carried out with the three quarz sands. They showed only very small sorption ($K_d$ = 0.001 $cm^3/g$) for the tracers $^{3}HHO$, $^{82}Br^-$, $^{51}Cr$-EDTA and flourescein. Thus, under these experimental boundary conditions, tracers were not absorbed to a measurable extent.

However, the percolation tests in the laboratory, performed over a longer period (1 year) than the batch tests (1 week), showed lower transport velocities for $^{51}Cr$-EDTA and fluorescein as compared to the tritiated water. In these tests the tracers $^{51}Cr$-EDTA and fluorescein have a retardation factor of $R_F$ = 1.2 to 2. Obviously sorption increases with time. This effect is said to be caused by diffusion of the solutant into the sand grains.

Even tritium cannot be considered an ideal tracer in these percolation tests. Although it is not absorbed in the quartz sand used in our laboratory experiments an unexpected change in concentration may occur due to convection, molecular diffusion, evaporation and condensation.

## 4. Laboratory results on percolation and dispersion in the zone of aeration

### 4.1 Test Set-up

Column experiments (Fig. 4) have been set up to study Wadi infiltration (arrangement I with 3 columns) and percolation due to infiltration of precipitation (arrangement II with 12 columns).

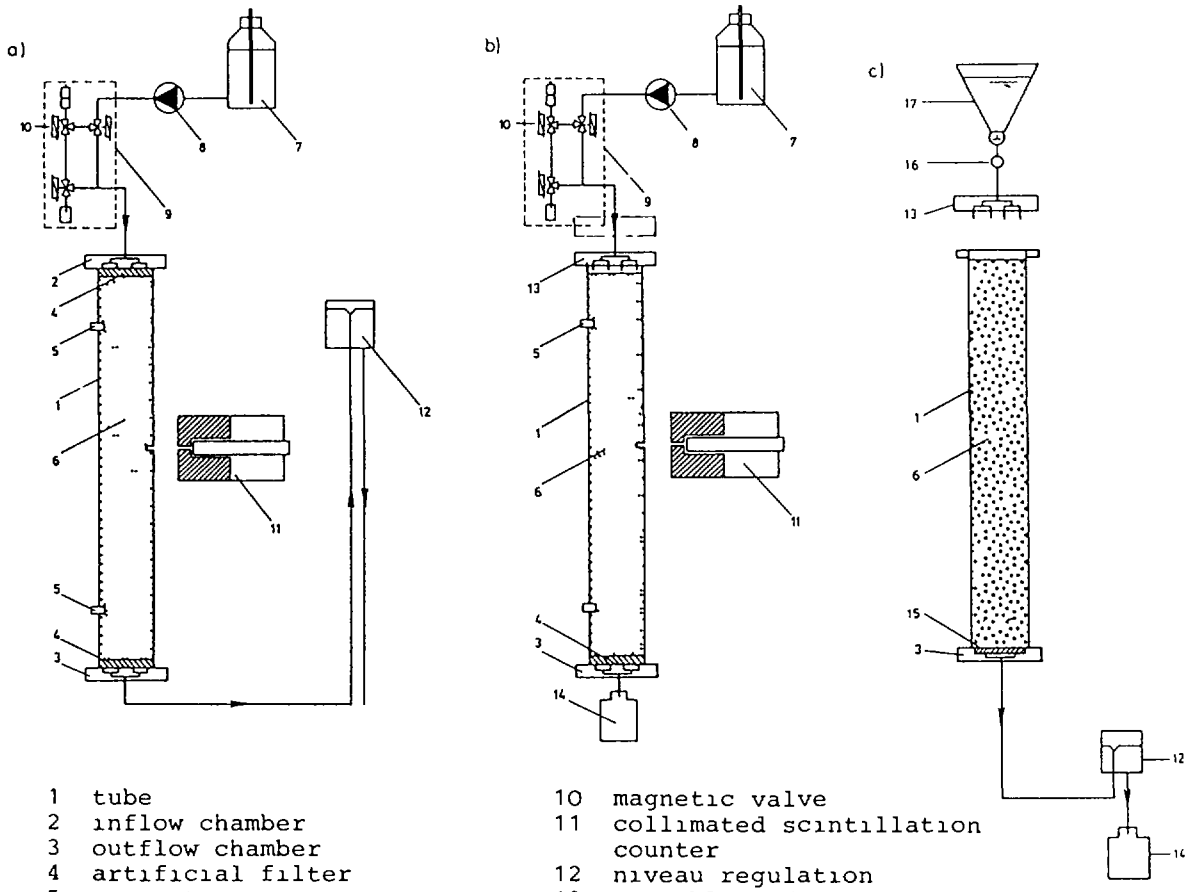


Fig. 4: Experimental set-up to study saturated (a) and unsaturated flow (b, c)

Two boundary conditions prevailed in the study of unsaturated flow:

- a short time sprinkling (about 15 minutes) and
- a continuous sprinkling.

Ten columns of arrangement II are in operation since 1980 (column set-up IIa); they are completely placed in a kind of climatic chamber, in order to protect them from rough climate changes in the laboratory. Unsaturated conditions were created in these columns by gravitational drainage for a period of one week.

Two columns of arrangement II (column set up IIb), in operation since 1982, are only with their upper part placed in a climate chamber. Unsaturated conditions were generated by suction plates at the outlet; dewatering lasted two weeks.

Tab. 2:

Review of the sands in the column experiments, the mode of sprinkling and the sprinkling rate

| column arrangement | column No. | sand | flow saturated | flow unsaturated | mode of sprinkling | rain amount (mm/a) |
|---|---|---|---|---|---|---|
| | 1 | A | + | + | continuous | 2000 |
| I | 2 | B | + | + | continuous | 2000 |
| | 3 | C | + | + | continuous | 2000 |
| | 4 | A | | + | instantaneous | 100 |
| | 5 | B | | + | instantaneous | 100 |
| | 6 | B | | + | instantaneous | 200 |
| | 7 | B | | + | instantaneous | 400 |
| IIa | 8 | C | | + | instantaneous | 100 |
| | 9 | A | | + | instantaneous | 200 |
| | 10 | B | | + | continuous | 100 |
| | 11 | B | | + | continuous | 200 |
| | 12 | B | | + | continuous | 400 |
| | 13 | C | | + | instantaneous | 200 |
| IIb | 14 | B | | + | instantaneous | 400 |
| | 15 | B | | + | instantaneous | 400 |

Table 2 reviews the sands in columns 1 to 15, the experimental set-up, as well as the mode and the yearly rate of sprinkling.

## 4.2 Evaluation of the results

When comparing water movement and tracer dispersion (Fig. 5) for saturated and unsaturated flow (arrangement I), we have to consider the fact that the water content in the unsaturated flow is very high (Table 3,4). This is due to the fine grain size of the sand and the gravitational draining the sample, which leaves the water content of the sands A and B very close to saturation. The coarse grained sand C however reaches only 50 % saturation.

For both saturated and unsaturated flow the relation between distance velocities ($v_A > 10^{-4}$ cm/s) and the longitudinal dispersion coefficients D can be expressed by:

$$D = B \times v_A^{1.07}$$

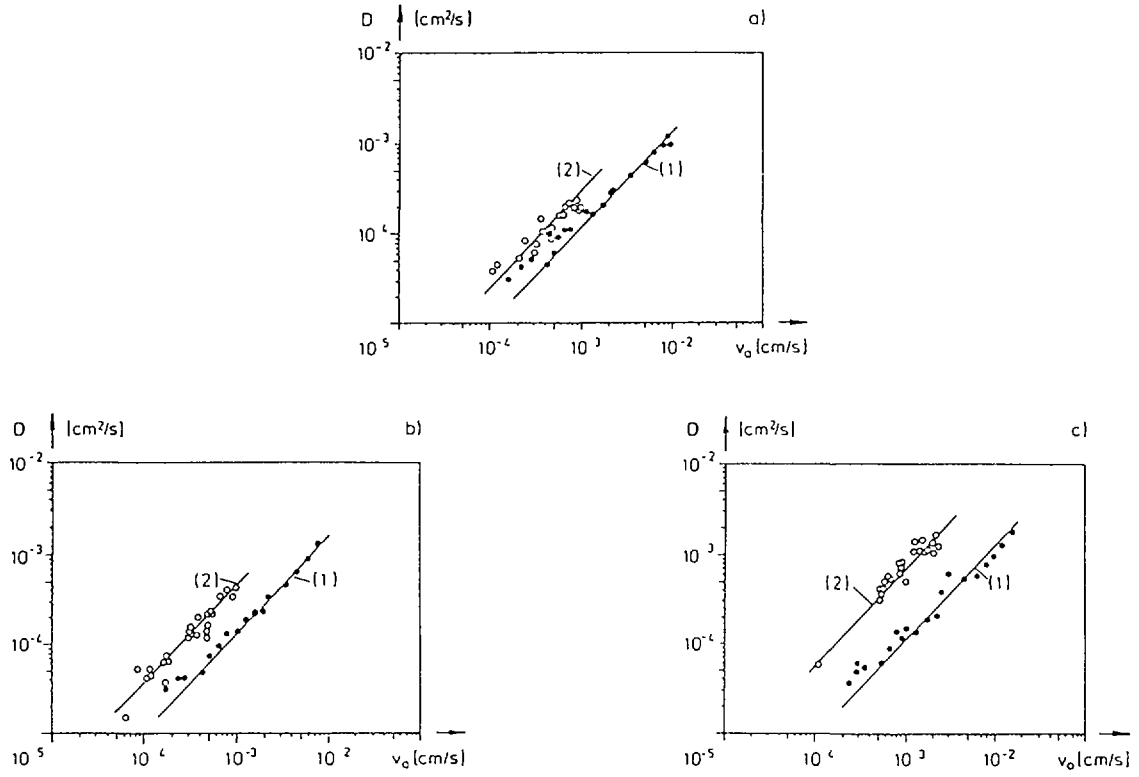


Fig. 5: Relation between dispersion coefficient and distance velocity

(1) saturated flow (2) unsaturated flow

a sand A
b sand B
c sand C

**Tab. 3:**

**Results of saturated and unsaturated flow from column arrangement at saturated and unsaturated flow.**

| column | No. | sand size range (mm) | porosity vol.% | saturated flow permeability cm/s | saturated flow effective porosity (vol %) | saturated flow dispers. (m) | unsaturated flow water cont. vol.% | unsaturated flow effective water content (vol. %) | dispersivity (cm) |
|---|---|---|---|---|---|---|---|---|---|
| 1 | A | 0,06-0,15 | 0,476 | $(3,1\pm0,2)10^{-3}$ | $0,48\pm0,2$ | 0,21 | 0,468 | $0,45\pm0,02$ | 0,5 |
| 2 | B | 0,08-0,2 | 0,500 | $(3,5\pm0,3)10^{-3}$ | $0,50\pm0,3$ | 0,23 | 0,481 | $0,46\pm0,01$ | 0,8 |
| 3 | C | 0,1-0,4 | 0,392 | $(2,0\pm0,2)10^{-2}$ | $0,39\pm0,2$ | 0,20 | 0,152 | $0,14\pm0,03$ | 1,3 |

Tab. 4:

Characteristics of the sands in columns 1 to 15 (arrangement IIa and IIb
N = total porosity, $O_A$, $O_E$ = total water content at the beginning and the end of the experiment, R amount of rain, V = evaporation, $v_t$ = transport velocity of tritiated water, $v_f$ = filter velocity, = coefficient of longitudinal dispersion

| Column No. | Sand | n | $O_A$ | $O_E$ | R (mm/a) | V (mm) | $v_f$ (cm/s) | $^3$H-loses (%) | $v_f/v_t$ | D ($cm^2$/s) | $D/v_t$ 1.0 (cm) |
|---|---|---|---|---|---|---|---|---|---|---|---|
| 4 | A | 0,480 | 0,471 | 0,444 | 100 | 62 | $7,1\ 10^{-7}$ | 45 | 0,40 | $6,6\ 10^{-6}$ | 25 |
| 5 | B | 0,492 | 0,469 | 0,428 | 100 | 71 | $7,2\ 10^{-7}$ | 46 | 0,40 | $6,7\ 10^{-6}$ | 25 |
| 6 | B | 0,500 | 0,471 | 0,448 | 200 | 57 | $1,3\ 10^{-6}$ | 18 | 0,47 | $5,6\ 10^{-6}$ | 11 |
| 7 | B | 0,488 | 0,463 | 0,442 | 400 | 62 | $2,7\ 10^{-6}$ | 3 | 0,46 | $8,9\ 10^{-6}$ | 8 |
| 8 | C | 0,395 | 0,187 | 0,154 | 100 | 52 | $1,9\ 10^{-6}$ | 20 | 0,16 | $2,6\ 10^{-5}$ | 34 |
| 9 | A | 0,481 | 0,469 | 0,433 | 200 | 79 | $1,3\ 10^{-6}$ | 26 | 0,47 | $5,9\ 10^{-6}$ | 12 |
| 10 | B | 0,492 | 0,457 | 0,444 | 100 | 79 | $6,9\ 10^{-7}$ | 72 | 0,34 | $5,9\ 10^{-6}$ | 23 |
| 11 | B | 0,505 | 0,467 | 0,445 | 200 | 83 | $1,5\ 10^{-6}$ | 48 | 0,42 | $1,1\ 10^{-5}$ | 19 |
| 12 | B | 0,503 | 0,459 | 0,445 | 400 | 91 | $2,3\ 10^{-6}$ | 34 | 0,44 | $2,1\ 10^{-5}$ | 23 |
| 13 | C | 0,394 | 0,183 | 0,168 | 200 | 65 | $3,6\ 10^{-6}$ | 16 | 0,16 | $8,5\ 10^{-6}$ | 6 |
| 14 | B | 0,497 | 0,369 | 0,128 | 400 | 307 | $2,4\ 10^{-6}$ | 25 | 0,45 | $2,8\ 10^{-5}$ | 24 |
| 15 | B | 0,489 | 0,220 | 0,110 | 400 | 177 | $4,8\ 10^{-6}$ | 6 | 0,22 | $6,7\ 10^{-6}$ | 33 |

Fig. 5 A-C show, that the longitudinal dispersion coefficient for unsaturated flow $B_u$ is greater than that for saturated flow, $B_g$; obviously in this range of saturation dispersion increases with decreasing water content, a result that has been found also for other sediment types. It is possible that in these unsaturated conditions the tracer movement takes place more along discrete flow paths than in a broad front. This assumption is confirmed by the observation, that in all these column experiments the percolation velocity is higher in the unsaturated than in the saturated state. For sprinkling rates around 400 mm/year the percolation velocities are above or around 1 m/year; for sprinkling rates below 200 mm/year they are lower than 1 m/year (Table 5).

In the case of unsaturated flow in the homogenous sand columns of arrangement I (saturation about 95 %, rain amount 2 m/year), the longitudinal dispersivities cover a range of mm to cm (Table 6). They are constant within measuring accuracy for percolation velocities $v_a > 10^{-4}$ cm/s in any type of sand.
This has also been observed in other sediments (e.g. KLOTZ 1980). This may be attributed to the fact that the mixing of

Tab. 5: Percolation velocities in columns 5 to 15.

| Sand | Column | Saturation (%) | Amount of Rain (mm/a) | Percolation Velocity (m/a) |
|---|---|---|---|---|
| A, B | 4, 5, 10 | ca. 95 | 100 | 0,2 |
| A, B | 6, 9, 11 | ca. 95 | 200 | 0,4 - 0,5 |
| A, B | 7, 12 | ca. 95 | 400 | 0,7 - 0,8 |
| B | 7 | ca. 95 | 400 | 0,8 |
| B | 14 | ca. 50 | 400 | 0,8 |
| B | 15 | ca. 25 | 400 | 1,5 |
| C | 8 | ca. 50 | 100 | 0,6 |
| C | 13 | ca. 50 | 200 | 1,1 |

Tab. 6: Longitudinal dispersion B in the sands A, B and C for different degrees of saturation, amount of rain and percolation velocities.

| Sand | Saturation (%) | Quantity of of Rain (mm/a) | Percolation Velocity (m/a) | Dispersivität B(m) |
|---|---|---|---|---|
| A | 100 | | | 0,2 |
| | ca. 95 | 2000 | 3000 | 0,5 |
| | ca. 95 | 200 | 0,4 | 12 |
| | ca. 95 | 100 | 0,2 | 25 |
| B | 100 | | | 0,2 |
| | ca. 95 | 2000 | 3000 | 0,8 |
| | ca. 95 | 400 | 0,8 | 8 |
| | ca. 95 | 200 | 0,4 | 11 |
| | ca. 95 | 100 | 0,2 | 25 |
| | ca. 50 | 400 | 0,7 | 24 |
| | ca. 25 | 400 | 1,5 | 33 |
| C | 100 | | | 0,2 |
| | ca. 50 | 2000 | 3000 | 1,3 |
| | ca. 50 | 200 | 0,6 | 6 |
| | ca. 50 | 100 | 1,1 | 34 |

the tracer due to diffusion is small as compared to that due to hydrodynamic dispersion. However for small percolation velocities the influence of molecular diffusion of the tracer gets more pronounced, which slows the decrease in dispersion with decreasing percolation velocity (Table 6).

When tritiated water is used as a tracer, evaporation and condensation effects can come into play, which result in a broadening of the concentration-position or the concentration-time curve. For slow percolation velocities we can no longer assume that the tracers move in a broad front, but their path is split up into several flow lines.

During the 3 years of the experiments the evaporation in arrangement IIa was only about 50 to 100 mm. This is mainly due to the climate chamber. Evaporation is slightly higher in the case of continuous sprinkling than in cases of 12 intermittent sprinklings per year. However the evaporation rates in the columns that were only partially climatized (arrangement IIb) were highest; it was 200 and 300 mm per test year.

## 5. Field results on flow and propagation of percolation water

All together 8 field experiments were carried out in four different regions of Upper Bavaria (Fig. 6). Only one of these experiments concernes infiltration of a river, that dries up in

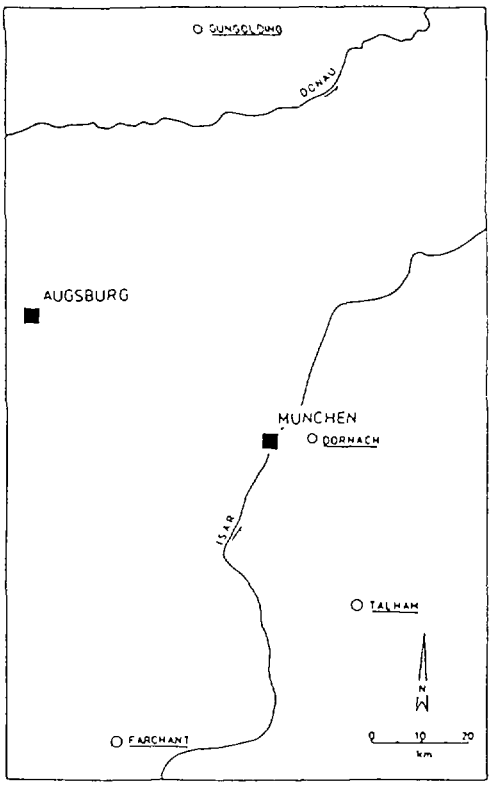


Fig. 6: The four experimental sites in Upper Bavaria

its bed. In all the other experiments point or line sprinkling was used with quantities of about 200, 50 or 25 mm/d. In no case was the infiltration capacity of the gravels reached.

## 5.1 Methodology

Sprinkling was performed with a self constructed sprinkler (Fig. 7) at a constant rate, regulated by a tube pump. Experiments started with constant sprinkling during one to two weeks, than the tracer (eosin or fluorescein) was added instantaneously to the percolation water, and sprinkling continued at the same rate for an additional week. In this way a more or less steady state percolation velocity was produced. Unsteady state conditions are no doubt more realistic in nature, but one can properly judge percolation and propagation processes in the zone of aeration under these conditions.

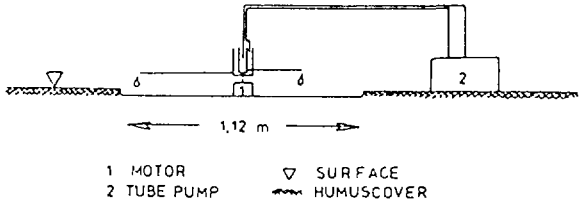


Fig. 7: Sprinkling device used in field experiments

The determination of flow and propagation of tracers in the zone of aeration is based on two different experimental set-ups:

In the case of a shallow water table, enough groundwater observation wells and high groundwater velocities, tracer input from the zone of aeration into groundwater was observed. This method enables better detection of the lateral propagation of percolation water.

In areas with a deep water table, a shaft was dug and horizontal tubes were inserted to the gravel at different depths. These tubes were perforated at their top to collect percolation water (Fig. 8). This set-up may cause a drying out of the unsaturated zone in the neighbourhood of the tube and thus influences percolation. In addition a capillary fringe is necessary before water can enter into the tube; this also influences

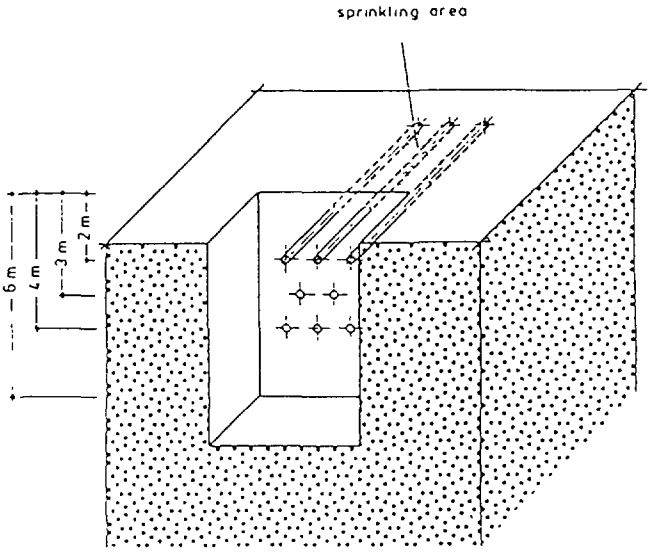


Fig. 8: Set-up for shaft experiments

the original percolation velocities. Thus these shaft experiments lead only to a rough approximation of flow velocities and give little information on lateral tracer propagation.

## 5.2 The results

A qualitative description of the results from the different test sites is followed by a discusion on propagation and on flow velocities in the zone of aeration.

### 5.2.1 Results from experimental site in Gungolding

Sprinkling and tracer injection were performed in Gungolding next to a pumping well; the infiltration rate was 20 mm/d. The water table during pumping was 2.5 m below ground, groundwater flow was about 100 m/d.

Percolation velocity was calculated from residence time between the surface and pumping well at 0.48 m/d. The in situ determination of water content in the unsaturated zone during the sprinkling experiment was not possible.

Unsaturated permeabilities from these gravels were determined by laboratory experiments (Fig. 9). If one assumes as a first approximation the permeability ($10^{-7}$ m/s) and the water content (6 vol. %) at field capacity (pF = 1,8 corresponding to 63

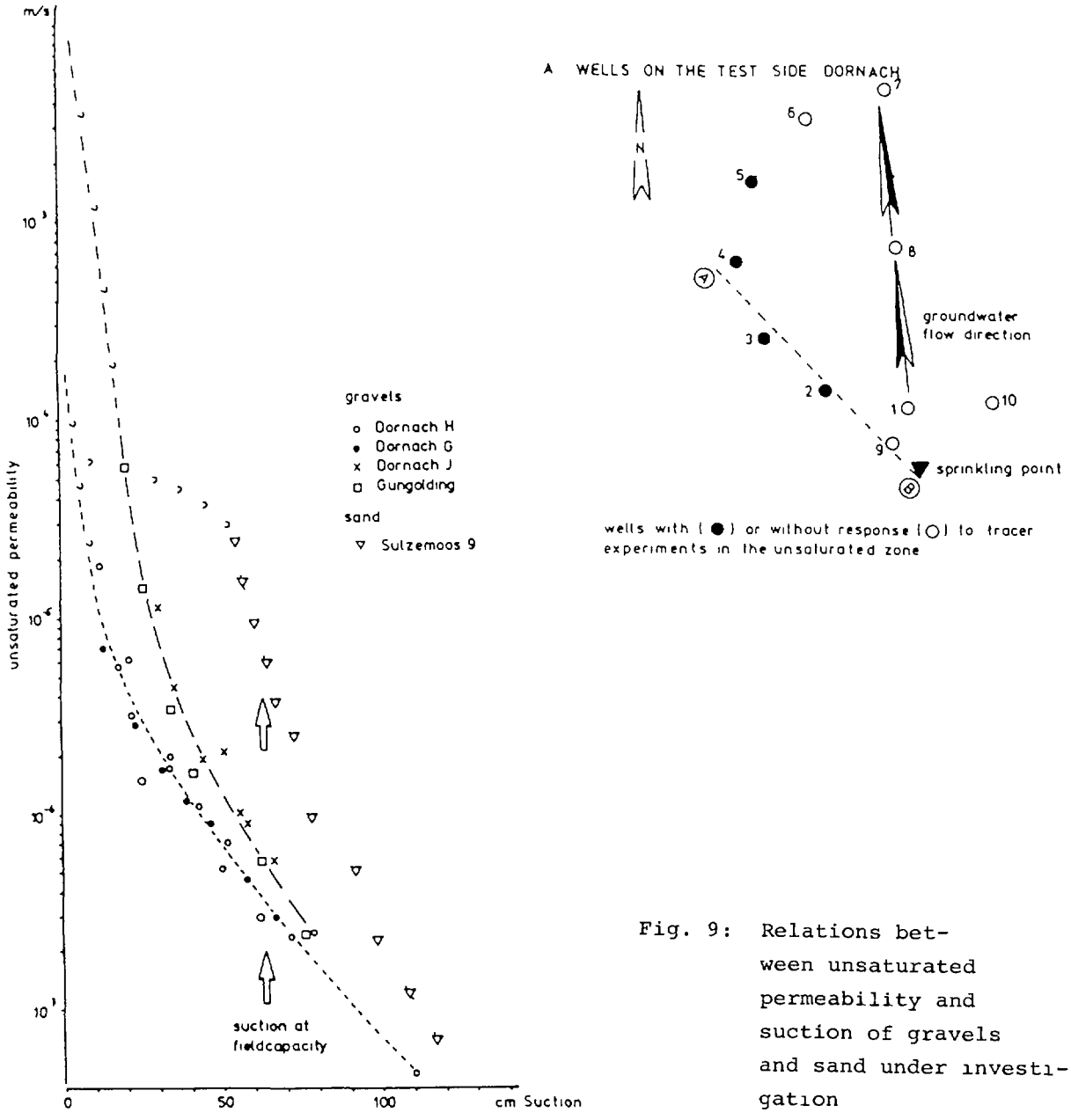


Fig. 9: Relations between unsaturated permeability and suction of gravels and sand under investigation

cm water column), a percolation velocity of 0,14 m/d is calculated. Field and laboratory data would be more consistent if water content in the zone of aeration was known; this water content was certainly higher than the water content at field capacity; in other words, the calculated velocity represents a minimum.

### 5.2.2 Results from Dornach experimental site

The groundwater table was 2 m below ground. Groundwater flow velocity was about 45 m/d and the flow direction is well known.

Tracers injected directly into the groundwater propagate as a narrow plume with an opening angle in the propagation zone of about 5° [3]. All deviations from this transverse tracer propagation in groundwater, arising when tracer is injected in the zone of aeration must be due to a more pronounced lateral tracer propagation in the unsaturated zone.

The experimental set-up is shown in fig. 10. Three experiments were carried out with sprinkling rates of 200 mm/d (1. experiment), 52 mm/d (2. experiment) and of 26 mm/d (3. experiment), each of which over an area of 1 $m^2$.

Calculated percolation velocities are discussed in chapter 5.4.

Observation well 9 is nearest to the sprinkling point; it was not reached by traced percolation water (Fig. 10). However the tracer cloud reached observation wells 2, 3, 4. Percolation water must propagate only to the west of the sprinkling point, because there was no tracer indication on the east side. The maximum of tracer concentration appears in the observation wells 3 and 4 earlier than in 2. This indicates a strong, unidirectional lateral tracer propagation (Fig. 10), that is not influenced by the thickness of the capillary fringe above groundwater (about 20 cm). It obviously is influenced by changes in unsaturated permeability (Fig. 14) due to bedding and by the inclination of this geological bedding.

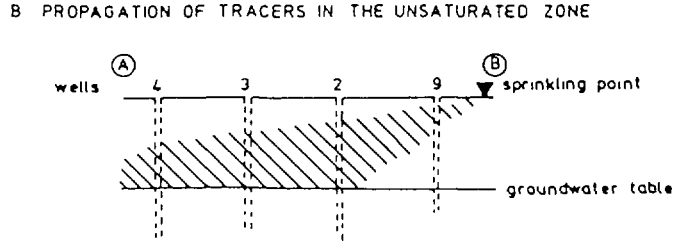


Fig. 10: A. Groundwater wells and sprinkling point at the test site of Dornach

B. Supposed propagation field of the tracer in the unsaturated zone

The third experiment was carried out with an infiltration rate of 26 mm/d. No tracer was found in the observation wells. Either the tracer amount was too small in comparision to the infiltration rate, or the percolation occured in such a narrow and vertical cone below the sprinkling site that no tracer reached the observation wells (see 5.3 and 6.3).

### 5.2.3 Results from Talham experimental side

In these experiments tracer was collected directly in the zone of aeration by using horizontal tubes (Fig. 8). In order to better study sidewards tracer propagation, a system of three sprinklers was used to water three adjacent areas, each of which then receving either eosin or fluorescein as tracer.

In any given experiment only a small number of tubes actually collected percolation water and the percolation velocity was unexpectedly high. Both facts tend to confirm the previously stated fear that such a set-up disturbs the percolation pattern of the water (see 5.1).

The two tracers were not detected directly below their injection site, but rather with a horizontal shift. Apparently a lateral flow component exists here as well as in Dornach.

### 5.2.4 Results from river infiltration in Farchant

The Kuhflucht river leaves hard rocks with a discharge of 0,3 $m^3/s$ and enters gravels in the Loisach valley.

The river was traced at its entrance to the valley (Fig. 11) and the effect of this tracing was observed in the nearby groundwater observation wells. Groundwater flow velocity was in the range of 20 m/d and its flow direction is well known.

Percolation water obviously spreads in all directions lateraly. This spreading pattern corresponds to a cone with large opening angle. In comparison the spreading cone in groundwater is much narrower. This difference can be explained if one considers the fact that the groundwater flows parallel to the bedding, where-

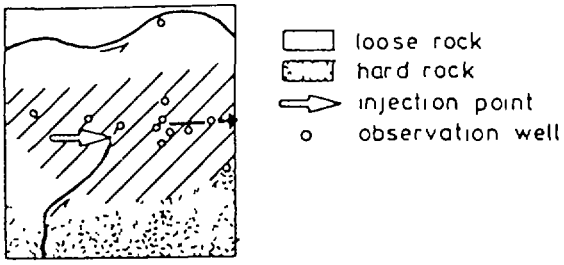


Fig. 11:

Propagation fields of tracers injected into groundwater (black arrow) and into unsaturated zone (hatched area) in connection with a river infiltration

as percolation water flows with the same velocity, but transverse to the bedding.

## 5.3 The role of bedding on lateral movement of percolation water

Tracer experiments in the zone of aeration from Dornach, Talham and Farchant show a pronounced lateral tracer propagation; only experiment No. 3 in Dornach does not agree with this statement.

In Dornach and Talham the bedding has a slight, but uniform slope. In Farchant however the slope of the bedding is multidirectional and steeper than in Dornach and Talham.

Along bedding a discontinuity in permeability exists that favours lateral tracer propagation. Although bedding slopes steeper in Farchant, the lateral tracer propagation is stronger than in Dornach and Talham. Thus the bedding slope is not the only factor influencing lateral tracer propagation; the other factor must be the rate of infiltration: The stronger the infiltration rate, the stronger the lateral propagation and vice versa can be. It is even possible that high infiltration rates could cause a partially saturated flow along beddings in the unsaturated zone.

The above mentioned interpretations of the causes of lateral tracer propagation includes experiment No. 3 of Dornach, that was performed with a sprinkling rate of 26 mm/d and that remained undetected in groundwater. In that case the low sprinkling rate favoured vertical flow and lateral flow may even be neglected; as a result the screen of observation wells was too wide to detect traced percolation water in groundwater. In chapter 6 the dependence of lateral flow is examined with the help of a mathematical model.

Transverse tracer propagation can not yet be expressed by means of transverse dispersivity in the unsaturated zone. Its qualitative effect on groundwater can be seen by comparing concentration-time curves from both tracing percolation water and only groundwater (Fig. 12). The boundary conditions in each pair of these experiments, especially flow velocity and length of flow path, were very similar to each other.

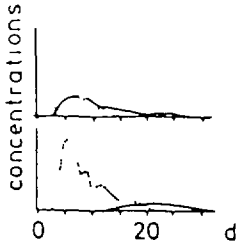


Fig. 12: Concentration-time-curves from tracer experiments in groundwater (dotted lines) and in the unsaturated zone (unbroken line). Distance between injection and detection point is for each case the same.

Tab. 7 Average percolation velocities derived from different experimental sites and experiments - n.d. = not determined

| percolation velocities [m/d] | | | |
|---|---|---|---|
| Infiltration quantity mm/d | refered to the thicknes of unsaturated zone | refered to the real flow path | experimental site |
| 200 | 0,09 | 0,31 | Dornach |
| 200 | 0,15 | 1,2 | Dornach |
| 52 | 0,02 | 0,09 | Dornach |
| 52 | 0,03 | 0,18 | Dornach |
| 26 | n.d. | n.d. | Dornach |
| 29 | - | 0,3 | Talham |
| 25 | - | 2 | Talham |
| 20 | 0,48 | 0,48 | Gungolding |
| river infiltration | - | 20,0 | Farchant |

## 5.4 Percolation velocities

Calculated percolation velocities by means of tracer tests are listed in table 7. The calculations are based on the thickness of the unsaturated zone and the suggested real flow path in it (Fig. 10).

In general measured percolation velocities in the gravels under research are above 0,1 m/d or 36,5 m/year. A plot of the percola- tion velocities as a function of infiltration rate is given in fig. 13. The results of the Dornach experiments can be summed up by a logarithmic straight line. The extrapolation of this line to an infiltration rate of 350 mm/year, corresponding to the groundwater recharge of Dornach, results in a flow velocity of 0,07 m/d or 25,5 m/year. This value agrees fairly well with the calculated one by means of hydraulics of 0,05 m/d or 18 m/year (permeability 4 x $10^{-8}$ m/s and water content 0,07, both at field capacity).

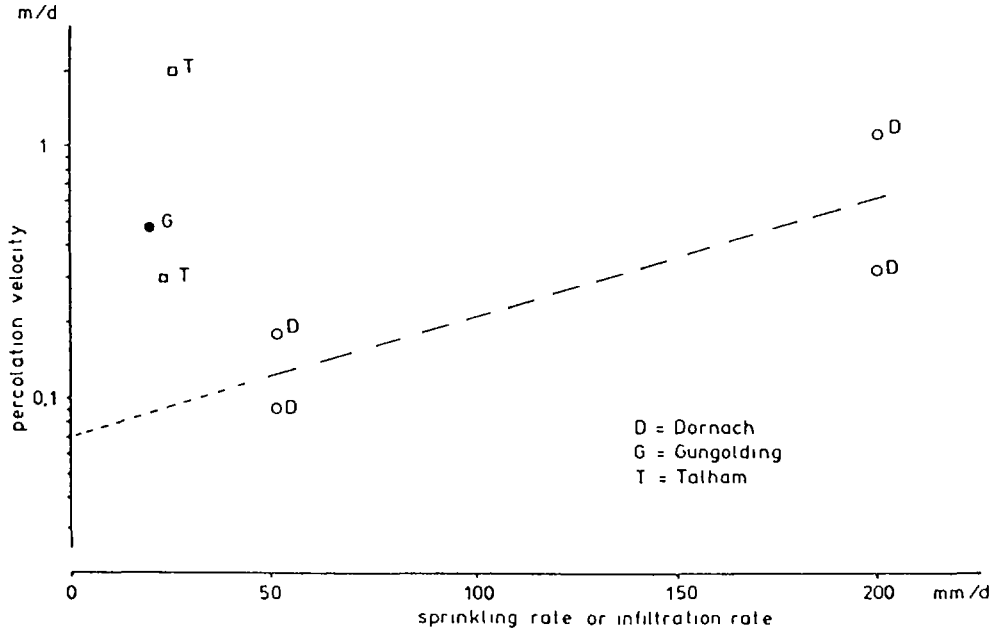


Fig. 13: Percolation velocities and their dependence on infiltration rate from field experiments.

## 6. The model problem and its geological boundary conditions

In Chapter 5 field tests were described, in which the sidewards movement of water in the unsaturated zone plays an important role. This sidewards movement is presumably due to a layering

of soils with different permeabilities. A number of questions remain unanswered or only partially answered:

1) How large a difference in permeability is necessary to produce such behaviour? The answer to this question obviously depends also on the slope of boundary between the soil layers under consideration.

2) How sensitive to changes in permeability and slope is this phenomenon?

3) Why does the sidewards component of the movement seem to increase with increasing infiltration speeds?

A plausible answer to question (3) can be found by refering to fig. 14. Plots of permeability K as a function of moisture potential $\Psi$ are given for a sandy soil and a gravel. One notes that for $\Psi$ =-660mm, the permeabilities of the two soils are approximately equal. As $\Psi$ increases toward 0, i.e. as the soils become wetter, the sand becomes more permeable than the gravel.

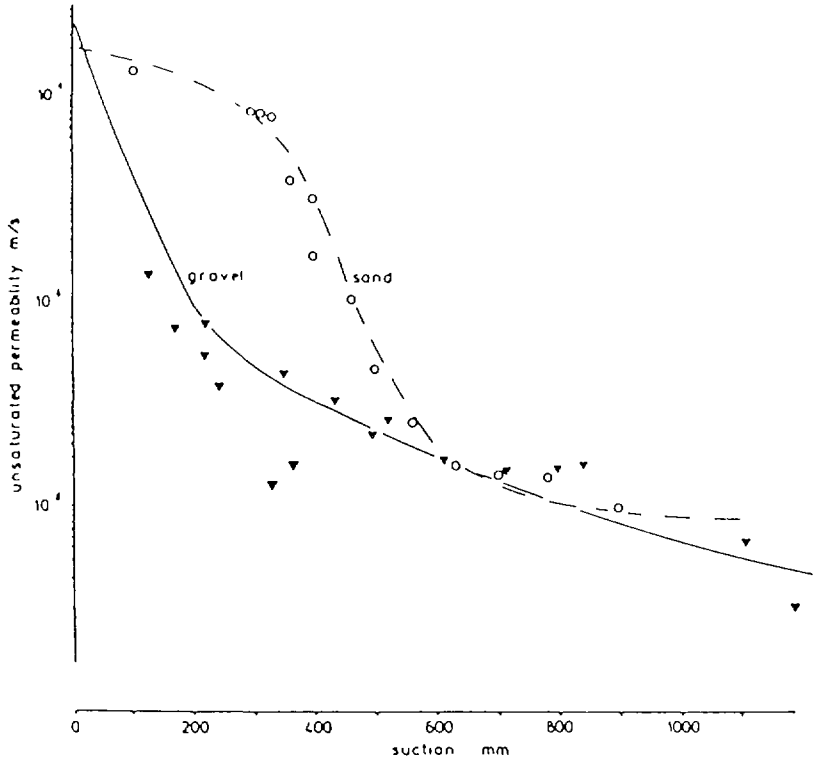


Fig. 14: Permeability K as a function of moisture potential (suction) for a sand and a gravel.

The difference between the two increases until, at values near $\Psi$ =-300mm, it reaches a maximum. Finally, as the moisture content approaches saturation, the two permeabilities start to approach each other again.

The permeability of the sand at $\Psi$ =-300mm is $K=6.76 \times 10^{-5}$m/sec. This corresponds to an infiltration rate due to gravity of 5.84m/d. Thus one would expect that, as the infiltration rate increases up to this point, the sidewards movement of water in layers of the above soils would become more pronounced. For larger infiltration rates, the two curves approach each other, and the sidewards movement should diminish.

To make this explanation more concrete, one needs answers to the questions (1) and (2) above. In particular, one should know if the differences in the curves of the two soils under question are in the ranges where effects similar to those observed in the field can take place.

We have attempted to answer these questions by using a mathematical model. The test situation is schematically described in fig. 15. The test area consists of a trough 2 meters high, 2 meters wide, and infinitely long. At the bottom of the trough

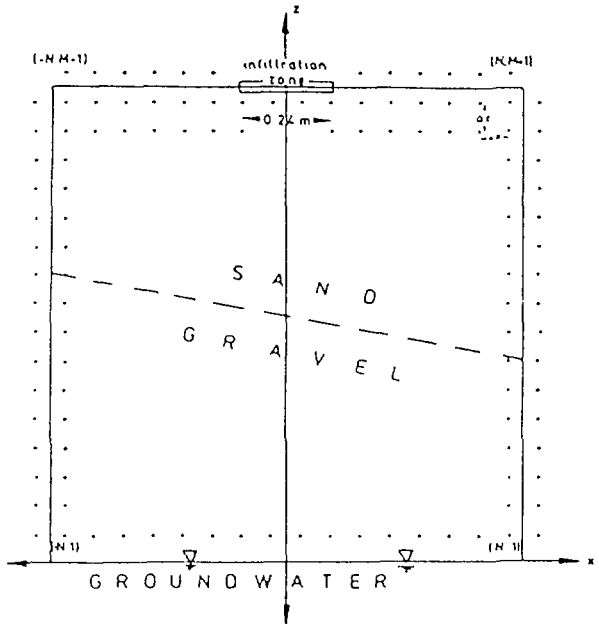


Fig. 15: Cross section of the model trough. The x-axis is placed at the bottom, along the groundwater table. The z-axis runs through the middle of the trough. The grid points, which are used in the numerical colution of the model equations, habe been drawn in along the boundary

is a ground water table, so that the bottom remains permanently saturated. The sides of the trough are impermeable, i.e. no water flows through them. Water infiltrates into the trough from the top, in an infinitely long strip, 0.24m wide, centered in the middle of the trough. The soil within the trough has two layers. The upper layer is the sand whose K-$\Psi$ curve appears in fig. 14. The lower layer is the gravel. The boundary between the two layers slopes to the right at an angle of 10°.

The steady state flow conditions, which arise when the infiltration is allowed to continue at a constant rate for an arbitrarily long time, were calculated using the model.

## 7.1 Description of the model

The mathematical model for water movement in unsaturated ground which was used is not new. More detailed discussions of its derivation can be found, for example, in [4 - 6].

The idea of the model is to determine the moisture potential within the ground as a function of position and time. We remark that when $\Psi$ is negative, the ground is unsaturated and $\Psi$ is a measure of the suction due to capillary forces within the soil When $\Psi$ is positive, the soil is saturated, and $\Psi$ is a measure of the hydrostatic pressure at the point in question.

The soil is assumed to obey a Darcy's law:

$$Q = -K(\Psi)\,\nabla\,\bar{\Psi} = -K(\Psi)\,\nabla\,(\Psi + z) \qquad (1)$$

where Q is the Darcy vector flow velocity, $K(\Psi)$ the permeability, and $\nabla\,\bar{\Psi}$ is the gradient of the total potential $\bar{\Psi}$ . $\bar{\Psi}$ is the sum of the moisture potential $\Psi$ and the potential due to gravity z, where z is the elevation above some fixed reference point. K is a constant for saturated soil, i.e. $K(\Psi)=K(0)$ for $\Psi > 0$. Plots of $K(\Psi)$ for $\Psi < 0$ appear in fig. 14 for the two soils used in the model situation.

Note that, if $\Psi$ is known as a function of position throughout the soil (assuming that the permeability $K(\Psi)$ is also known),

then (1) can be used to calculate Q, which is the information one seeks. In this way the problem of calculating the flow pattern in the soil is reduced to calculating the function

The continuity equation tells us that, for volumetric water content $\theta$,

$$\frac{\partial \theta}{\partial t} = - \nabla Q$$

where $\nabla Q$ is the divergence of Q.

When steady state flow exists, $\theta$ remains constant in time, so that we obtain

$$- \nabla Q = 0$$

or, using (1),

$$\nabla ( K(\Psi) \nabla (\Psi + z) = 0 \qquad (2)$$

The function $\Psi$ in equation (2) can be numerically determined, once we specify suitable boundary conditions. These are (see fig 16):

a) $\Psi (x, 0) = 0 \quad , \quad -1000\ mm \leq x \leq 1000\ mm$

b) $Q^x(-1000\ mm, z) = Q^x(1000\ mm, z) = 0 \qquad 0 \leq z \leq 2000\ mm \qquad (3)$

c) $Q^z(x, 2000\ mm) = 0 \quad , \quad |x| > 1200\ mm$

$= -q \quad ,$ a constant for $|x| < 120\ mm$

Here we have written the vector $Q=(Q^x, Q^z)$ in components using the coordinate system (x,z) in the trough. Equation (a) says that the soil at the ground water table is at saturation and under no hydrostatic pressure. Equations (b) say that no water can flow through the sides of the trough. Equation (c) specifies the infiltration rate q of water into the soil from above.

## 7.2 Results

Flow patterns for the model situation were calculated for the three different infiltration velocities q: 200mm/day, 50mm/day and 20mm/day. Normalized flow diagrams for these situations are given in figs. 16 A, B, C.

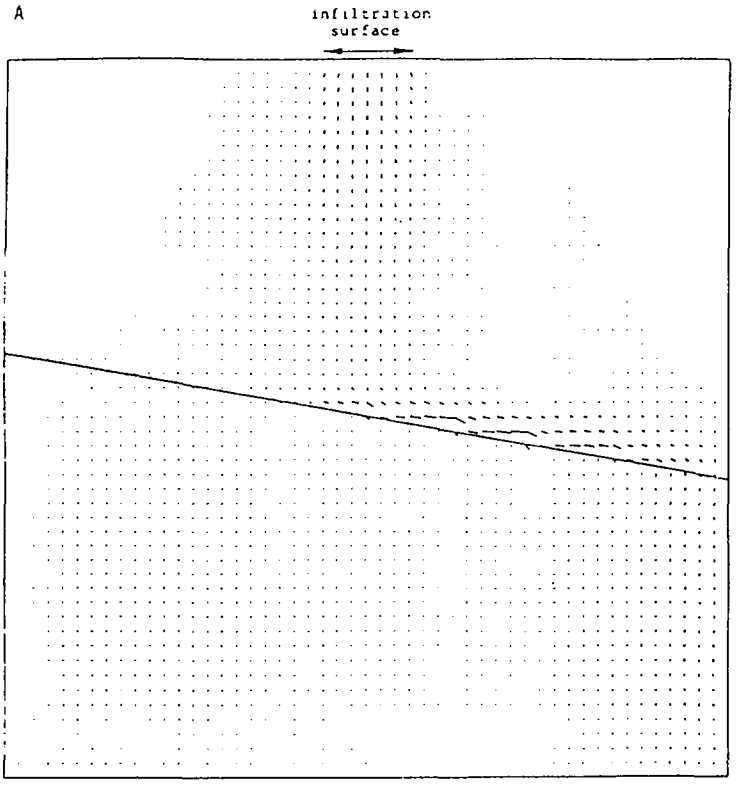
A
infiltration
surface

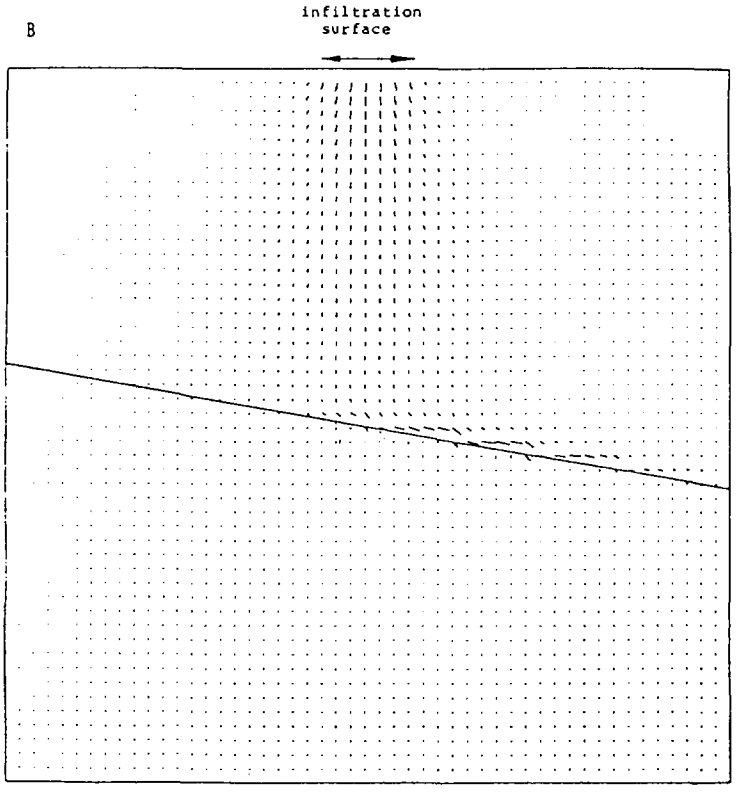
B
infiltration
surface

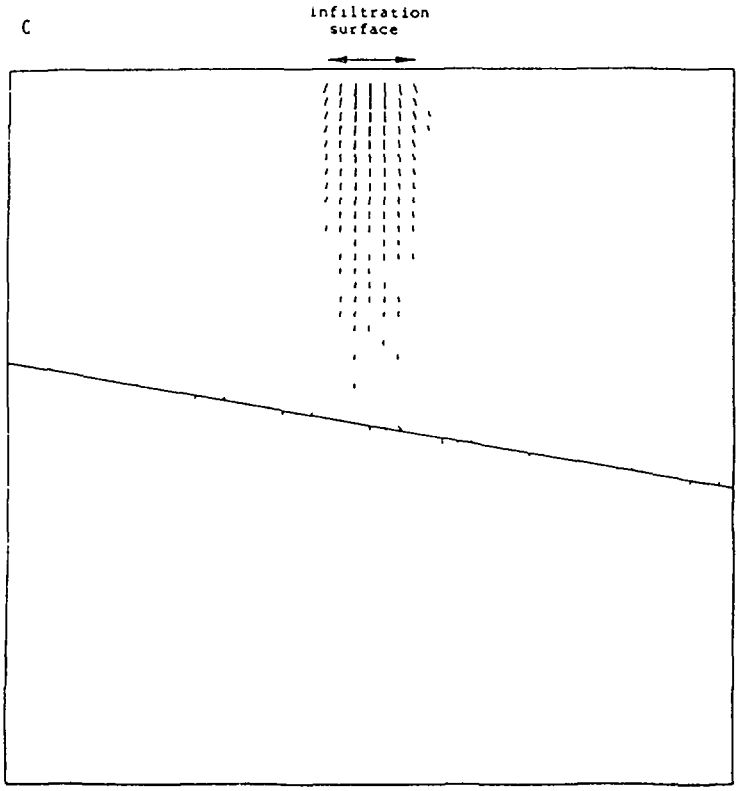


Fig. 16: Flow diagrams for the model situation with surface infiltration rates of 200 mm/d (A), 50 mm/d (B) and 200 mm/d (C). At each grid point a vector is drawn, representing the Darcy flow. The flow vectors in each diagram have been normalized, so that the maximum flow appears as a vector whose length is equal to the distance between grid points. This must be taken into consideration, when comparing flow vectors in two different diagrams.

In all three cases, the degree of saturation, which is reached just below the surface of infiltration, is such that the permeability is equal to the rate of infiltration. Thus, for example, when q=200mm/day, the value for K just below the infiltration surface is $2.315 \times 10^{-6} m/s = 200 mm/d$. This enables the potential gradient due to gravity to transport the water away from the surface. At greater depths below the surface, the ground becomes drier and the permeability decreases. Finally, near the boundary between the two soil layers, the saturation and permeability increase again.

In case I (200mm/d=2.315x10$^{-6}$m/s) there is a strong sidewards flow of water along the boundary between the two layers. On the upper side of this boundary, directly below the region of infiltration, the K-values are approximately 5.6x10$^{-5}$m/s, or around 25 times larger than at the surface. On the lower side of the boundary, the permeability is approximately 2.3x10$^{-7}$m/s, or less than 1/200 the permeability on the upper side. It is this sudden drop in permeability which forces the water to flow above and along the boundary, instead of flowing across it. The maximum flow velocity occurs here along the boundary: about 400mm/d, or twice the infiltration rate at the surface.

In case II (50mm/d=5.79x10$^{-7}$m/s) the sidewards flow along the boundary between the layers is still quite noticeable, although considerably weaker than in case I. On the upper side of the boundary, directly below the region of infiltration, the K-values are approximately 6.1x10$^{-6}$m/s, or around 10 times larger than at the surface. On the lower side of the boundary the K-values are around 1x10$^{-7}$m/s, or 1/60 of those on the upper side. The maximum flow velocity again occurs along the boundary. It is about 60mm/d, or somewhat more than at the surface.

In case III (20mm/d=2.315x10$^{-7}$m/s) the lateral flow component is hardly noticeable. Along the upper side of the boundary and below the region of infiltration, the K-values are about 3.4x10$^{-7}$m/s, about 1.5 times the values at the surface. On the lower side of the boundary, it is about 6x10$^{-5}$m/s, or about 1/6 of the value on the upper side. The maximum flow velocity occurs at the infiltration surface. Directly below it, water flows across the boundary between the layers with a flow velocity of approximately 6mm/d, or about 1/3 the velocity at the surface.

The results presented here offer estimates of certain conditions necessary for the presence of steady state lateral flow along a boundary with 10° slope between two soil layers with different permeability. When the permeability above the boun-

dary is at least 60 times greater than that below the boundary (as in case II), lateral flow is quite noticeable. When it is only 6 times as great (as in case III), very little sidewards flow is observed.

For permeability curves similar to the ones studied here, the transition between these two states can occur for infiltration rates between 20 and 50mm/d. It should be noted however that, when sidewards flow occurs, the impermeable walls of the trough cause a flow back-up which raises the moisture content in the upper layer. If these walls were not present, the moisture content, and hence the permeability would drop somewhat. This would presumably result in a somewhat diminished sidewards motion, because, as the soils become drier, the permeabilities of the sand and gravel approach each other.

It is also worth noting that, even in case I where the lateral flow is so pronounced, the water content does not reach saturation along the boundary.

References

[1] SAJJAD, M.J., HUSSAIN, S.D., WAHEED, R., SEILER, K.-P., STICHLER, W., TASNEEN, M.A., Study of downward movement of soil moisture in unsaturated zone. - In this Tec. Doc., 1985

[2] KLOTZ, D., Untersuchungen zur hydrodynamischen Dispersion in wasserungesättigten porösen Medien. - Dt. gewk. Mitt., 24: 158-163; Koblenz 1980

[3] BEHRENS, H., SEILER, K.-P., Field tests on propagation of conservative tracers in fluvioglacial gravels of upper Bavaria. - Proc. Quality of Groundwater: 649-657; Nordwijkerhoud 1981

[4] PHILIPS, J. R., Theory of infiltration. - In: Advances in Hydroscience, 5; Academic Press 1969

[5] IASH, Water in the unsaturated zone. - Proceedings of the Wageningen Symposium, two volumes 1968

[6] HORNUNG, U., MESSING, W., Poröse Medien: Methoden und Simulation. - Unpublished rep. Inst. für Numerische und Instrumentelle Mathematik der Universität Münster 1982

[7] BAKER, D., SEILER, K.-P., Zur Wasserbewegung in wasserungesättigten Lockergesteinen. - Beitr. über hydrol. Tracermethoden und ihre Anwend., GSF-Ber. R 290: 166-174; Neuherberg 1982

# GROUNDWATER FORMATION UNDER DESERT CONDITIONS

A.S. ISSAR*, J.R. GAT**, A. KARNIELI*,
R. NATIV*, E. MAZOR**

* J. Blaustein Institute for Desert Research,
Ben Gurion University of the Negev, Sede-Boqer Campus

** Department of Isotopes,
Weizmann Institute of Science,
Rehovoth

Israel

**Abstract**

Two complementary approaches were taken with regards to the problem of the physical and isotopic behaviour of soil moisture in the zone of aeration. Direct measurements on the moisture were carried out mainly by the Heidelberg group. The second approach was that of studying the isotopic and chemical composition of water at the two boundaries of this zone, namely the input from the surface and the water in the saturated zone. From the comparison of these waters the role of the aerated zone is inferred.

Three major recharge pathways were identified and found to differ in their effect on the isotopic composition: these are direct infiltration into sand dunes; local surface flow in fracturated rocky terrain and recharge through the intermediary of floodflows.

The following conclusions were reached:

1. In the sand dune column the water held in the unsaturated zone is enriched in the heavy isotopic species along a low slope evaporation line.
2. Practically no direct infiltration into groundwater occurs in lowest covered terrain.
3. In fractured rocky terrain the zone of aeration does not much affect the isotopic composition of the infiltrating on water. In most cases composition of groundwater resembles that of rain water.
4. Some enrichment of isotopes in the alluvial fan aquifers is believed to be due to evaporation of flood water.

## 1. Introduction

This paper is a final report on the research conducted under contract no. 2812/GS, signed in the beginning of 1981 with the Weizmann Institute of Science and the Institute for Desert Research. This research

was carried out with the collaboration of the Department für Umweltphysik, University of Heidelberg, W. Germany. This latter group put the emphasis on its research on the isotopic composition of the water on the zone of aeration in sand and loess terrains (Pfeilsticker, 1981). The Israeli group emphasized the study of the changes in the isotopic composition at the two extreme boundaries of the zone of aeration, namely precipitation and flood water on one hand and groundwater on the other.

For this purpose a number of different topographic and geological settings were chosen and compared as to the pattern of response to the

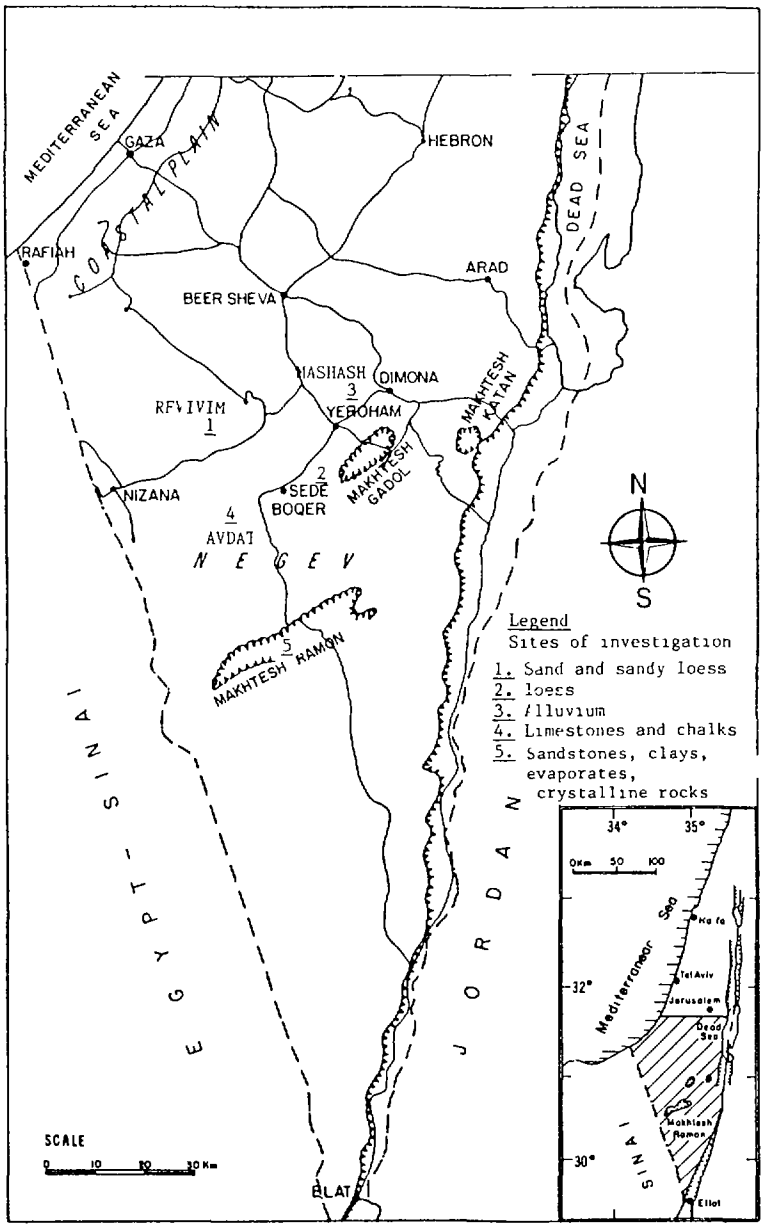


Fig. 1

rain input. These included Fig. 1:

1. Sands and sandy loess of aeolian origin which cover the foothills of the Western Negev.
2. A loess soil of pluvio-aeolian origin, of the type which covers the plateau of the Northern Negev.
3. Alluvial deposits in wadi-beds.
4. The limestone and chalk bedrock which build the foothills and high plateau of the Negev.
5. An area built of different types of rocks including sandstones, limestones clays, crystalline rocks and evaporites.

The annual average precipitation in the areas of research is from 50 to 100 mm. Average temperatures fluctuate between 10°C in December and 26° in July.

## 2. Isotopic and chemical composition of rainfall in the Negev

As stated before, although the main object of this research was to trace the behaviour of water in the zone of aeration it became clear in the early stages of the research that a knowledge of the isotopic and chemical composition of the rain water input and of the flood waters is a pre-requisite. This view was established after the sampling of rains and floods by special sequential samplers (Adar et al., 1980, Levin et al. 1980) showed a high variability in the isotopic and chemical composition between the different stages of each storm and each flood, as well as between different storm and flood events.

This variability in the isotopic composition between different rain events was found to be related to the air-mass trajectories of these rain storms (Leguy et al., 1983). In a very general way it can be concluded that rains which are most depleted in the heavy isotopes (but have a rather low "d" value) are connected in most cases with trajectories approaching the region from the south and southwest. These air

masses originated, presumably, as cold polar air masses but spent at least 24 hours over the continental deserts of northwestern Africa.

The group with the highest "d" value (+22‰) is mainly related to air masses reaching the area from the north-northwest, namely from over the Mediterranean sea. These air masses correspond to the classic "Mediterranean air masses" with a high "d" excess value, as described by Gat and Carmi (1970) (Fig. 2). Samples with isotope characteristics intermediate between these two extreme groups cannot be defined as clearly with regards to their trajectories and flow pattern.

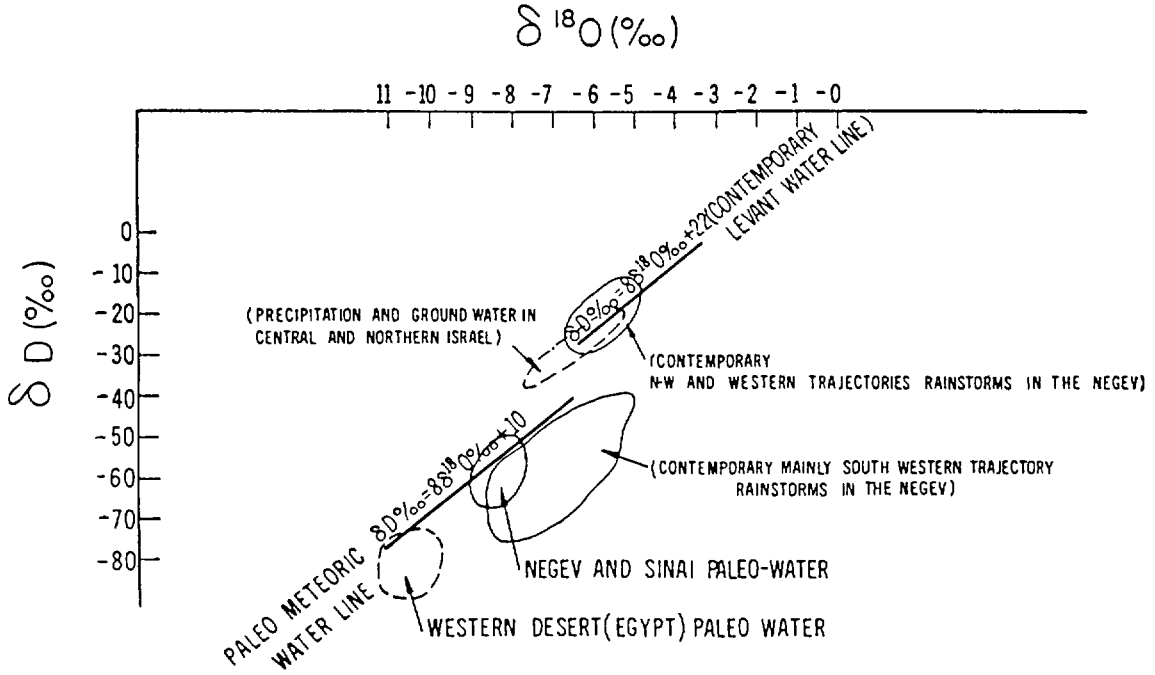


Fig. 2

An additional parameter related to the trajectories of air masses was found to be the sulfate content of the rain (Nativ et al. manuscript). It was found that a typical sulfate rich rain in mid winter is associated with a low pressure system located to the west of the Levant coast. The surface winds blow prior to the rain event from the eastern to southern quadrant and during the event from a southwestern to western direction. In these cases the rain events are small in quantity and have a relatively heavy isotopic composition

The tritium content may also be used to characterize the origin of the air masses. European humid air masses were found to be relatively high in tritium, while proper Mediterranean air masses were found to be much poorer in tritium. This observation parallels that of Gat and Carmi (1970) regarding precipitation in northern Israel.

A by-product of these results is a better understanding of the differences in the chemical and isotopic composition between the paleo- and contemporary groundwaters.

The paleo-climatic model proposed is that of a relatively higher frequency of storms akin to those which nowadays reach our area from the south-west to western direction; these air masses presumably originated over the northern hemisphere but were deflected towards the south due to the southern shift of the westerlies (Issar and Zangwil, manuscript). Their passage over a "sabkha" type continental shelf, created by the regression of the sea, may have caused the enrichment of sulfates in the paleo-waters.

## 3. Isotopic and chemical composition of flood water

The present work has put its main emphasis on the study of the composition of water of small watersheds and an attempt to correlate this with the hydrological regime of these watersheds.

Hydrological research which had been carried out in this region (Shanan 1975) showed that in a small watershed a threshhold value of 1.5mm-3.5mm of rain is necessary for the the formation of surface flow; this is conditioned by the intensity of the storm. A momentary intensity of less than 6mm/hour may not form any flow altogether.

The observations of Yair et al. (1978) have shown that in a small watershed, composed of bedrock in its higher part and colluvium in its lower part, a threshold of 0.5mm exists for the initiation of surface flow on the limestone outcrops. In most cases, however, the waters from

these outcrops do not reach the main wadi channel but infiltrate and evaporate before reaching the lower part of the watershed.

Issar et al (1984) have used the small watershed established by Yair et al. (op. cit.), to correlate the rain-runoff relations with their isotopic composition. The details of these observations were presented at the International Symposium on Isotope Hydrology in Water Resources Development, IAEA, 1983.

The main conclusions were the following:

1. Surface flows are of a lighter isotopic composition than that of the first 2mm of rain, which shows that they are generated only after this 2mm threshhold was passed.
2. The rains below the threshold evaporate totally, leaving the salts on the watershed. These salts are flushed afterwards by the rains which generate the floods. In other words it can be stated that floods `remember' the chemical composition of the rains below the threshhold but `forget' their isotopic composition.
3. No significant evaporation takes place from the floodwaters in the mainstreams.

These conclusions were found to be relevant also to bigger drainage basins. It can be seen from the statistics of the distribution of isotopic values (Fig. 3), where the mean value of the composition of the rainwater, floods and springs were calculated, that in all basins the floods have a lighter isotopic composition (more depleted in the heavy isotopes) than the average isotopic composition of the rains which generated them. This seems to be a result of the fact that the first portion of the rains, which are in most cases enriched in the heavy isotopes due to primary evaporation, are either below the threshold or are captured in the dry soil, sands and gravel. Only the main bulk of the storm and especially the more intense fractions thereof which have a characteris-

```
---------- DESCRIPTIVE STATISTICS ----------
HEADER DATA FOR: B:SPR+WLL    LABEL: SPRINGS + WELLS
NUMBER OF CASES: 160   NUMBER OF VARIABLES: 2

NO.   NAME     N          MEAN      STD. DEV.      MINIMUM       MAXIMUM
  1    018   160       -4.4564         1.5783       -6.3200        5.3200
  2     CL   158     1017.0206      1263.5213      124.0700     7476.3000

=====CLASS LIMITS====  FREQUENCY .............................
    -7.00 <     -6.25          5 |==
    -6.25 <     -5.50         23 |============
    -5.50 <     -4.75         53 |==============================
    -4.75 <     -4.00         36 |====================
    -4.00 <     -3.25         30 |================
    -3.25 <     -2.50          2 |=
    -2.50 <     -1.75          0 |
    -1.75 <     -1.00          6 |===
    -1.00 <      -.25          3 |=
     -.25 <       .50          0 |
      .50 <      1.25          0 |
     1.25 <      2.00          0 |
     2.00 <      2.75          0 |
     2.75 <      3.50          0 |
     3.50 <      4.25          0 |
     4.25 <      5.00          1 |
     5.00 <      5.75          1 |

---------- DESCRIPTIVE STATISTICS ----------
HEADER DATA FOR: B:RAIN    LABEL: RAIN 1977-
NUMBER OF CASES: 337   NUMBER OF VARIABLES: 2

NO.   NAME     N          MEAN      STD. DEV.      MINIMUM       MAXIMUM
  1    018   327       -4.3484         2.5305      -10.4800        3.7500
  2     CL   147       16.4435        10.2626        1.8500       45.5800
---------- FREQUENCY DISTRIBUTIONS ----------
HEADER DATA FOR: B:RAIN    LABEL: RAIN 1977-
NUMBER OF CASES: 337   NUMBER OF VARIABLES: 2

=====CLASS LIMITS====  FREQUENCY .............................
   -11.00 <    -10.25          1 |
   -10.25 <     -9.50          5 |===
    -9.50 <     -8.75          9 |=======
    -8.75 <     -8.00         12 |========
    -8.00 <     -7.25         27 |===================
    -7.25 <     -6.50         16 |==========
    -6.50 <     -5.75         21 |===============
    -5.75 <     -5.00         40 |============================
    -5.00 <     -4.25         32 |======================
    -4.25 <     -3.50         43 |==============================
    -3.50 <     -2.75         39 |===========================
    -2.75 <     -2.00         35 |=========================
    -2.00 <     -1.25         24 |=================
    -1.25 <      -.50         20 |==============
     -.50 <       .25          3 |==
      .25 <      1.00          0 |
     1.00 <      1.75          4 |==
     1.75 <      2.50          4 |==
     2.50 <      3.25          0 |
     3.25 <      4.00          2 |=

---------- DESCRIPTIVE STATISTICS ----------
HEADER DATA FOR: B:FLOODS    LABEL:
NUMBER OF CASES: 224   NUMBER OF VARIABLES: 2

NO.   NAME     N          MEAN      STD. DEV.      MINIMUM       MAXIMUM
  1    018   224       -5.2445         1.9917      -10.1600         .5000
  2     CL    84       39.6265        25.4945        4.1000      117.0000

---------- FREQUENCY DISTRIBUTIONS ----------
HEADER DATA FOR: B:FLOODS    LABEL:
NUMBER OF CASES: 224   NUMBER OF VARIABLES: 2

=====CLASS LIMITS====  FREQUENCY .............................
   -11.00 <    -10.25          0 |
   -10.25 <     -9.50          7 |====
    -9.50 <     -8.75          1 |
    -8.75 <     -8.00          6 |====
    -8.00 <     -7.25          5 |===
    -7.25 <     -6.50         39 |===========================
    -6.50 <     -5.75         41 |=============================
    -5.75 <     -5.00         29 |====================
    -5.00 <     -4.25         29 |====================
    -4.25 <     -3.50         37 |==========================
    -3.50 <     -2.75         10 |=======
    -2.75 <     -2.00          6 |====
    -2.00 <     -1.25          3 |==
    -1.25 <      -.50          5 |===
     -.50 <       .25          2 |=
      .25 <      1.00          4 |==
```

Fig. 3

tic composition which is more depleted than the average rainwater, will contribute to the flood flow.

Evenari et al. (1978) has shown that the runoff to rainfall ratio decreases with the size of the drainage basin, implying that water is lost during the surface flow. This should have been observed in the isotopic record if that loss is due to evaporation from the surface. There is no evidence for this in the data.

One has, therefore, to assume that the main loss of the water from the floods between the upper to the lower parts of the catchment area, is not by evaporation but due to other reasons:

1. The ratio of the area of the surface drainage system versus the area on which the convective rain falls increases as the area increases, due to the patchy nature of the desert rainfall, and thus the ratio of runoff/rain decreases.
2. Part of the water which disappears infiltrates to the subsurface to create groundwater.

In order to find out which of these mechanisms operate, a denser sampling and measuring network of rainwater and floodwater is needed. Radar mapping of rain events can also be very useful.

Not all the water which infiltrates to the subsurface during the process of the floods reaches the saturated zone and becomes groundwater. Part of it may be reclaimed by the vegetation which thrives along river beds in arid regions and is then transpired. The efficiency by which the annual runoff (R) is reduced in relation to the annual depth of precipitation over the region (D) is a function of the area of the watershed (A) and given by the function: $R/D=12.3A^{-0.4}$ (Ben Asher et al. manuscript).

Regarding the total quantity of salts brought into the region as aerosols by the rain storms, it was found (Nativ et al., 1983) that in an average year more salts are imported into such a region than exported by

the floods. This explains the phenomena of salinization of arid lands. It should be borne in mind, however, that during extreme wet years export will exceed import and at the same time more salts may be flushed out from the soils into the groundwater.

## 4. Mechanisms of groundwater recharge as revealed by isotopic characteristics

4a. Sands and sandy loess areas. The study of the sand area was carried out by Mr. Klaus Pfeilsticker from the University of Heidelberg group and involved the use of the tracing of the naturally occuring stable isotopes of $^{18}O$ and $^{2}H$ and of artificially introduced tritium. In this study, soil cores of up to 5 m in length were taken, the soil moisture was extracted and subjected to isotopic analysis at the laboratory of the Institut für Umweltphysik, of the University of Heidelberg.

The input of the stable isotopic tracer was controlled by rain collection and by continuous sampling of atmospheric moisture at Sede Boker. The tritium input was by artificial injection of tritiated water below the surface.

The main conclusions of the study regarding the sandy soils is that the infiltration below the capillary zone may reach 5% to 35% of the total annual rain (Pfeilsticker 1981). The percentage of infiltration from a storm of 30 mm rain as measured by Pfeilsticker (1981), was 60% (Issar et al., 1984 ). The apparent discordance between these conclusions can be explained by taking into account that about 40% of the precipitation in the Negev is in the form of isolated storms of less than 5 mm. Such storms are not effective for replenishment due to the fact that they saturate a depth of less than 50 cms and are redrawn to the surface either by capillary or by evapo-transpiration processes.

Thus it can be concluded that in the part of the Negev built of bare sand dunes, about 30% of the total annual rain is left for the replen-

ishment to groundwater. This calculation does not take into consideration deep rooted vegetation which may transpire the water even below the capillary zone.

The general equation for annual infiltration into the sand dunes can be given in the form of

$$R = 0.4\ P - Tr$$

where R = replenishment to groundwater in mm

P = annual precipitation in mm

Tr = annual transpiration from deep rooted vegetation in mm.

It is suggested to investigate the possibility of using the ratio of enrichment of environmental isotopes in the subsurface in relation to salts, in order to obtain a better estimate of Tr.

4.b. Loess covered areas. In his research on a loess soil column in the area of Sede-Boker, Pfeilstiker (1981) arrived at the conclusion that about 5% of the annual fall infiltrated below the 1 meter depth. It should be taken into consideration that the year of investigation was one with an unusually high annual precipitation of 162mm, which has a rather low probability to reoccur. As the infiltration is a function of the depth of the soil column which is saturated, as well as the thickness of the column of loess, it is suggested to continue this research to depths of more than 1 meter and over longer period of years.

4.c. Infiltration into alluvial beds. For the purpose of this research two wells were chosen in a river bed. One of them had been dug into the alluvial layers and the other into chalks of Eocene age near the river bed. A year long study of the oxygen isotope composition of the water in these two wells revealed abrupt changes in the isotopic content of the water in the well (Mashash 1, 2nd progress report) A closer investigation has shown that artificial recharge to the well from a nearby tank was the reason for this anomaly.

The $^{18}O$ content of the water of the alluvial well (Mashash 2) show a rather low variability and there is a hint of a positive deviation during the rainy season. This may be a result of the pushing in of water from the loess rich colluvium layers, or even the chalks bordering the alluvium. Similar but a more pronounced change in the tritium content of the water was observed in wells which penetrated chalk layers underlying gravel-beds (Issar et al. 1984).

The water found in the alluvial fill of the Rift Valley of the Arava is heavier by about 1‰ in $^{18}O$ than the water found in the Negev highlands (Gat and Galai, 1982; Issar et al., 1984 ). The question remains open whether this is due to the fact that the water which arrives at the alluvial fans of the Rift into which they infiltrate have before passed through some evaporation phase. If such is indeed the case than it would appear that although no effect of evaporation from the floods could be observed in the range of a few kms of flood travel, when it comes to a travel along tens of kilometers some evaporation may take place.

4.d. Infiltration into limestone aquifers. The samples which were collected from springs and wells in the limestone aquifer of the Avdat plateau of the Central Negev have confirmed the values which were observed in previous years, namely small fluctuations around an average of $\delta^{18}O = -4.45‰$.

The continuing sampling of rain has not changed the preliminary conclusion (Levin et al. 1980) regarding the existence of an enrichment trend in the groundwaters relative to the rain. The high standard deviation of the mean isotopic composition of the rain ($\pm 2.5‰$) does not permit to be too conclusive about this effect, however.

Comparison of the frequency distribution of the isotopic composition of the rain with that of the floods and the groundwaters from the Negev highlands, shows the averaging effect of the groundwater storage.

The rather big mean deviation coefficient which characterize the composition of the rain storms and the floods (although the latter is a little lower) strengthens the general conclusion expressed in the first part of this report regarding the large differences in the isotopic composition between one storm to the other and in between storms. To these variations along the coordinate of time one has to add the differences along the coordinates of space; Storms do not occur simultaneously all over the region.

The preliminary estimate of the infiltration rate into the limestone of the Avdat plateau does not exceed 2% of the total quantity of rainfall which falls over the area. This estimate is again preliminary, as it multiplies the value of precipitation observed in the different stations by the total area, without taking into consideration the spatial distribution of the rain.

Statistically, the spatial variability of rains of the entire area converges to at a certain constant value over a long period of time which does not exceed that of the retention period of such an aquifer (An assumption possible in view of the low tritium values observed at Ein Kudeirat and Ein Avdat during most of the years). One can estimate that the low percent gives the correct order of magnitude of infiltration.

The desert rains and the floods generated by them show great spatial variability. The function defining the replenishment percent in relation to precipitation ($R/D=30A^{-0.4}$) over a large area attains an asymptotic value of a few percent not exceeding that of 2%. Infiltration into groundwater operates at an early runoff stage in rather small basins, namely when the ratio of runoff to precipitation is about 1:10. Comparing the mean value of the isotopic composition of the groundwater $\delta^{18}O = -4.4\pm1.5‰$ to that of the floods $\delta^{18}O = -5.2\pm1.9‰$ and rain $\delta^{18}O = -4.3\pm2.5‰$, one might detect a trend of evaporation between the flood

stage and that of groundwater. Due to the relatively high standard deviation in the data it is suggested, however, not to consider these values as conclusive and to wait for more data such as deuterium analysis and the computation of the "d" values (which is a powerful indicator of the occurence of an evaporative water loss), as well as more field data on the composition of rains, floods and groundwaters.

The observations in the lower part of the Avdat plateau in wells near main riverbeds cutting into the chalks have shown (Issar et al. 1984) that the big floods in these river-beds influence the tritium content in these wells.

One can thus suggest that from the regional point of view the infiltration into groundwater occurs at all levels of the watershed and that the limestones aquifer acts as a rather good medium for mixing water both spatially and chronologically. As a result the water at the outlet shows a rather stable isotopic mean value.

4.e. Infiltration into chalk terrain. The correlation between the water levels, tritium content and flood events in wells near river beds in chalky terrain (Issar et al. 1984) has shown that the infiltration into this aquifer is by a piston action mechanism which drives older and more saline water into the aquifer. Younger water recharged by the flow arrive gradually later in the season.

This mechanism is of interest for understanding the nature of the aquiferous properties of chalky terrains and the spatial distribution of its permeable zones.

The continuation of this research needs however a rather extensive network of observation stations, hydrological as well as hydrochemical.

## 5. The Makhtesh Ramon Basin

During the last two years of research the watershed inside the erosion cirque of the Ramon has been monitored. In this watershed a network of

TABLE 1

Ramon Western Station (800 m a.s.l.) analytical data

| Sample | Date | Cont | cc | rain mm | total mm | Ca | Mg | Na | K | Cl | $SO_4$ | $HCO_3$ | TDI | Cont | pH | $^{18}O$ | $^{3}H$ TU |
|---|---|---|---|---|---|---|---|---|---|---|---|---|---|---|---|---|---|
| 23 | 050182 | 1 | 500 | 4.0 | 5.0 | 17.6 | 3.9 | 5.8 | 1.0 | 19.6 | 14.5 | 32.0 | 96.4 | 105. | 7.34 | -5.87 | 23.0 |
| | | | | | | 0.88 | 0.32 | 0.25 | 0.03 | 0.55 | 0.30 | 0.53 | 2.93 | | | ±0.06 | ±4 |
| 26 | 270182 | 1 | 250 | 2.8 | 2.8 | 14.4 | - | 3.0 | 0.9 | 10.6 | 8.8 | 32.0 | - | 88. | 7.35 | +1.52 | |
| | | | | | | 0.72 | - | 0.13 | 0.02 | 0.30 | 0.18 | 0.61 | | | | ±0.13 | |
| 27 | 030282 | 1 | 500 | | | 28.0 | 4.9 | 9.1 | 0.9 | 41.5 | 24.7 | 57.1 | 166.2 | 140. | 7.76 | -7.13 | 24.0 |
| | | | | | | 1.40 | 0.40 | 0.40 | 0.02 | 1.17 | 0.51 | 0.94 | 4.82 | | | ±0.05 | ±5 |
| 28 | 030282 | 1 | 500 | 3.7 | 3.7 | 20.4 | 1.5 | 8.7 | 1.1 | 20.2 | 19.8 | 41.7 | 113.4 | 133. | 7.73 | -5.61 | 25.0 |
| | | | | | | 1.02 | 0.12 | 0.38 | 0.03 | 0.57 | 0.41 | 0.68 | 3.23 | | | ±0.03 | ±4 |
| 30 | 170282 | 1 | 500 | 4 | 4 | 20.0 | 5.3 | 4.3 | 0.9 | 12.9 | 18.2 | 59.0 | 120.6 | 116. | 7.24 | -2.45 | 28.0 |
| | | | | | | 1.00 | 0.44 | 0.19 | 0.02 | 0.38 | 0.38 | 1.00 | 3.42 | | | ±0.05 | ±4 |
| 33 | 230282 | 1 | 500 | 4 | 14.7 | 23.2 | 2.4 | 4.1 | 0.9 | 10.6 | 17.1 | 51.5 | 109.8 | 123. | 7.77 | -4.79 | 18.0 |
| | | | | | | 1.16 | 0.20 | 0.18 | 0.02 | 0.30 | 0.36 | 0.85 | 3.12 | | | ±0.26 | ±3 |
| 34 | 230282 | 2 | 500 | 4 | 14.7 | 12.4 | 0.7 | 1.2 | 0.3 | 3.4 | 6.8 | 34.3 | 59.1 | 56. | 7.50 | -5.51 | 16.0 |
| | | | | | | 0.62 | 0.06 | 0.05 | 0.01 | 0.10 | 0.14 | 0.56 | 1.61 | | | ±0.05 | ±3 |
| 37 | 030382 | 1 | 200 | 2.2 | 2.2 | 24.0 | - | 3.0 | 0.8 | 8.2 | - | 58.9 | - | 130. | 7.78 | -2.82 | 17.0 |
| | | | | | | 1.20 | - | 0.13 | 0.02 | 0.20 | - | 1.00 | | | | ±0.03 | ±5 |
| 38 | 130382 | 1 | 500 | 4.0 | 5.3 | 24.4 | 3.2 | 9.2 | 1.1 | 31.8 | 18.5 | 67.2 | 154.6 | 138. | 7.41 | -4.14 | 29.0 |
| | | | | | | 1.22 | 0.26 | 0.40 | 0.03 | 0.87 | 0.38 | 1.10 | 4.33 | | | ±0.03 | ±4 |
| 43 | 250382 | 1 | 500 | 7.0 | 7.0 | 32.4 | 2.2 | 8.9 | 1.3 | 29.8 | 14.7 | 109.5 | 198.8 | 175. | 7.40 | -2.35 | 21.0 |
| | | | | | | 1.62 | 0.18 | 0.39 | 0.03 | 0.84 | 0.31 | 1.80 | 5.13 | | | ±0.03 | ±5 |
| 49 | 050482 | 1 | 150 | 1.6 | 1.6 | 23.2 | - | 3.1 | 1.1 | - | - | 81.7 | - | 112. | 7.62 | -1.55 | 7.0 |
| | | | | | | 1.16 | - | 0.14 | 0.03 | - | - | 1.34 | | | | ±0.04 | ±3 |
| 52 | 130582 | 1 | 250 | 2.9 | 2.9 | 44.8 | - | 7.4 | 1.7 | - | 38.1 | 66.7 | - | 42. | 8.04 | -0.65 | 31.0 |
| | | | | | | 2.24 | - | 0.32 | 0.04 | - | 0.79 | 1.09 | | | | ±0.04 | ±4 |
| 90 | 051182 | 2 | 500 | 4.0 | 40 | 14.0 | 1.5 | 6.2 | 1.0 | 14.6 | 16.4 | 19.9 | 73.6 | 89. | 7.22 | -7.98 | 23.0 |
| | | | | | | 0.70 | 0.12 | 0.27 | 0.03 | 0.41 | 0.34 | 0.33 | 2.13 | | | ±0.10 | ±4 |
| 91 | 051182 | 3 | 500 | 4.0 | 40 | 10.4 | 0.00 | 2.9 | 0.3 | 4.4 | 6.5 | 41.2 | 65.7 | 52. | 6.98 | -9.55 | 22.0 |
| | | | | | | 0.52 | 0.00 | 0.13 | 0.01 | 0.12 | 0.13 | 0.68 | 1.51 | | | ±0.09 | ±5 |
| 92 | 051182 | 4 | 500 | 4.0 | 40 | 9.2 | 0.00 | 2.3 | 0.2 | 8.4 | 5.5 | 19.0 | 44.6 | 45. | 7.20 | -8.85 | 18.0 |
| | | | | | | 0.46 | 0.00 | 0.10 | 0.01 | 0.24 | 0.11 | 0.31 | 1.21 | | | ±0.09 | ±5 |
| 93 | 051182 | 5 | 200 | 1.6 | 40 | 8.4 | - | - | - | 7.8 | - | 16.1 | - | 43. | 7.14 | -4.93 | 13.0 |
| | | | | | | 0.42 | - | - | - | 0.22 | | 0.36 | | | | ±0.12 | ±5 |
| 97 | 231182 | 1 | 450 | 6.0 | 7.3 | 12.0 | 1.2 | 5.0 | 0.7 | 11.2 | 12.2 | 30.9 | 73.2 | 67. | 7.00 | -3.17 | 8.0 |
| | | | | | | 0.60 | 0.10 | 0.22 | 0.02 | 0.32 | 0.25 | 0.51 | 2.02 | | | ± 0.09 | ±5 |
| 98 | 231182 | 2 | 100 | 1.3 | 7.3 | - | - | 4.7 | 0.4 | - | - | 22.9 | - | 59. | 7.06 | -3.79 | 10.0 |
| | | | | | | - | - | 0.20 | 0.01 | - | - | 0.38 | - | | | ± 0.20 | ±4 |
| 102 | 211282 | 1 | 500 | | | 18.8 | 2.2 | 5.0 | 0.5 | 11.1 | 12.1 | 57.2 | 104.9 | 106. | 7.04 | -4.50 | |
| | | | | | | 0.94 | 0.18 | 0.22 | 0.01 | 0.31 | 0.25 | 0.94 | 2.81 | | | ± 0.04 | |
| 105 | 060183 | 1 | 120 | | | 25.6 | - | 10.9 | 1.1 | - | - | 50.7 | - | 148. | 7.09 | -6.26 | |
| | | | | | | 1.28 | - | 0.48 | 0.03 | - | - | 0.83 | - | | | ± 0.05 | |
| 107 | 150183 | 1 | 500 | 4.0 | 10 | 15.6 | 1.7 | 4.6 | 0.5 | 12.4 | 11.6 | 28.9 | 75.3 | 82. | 7.22 | -6.93 | |
| | | | | | | 0.78 | 0.14 | 0.20 | 0.01 | 0.35 | 0.24 | 0.48 | 2.1 | | | ± 0.01 | |
| 113 | 230183 | 1 | 500 | 4.0 | 20.7 | 24.8 | 1.9 | 12.5 | 1.1 | 23.2 | 27.4 | 41.4 | 132.3 | 170. | 7.75 | -5.05 | 27 |
| | | | | | | 1.24 | 0.16 | 0.54 | 0.03 | 0.66 | 0.57 | 0.68 | 3.93 | | | ±0.19 | |
| 115 | 020283 | 1 | 400 | 3.6 | 3.6 | 17.2 | 2.6 | 2.2 | 0.3 | 7.1 | 8.1 | 52.8 | 90.3 | 70. | 7.23 | -5.19 | |
| | | | | | | 0.86 | 0.22 | 0.10 | 0.01 | 0.20 | 0.17 | 0.87 | 2.51 | | | ±0.09 | |
| 118 | 130283 | 1 | 450 | 4.6 | 4.6 | 19.6 | 1.9 | 2.2 | 0.5 | 9.2 | 11.9 | 46.7 | 92.0 | 89. | 7.36 | +1.31 | |
| | | | | | | 0.98 | 0.16 | 0.10 | 0.01 | 0.26 | 0.25 | 0.77 | 2.61 | | | ± 0.05 | |
| 120 | 240283 | 1 | 400 | 3 | 3 | 25.6 | 2.1 | 14.6 | 1.2 | 31.2 | 23.9 | 64.1 | 162.7 | 154. | 7.05 | -3.83 | |
| | | | | | | 1.28 | 0.18 | 0.64 | 0.03 | 0.88 | 0.50 | 1.05 | 4.63 | | | ± 0.07 | |
| 123 | 040383 | 1 | 300 | 4.0 | 35.5 | 20.4 | 1.7 | 5.7 | 0.7 | 17.8 | 9.2 | 40.3 | 95.7 | 99. | 7.13 | -7.58 | |
| | | | | | | 1.02 | 0.14 | 0.25 | 0.02 | 0.51 | 0.19 | 0.66 | 2.72 | | | ± 0.04 | |
| 124 | 040383 | 2 | 150 | 1.5 | 35.5 | 19.6 | - | - | - | - | - | 43.3 | - | 65. | 6.85 | -5.73 | |
| | | | | | | 0.97 | - | - | - | - | - | 0.72 | - | | | ± 0.04 | |
| 128 | 150383 | 1 | 500 | 5.1 | 5.1 | 14.0 | 1.4 | 1.7 | 0.3 | 8.8 | 4.3 | 38.3 | 69.3 | 46. | 7.38 | -8.07 | |
| | | | | | | 0.70 | 0.12 | 0.08 | 0.01 | 0.25 | 0.09 | 0.64 | 1.81 | | | ± 0.03 | |
| 130 | 210383 | 1 | 450 | 6 | 6 | 18.0 | 1.9 | 1.8 | 0.4 | 13.9 | 7.7 | 37.6 | 81.3 | 82. | 7.09 | -4.51 | |
| | | | | | | 0.90 | 0.16 | 0.08 | 0.01 | 0.39 | 0.16 | 0.62 | 2.41 | | | ± 0.07 | |

Date: The first day of event.
Container: Number of successive collecting container representing 4mm rain.
cc: Volume of rain sampled by the container as measured in the lab.
rain mm: Mw rain collected in respective container. (measured in the lab).
total mm: The total amount of rain during the event (measured by the recorder).
Dissolved ions and TDI in mg/l and below in meq/l.
Conductivity in microSiemens.
pH: Determined in the lab.

TABLE 2

Ramon Central Station (500 m a.s.l.) analytical data

| Sample | Date | Cont. | cc | rain mm | total mm | Ca | Mg | Na | K | Cl | SO4 | HCO3 | TDI | Cond | pH | $^{18}O$ | $^{3}H$ TU |
|---|---|---|---|---|---|---|---|---|---|---|---|---|---|---|---|---|---|
| 24 | 050182 | 1 | 450 | 3.6 | 3.6 | 39.6 | 3.2 | 13.9 | 2.0 | 42.1 | 53.2 | 34.3 | 188.3 | 245. | 7.25 | -3.57 | 12.0 |
| | | | | | | 1.98 | 0.26 | 0.60 | 0.05 | 1.19 | 1.11 | 0.56 | 5.85 | | | ±0.07 | ±4 |
| 25 | 270182 | 1 | 250 | 2.7 | 2.7 | 26.8 | - | 9.3 | 1.4 | 24.7 | 36.1 | 36.2 | - | 175. | 7.35 | +1.18 | |
| | | | | | | 1.34 | - | 0.40 | 0.04 | 0.75 | 0.75 | 0.59 | - | | | ±0.07 | |
| 29 | 030282 | 1 | 500 | 3.3 | 3.3 | 27.6 | 1.5 | 10.6 | 1.1 | 22.9 | 32.3 | 51.3 | 147.3 | 175. | 7.77 | -5.05 | 14.0 |
| | | | | | | 1.38 | 0.12 | 0.46 | 0.03 | 0.65 | 0.67 | 0.84 | 4.13 | | | ±0.05 | ±4 |
| 31 | 230282 | 1 | 500 | 4 | 14.5 | 24.8 | 2.2 | 4.4 | 0.8 | 11.8 | 26.0 | 43.1 | 113.1 | 130. | 7.61 | -4.71 | 17.0 |
| | | | | | | 1.24 | 0.18 | 0.19 | 0.02 | 0.33 | 0.54 | 0.71 | 3.30 | | | ±0.05 | ±4 |
| 32 | 230282 | 2 | 500 | 4 | 14.5 | 9.2 | 1.2 | 1.0 | 0.5 | 1.9 | 4.2 | 27.1 | 45.1 | 41. | 7.33 | -5.84 | 14.0 |
| | | | | | | 0.46 | 0.10 | 0.04 | 0.01 | 0.05 | 0.09 | 0.45 | 1.26 | | | ±0.05 | ±4 |
| 39 | 130382 | 1 | 500 | 2.2 | 2.2 | 29.6 | 1.5 | 8.5 | 0.9 | 44.0 | 16.0 | 61.6 | 162.1 | 165. | 7.90 | -2.73 | 12.0 |
| | | | | | | 1.48 | 0.12 | 0.37 | 0.02 | 1.24 | 0.33 | 1.01 | 4.52 | | | ±0.03 | ±4 |
| 44 | 250382 | 1 | 350 | 2.8 | 2.8 | 35.6 | 3.4 | 10.1 | 1.1 | 29.0 | 28.0 | 85.5 | 192.7 | 215. | 7.79 | -1.36 | 23.0 |
| | | | | | | 1.78 | 0.28 | 0.44 | 0.03 | 0.82 | 0.58 | 1.40 | 5.33 | | | ±0.03 | ±4 |
| 47 | 050482 | 1 | 500 | 4.4 | 5.7 | 18.0 | 1.7 | 2.5 | 1.0 | 9.1 | 4.1 | 65.4 | 101.8 | 88. | 7.50 | -2.94 | 14.0 |
| | | | | | | 0.89 | 0.14 | 0.11 | 0.03 | 0.26 | 0.09 | 1.07 | 2.73 | | | ±0.03 | ±4 |
| 48 | 050482 | 2 | 150 | 1.3 | | 15.2 | - | 2.8 | 1.2 | - | - | 80.4 | - | 81. | 7.27 | -2.56 | 28.0 |
| | | | | | | 0.76 | - | 0.12 | 0.03 | - | - | 1.32 | - | | | ±0.04 | ±5 |
| 53 | 130582 | 1 | 400 | 2.7 | 5.8 | 43.2 | 1.5 | 8.0 | 2.2 | 23.6 | 49.1 | 51.4 | 179.0 | 250. | 8.00 | -0.24 | 21.0 |
| | | | | | | 2.16 | 0.12 | 0.35 | 0.06 | 0.66 | 1.02 | 0.84 | 5.16 | | | ±0.04 | ±3 |
| 54 | 130582 | 2 | 450 | 3.1 | 5.8 | 19.6 | 2.4 | 2.2 | 0.6 | 6.8 | 14.5 | 42.7 | 88.8 | 160. | 7.99 | -0.97 | 30.0 |
| | | | | | | 0.98 | 0.20 | 0.09 | 0.02 | 0.19 | 0.30 | 0.70 | 2.52 | | | ±0.02 | ±4 |
| 56 | 051182 | 1 | 450 | 3.2 | 8.6 | 36.6 | 1.5 | 13.3 | 1.9 | 29.4 | 42.3 | 66.3 | 191.5 | 220. | 7.03 | -6.02 | 9.0 |
| | | | | | | 1.64 | 0.12 | 0.58 | 0.05 | 0.83 | 0.88 | 1.09 | 5.35 | | | ±0.01 | ±5 |
| 57 | 051182 | 2 | 500 | 3.6 | 8.6 | 11.2 | 0.2 | 3.1 | 0.5 | 8.5 | 7.5 | 22.7 | 53.7 | 64. | 6.97 | -5.81 | - |
| | | | | | | 0.56 | 0.02 | 0.14 | 0.01 | 0.24 | 0.16 | 0.37 | 1.71 | | | ±0.08 | |
| 58 | 051182 | 3 | 250 | 1.8 | 8.6 | 12.8 | - | 4.1 | 0.5 | 11.5 | - | 20.2 | - | 68. | 7.02 | -3.88 | 7.0 |
| | | | | | | 0.64 | - | 0.18 | 0.01 | 0.32 | - | 0.33 | - | | | ±0.09 | ±4 |
| 99 | 231182 | 1 | 450 | 3.9 | 5.6 | 17.6 | 1.9 | 7.0 | 0.8 | 15.6 | 21.6 | 25.6 | 90.1 | 104. | 7.19 | -2.93 | 8.0 |
| | | | | | | 0.88 | 0.16 | 0.30 | 0.02 | 0.44 | 0.45 | 0.42 | 2.62 | | | ±0.09 | ±4 |
| 100 | 231182 | 2 | 200 | 1.7 | 5.6 | 8.8 | - | 3.1 | 0.3 | 4.1 | - | 20.3 | - | 41. | 6.88 | -4.74 | 13.0 |
| | | | | | | 0.44 | - | 0.14 | 0.01 | 0.12 | - | 0.33 | - | | | ±0.05 | ±4 |
| 101 | 051282 | 1 | 200 | 2.2 | 2.2 | 33.2 | - | 15.0 | 1.1 | 36.6 | - | 73.2 | - | 215. | 7.01 | -3.48 | |
| | | | | | | 1.66 | - | 0.65 | 0.03 | 1.03 | - | 1.20 | - | | | ±0.07 | |
| 104 | 211282 | 1 | 300 | 3.0 | 3.0 | 20.4 | - | 5.5 | 1.0 | 18.9 | - | 29.6 | - | 104. | 7.10 | -5.07 | |
| | | | | | | 1.02 | - | 0.24 | 0.03 | 0.49 | - | 0.53 | - | | | ±0.07 | |
| 109 | 150183 | 1 | 200 | 1.7 | 1.7 | 38.0 | - | 10.6 | 2.4 | 30.9 | - | 47.0 | - | 215. | 7.34 | -4.69 | |
| | | | | | | 1.90 | - | 0.46 | 0.06 | 0.87 | - | 0.77 | | | | ±0.16 | |
| 111 | 150183 | 1 | 450 | 4.7 | 8.7 | 10.4 | 0.0 | 8.8 | 0.6 | 17.1 | 8.3 | 24.0 | 69.2 | 90. | 7.22 | -5.32 | |
| | | | | | | 0.52 | 0.00 | 0.39 | 0.02 | 0.49 | 0.17 | 0.40 | 2.02 | | | ±0.18 | |
| 112 | 150183 | 2 | 350 | 3.8 | 8.7 | 18.8 | 1.9 | 6.9 | 0.7 | 14.7 | 11.1 | 40.6 | 94.7 | 115 | 7.50 | -5.24 | |
| | | | | | | 0.94 | 0.16 | 0.30 | 0.02 | 0.42 | 0.23 | 0.66 | 2.72 | | | ±0.18 | |
| 114 | 230183 | 1 | 370 | 4.6 | 4.6 | 22.4 | 2.1 | 13.5 | 1.0 | 18.7 | 27.9 | 36.2 | 121.8 | 150. | 7.56 | -4.18 | 21 |
| | | | | | | 1.12 | 0.18 | 0.59 | 0.03 | 0.53 | 0.58 | 0.59 | 3.63 | | | ±0.16 | |
| 116 | 020283 | 1 | 300 | 3.8 | 10.0 | 18.8 | 2.1 | 2.7 | 0.6 | 8.6 | 14.8 | 36.2 | 83.8 | 84. | 7.39 | -2.93 | |
| | | | | | | 0.94 | 0.18 | 0.12 | 0.02 | 0.24 | 0.31 | 0.59 | 2.31 | | | ±0.09 | |
| 117 | 020283 | 2 | 500 | 6.2 | 10.0 | 7.6 | 0.0 | 1.0 | 0.2 | 5.2 | 0.0 | 16.4 | 30.4 | 31. | 6.83 | -3.84 | |
| | | | | | | 0.38 | 0.00 | 0.04 | 0.01 | 0.15 | 0.00 | 0.27 | 0.85 | | | ±0.09 | |
| 119 | 130283 | 1 | 120 | 3.1 | 3.1 | 34.8 | - | - | 0.0 | 19.0 | - | - | - | 170. | 7.22 | -1.21 | |
| | | | | | | 1.74 | - | - | 0.00 | 0.54 | - | - | - | | | ±0.09 | |
| 121 | 250283 | 1 | 300 | 0.3 | 0.3 | 36.4 | 2.6 | 25.0 | 1.7 | 52.5 | 46.5 | 57.2 | 221.9 | 260. | 7.16 | -1.62 | |
| | | | | | | 1.82 | 0.22 | 1.09 | 0.04 | 1.48 | 0.97 | 0.94 | 6.54 | | | ±0.09 | |
| 125 | 040383 | 1 | 350 | 4.6 | | 20.0 | 1.4 | 6.6 | 0.7 | 11.7 | 20.7 | 46.6 | 97.7 | 112. | 7.32 | -6.86 | |
| | | | | | | 1.00 | 0.12 | 0.29 | 0.02 | 0.33 | 0.22 | 0.76 | 2.79 | | | ±0.02 | |
| 126 | 040383 | 2 | 500 | 6.0 | | 14.4 | 0.0 | 3.2 | 0.3 | 13.9 | 7.3 | 36.3 | 75.4 | 72. | 6.56 | -3.37 | |
| | | | | | | 0.72 | 0.00 | 0.14 | 0.01 | 0.39 | 0.15 | 0.60 | 2.01 | | | ±0.02 | |
| 127 | 040383 | 3 | 100 | 2.0 | | 9.6 | - | 6.4 | 0.3 | 9.0 | - | 26.2 | - | 69. | 6.52 | -5.67 | |
| | | | | | | 0.48 | - | 0.28 | 0.01 | 0.26 | - | 0.48 | - | | | ±0.02 | |
| 129 | 150383 | 1 | 250 | 3.1 | 3.1 | 18.0 | 0.0 | 5.0 | 0.8 | 18.0 | 13.1 | 39.4 | 94.3 | 97. | 6.69 | -6.59 | |
| | | | | | | 0.90 | 0.00 | 0.22 | 0.02 | 0.51 | 0.27 | 0.65 | 2.52 | | | ±0.03 | |
| 131 | 210383 | 1 | 400 | 5.4 | 6.3 | 19.6 | 2.1 | 3.9 | 0.3 | 14.3 | 12.6 | 39.2 | 92.0 | 104. | 7.34 | -5.30 | |
| | | | | | | 0.98 | 0.18 | 0.17 | 0.01 | 0.40 | 0.26 | 0.64 | 2.71 | | | ±0.07 | |
| 132 | 210383 | 2 | 70 | 0.9 | 6.3 | - | - | - | - | 12.7 | - | - | - | 104. | 7.29 | -0.97 | |
| | | | | | | - | - | - | - | 0.36 | - | - | - | | | ±0.03 | |

Date: The first day of event.
Container: Number of successive collecting container (text).
cc: Volume of rain sampled by the container as measured in the lab.
rain mm: Mw rain collected in respective container.
total mm: The total amount of rain during the event (measured by the recorder).
Dissolved ions and TDI in mg/l and below in meq/l.
Conductivity in microSiemens.

rain and flood collection stations which sampled all rain events and intercepted flood flows at two transects across the basin, have been established. In addition water was collected from springs and observation wells.

As can be seen from tables 1 and 2 the differences in the $^{18}O$ compositions of individual rains is rather large, the most depleted value being -10.1‰ and the heaviest +4.2‰.

A comparison between the western and the more eastern rain station shows that the western one, which is at a higher elevation (about 300m higher than the other one), shows a composition which is depleted by about 0.8‰ to 1.6‰ in $^{18}O$.

A trend of depletion in the $^{18}O$ composition of the rain during the storms could be observed also in the Ramon area. In some cases when the rain stopped for a few hours and started again the same trend was observed again.

The range of the tritium values in the two stations is rather big - namely from $0\pm4$ to 39. The extremely low level tritium is worth special attention. Previous studies in the Negev have shown such low values to be characteristic to air masses which originate in the Indian Ocean region (monsoonal).

A general trend of decrease in the tritium values in the two years is observed. Such a trend could be seen also in the value of tritium in the rain at Sede Boker sampled since 1977. No trend has been observed in the values of tritium as they relate to two different stages of each storm.

Seven flood events have been recorded during the two years of observation (1981/1 - 3 events, 1982-3 4 events) although the precipitation value in 1982/3 was double that of 1981/2.

The $^{18}O$ composition of floods compared with that of the rains, show that the same characteristics described before exist, namely that the

floods 'forget' the $^{18}O$ composition of the light rains but remember their salt content. The mean $^{18}O$ composition of the groundwater $\delta^{18}O=(3.9\pm1.1‰)$ is similar to that of the groundwater of the Avdat plateau ($\delta_{18}=-4.3‰$), although the layers differ in their character and the area in its magnitude.

The tritium content of the well waters differ from one place to the other: the more enriched ones in tritium are more depleted in $^{18}O$. These water holes are located in the alluvium and are readily affected by the floods as well as by evaporation.

An interesting observation is related to Ein Saharonim where the tritium content is very low. The $^{14}C$ was found to be 54PMC. Another well, Ein Mishor, with about 4TU, show a $^{14}C$ value of 58 PMC. The $^{18}O$ and chemical composition of these wells are not outstanding, however.

A more detailed field examination of Ein-Saharonim and Ein Mishor has shown that these wells show an anomaly also from the hydrogeological point of view, as they emerge along a dike cutting through layers of Triassic age. Deposits of travertines were found along the dike, an evidence for groundwaters emerging from bigger depths. A detailed investigation of trace elements and general geochemistry of the travertines and these waters is being conducted.

## Summary and Conclusions

One can distinguish three major recharge mechanisms which operate in the arid environment. Direct infiltration can take place when relatively heavy rains above the threshold of about 2 mm fall on sand dune exposures, by virtue of the open pore structure of the sand and absence of plant interceptors (route I); on rock exposures and boulder-covered hills, recharge follows a modest scale of surface runoff, whereby a sufficient water depth is achieved to infiltrate throuch cracks or soil accumulators (II). The third major pathway for recharge utilizes the

large scale regional floods (III), which occur following intense downpours.

Paradoxically, the first mechanism may reach the highest water yield locally (in term of percentage of rain utilisation for a unit area) but its overall importance in the arid groundwater balance of the Negev Desert is quite limited, because of the reforestration of most of the dune areas. The floodflow mechanism which feeds some of the important regional aquifers (Gat and Galai, 1982) is rather inefficient in terms of water yield, simply because only a minor part of the rain ever reaches the floodflow scale.

From the isotope composition point of view these three pathways are quite distinct and the isotopic composition of groundwaters is thus a useful diagnostic tool. Again, paradoxically, the direct pathway of infiltration through sand dunes yield the most highly enriched (in heavy isotopic species) groundwaters, by virtue of the evaporative water loss from within the sand column. The floodflow mechanism is characterized by depletion in the heavy isotopes, due to the selection of intense showers in the flood's inception. Evaporation plays a minimal role in the big flash flood events. Pathway II, which involves some delay of waters near the surface carries the signature of evaporative enrichment to a small degree. All three pathways discrimate against the rains of

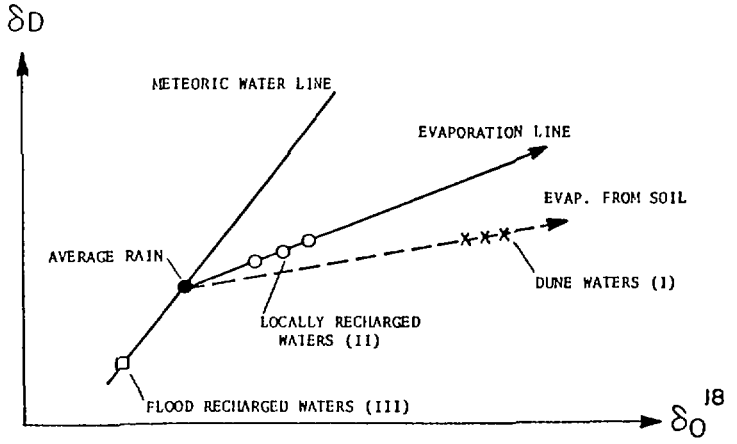


Fig. 4 Isotopic signature of the desert waters.

less than a few mms, and therefore the isotopic input (before secondary surface and subsurface processes take over) is somewhat depleted when compared to the mean annual rainfall (Fig. 4).

References

Adar, E., M. Levin and A. Barzilai, Development of a self sealing rain sampler for arid zones, Water Resources, 16 (1980) 592.

Evenari, M., L. Shanan and N.H. Tadmor, Runoff farming in the Negev desert of Israel, Department of Botany, Hebrew University, Jerusalem (1968) 47.

Gat, J.R. and I. Carmi, Evolution of the isotopic composition of atmospheric waters in the Mediterranean Sea area, J. Geophys. Res. 75 (1970) 3039.

Gat, J.R. and A. Galai, Groundwaters of the Arava Valley: an isotopic study of their origin and interrelationships, Israel J. Earth Sciences, 31 (1982) 25.

Issar, A., J.R. Gat, R. and R. Nativ and A. Karnielli, Isotopic evidence concerning the origin of groundwater in arid zones, Isotope Hydrology (1983), IAEA (1984).

Leguy, C., M. Rindsberger, A. Zangvil, A. Issar and J.R. Gat, The relationship between the Oxygen-18 and Deuterium contents of rainwater in the Negev Desert and air mass trajectories, Isotope Geoscience 1 (1983) 205.

Levin, M., J.R. Gat and A. Issar, Precipitation, flood and groundwaters of the Negev Highlands: an isotopic study of desert hydrology. "Arid Zone Hydrology: investigations with isotope techniques", IAEA (1980) 3.

Nativ, R., A. Issar and J. Rutledge, Chemical composition of rainwater and floodwaters in the Negev Desert, Israel, J. Hydrology, 62 (1983) 201.

Pfeilsticker, K. Deuterium und $^{18}O$ in Regen, Luft und Bodenfeuchte von Sde-Boqer (Negev), Lokale Grundwasserspende, Diplomarbeit Inst. fur Umweltphysik, Univ. Heidelberg (1981).

Shanan, L., Rainfall and runoff relationships in small watersheds in the Avdat region of the Negev desert highlands, Ph.D. thesis, the Hebrew University, Jerusalem (1975).

Yair, A., D. Sharon and H. Lavee, An instrumental watershed for the study of partial area contribution of runoff in an arid zone, Zeitschr. fur Geomorphologie, Suppl. 29 (1978) 71.

# SOIL WATER MOVEMENT IN SEMI-ARID CLIMATE – AN ISOTOPIC INVESTIGATION

P. SHARMA, S.K. GUPTA
Physical Research Laboratory,
Ahmedabad, India

**Abstract**

Soil moisture movement in the arid region of Thar desert, Rajasthan, has been studied using the tritium tagging method. It was found that groundwater recharge in the area varies between 6-14% of the precipitation input. The important factors which control the groundwater recharge are: i) vegetation cover; ii) nature of surface soil; and iii) topography. It was found that groundwater recharge is higher in the regions of shifting unconsolidated sands as compared to stabilised sand dunes having vegetation cover. In addition, a slight inclination of the land surface results in considerable reduction in the soil moisture transfer as compared to flat areas or areas which are situated in slight depression.

A simple conceptual model has been employed to understand the mechanism of soil moisture movement. The model involves estimation of precipitation excess for individual months taking into account the requirement of soil moisture storage and evapotranspiration. Using this model, the computed groundwater recharge for the semi-arid regions of Gujarat has been found to be in very good agreement with the experimental values obtained by the tritium tagging method.

## I. Introduction

We have been studying the phenomenon of groundwater recharge in the Sabarmati Basin, Gujarat, for the last few years by means of radioisotopic and conventional methods (Datta et al 1979, a, b; 1980, a, b; Bhandari et al, 1982 and Gupta and Sharma, 1984). Our studies indicate that groundwater recharge in the semi-arid regions is a complex phenomenon, depending not only on the amount and intensity of rainfall but also on the climate and soil texture.

In this report, we present results of tritium tagging experiments in the Thar Desert, Rajasthan (Fig. 1) and compare these with the results obtained at Ahmedabad (23.0°N, 72.6°E), a region of about three times higher rainfall than the Thar Desert but still on the fringe of the desert in the semi-arid region of NW India.

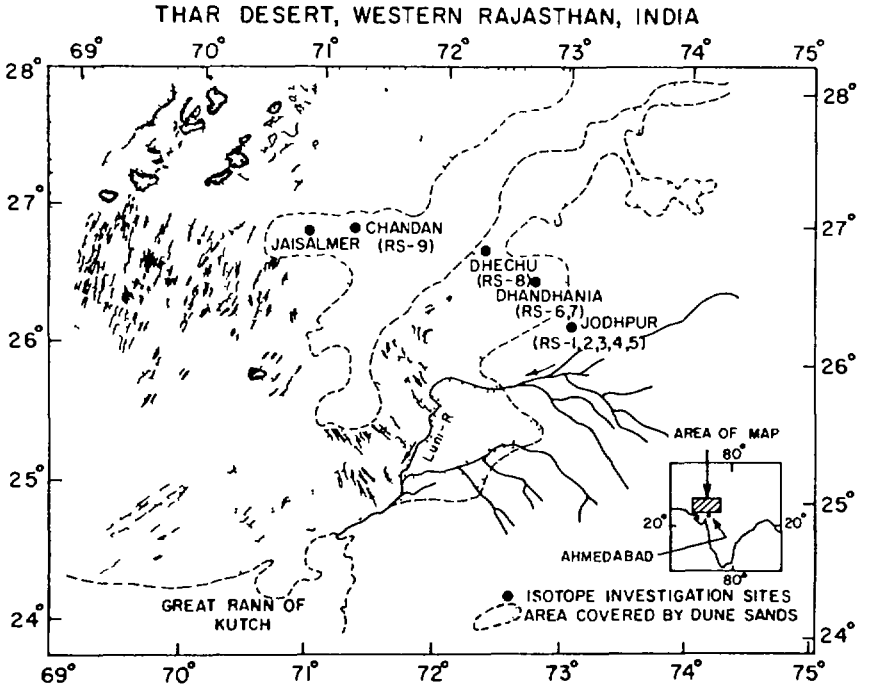


Fig. 1. Schematic map of Thar Desert, western Rajasthan, showing the isotopic investigation sites.

## II. Project Area: Geology and Climate

Fig. 1 shows the locations of stations established for this study in the Thar Desert. The area not covered by dune sands represents the rocky desert with a thin (3-4 m) soil cover. The rock type in the region around Jodhpur are pre-Cambrian granites of the Aravalli system while those near Chandan and Jaisalmer are low grade metamorphic sedimentary rocks of "Lathi" formation.

The long term (1901-50) monsoon means rainfall (June-September) in the Thar Desert is about 328 mm at Jodhpur and about 152 mm at Jaisalmer, the coefficient of variation of rainfall being in the range of 55-70% in the region between Jodhpur and Jaisalmer (Gupta and Prakash, 1975). In comparison, the long term (1901-73) mean annual rainfall at Ahmedabad is 774 mm (UNDP, 1976) with a coefficient of variation of about 40%.

Fig. 2(a) gives the long term monthly estimate of potential evaporation at Jodhpur by Penman and Thorntwaite methods. The observed values by the Class-A Pan (wire mesh type) are also given. Fig. 2(b) gives the same for Ahmedabad.

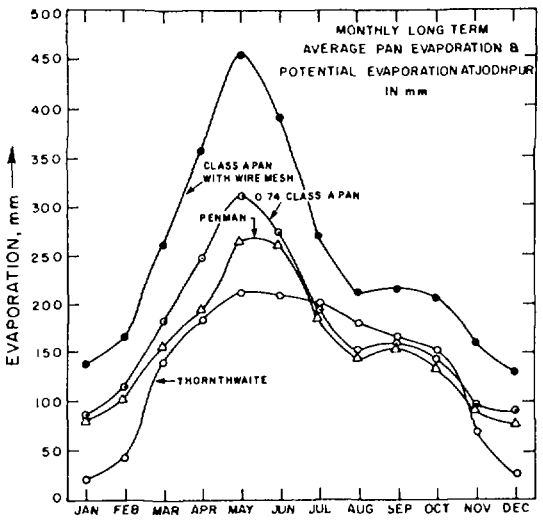


Fig. 2(a). Monthly mean long term average pan evaporation potential evaporation data at Jodhpur (UNDP, 1976)

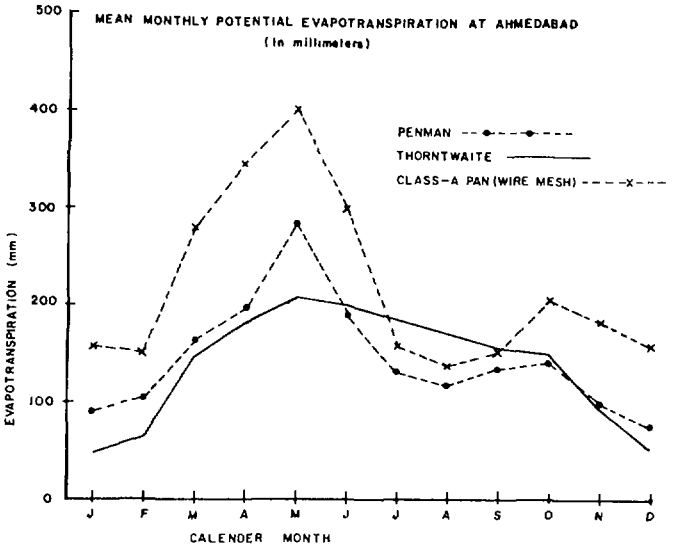


Fig. 2(b). Monthly mean long term average pan evaporation potential evaporation data at Ahmedabad (Gupta, 1984)

## III. Experimental Details; Methodology and Results

Nine experimental stations (RS 1-9) were established in the Thar Desert in September 1982, RS 1 to RS 5 at/around Jodhpur, RS 6 and RS 7 on the stabilized sand dune at Dhandhania, about 55 km NW of Jodhpur, RS 8 at Dhechu on a dune about 100 km NW of Jodhpur. The field station RS 9 was established at Chandan, about 40 km east of Jaisalmer (Fig. 1).

The field conditions at the time of injection/sampling at these sites are given in Table 1. It may be noted that we could not sample two of the sites RS 7 and RS 8. The site RS 7 is located about 100 m away from RS 6 at nearly the same elevation on the sand dune at Dhandhania. RS 8 is located at the base of the stabilized sand dune near village Dhechu. A hard clay/kankar bed was encountered at about 1 m at both these locations and the sampling had to be abandoned.

The details of the tritium tagging method for estimating the soil moisture movement are given in a recent paper by Gupta and Sharma (1984). Briefly, tritiated water (approx. 2 ml, activity 10 μCi/ml) was injected at a depth of 0.75 m below the ground surface, usually 3-4 sets at any given station. A hand auger was used for sampling the soil in steps of 10 cm.

The soil moisture was extracted by a batch distillation system under vacuum fabricated especially for this study. The moisture content was

Table 1: Details of field site and tritium tagging experiment conducted at the isotopic investigation stations established in the Thar Desert, Rajasthan

| Station Code | Station Name | Details of the location | Soil type (median grain size of top 0.5m layer, $\mu$ m) | Date of Injection | Date of Sampling | Net Moisture transfer (cm) | Water input** (cm) | Fractional recharge (%) |
|---|---|---|---|---|---|---|---|---|
| RS-1 | Jodhpur | CAZRI* campus. Barren land, sparsely planted desert plants exist at the site. RS-1 is about 500 m away from the location of RS-4/5 | (150 $\mu$m) | 7.9.82 | 24.7.83 | 2.57 | 21.88 | 11.7 |
| RS-2 | Subhavaton ki Dhani | Pasture land in the Doli-Pal basin on the outskirts of Jodhpur. Seasonal grass cover 0.5 m in height at the time of injection. | (190 $\mu$m) | 7.9.82 | 25.7.83 | 2.21 | 21.88 | 10.1 |
| RS-3 | Subhavaton ki Dhani | Same as RS-2 on a barren part of the land located in a slight depression, about 100 m from RS-2 | (210 $\mu$m) | 7.9.82 | 2.8.83 | 4.68 | 38.91 | 12.0 |
| RS-4 | Jodhpur | Experimental field of CAZRI in the CAZRI campus, Cowpeas crop under drip irrigation (no return seepage of irrigation water with this type of irrigation) | (185 $\mu$m) | 7.9.82 | 24.7.83 | 1.66 | 21.88 | 7.6 |
| RS-5 | Jodhpur | Experimental field of CAZRI in the CAZRI campus, rainfed Guvar (a kind of beans) raised in the field RS-5 is about 50 m away from RS-4 in the same field. | (210 $\mu$m) | 7.9.82 | 24.7.83 | 1.74 | 21.88 | 7.9 |
| RS-6 | Dhandhania | Stabilized sand dune near village Dhandhania 55 km from Jodhpur on Jodhpur-Jaisalmer State Highway, sparse shrub cover over the dune, station is on the wind-ward side of the dune at a surface slope of about 5°. | (225 $\mu$m) | 8.9.82 | 31.7.83 | 2.18 | 38.91 | 5.6 |
| RS-9 | Chandan | CAZRI Campus at Chandan, about 40 km from Jaisalmer on Jodhpur-Jaisalmer State Highway. Stabilized sand dune with a thin cover of shifting sands. | (225 $\mu$m) | 9.9.82 | 30.7.83 | $\geq$2.23 | 16.49 | $\geq$13.5 |

*Central Arid Zone Research Institute, Jodhpur.

measured gravimetrically. After a site was sampled up to the desired depth, in situ soil density was measured by the sand logging method. For the study region, the in situ soil density is about 1.75 gm.cm$^{-3}$.

The net moisture transfer, M (in cm), has been obtained using

$$M = m.\ D.\ x. \qquad \ldots\ (1)$$

where

m = moisture content (gm per gm of the field soil)

D = in situ density of the field soil (gm. cm$^{-3}$) obtained by sand logging

x = observed displacement (in cm) of the tagged layer, given by the depth difference between the depth of injection (75 cm) and position of the centre of gravity (C.G.) of the tracer activity profile.

In actual practice, as there is variation of both 'm' and 'D' with depth, the computation of 'M' is done by summation, the values obtained from equation (1) for each 10 cm depth interval for which both 'm' and 'D' are available.

Figs. 3-9 show the observed depth profiles of tritium activity as well as moisture content at seven of the field stations RS 1-5, RS 6 and RS 9 established in the Thar Desert. It may be noted that the moisture content of the soil is low in these regions, about 2-6% only as compared to 5-15% at Ahmedabad (Fig. 10) and other stations in Gujarat (Bhandari et al, 1982).

From Table 1, it is seen that the three stations RS 1, RS 4 and RS 5 at the Central Arid Zone Research Institute (CAZRI) campus at Jodhpur show fractional recharge in the range of about 8-12%. The two stations RS 4 and RS 5 which are about 50 m apart in the same field show close agreement in the fractional recharge values, being 7.6% and 7.9% respectively at these two stations.

The site RS 1 (barren plot) about 500 m away from the location of RS 4/5 in the CAZRI campus show a higher recharge (11.7%) as compared to nearby RS 4 and RS 5 locations (cultivated plots). The difference could be due to consumptive use of soil moisture by plants over and above the drip irrigation at RS 4.

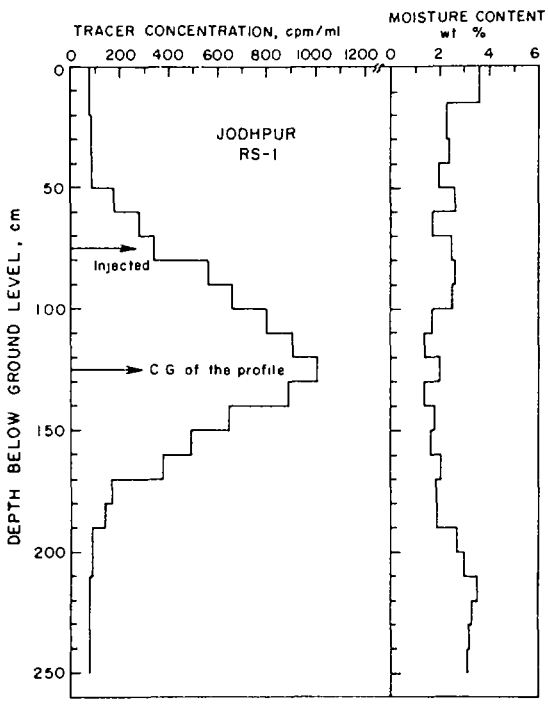


Fig. 3. Tracer activity profile and the soil moisture content for the station RS 1 at CAZRI Campus, Jodhpur.

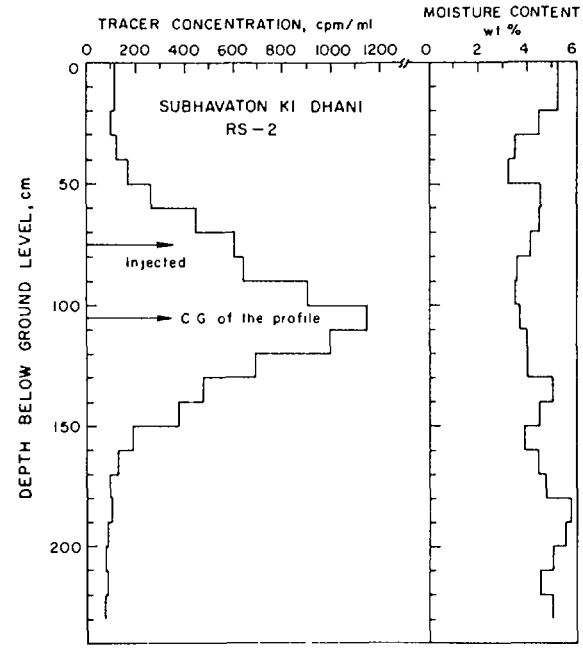


Fig. 4. Tracer activity profile and the soil moisture content for the station RS 2 at Village Subhavaton Ki Dhani on the outskirts of Jodhpur.

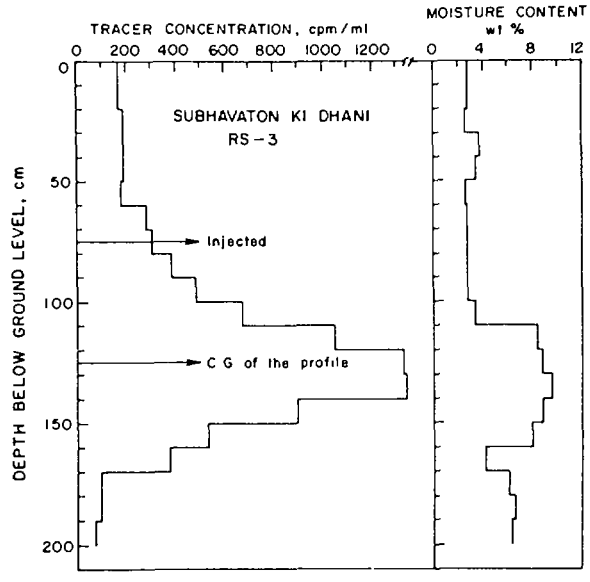


Fig. 5. Tracer activity profile and the soil moisture content for the station RS 3 at Village Subhavaton Ki Dhani on the outskirts of Jodhpur.

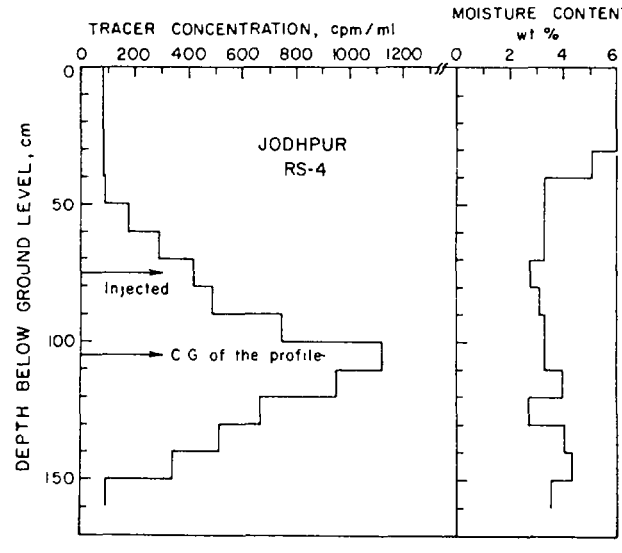


Fig. 6. Tracer activity profile and the soil moisture content for the station RS 4 at the CAZRI Campus, Jodhpur.

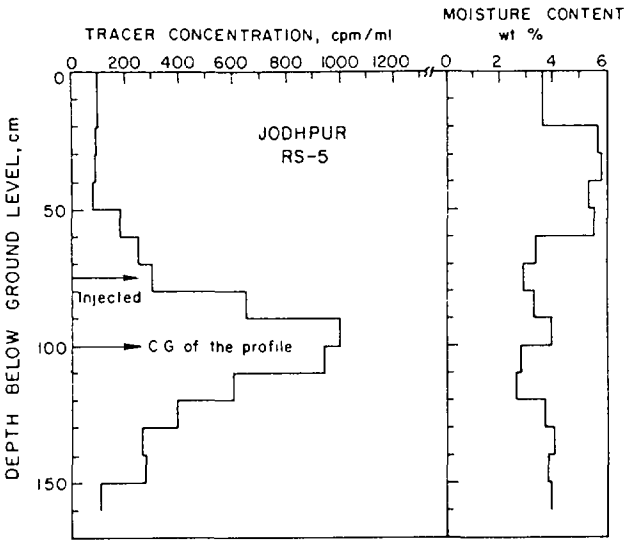


Fig. 7. Tracer activity profile and the soil moisture content for the station RS 5 at the CAZRI Campus, Jodhpur.

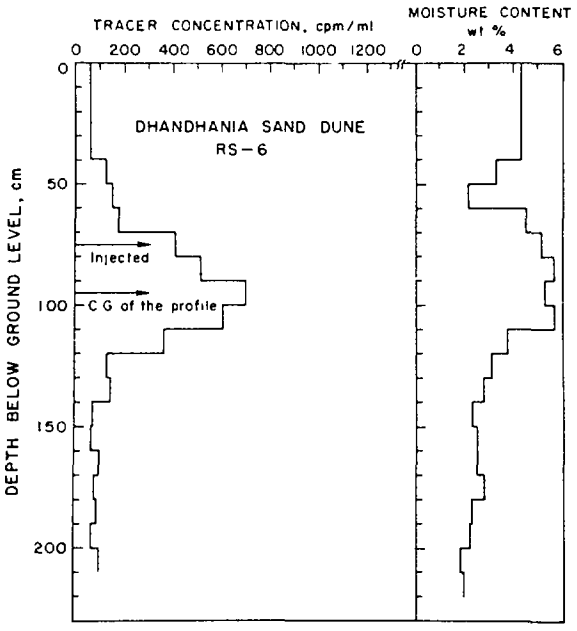


Fig. 8. Tracer activity profile and the soil moisture content for the station RS 6 at the stabilized sand dune near Village Dhandhania.

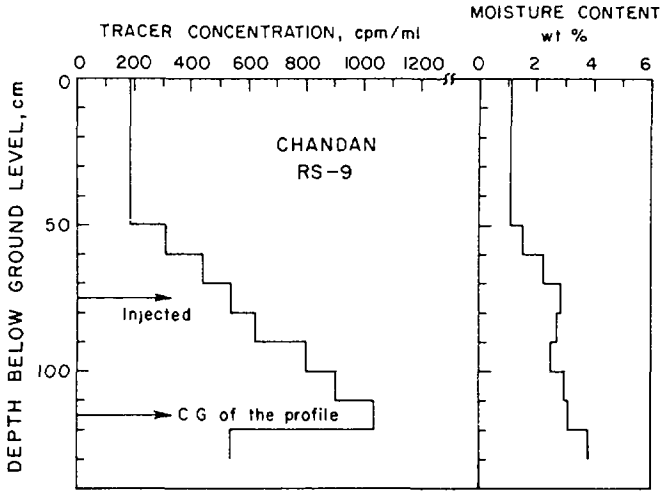


Fig. 9. Tracer activity profile and the soil moisture content for the station RS 9 at CAZRI Campus, at Chandan.

For the station RS 2 at Subhavaton Ki Dhani on the outskirts (about 3 km) of Jodhpur, the fractional recharge value of 10.1% is of the same order as for the stations RS 1, 4 and 5 at CAZRI campus, Jodhpur. However, between RS 2 and RS 3, within about 100 m distance of each other the slightly higher recharge at RS 3 (12.0%) could be due to absence of any vegetation and/or slight depression of the tritium injection site resulting in a ponding of water after a rainfall event, as we noticed during the sampling.

The station RS 6 at the stabilized sand dune at Dhandhania which has almost the same type of topsoil as at Jodhpur, has a prominently low recharge value (5.6%). The exact rainfall data for this station is not available in the absence of a raingauge station in the vicinity. We have, therefore, used the rainfall data of Jodhpur. However, as can be seen from the contours of annual rainfall, as given in Gupta and Prakash (1975), the variation of rainfall between Jodhpur and Dhandhania is less than 50 mm, which gives us confidence in using the rainfall data of Jodhpur for this site. Thus the low value of fractional recharge at RS 6 could be partly due to the surface slope (about $5^{o}$) resulting in higher run-off.

The station RS 9 at CAZRI campus at Chandan shows a higher recharge ( 13.5%). This site could not be sampled beyond 130 cm depth due to collapsing of the auger hole as a result of loose sand (low moisture content). However, a clear peak of tracer can be seen from Fig. 9 and can be taken as the position of C.G. of the profile. In such a case in the absence of the complete tracer activity profile, the fractional recharge estimated is the lower limit. The site has a thin layer of shifting loose sand with no vegetation cover and the observed high recharge value probably is due to high rate of infiltration through the sand.

Thus, the results of our experiments indicate significant recharge in the range 6-14% of rainfall as against the average recharge of 14.5% (range being from 5-35%) in the alluvial parts of the Sabarmati basin, Gujarat (Gupta and Sharma, 1984). The control of various factors giving rise to the observed variability is also indicated.

## IV. Mechanism of soil water movement

In the previous discussion, it has been implicitly assumed that the tracer is carried downward or upward in response to the soil moisture movement. With a view to describe the tracer behaviour over a long period of time, a special study was undertaken at Ahmedabad.

A set of 8 tritium injections were made 1 m apart from each other in a non-irrigated agricultural field at Thaltej ($23.0^{o}$N, $72.6^{o}$E) on the outskirts of Ahmedabad. Table 2 and Fig. 10 give details of the results of periodic sampling (one by one) of the 8 injection points during the two years period 6.8.1977-16.10.1979.

Table 2: Results of multiple sets of injection at Thaltej, Station Code-37 (Injection depth = 75 cm)

| Inj. No. | Date of Injection | Date of Sampling | Displacement of tracer Peak (cm) | Water input (Precipitation) (cm) | Net downward moisture transfer (cm) | Fractional Recharge (%) |
|---|---|---|---|---|---|---|
| 1. | 6-8-77 | 6-8-77 | 0.0 | 0.0 | 0.0 | 0.0 |
| 2. | 6-8-77 | 17-8-77 | +12.0 | 18.4 | 2.85 | 15.5 |
| 3. | 6-8-77 | 9-9-77 | +14.0 | 25.6 | 3.40 | 13.3 |
| 4. | 6-8-77 | 10-12-77 | -10.0 | 26.5 | -2.0 | - |
| 5. | 6-8-77 | 12-4-78 | -20.0 | 26.5 | -3.7 | - |
| 6. | 6-8-77 | 25-10-78 | +21.0 | 91.8 | 7.23 | 11.1 |
| 7. | 6-8-77 | 13-6-79 | +21.0 | 96.6 | 6.31 | 9.0 |
| 8. | 6-8-77 | 16-10-79 | +26.0 | 150.1 | 10.97 | 8.9 |

The case I (Fig. 10 and Table 2) giving the results of sampling of the first injection point on the same day of injection (6.8.1977) shows no displacement of the tracer peak and consequently no net moisture transfer, in the absence of any precipitation on that day. Case II, obtained by sampling the second injection point on 17.8.1977, eleven days after the injection, shows a downward displacement of 12 cm of the tracer in response to precipitation of 18.4 cm during the 11 day interval (Table 2). The tracer peak for the case III on 9.9.1977 is found to be at 89 cm, i.e. a net downward displacement of 14 cm from the depth of injection in response to the total precipitation of 25.6 cm during the interval between injection and sampling. For the cases IV and V, obtained on 10.12.1977 and 12.4.1978 respectively, there was negligible precipitation input (0.9 cm) after the III sampling. The tracer peak for these cases show upward displacement of 10 cm and 20 cm respectively in response to progressive evapotranspiration loss; the net (upward) moisture transfer between the depth of injection and tracer activity peak, using equation (1), for the cases IV and V are found to be -2.0 and -3.7 cm respectively.

Case VI, corresponding to sampling on 25.10.1978, indicates the tracer peak at 96 cm depth, a displacement of 41 cm, from the previous position (on 12.4.1978), in response to 65.3 cm of rainfall during the interval 12.4.1978 to 25.10.1978.

For the case VII, obtained on 13.6.1979, there is no shift in the position of the C.G. of the tracer profile which remains at the same position as for Case VI. However, there is a considerable depletion of soil moisture for the

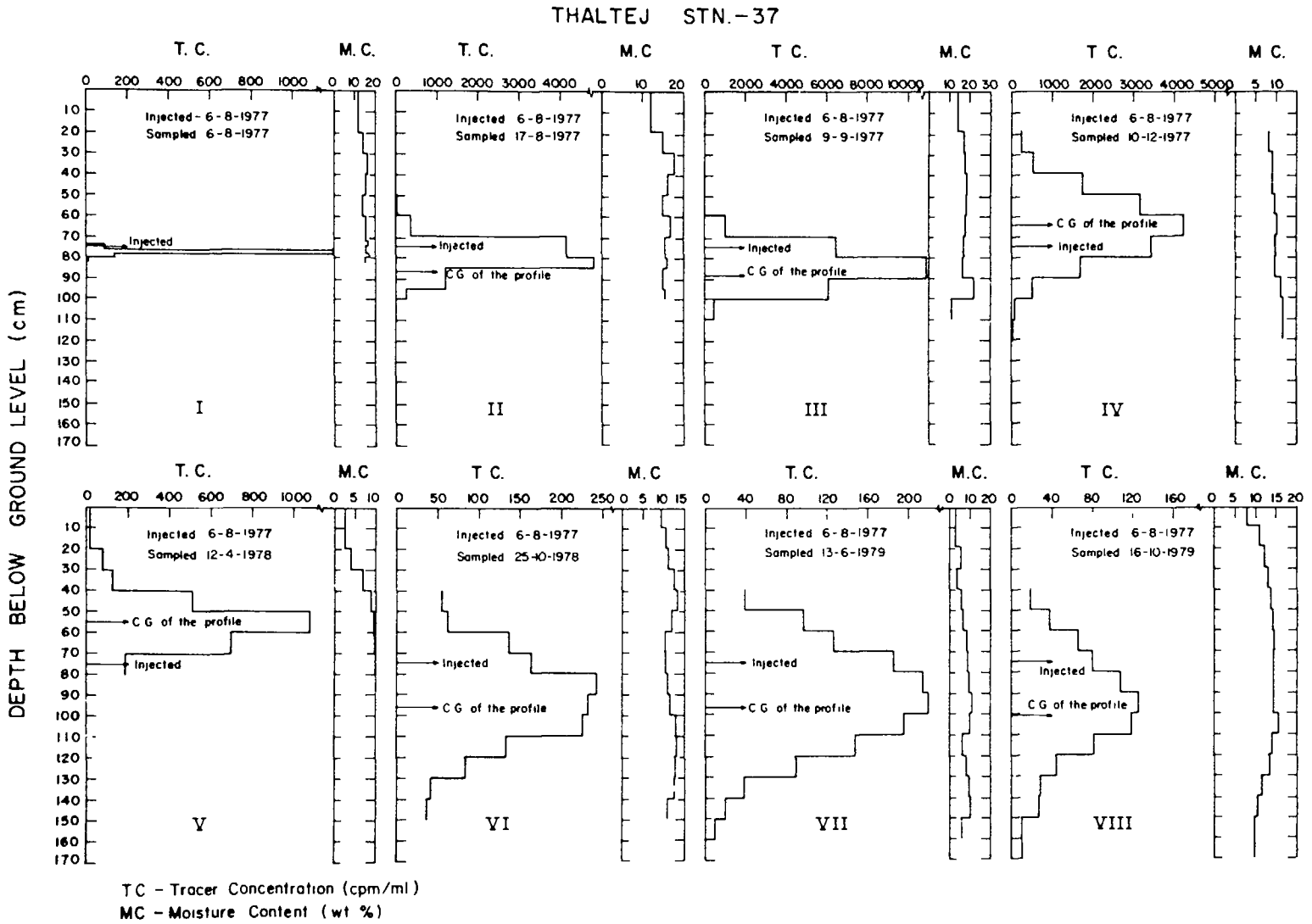


Fig. 10. Tracer activity and the moisture content profiles obtained by successive sampling (I to VIII) of the 8 injection points at Thaltej (Station Code 37), near Ahmedabad during the period 1977-1979 (Bhandari et al, 1982).

top 60 cm layer in response to evapotranspiration. For the case VIII on 16.10.1979 there is a further downward displacement of 5 cm of the tracer in response to 53.5 cm of rainfall after the last sampling. A closer look at the moisture profiles for the two cases VII and VIII shows that there is a considerable build up of the soil moisture at the depths sampled and it appears that the displacement of the tracer occurs only after the soil moisture exceeds the field capacity. The net groundwater recharge for the two year period between case I and case VIII is 8.9% of the total rainfall.

The above examples clearly illustrate that the soil moisture movement occurs in pulses after an infiltrating sheet of water after a rainfall event satisfies the soil moisture deficit. Based on the above understanding of the soil water movement, we have developed a simplified evapotranspiration-runoff model to estimate the fraction of annual precipitation that would be available for groundwater recharge after accounting for the runoff and evapotranspiration processes.

Several methods for estimating evapotranspiration such as Penman's, the Thorntwait's and others are available (see e.g. Grant, 1975). Often, they cannot be used for want of necessary soil and meteorological data. Even when the required data are available, evapotranspiration estimates using different formulae differ by as much as 50 to 100% (Fig. 2, a and b). It was therefore felt that it is necessary to develop simple evapotranspiration models and calibrate these with measurable quantities such as pan evaporation data or groundwater recharge estimated using soil water tracing studies. One thing, however, is clear that temperature, relative humidity and the availability of soil moisture, have a first order effect on actual evapotranspiration.

It was observed that there exists an approximate similarity of distribution of average monthly evapotranspiration, E (t), and saturation deficit, V(t), in the atmospheric moisture at two lysimeter stations, Sindorf and Libergerhof in West Germany (Esser, 1980). We can therefore assume (Thoma et al, 1979) that

$$E(t) \propto V(t) \text{ or } E(t) = K.V(t) \qquad \ldots\ (2)$$

with

$$V = P_s(T).(1-h) \qquad \ldots\ (3)$$

where $P_s(T)$ is the saturation vapour pressure of atmospheric moisture at average temperature (T) of the appropriate month, and h is the average

relative humidity (fractional) of the appropriate month. The proportionality constant, K. called evapotranspiration constant (mm. month$^{-1}$. torr$^{-1}$) is determined by the condition that long term integration of equation (2) is equal to long term total potential evapotranspiration. Actual evapotranspiration equals potential evapotranspiration if precipitation in a given month exceeds sum of potential evapotranspiration and soil moisture deficit of previous month, if any.

Under European conditions, where precipitation (either rain or snowfall) occurs almost round the year and temperatures are low, the actual evapotranspiration can approximately be taken the same as potential evapotranspiration given by equation (2). However, under Indian conditions there is a large discrepancy in the values of actual and potential evapotranspiration (except for the 2-3 months of rainy season), the actual evapotranspiration being much less than potential evaporation as there is simply no water available for evaporation. Therefore, if the precipitation is not sufficient to satisfy the soil moisture deficit or there is continued aridity, actual evapotranspiration is estimated by an exponential relation between aridity and soil moisture deficit such as Thorntwaite graph (Fig. 11, taken from Szalay, 1972). In using the Thorntwaite graph, the difference (P(t)-E(t)) is computed for all the months. It is followed by the computation of summation of the successive negative values. From the successive negative totals $\Sigma(P(t)-E(t))$, the value of change in the moisture capacity (water holding capacity) of the soil is computed for an assumed total water holding

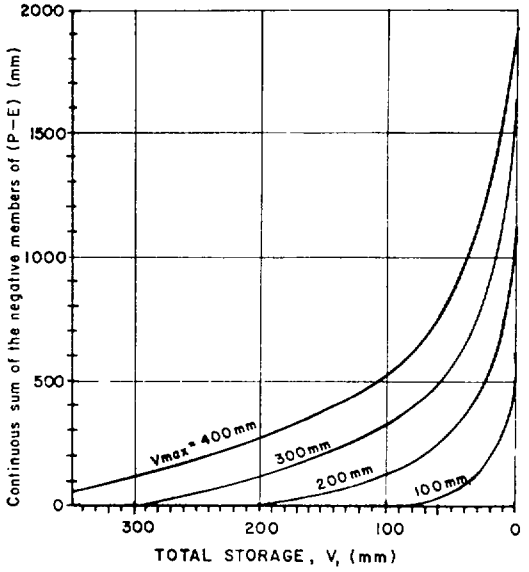


Fig. 11. Thorntwaite graph for estimating the effect of aridity on soil moisture depletion (Szalay, 1972).

capacity of the soil (100 to 500 mm; average 300 mm). Actual evapotranspiration for the month with aridity is then given by the change in soil moisture capacity. Further, if the precipitation excess after fulfilling the requirement of soil moisture storage and potential evapotranspiration during the month is higher than 50 mm (this number can be estimated from rainfall-funoff relation for a given catchment area and depends essentially on the slope of the terrain and is smaller for sharply undulating terrain), the excess is lost as runoff. Precipitation excess up to 50 mm for any month results in groundwater recharge according to the mechanism discussed subsequently.

Unfortunately because of the non-availability of temperature and relative humidity data for the project area, for the period under study, we have not been able to apply this model for simulation of the present results. However, the groundwater recharge estimated at two stations, Ahmedabad and Idar (23.9°N, 73.0°E) using the above model are shown in Table 3. These compare reasonably well with the data of tritium tagging studies in the Sabarmati basin (Gupta and Sharma, 1984). Datta et al (1979, b; 1980, b),

Table 3 : Estimates of groundwater recharge using evapotranspiration-runoff model and tritium tagging method at Ahmedabad and Idar, in Gujarat

| Year | Precipitation (mm) | Recharge based on soil moisture storage capacity 300 mm (mm) | 300 mm % Rainfall | 200 mm (mm) | 200 mm % Rainfall | Recharge based on tritium tagging experiment % rainfall |
|---|---|---|---|---|---|---|
| Station : | Ahmedabad | | | | | |
| 1976 | 1026 | 90.1 | 8.8 | 110.3 | 10.8 | |
| 1977 | 1252 | 100.3 | 8.0 | 122.8 | 9.8 | |
| 1978 | 700 | 69.4 | 9.9 | 95.8 | 13.7 | Average of 1977-79 |
| 1979 | 600 | 63.6 | 10.6 | 79.3 | 13.7 | |
| Mean | 894 | 80.9 | 9.0 | 102.1 | 11.4 | 8.9 |
| Station : | Idar | | | | | |
| 1971 | 552 | 75 | 13.6 | 103 | 18.7 | |
| 1972 | 349 | 13 | 4.0 | 65 | 18.6 | |
| 1973 | 1377 | 155 | 11.3 | 163 | 11.8 | |
| 1974 | 321 | 9 | 2.8 | 57 | 17.8 | |
| 1975 | 1252 | 145 | 11.6 | 152 | 12.1 | |
| 1976 | 1098 | 133 | 12.1 | 169 | 15.4 | |
| 1977 | 1196 | 195 | 11.3 | 173 | 14.5 | |
| 1978 | 855 | 111 | 13.0 | 144 | 16.8 | |
| 1979 | 510 | 64 | 12.5 | 111 | 21.8 | |
| 1980 | 785 | 102 | 13.0 | 144 | 16.3 | Average of 1978-79 |
| 1981 | 739 | 93 | 12.6 | 120 | 16.2 | |
| Mean | 821 | 94 | 11.5 | 126 | 15.3 | 11.9 |

Thoma et al (1979) and Gupta (1983) have described a conceptual model involving a pulsed movement through a series of hypothetical boxes (mixing cells) sub-dividing the soil column for describing the movement of tracer through the unsaturated zone.

Briefly, in the model the soil is assumed to be made up of a series of inter-connected expandable boxes with its moisture content at field capacity. The average field capacity of the entire soil column is assumed to be equal to the observed average moisture content of the soil profile. A fraction of monthly precipitation (total precipitation less estimated evapotranspiration and runoff) with its tracer content is then allowed to pass through the interconnected series of boxes in small pulses of equal size. It can be easily shown that the process of mixing of an advancing recharge pulse in successive boxes of equal size, H, mathematically simulates the dispersion process according to the relation $D = H^2F/t$ where H is the size of each box, F, the fraction representing the size of the recharge pulse in terms of the box size and t the time step of iteration, i.e. the interval at which successive recharge pulses are added to the system. A recharge pulse during transit through the boxes undergoes a change in its tracer concentration by mixing with the fluid in each box and leaving the trailing box at its assumed field capacity. The size of the advancing recharge pulse may be reduced or it may completely exhaust itself before reaching the water table depending on the moisture content of the soil column at the end of the previous evapotranspiration cycle.

The above two models in combination represent our basic understanding of the evapotranspiration, runoff and soil moisture movement processes in the arid regions of Thar Desert. Our studies also indicate that even in a very low rainfall region, the groundwater recharge can be quite substantial, amounting to about 6-14%.

ACKNOWLEDGEMENTS

We thank Shri T.N. Mehra, Chief Engineer, and Shri D.C. Sharma, Superintending Hydrogeologist, Groundwater Department, Rajasthan, for discussions and help during field work in Rajasthan. We also thank Shri K.A. Shankaranarayanan, Director and Shri P.C. Chatterji, Geologist, of CAZRI for kind permission to conduct experiments in their campus and for logistic support.

REFERENCES


BHANDARI, N., GUPTA, S.K., SHARMA, P., PREM SAGAR, AYACHIT, V. and DESAI, B.I. (1982). Hydrogeological investigations in Sabarmati basin and coastal Saurashtra using radioisotopic methods. Report HYD-82-01, Physical Research Laboratory, Ahmedabad, India.

DATTA, P.S., DESAI, B.I. and GUPTA, S.K. (1979, a). Comparative study of groundwater recharge rates in parts of Indo-Gangetic and Sabarmati alluvial plains. Mausam 30(1), p. 29-33.

DATTA, P.S., GUPTA, S.K. and SHARMA, S.C. (1979, b). Simulation of water movement through vadose zone, in Current Trends in Arid Zone Hydrology (ed. Gupta, S.K. and Sharma, P.), Today & Tomorrow's Printers & Publishers, New Delhi, p. 93-101.

DATTA, P.S., DESAI, B.I. and GUPTA, S.K. (1980, a). Hydrogeological investigations in Sabarmati basin. I. Groundwater recharge estimation using tritium tagging method. Proc. Indian Nat. Sci. Acad., Part A, 46(1), p. 84-98).

DATTA, P.S., GUPTA, S.K. and SHARMA, S.C. (1980, b). A conceptual model of water transport through unsaturated soil zone. Mausam, 31(1), p. 9-18.

ESSER, N. (1980). Bonbentritium-Zeitverhalten Seit 1963 in Abfluss Mittleeuropascher Flusse and Kleiner Hydrologischer Systeme. Dipl. Thesis, Inst. fur Umweltphysik, Univ. Heidelberg.

GRANT, D.R. (1975). Comparison of evaporation measurements using different methods. Quat. J. Roy. Met. Soc., 101, p. 543.

GUPTA, S.K. (1983). An isotopic investigations of a near surface groundwater system. Hydrological Sciences Journal, 28(2), p. 261-272.

GUPTA, S.K. (1984). A radiotracer study of soil moisture movement during groundwater recharge', Hari Om Ashram Prerit Vikram Sarabhai Award Lectures, Physical Research Laboratory, Ahmedabad, India, p. 57-76.

GUPTA, S.K. and PRAKASH, I. (1975). Environmental analysis of the Thar Desert, English Book Depot, India.

GUPTA, S.K. and SHARMA, P. (1984). Soil moisture transport through the unsaturated zone: tritium tagging studies, in Sabarmati Basin, Western India. Hydrological Sciences Journal, 29(2), p. 177-189.

SZALAY, M. (1972). Hydrometeorology and water balance, lecture notes, International Postgraduate Course, Research Institute for Water Resources Development (VITUKI), Budapest, Hungary.

THOMA, G., ESSER, N., SONNTAG, C., WEISS, W., RUDOLPH, J. and LEVENE, P. (1979). New technique of in situ soil moisture sampling for environmental isotope analysis: applied at Pilat sand dune near Bordeaux, in Isotope Hydrology, 1978, Vol. II, IAEA, Vienna, p. 753-768.

United Nations Development Programme (UNDP, 1976). Groundwater Surveys in Rajasthan and Gujarat, India. Technical Report, United Nations.

# DEUTERIUM AND CHLORIDE CONTENT OF SOIL MOISTURE, GROUND AND SURFACE WATERS FROM MARVANKA BASIN, ANANTAPUR, INDIA

B. KUMAR, D.J. PATIL, R. MATHUR
National Geophysical Research Institute,
Hyderabad, India

**Abstract**

The report contains the results of isotopic and chloride behaviour studies of soil moisture, ground and surface waters from a semi-arid basin located in a hard rock area of Southern India. About 300 soil cores in 10 cm sections, were collected during two field seasons from different soil types (red loamy sandy, black loamy sandy, black clayey, black soil with calcareous material and alluvial sandy soil) occuring in the Marvanka Basin, Andhra Pradesh, and its nearby areas in the Anantapur district.

The moisture in the wet weight percentage ($M_w$ %) of all the soil cores was determined and the data was used to compute the equivalent depth values for different soil types. The values were found to vary narrowly (7.5 cm - 10 cm) for red soils and significantly for black soils (4.1 cm - 35 cm). The average value of equivalent depth of 9 cm for red soils suggest that about 9 cm of water per 100 cm of soil column is available which may contribute to the groundwater.

Deuterium and chloride analyses of about 90 soil water samples and few surface and groundwaters were carried out. The data for soil moisture show large scatter. Isotopically, each soil core was found to behave independently favouring the piston flow concept of recharge to the groundwater. The weighted mean $\delta D$ values for soil water are comparable to groundwater $\delta D$ values in case of red and alluvial sandy soils and are different for black soils.

## I INTRODUCTION

Study of soil moisture movement and its behaviour in different types of soils is important for evaluating the water balance of unsaturated zone and recharge to the groundwater. The soil moisture shows large variations in arid and semi-arid regions and study of its behaviour using environmental tracers ($^2H$, $^{18}O$, $Cl^-$), has been attempted by several workers [1-3]. The present work

is a similar attempt in Marvanka Basin, a semi-arid basin located in a hard rock area in Anantapur district of Andhra Pradesh (A.P.), India. The basin lies between Lat. $14^{o}18'$ - $14^{o}55'$N and Long. $77^{o}22'$ to $77^{o}53'$E and covers an area of about 2044 sq. km. Anantapur is the driest district of A.P. and the area has been subjected to recurrent drought conditions. The surface water potential in the basin is very much limited and the biota of the district is severely dependent on groundwater resources. Therefore, the information on water balance of unsaturated zone and recharge to the groundwater is very vital for this basin.

## II HYDROLOGY, DRAINAGE, SOILS AND CLIMATE OF THE MARVANKA BASIN

Fig. 1 shows the geological and structural map of the basin [4]. The main rock formation in the basin is the Precambrian gneissic complex comprising, gneisses (migmatites), pink and grey granite, granitic gneisses and schists, quartz veins and basic dykes, etc. A small patch in the NE corner of the basin is covered by Vempalli dolomites. The basin area appears to have been intensively fractured at places and groundwater occurs in unconfined, semi confined and confined systems [4, 5].

Marvanka is a tributary of the Pennar river and it has three ephemeral sub-tributaries namely, Tadakaleru, Pandemeru and Kutaleru. The basin has several irrigation tanks of which two major ones are the Anantasagar (tank located near Anantapur town) and the Singanamala tank. Both the major tanks are interconnected. The Pandemeru drains to the Anantasagar tank and the Tadakaleru into the Singanamala tank, and the surplus water of both the major tanks drains into the Marvanka stream.

The soils of the area are mostly of residual origin derived mainly from granite and its associated rocks. They are represented by three principal soil types; red loamy sandy soil, black loamy sandy soil and black clayey soil, covering about 82%, 12% and 6% area of the basin respectively. The soil thickness varies from a few centimeters to a few meters and the maximum thickness of weathered rock is found to be about 30 m [6].

The basin forms a part of semi-arid tract of Southern India and receives meagre rainfall from both the south-west and north-east monsoon. The average rainfall in the basin is about 550 mm in which about 60-65% is contributed by

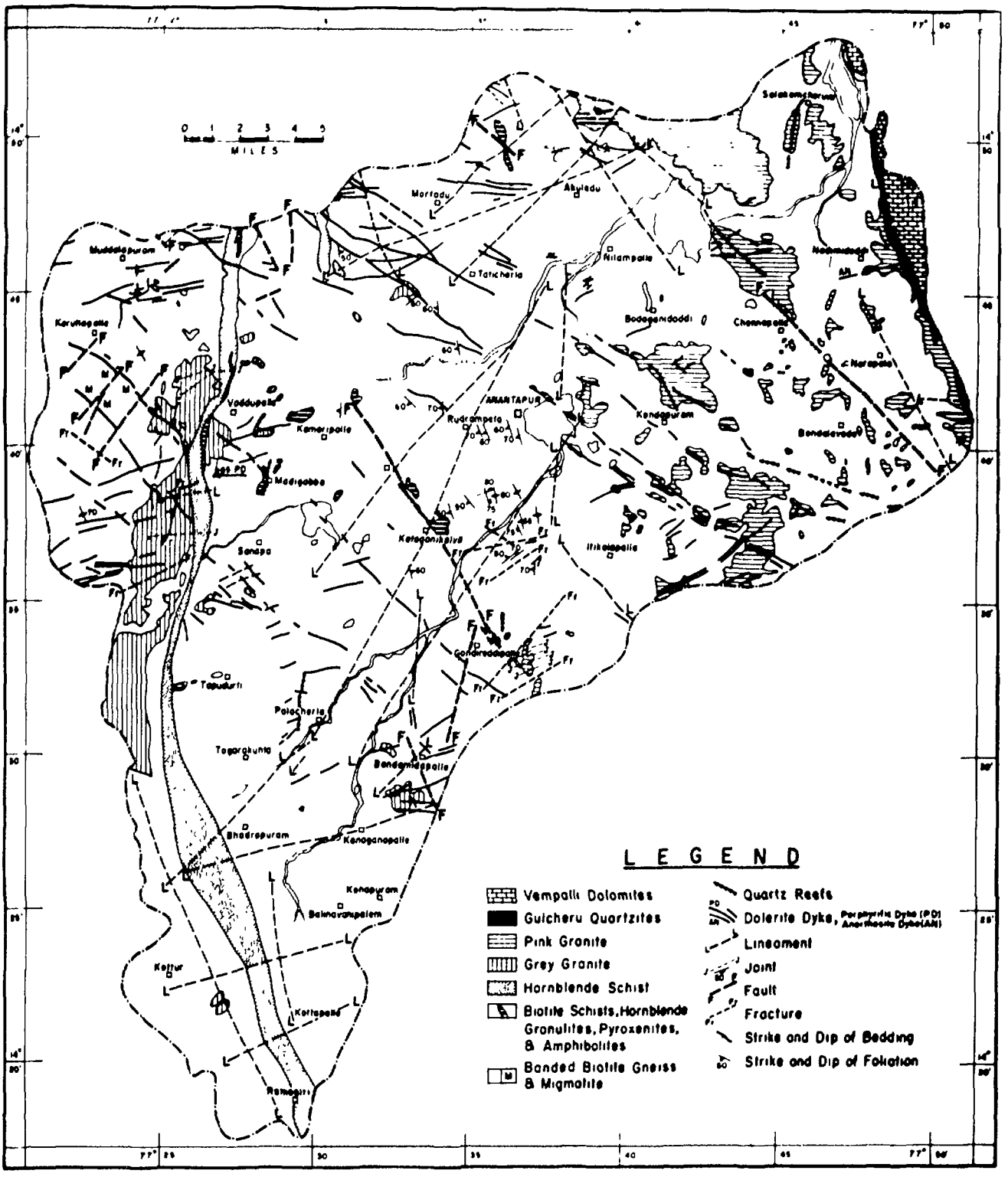


Fig. 1. Geological and structural map of Marvanka basin, Anantapur Dist. (After Radhakrishna et al., 1984).

*SW monsoon and remaining by NE monsoon.* The climate in general is hot and dry. The mean daily maximum and minimum temperature during the winter season are 28°C and 16°C.

## III SAMPLING

Soil core samples in 10 cm sections were collected in two phases first during August 1982 (second and third weeks of August) and next during August 1983 (first week of August). The heavy wall mild steel pipes of various lengths with a sharp edge at one end and steel cap at the other end were hammered manually for collecting the soil samples from different depths (Fig. 2). Pipes having inner diameter (i.d.) of 4 cm were used for obtaining soil cores up to 1.7 m and pipes having i.d. of 3.4 cm were used for deeper samples up to 3.5 m. Further deeper samples were collected by making pits of size 2 m dia x 3 m deep and by conducting the field operation from the bottom of the pit.

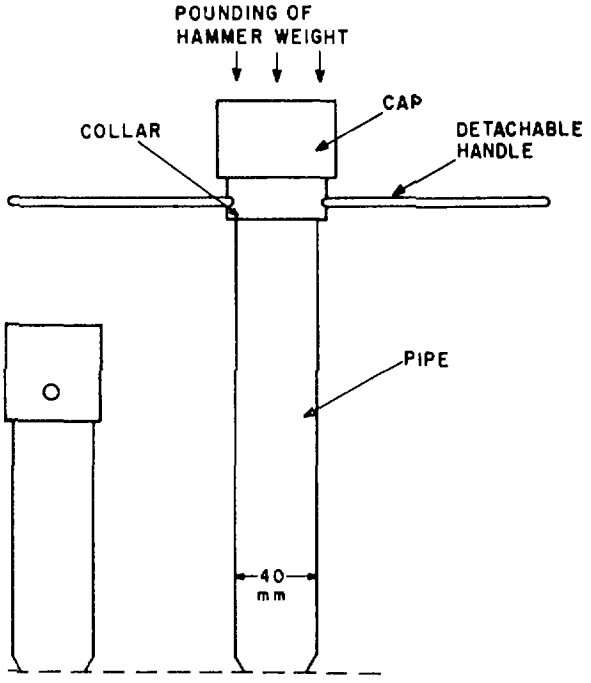


Fig 2 Cross-sectional view of soil coring pipe

In total, samples from 19 profiles (17 profiles in the basin and 2 profiles outside the basin) were collected during 1982 and from 8 profiles (6 profiles in the basin and 2 profiles outside the basin) during 1983. The second phase of sampling was the repeat sampling. Figure 3 gives the soil profile location map of the Marvanka Basin. The selection of profile was made

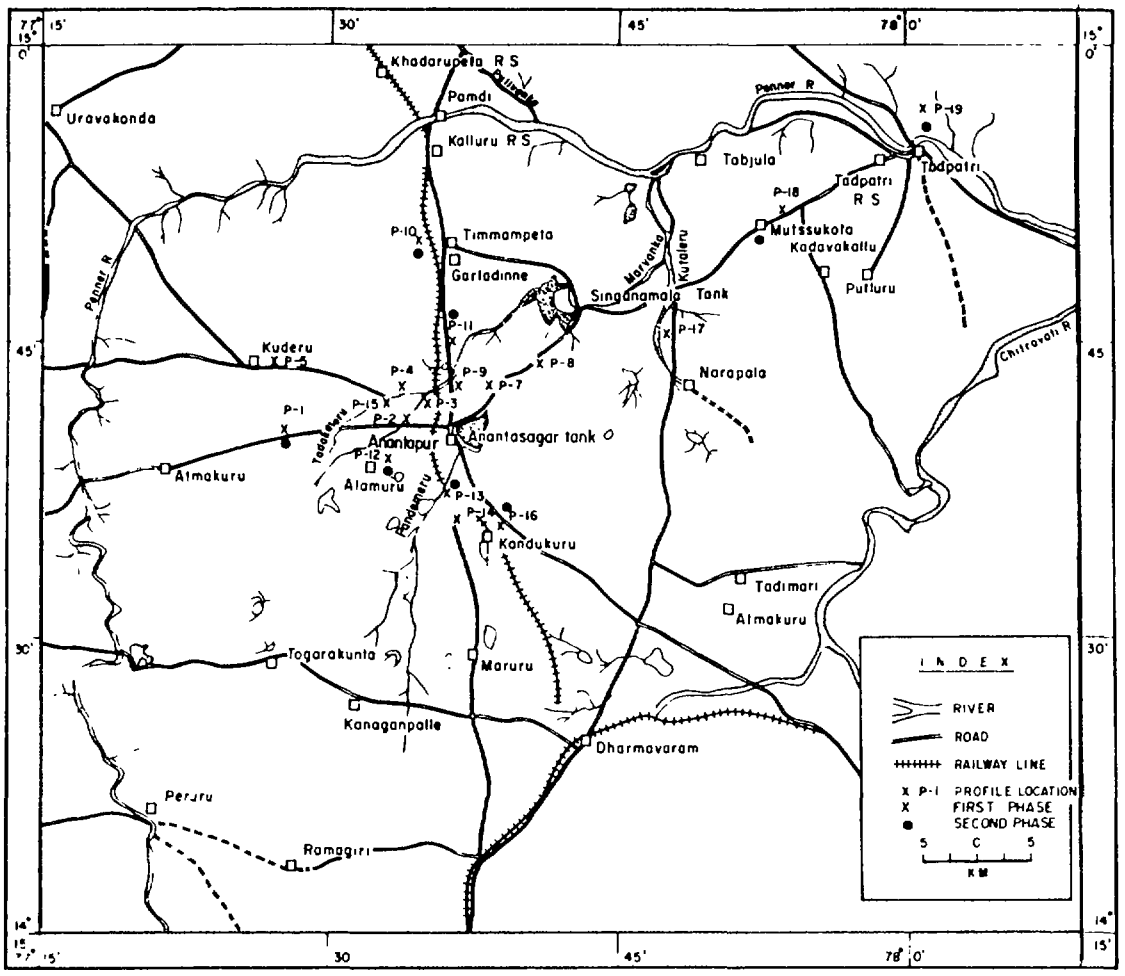


Fig 3 Soil profile location map of Marvanka basin, Anantapur.

mainly on soil types and accessibility. Two profiles outside the basin are from Mutssukota (black soil with calcareous material) and from Tadpatri (alluvial sandy soil).

The groundwater samples from borewells and dug wells representing some soil profiles along with two samples of surface waters were also collected.

## IV EXPERIMENTAL TECHNIQUES

### Soil moisture distillation

Two methods namely; azeotropic distillation and vacuum distillation were attempted for distilling soil samples. The vacuum distillation was preferred over azeotropic distillation as the experiments with azeotropic distillation did not give the required reproducibility of $\delta D$ ($^2H$) measurements.

A multibatch vacuum distillation apparatus was fabricated for the distillation of soil samples (Fig. 4). The vacuum distillation was carried

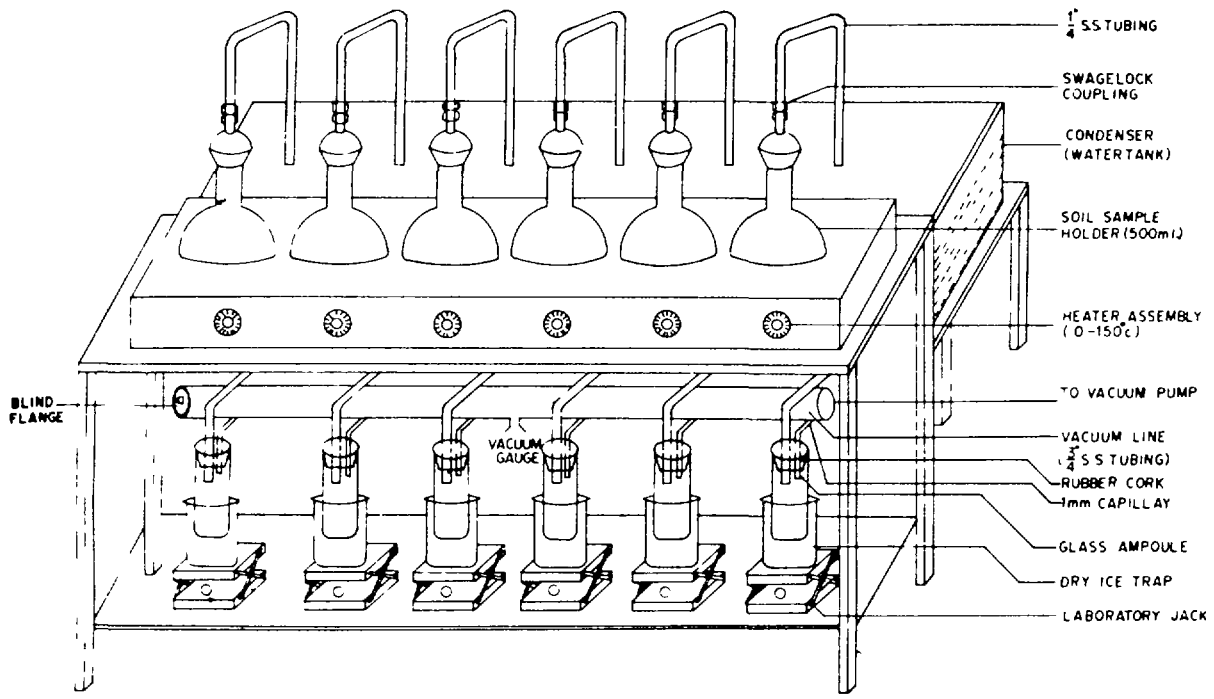


FIG 4 MULTIBATCH VACUUM DISTILATION APPARATUS FOR DISTILLING SOIL SAMPLES.

out for 2-3 hours in dynamic mode at 120°C for red loamy sandy, black loamy sandy, alluvial sandy soil and at 150°C for black clayey and black soil with calcareous material. The soil water was collected in a glass ampoule cooled at dry ice and acetone temperature. The experiments with repeated distillation on the same soil showed that $\delta D$ reproducibility was within ± 2.0‰ except in the case of black clayey soil with moisture values of 2% or less, where irratic $\delta D$ values were observed.

Soil moisture content ($M_w$ %)

Soil moisture content in the lab was determined by three different methods: (i) using an infra red torsion balance, (ii) loss in weight of wet soil, and (iii) the amount of water collected while distilling the soil moisture. All three values were found to be in good agreement within the experimental errors (± 0.5‰).

Isotopic and chloride analyses

Deuterium analyses on water samples (soil moisture distillate, surface and groundwaters) were carried out using VG Micromass 602-C mass spectrometer and isotopic data are given in ‰ versus V-SMOW (Vienna-Standard Mean Ocean Water). Some samples were analysed in duplicate and reproducibility was found to be within ± 1.5‰.

The chloride analyses was carried out using the silver nitrate titration method with potassium chromate as indicator. The 50 gm representative sample of soil was mixed with 50 ml of deionised distilled water. The soil water mixture was stirred with a glass rod and left to soak for 30 minutes, restirred and left to soak for a further 30 minutes. After this time the liquid was decanted into clean 50 ml tubes which were then centrifuged for 10-20 minutes at 2500 RPM to get clear aqueous solution. The 10 ml portion of clear aqueous solution was removed and used for titration. The precision for chloride measurement was within ± 1 ppm.

## V RESULTS AND DISCUSSION

### Soil moisture data

The soil moisture data of different soil profiles was used to calculate the Mw(wt.) % i.e. mean value of moisture content and equivalent depth for 0-100 cm and 100-200 cm of soil column for the samples collected during the first and second phase of sampling. The term equivalent depth denotes the amount of water contained in 1 m deep soil profile and was computed based on the formula given by Hillel [7].

$$\text{Equivalent depth} = \frac{W \times \rho_b \times L}{\rho_w}$$

where, $W$ = means mass wetness of soil core
$\rho_p$ = bulk density in $gm/cm^3$
$\rho_w$ = density of water
$L$ = length of the soil column in cm

The TABLE I gives values of mean of $M_w$(wt.) and equivalent depths for 0-100 cm and 100-200 cms of soil columns for 16 soil profiles collected during the first phase and for 8 soil profiles collected during the second phase. The red soils, which cover about 82% area of the basin, show very interesting behaviour. The equivalent depth for all the profiles in red soil except the profile No. 14 (which was near to an irrigated field) vary narrowly between 8.6 to 10.2 cm for the soil samples collected during the first phase and between 7.5 to 10.0 cm for the samples collected during the second phase. The mean of equivalent depths (excluding Profile Number 14) for 0-100 cm and for 100-200 cm sections are 9.2 cm and 9.9 cm for Phase I and 8.7 cm and 7.7 cm

TABLE I. THE MEAN VALUE OF MOISTURE CONTENT AND EQUIVALENT DEPTH VALUES FOR 0-100 AND 100-200 CM OF SOIL COLUMNS, FOR THE SAMPLES COLLECTED DURING IST AND IIND PHASE.

| Profile No. | Location | Depth of soil column cm | Ist phase | | IInd phase | |
|---|---|---|---|---|---|---|
| | | | $\bar{M}_u$(ut.) % | Eq. depth cm | $\bar{M}_u$(ut.) % | Eq. depth cm |
| Red loamy sandy soil: | | | | | | |
| 7 | Bukkarayasamudram | 0-100 | 5.0 | 8.8 | - | - |
| | | 100-200 | - | - | - | - |
| 8 | Near Reddy Palli village | 0-100 | 5.9 | 9.6 | - | - |
| | | 100-200 | 5.3 | 10.3 | - | - |
| 10 | Garaladinne | 0-100 | 6.2 | 10.0 | 6.2 | 7.5 |
| | | 100-200 | 4.4 | 10.2 | - | 7.7 |
| 14 | On Kendukuru+ Road | 0-100 | 10.0 | 18.6 | - | - |
| | | 100-200 | 5.0 | 9.1 | - | - |
| 16 | Itkalapalli | 0-100 | 5.4 | 8.9 | 7.8 | 10.0 |
| | | 100-200 | - | - | - | - |
| 17 | Near Narpala | 0-100 | 5.8 | 8.6 | - | - |
| | | 100-200 | - | - | - | - |
| +near a irrigated field | | | | | | |
| Black loamy sandy soil: | | | | | | |
| 1 | Vaddipalli | 0-100 | 7.9 | 14.0 | 5.7 | 8.3 |
| | | 100-200 | 8.6 | 18.0 | 3.4 | 6.5 |
| 4 | After crossing Tadakaleru | 0-100 | 12.1 | 15.8 | - | - |
| | | 100-200 | 15.8 | 33.0 | - | - |
| 5 | Near Kuderu | 0-100 | 8.4 | 15.1 | - | - |
| | | 100-200 | 2.7 | 5.4 | - | - |
| 9 | Anantapur Hyderabad Road | 0-100 | 10.0 | 16.3 | - | - |
| | | 100-200 | 6.7 | 13.2 | - | - |
| Black loamy sandy soil: | | | | | | |
| 12 | Alamuru | 0-100 | 9.4 | 16.8 | 6.6 | 6.4 |
| | | 100-200 | 14.3 | 24.9 | 9.0 | 16.7 |
| 13 | Near Raptadu | 0-100 | 14.9 | 25.0 | 11.6 | 24.3 |
| | | 100-200 | 16.8 | 35.3 | 13.2 | 25.0 |
| Black clayey soil: | | | | | | |
| 11 | Anantapur Hyderabad Road | 0-100 | 14.7 | 22.7 | 15.2 | 21.0 |
| | | 100-200 | 5.3 | 9.4 | 4.4 | 7.4 |
| 15 | Rachnapalli | 0-100 | 12.0 | 24.0 | - | - |
| | | 100-200 | 13.5 | 27.5 | - | - |
| Black soil with calcareous material: | | | | | | |
| 18 | Mutsukota | 0-100 | 8.0 | 11.7 | 6.0 | 4.1 |
| | | 100-200 | 8.0 | 14.7 | 4.0 | 5.5 |
| Alluvial sandy soil: | | | | | | |
| 19 | Tadpatri | 0-100 | 4.1 | 6.9 | 1.5 | 1.5 |
| | | 100-200 | 6.7 | 8.8 | 1.0 | 1.8 |

(one value only) for Phase II samples respectively. The overall mean of equivalent depths for red soils is 9.2 cm, and if the piston flow model proposed by [3, 8, 9] is valid, we can say that about 9 cm of water per 100 cm of soil column is available which may contribute to the groundwater in case of red soils. The model assumes that the percolating soil moisture moves downward in discrete layers and any addition of a fresh layer of moisture at the surface, would push down an equal amount of water immediately below and so on, till the last such layer in the unsaturated zone will be added to the saturated regime or the water table.

Our above mentioned estimate of annual recharge of about 9 cm for red soils (which cover about 82% area of the basin) lies in between the estimates of 11 cm by Raje et al [6] for the Anantapur taluq and of 4 cm by Athavale et al [5] for the Marvanka basin. The Anantapur taluq covers an area of about 2400 sq. km. and the Marvanka basin lies in the Anantapur taluq. The recharge estimate of Raju and coworkers was based on slope classification, land use particulars, and other hydrogeological parameters and of Ahtavale and coworkers on injected tritium method.

The equivalent depth values for black loamy sandy soil and black clayey soil show large variations. This is due to the fact that in black soils depending upon the clay percentage in the soil column, the permeability decreases with the increase in clay content.

As shown above, the equivalent depth values for red soils vary narrowly between the first and second phase samples. This suggests that the water balance of unsaturated zone in red soils have not changed significantly from August 1982 to August 1983. The periodic measurement of equivalent depth in red soils, therefore, may provide a simple means of establishing the periodic changes in water balance of unsaturated zone.

Deuterium and chloride data of soil moisture profiles

The $\delta D$ and moisture content data (Mw) of some selected soil profiles (one profile in each soil type i.e. red loamy sandy soil, black loamy sandy soil, black soil with calcareous material and alluvial sandy soil) are given in TABLE II. The $\delta D_1$ and $Mw_1$ corresponds to first phase sampling and $\delta D_2$ and $Mw_2$ corresponds to second phase sampling. The isotopic and moisture content data vs. depths are plotted in figures 5-8. The $\delta D$ values in

TABLE II. δD AND MOISTURE CONTENT (Mw) VS. DEPTH VALUES OF DIFFERENT SOIL PROFILES FROM MARVANKA BASIN ($\delta D_1$, $Mw_1$ - IST PHASE; $\delta D_2$, $Mw_2$ - IIND PHASE).

| Depth in cms | P.No. 10 Red loamy sandy soil | | | | P.No. 12 Black loamy sandy soil | | | |
|---|---|---|---|---|---|---|---|---|
| | $\delta D_1$ ‰ | $Mw_1$ % | $\delta D_2$ ‰ | $Mw_2$ % | $\delta D_1$ ‰ | $Mw_1$ % | $\delta D_2$ ‰ | $Mw_2$ % |
| 20-30 | -20 | 4.7 | - 8 | 5.8 | -19 | 3.1 | 18 | 1.4 |
| 40-50 | -25 | 9.6 | -33 | 5.5 | -21 | 7.9 | 21 | 2.4 |
| 60-70 | -20 | 8.8 | 8 | 6.0 | -13 | 14.1 | 3 | 10.4 |
| 80-90 | 20 | 4.4 | 45 | 6.3 | -22 | 15.0 | -7 | 11.2 |
| 100-110 | -11 | 8.2 | - 6 | 5.9 | -24 | 5.6 | -6 | 11.6 |
| 120-130 | -29 | 5.5 | 12 | 3.3 | -12 | 12.9 | 8 | 8.1 |
| 140-150 | -23 | 2.6 | 5 | 2.8 | -31 | 17.7 | 16 | 8.7 |
| 160-170 | -13 | 3.5 | - | - | -17 | 18.7 | 9 | 7.5 |
| 180-190 | -14 | 6.5 | - | - | -29 | 14.0 | 10 | 5.6 |
| 200-210 | -27 | 2.8 | - | - | -11 | 19.0 | - | - |
| 220-230 | - | - | - | - | -22 | 12.9 | - | - |
| 240-250 | - | - | - | - | - 8 | 21.0 | - | - |
| 260-270 | - | - | - | - | - 7 | 5.6 | - | - |
| 280-290 | - | - | - | - | -16 | 13.3 | - | - |

| Depth in cms | P.No. 18 Black soil with calcareous material | | | | P.No. 19 Alluvial sandy soil | | | |
|---|---|---|---|---|---|---|---|---|
| | $\delta D_1$ ‰ | $Mw_1$ % | $\delta D_2$ ‰ | $Mw_2$ % | $\delta D_1$ ‰ | $Mw_1$ % | $\delta D_2$ ‰ | $Mw_2$ % |
| 20-30 | -12 | 6.9 | - | - | -12 | 3.7 | - | - |
| 40-50 | -18 | 5.8 | 7 | 10.0 | 12 | 4.6 | 25 | 2.1 |
| 60-70 | -13 | 9.3 | 28 | 3.0 | 18 | 4.7 | 23 | 1.4 |
| 80-90 | -10 | 7.6 | 7 | 2.4 | 17 | 4.0 | - | 0.9 |
| 100-110 | - 5 | 8.6 | 11 | 5.4 | 18 | 5.4 | 42 | 0.8 |
| 120-130 | 6 | 6.8 | 2 | 3.4 | 15 | 5.2 | 93 | 0.8 |
| 140-150 | -10 | 8.2 | -1 | 3.1 | -20 | 4.4 | 57 | 1.3 |
| 160-170 | -18 | 6.8 | 15 | 3.4 | 5 | 4.8 | 8 | 1.1 |
| 180-190 | -15 | 8.8 | 15 | 2.7 | 11 | 5.0 | 100 | 1.1 |
| 200-210 | -19 | 7.5 | 25 | 2.6 | -27 | 17.2 | 8 | 3.7 |
| 220-230 | -34 | 7.9 | - | - | -33 | 15.7 | -32 | 16.6 |
| 240-250 | -11 | 4.4 | - | - | -29 | 16.9 | - 9 | 16.4 |
| 260-270 | -34 | 4.7 | - | - | - | - | 13 | 9.2 |
| 280-290 | 3 | 5.9 | - | - | - | - | 5 | 13.7 |
| 300-310 | -16 | 7.8 | - | - | - | - | -10 | 12.0 |
| 320-330 | -17 | 5.5 | - | - | - | - | -36 | 10.2 |
| 340-350 | - | - | - | - | - | - | - 7 | 11.4 |

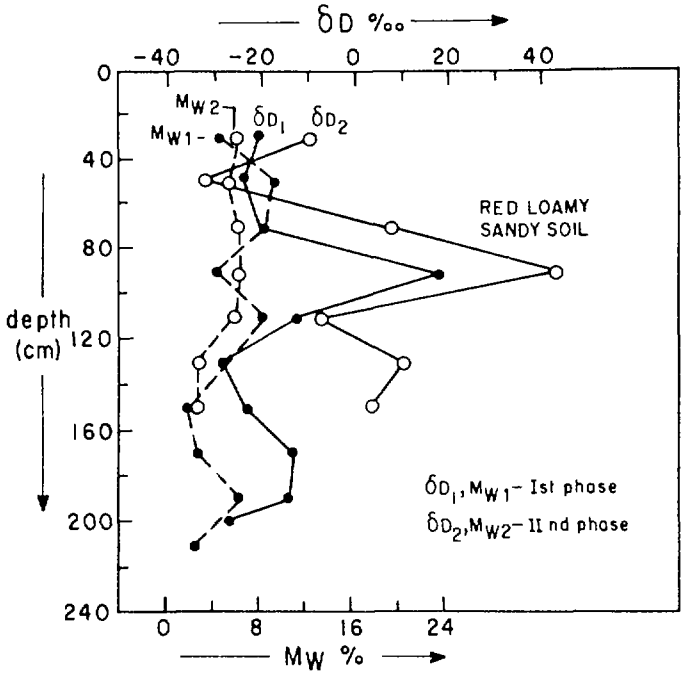


Fig 5

δD and moisture content vs. depth in a soil profile near Garlodinne (Profile No 10).

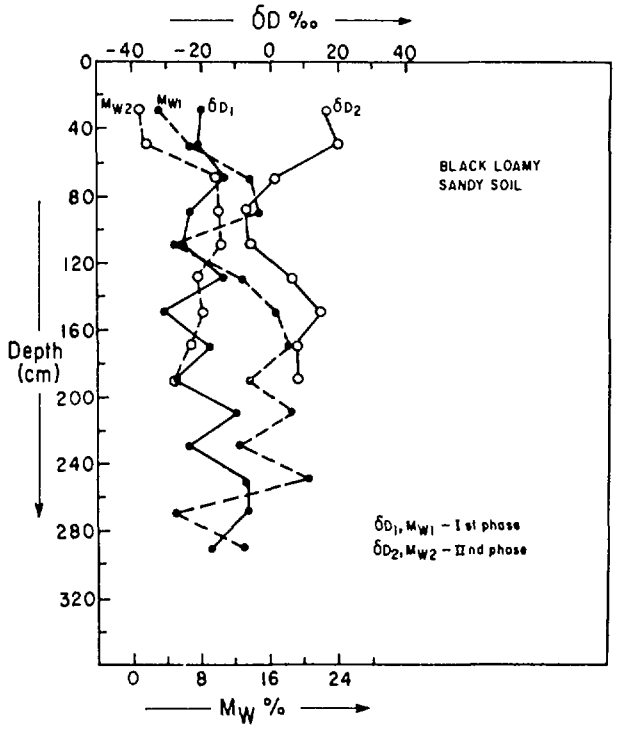


Fig 6

δD and moisture content vs depth in a soil profile near Atamuru (Profile No 12).

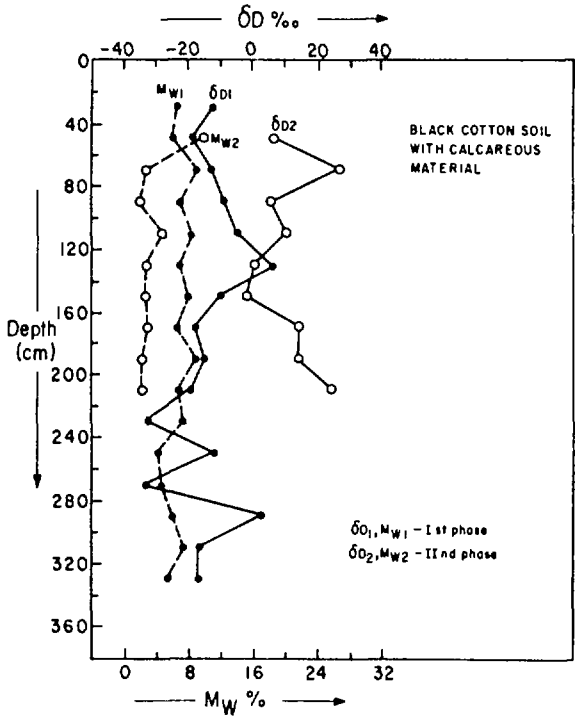


Fig 7

δD and moisture content vs depth in a soil profile near Mutssukota (Profile No 18).

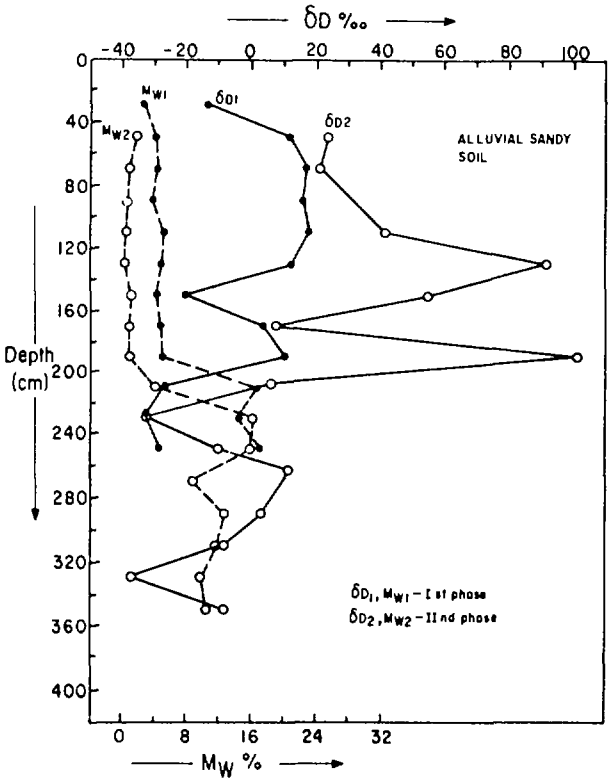


Fig 8

δD and moisture content vs depth in a soil profile near Tadpatri (Profile No 19).

general are enriched for the soil cores collected during the second phase. At the time of the first phase sampling the basin had received about 225 mm of rainfall and while at the time of the second phase sampling the rainfall received was only 170 mm. The enriched δD values for the IInd phase soil moisture samples suggest that the first few cm of rainfall resulting from onset of the monsoon in a semi arid basin does not seem to normally contribute to the groundwater. It is mainly lost due to evapotranspiration. The rainfall starts contributing to the groundwater only when a certain balance is established. Isotopically, each soil core seems to behave independantly supporting the piston flow model of recharge to the groundwater.

The Marvanka Basin as stated earlier lies in a semi-arid climate and is a hard rock area. The basin receives meagre rainfall from both the SW and NE monsoon. The isotopic data on soil moisture profiles suggest that the quantitative representation of water balance of unsaturated zone using stable isotopes may not be possible in such a case. However, the data provide a useful basis for qualitative interpretation.

The chloride data versus depth for different soil profiles is given in TABLE III. The chloride behaviour of soil moisture in case of each profile is different irrespective of soil type. The relatively low chloride value for soil moisture in the same soil type can be attributed to high recharge zones in the area.

In case of alluvial sandy soil the soil moisture has very low and consistent chloride content but on the other hand the δD values suggest significant loss of moisture due to evaporation. The loss of moisture should have normally resulted in high chloride values for soil moisture; but it is not the case. This may be due to the fact that the alluvial sandy soil has high permeability and chloride is flushed down with the new recharge input.

Deuterium and chloride data of ground and surface waters

The δD in ‰ versus V-SMOW and chloride in ppm for ground and surface waters are given in TABLE IV. The δD values vary from -24.4‰ to -2.5‰ for groundwaters. Surface water has positive δD values. A mass balance approach for calculating the weighted means gave interesting results. The following formula has been used for this purpose:

TABLE III. CHLORIDE CONTENT IN PPM VS. DEPTH VALUES OF DIFFERENT SOIL PROFILES FROM MARVANKA BASIN (SAMPLES COLLECTED DURING IIND PHASE).

| Depth in cms | Red loamy sandy soil | | Black clayey soil |
|---|---|---|---|
| | P.No. 10 | P.No. 16 | P.No. 11 |
| | Cl in ppm | | Cl in ppm |
| 10-20 | - | 9100 | 82 |
| 30-40 | - | 4936 | 38 |
| 50-60 | 280 | 4578 | 59 |
| 70-80 | 278 | 4794 | 52 |
| 90-100 | 278 | 2849 | 40 |
| 110-120 | 336 | 2030 | 68 |
| 130-140 | 373 | 603 | 31 |
| 150-160 | 476 | 69 | 123 |
| 170-180 | 476 | - | 142 |
| 190-200 | - | - | 158 |
| 210-220 | - | - | 158 |

| Depth in cms | Black loamy sandy soil | | | Black soil with calcareous material | Alluvial sandy soil |
|---|---|---|---|---|---|
| | P.No.1 | P.No. 12 | P.No.13 | P.No. 18 | P.No. 19 |
| | | Cl in ppm | | Cl in ppm | Cl in ppm |
| 10-20 | 5 | 3092 | 8155 | 51 | 5 |
| 30-40 | 5 | - | 999 | 19 | 5 |
| 50-60 | 5 | 2861 | 1039 | 41 | 5 |
| 70-80 | 5 | 3823 | 966 | 142 | 8 |
| 90-100 | 5 | 3911 | 754 | 142 | 5 |
| 110-120 | 5 | 2081 | 806 | 127 | 5 |
| 130-140 | 20 | 4858 | 456 | 96 | 8 |
| 150-160 | 5 | 4179 | 981 | 183 | 5 |
| 170-180 | 5 | 2732 | 201 | 280 | 8 |
| 190-200 | 5 | 8304 | 239 | 253 | 8 |
| 210-220 | 5 | 3035 | 264 | 400 | 5 |
| 230-240 | - | 812 | 668 | - | 31 |
| 250-260 | - | 387 | - | - | 5 |
| 270-280 | - | 957 | - | - | 5 |
| 290-300 | - | 992 | - | - | 5 |
| 310-320 | - | 195 | - | - | 5 |
| 330-340 | - | 117 | - | - | 5 |
| 350-360 | - | 124 | - | - | 5 |
| 370-380 | - | 159 | - | - | 5 |
| 390-400 | - | 88 | - | - | 34 |

TABLE IV. δD AND Cl VALUES OF GROUND AND SURFACE WATERS FROM MARVANKA BASIN.

| S. No. | Sample Location | Soil type | δD ‰ | Cl in ppm |
|---|---|---|---|---|
| 1. | Vaddipalli borewell water (P-1) | black loamy | -23 | 40 |
| 2. | Dugwell (P-4) | black loamy | -24 | - |
| 3. | Reddipally dug well (P-8) | red | - 3 | - |
| 4. | Garladinne dug well (P-10) | red | - 6 | 30 |
| 5. | Alamuru bore well (P-12) | black loamy | -23 | 40 |
| 6. | Raptadu soil profile water (P-13) | black loamy | - 7 | - |
| 7. | -do- | black loamy | - 3 | - |
| 8. | Borewell (P-14) | red | -12 | - |
| 9. | Itkalapalli dug cum borewell (P-16) | red | -20 | 35 |
| 10. | Mutssukota dug well (P-18) | black calcareous | -21 | 32 |
| 11. | Tadpatri dug well (P-19) | alluvial sandy | -11 | 238 |
| 12. | Tadpatri bore well (P-19) | alluvial sandy | -18 | - |
| 13. | Canal water near Garladinne | - | + 4 | - |
| 14. | Singanamala tank | - | +24 | 111 |

$$\delta D = \frac{(\delta D_i \times M_w)_{20-30} + (\delta D \times_i M_w)_{40-50} + \cdots}{(M_w)_{20-30} + (M_w)_{40-50} + \cdots}$$

where,

. δD = The weighted mean δD of the whole soil moisture profile.

. $\delta D_i$ and $M_w$ content of soil cores from 20-30 cm, 40-50 cm, 60-70 cm, etc., sections.

The weighted mean δD value for the first phase samples are denoted by $X_1$, and for the second phase samples by $X_2$. A comparison of weighted mean δD values for soil water for the first phase and second phase sampling and δD value for groundwater is shown in Fig. 9, for the soil profiles 10, 12, 18 and 19.

In case of profile 10 (red loamy sandy soil) the groundwater δD value lies between $X_1$ and $X_2$ and for profile 19 (alluvial sandy soil) $X_1$ and

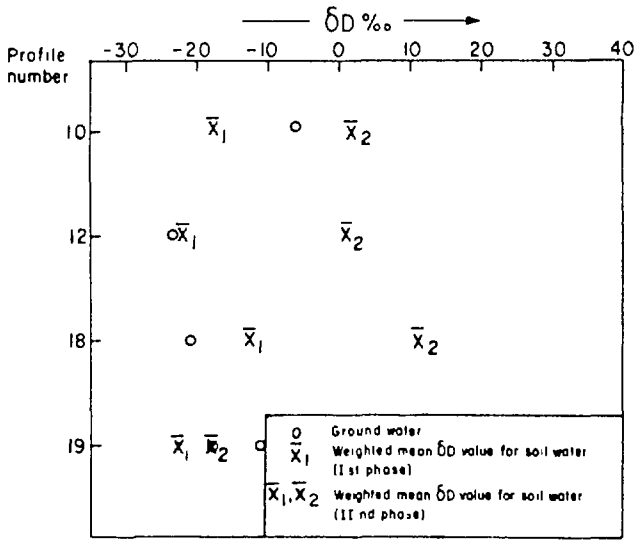


Fig. 9.
A comparison of δD value of ground waters with the weighted mean δD value for soil water.

$X_2$ are more or less similar to groundwater δD values. The profile 12 and 18 are from black loamy sandy soil and black soil with calcareous material. For these samples $X_1$ and $X_2$ values are different than the groundwater δD values (FIG. 9). The equivalent depth values for black soil (TABLE I) also gave different values for each soil profile, thereby, suggesting that the moisture and isotopic behaviour of soil moisture in case of the black soil is very intricate.

The chloride values for groundwaters are normal except for sample number 11 (TABLE IV). Sample number 11 is from a profile in alluvial sandy soil and high chloride content may be due to high permeability and significant loss of moisture from this soil type.

## VI CONCLUSIONS

The moisture content of soil cores, deuterium, and chloride contents of soil moisture, and surface, and subsurface waters from the Marvanka Basin has revealed the following:

1. The equivalent depth values for different soil profiles in red soil show small variations and for profiles in black soil show large variations.

2. The recharge estimates of 9 cm for red soils as annual recharge based on the equivalent depth analogy lie in between the estimates made by the previous workers.

3. The periodic measurement of equivalent depth in red soils may provide a simple means of establishing the periodic changes in water balance of unsaturated zone.

4. Isotopically, each soil core was found to behave independantly supporting the piston flow model of recharge.

5. A quantitative representation of water balance of unsaturated zone in a basin located in a hard rock area with semi-arid climate may not be possible by using stable isotopic and chloride behaviour studies of soil moisture profiles. However, the data provide an important tool for qualitative interpretation.

6. The weighted mean $\delta D$ values for soil water are more or less similar to groundwater $\delta D$ values for red loamy and alluvial sandy soil.

ACKNOWLEDGEMENTS

Research leading to preparation of this report has been partly supported by the International Atomic Energy Agency (IAEA), Vienna, Austria by agency research contract no. 2929GS. We gratefully acknowledge the financial support by IAEA. Authors are thankful to Prof. V.K. Gaur, Director, National Geophysical Research Institute, Hyderabad for granting permission to publish this report. Dr. I. Radhakrishna provided help in field work and took part in many useful discussions.

REFERENCES

[1] ALLISON, G.B., HUGHES, M.W. The use of natural tracers as indicators of soil water movement in a temperate semi-arid region, J. Hydrol. 60: (1983) 157-173.

[2] DINCER, T., AL-MUGRIN, A., ZIMMERMAN, U. Study of the infiltration and recharge through the sand dunes in arid zones with special reference to the stable isotopes and thermonuclear tritium, J. Hydrol. 23: (1974) 79-109.

[3] ZIMMERMANN, U., EHHALT, D., MUNNICH, K.O. Soil-water movement and evapotranspiration: changes in the isotopic composition of the water, In: Isotopes in Hydrology, IAEA, Vienna (1967) 567-584.

[4] RADHAKRISHNA, I., SUBRAMANYAN, K., DESHMUKH, S.D., KRISHNA, G.S.R. Groundwater movement, chemistry and resources in Marvanka basin Anantapur district, Andhra Pradesh, geophy. Res. Bull. 22: No. 2 and 3 (1984) 61-75.

[5] ATHAVALE, R.N., RAMESH CHAND, MURALIDHARAN, D., MOHAN MURALI, D., MURTI, C.S. Measurement of groundwater recharge in Marvanka basin, Anantapur district. Paper presented at the seminar on "Assessment Development and Management of groundwater resources" held at New Delhi (1983) April 29-30.

[6] RAJU, K.C., KAREEMUDDIN, M., RAO, P.K. Operation Anantapur Miscellaneous Publication of the Geol. Surv. India, No. 47, GSI Publication (1979) 1-57.

[7] HILLEL, D. Fundamental of soil physics, Academic Press Inc., New York (1980).

[8] ZIMMERMANN, U., MUNNICH, K.O., ROETHER, W. Downward movement of soil moisture traced by means of hydrogen isotopes. In: Geophys. Monogr. No. 11, Isotope Techniques in the Hydrologic Cycle, AGU, Washington (1967) 28-36.

[9] MUNNICH, K.O. Moisture movement measurement by Isotope tagging, In: Guidebook on Nuclear Technique in Hydrology, IAEA, Vienna (1968) 112-117.

# STUDY OF DOWNWARD MOVEMENT OF SOIL MOISTURE IN UNSATURATED ZONE

M.I. SAJJAD*, S.D. HUSSAIN*, R. WAHEED**,
K.P. SEILER***, W. STICHLER***, M.A. TASNEEN*

* Pakistan Institute of Nuclear Science and Technology, Rawalpindi

** Nuclear Institute for Agriculture and Biology (NIAB), Faisalabad

Pakistan

*** Institut für Radiohydrometrie, Gesellschaft für Strahlen- und Umweltforschung, Munich, Federal Republic of Germany

**Abstract**

Experiments carried out to study the relative contribution from canal system, precipitation and irrigated fields to water table have been described. The normal mode (delta) of irrigation water does not seem to have any appreciable effect on the water table through heavy textured soil. The contribution from irrigated fields/rains through sandy soils is significant. However, the groundwater rise (water logging) is mainly due to the infiltration from the canal system.

## 1. INTRODUCTION

The study of downward movement of soil water in unsaturated zone was initiated in December, 1980 under IAEA/GS Project 2734/GS.

During the study period of 3 years four fields with quite different soil texture are selected. Efforts have been made to find flow velocities due to irrigation practices, monsoon rains and prolonged irrigation of the fields.

It may be pointed out that the present work is a part of the study which was meant to distinguish between the infiltration from:

- canals and their distributaries,
- monsoon rains,
- irrigated fields.

## 2. AREA OF STUDY

The four fields each measuring 170 $m^2$ were selected in the area of Faisalabad (Fig. 1). These are located in Rechna Doab (land between the rivers Ravi and Chenab), which is badly hit by the problem of water logging and salinity. The water table in the area is 1-4 m below the ground surface. At some places it appears on the ground surface too.

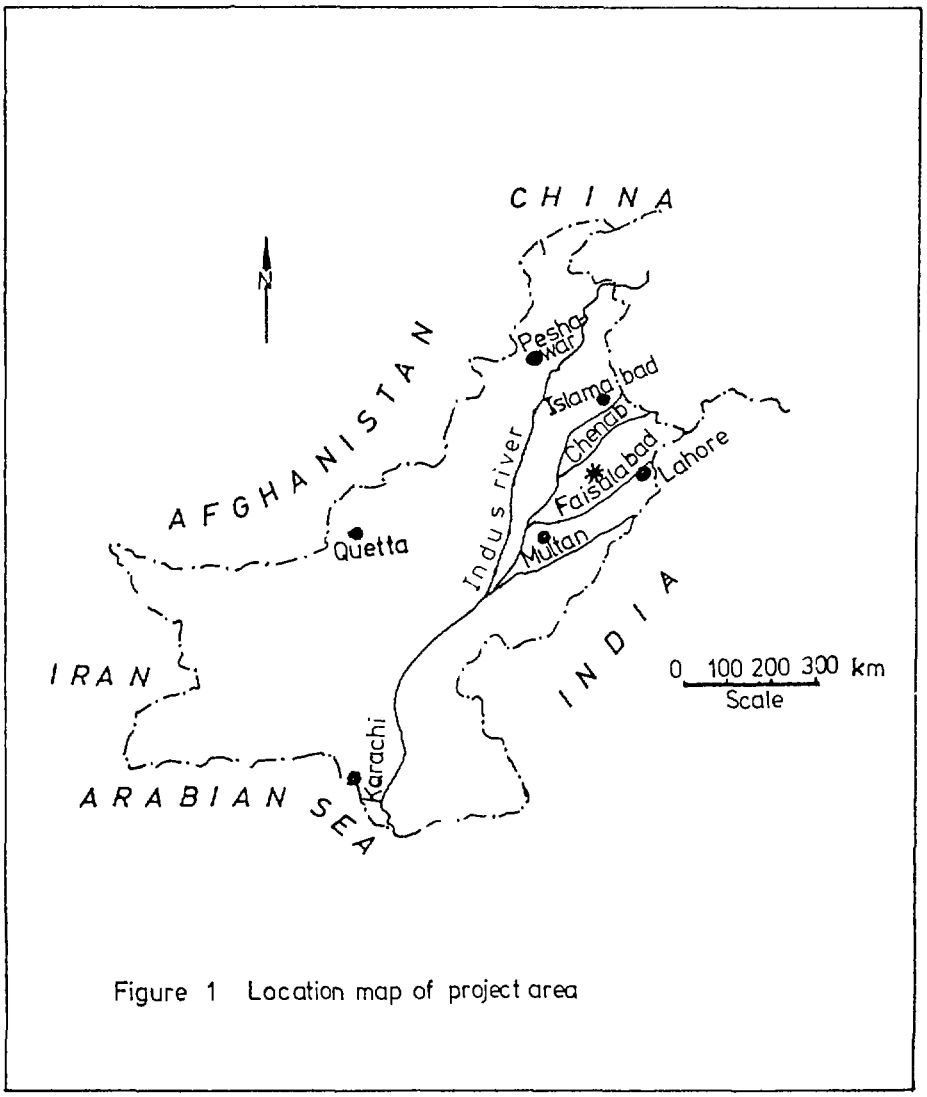


Figure 1 Location map of project area

### 2.1 Geology

The Faisalabad area forms part of the Punjab plains which is an extension of the upper Indus plains. The area was originally a sea bed. It had some extension of the Aravali mountain ranges of Northern India.

The mountains are burried under alluvium, with some hill tops still exposed as out-crops in the vast flat plains of the Indus. The average elevation of the area is about 215 m above sea level. The thickness of the alluvial deposits is about 450 m in the project area (1, 2, 3).

The area is filled by flood deposits comprising of unconsolidated clay, silt and fine to medium grained sand. These sediments are interconnected in an irregular way. Fine grained sediments prevail in the upper 3-5 m depth while medium grained sands are predominant below 5 m.

## 2.2 Climate

The project area falls in arid to semi-arid zone. For most of the winter months (November to January) the weather is characterized by dry air and bright sun during the day. Some of the climatological features are discussed below:

### 2.2.1 Temperature

January is the coldest month in winter and June is the hottest month in summer. The maximum temperature during January is 20°C, while minimum during this month is 5°C.

From February to June the temperature shows rising trend and June becomes the hottest month. The maximum temperature is 47°C, while minimum temperature is 32°C.

In July and August temperature falls to some extent due to the onset of monsoons. The annual maximum temperature is 32°C and minimum is 17°C.

### 2.2.2 Humidity

May and June are the driest months of the year, with 17 % mean relative humidity. The relative humidity during the month of July and August is about 70 %. The wet bulb temperature is about 23°C in these months making the weather more uncomfortable.

### 2.2.3 Rainfall

Rainfall occurs mainly in summer due to monsoons. The area also recieves winter showers of lesser intensity. Monsoon operates during July - September whereas in Winter, showers occur during December - February. The average annual rainfall is about 40 cm.

## 3. MATERIALS AND METHODS

Both isotopic techniques and conventional methods were employed during the course of this study. Further the study was conducted using:

a) a normal mode of irrigation in the fields with dfferent soil texture,
b) the rainy events only and
c) prolonged irrigation of the fields.

### 3.1 Isotopes used in the study

The environmental stable isotopes Deuterium (D), Oxygen-18 and radioactive isotope Tritium (T)) were studied. All these isotopes are produced in nature, form a part of water molecule and are transported through precipitation. Further, these isotopes do not react with the aquifer and therefore, serve as conservative tracers in the study of movement of groundwater.

The varying proportions of D and $^{18}O$ in terrestrial waters can be measured by a mass spectrometer with a precision of 0.1 ‰ for oxygen-18 and 1,0 ‰ for Deuterium. All the non-evaporated waters fall on a line with slope 8

$$\delta D = 8\ \delta O^{18} + Y$$

$$\text{where } \delta = \frac{R_{Sample} - R_{SMOW}}{R_{SMOW}} \times 1000;\ R = O^{18}/O^{16} \text{ or } D/H$$

The excess of deuterium (Y) may vary, but is normally in the range of +10 to +22. However, waters which have been subjected to evaporation are found to fall off the general line of slope 8. In these cases lines having a slope between 4 and 6 have been observed (4,5,6).

The occurrance of tritium in precipitation results in an overall labelling of water in the hydrological cycle. Tritium is, therefore, found to varying degrees not only in precipitation but also in surface waters, groundwaters and the oceans (6).

### 3.2 Other tools used

The neutron soil moisture gauge was used for the measurement of soil water content in the field. This offered a means of determining water content at various depths and intervals of time in case of the continuous irrigation of the field.

The count rate of the detector is translated into volumetric soil moisture content by means of appropriate calibration curve of the form (7):

$$Q = g.\ R' + C$$

where
- $Q$ = volumetric water content
- $g$ = slope of the calibration curve
- $R'$ = the count rate ratio $R/R_W$
- $R$ = count rate in soil
- $R_W$ = count rate in water standard
- $C$ = calibration constant, the negative intercept on Q axis.

Chloride and electrolytical conductivity measurements of soil water were also made to supplement the isotopic data.

## 4. Experimental set-up

Core samples were taken using an auger in the center of the field. It was ensured that the auger hole was at least one meter away from the position of the previous core. The soil

core sections each of 25 cm length were taken up to 4 meter below the ground surface. These core samples were properly sealed in PVC tubes and transported to laboratory.

Samples of irrigation water standing in the experimental fields were taken at different times to see the effect of evaporation on the isotopic composition of the infiltrating water.

The temperature of soil at various depths was measured just by putting the tip of a thermometer in the soil section while still in the auger.

Water samples from various hand-pumps penetrating up to a depth of about 10 m and tubewells exceeding 75 m were collected to see the effect of irrigation waters.

The moisture content of each soil core was also determined by drying it for 24 hours in an oven at 105°C and noting the loss of the weight. Sand/Clay/Silt Percentage was determined by mechanical method and is presented in Tables I and II.

Table I

Variation of Sand, Silt and Clay with depth in Field No. 2

| Depth (cm) | % Sand | % Silt | % Clay | Soil Class (11) |
|---|---|---|---|---|
| 0-25 | 55 | 26 | 19 | Clay loam |
| 26-50 | 57 | 24 | 19 | Sandy clay loam |
| 51-75 | 57 | 24 | 19 | - do - |
| 76-100 | 58 | 24 | 18 | - do - |
| 101-125 | 64 | 23 | 13 | Loam |
| 126-150 | 61 | 26 | 13 | - do - |
| 151-175 | 55 | 32 | 13 | - do - |
| 176-200 | 47 | 35 | 18 | Clay loam |
| 201-225 | 62 | 23 | 15 | Sandy clay loam |
| 226-250 | 78 | 14 | 8 | Sandy loam |
| 251-275 | 84 | 8 | 8 | Sandy loam |
| 176-300 | 88 | 8 | 4 | Loamy sand |
| 301-325 | 90 | 8 | 2 | - do - |
| 326-350 | 94 | 4 | 2 | - do - |
| 351-375 | 93 | 4 | 3 | - do - |
| 376-400 | 92 | 5 | 3 | - do - |

Table II

Variation of Sand, Silt and Clay with depth in Field No. 3

| Depth (cm) | % Sand | % Silt | % Clay | Soil Class (11) |
|---|---|---|---|---|
| 0-25 | 64 | 26 | 10 | Loam |
| 26-50 | 66 | 22 | 12 | Sandy loam |
| 51-75 | 66 | 22 | 12 | - do - |
| 76-100 | 68 | 21 | 11 | - do - |
| 101-125 | 70 | 20 | 10 | - do - |
| 126-150 | 72 | 21 | 7 | - do - |
| 151-175 | 75 | 18 | 7 | - do - |
| 176-200 | 68 | 24 | 8 | - do - |
| 201-225 | 73 | 22 | 5 | - do - |
| 226-250 | 67 | 25 | 8 | - do - |
| 251-275 | 60 | 30 | 10 | Loam |
| 276-300 | 70 | 24 | 6 | Sandy loam |
| 301-325 | 83 | 15 | 2 | - do - |
| 326-350 | 91 | 9 | - | Loamy sand |
| 351-375 | 94 | 6 | - | - do - |

The moisture extraction from the soil cores was done in a vacuum distillation assembly with four units as shown in Figure 2. To check the performance of the system, water of known isotopic composition ($^{18}O$) was added to dry soil samples and then these wet soil samples were processed in the vacuum distillation units and isotopic contents of extracted water compared with those of the original water. The results were reproducible and well within the acceptable error limits.

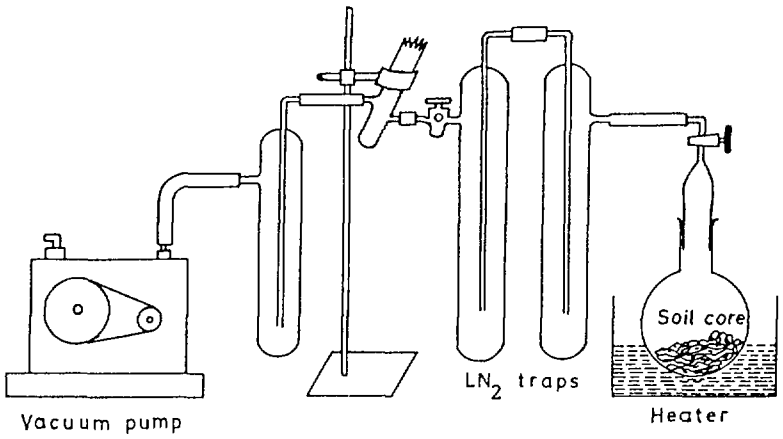


*Fig- 2 Vacuum distillation assembly for water extraction from cores*

The extracted water samples were analysed for $^{18}O$ and D contents by a Mass Spectrometer equipped with a double ion collector system and automatic $^{3}H$ - compensation unit. The tritium (T) content was determined by a Packard Tricarb Liquid Scintillation Spectrometer System.

In case of prolonged irrigation experiment a hole was drilled in the centre of each field. The diameter of this hole was kept smaller than the outer diameter of aluminium pipe used with neutron moisture probe as access tube. Under the situation, the access tube when lowered into hole cuts the soil edges keeping the soil profile undisturbed. Before irrigation of the field a background moisture measurement was made along the soil profile at depth intervals of 25 cm. This was then repeated at different time intervals after maintaining a constant water head of 100 mm.

## 5. RESULTS AND DISCUSSION

### 5.1 Hydrogeological properties

The representative grain size distributions for field 2,3 and 4 are given in Figure 3. In case of field 1, only clay and silt contents were determined. Differences in the granulometric com-

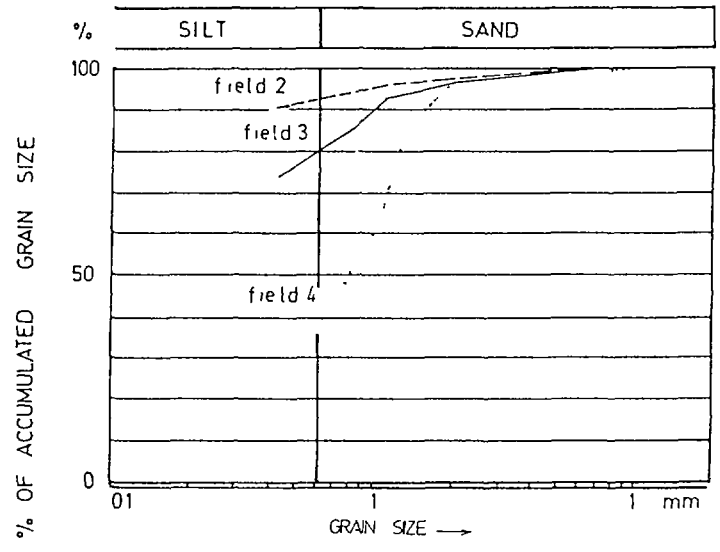


FIGURE-3 CLAY AND SILT CONTENT IN % OF ACCUMULATED GRAIN SIZE DISTRIBUTION

position of these sediments are best expressed by their silt and clay content as given in Table III. Parallel to the clay and silt content the hydraulic conductivity varies qualitatively.

The common irrigation practice is done by flooding the fields till water reaches a level of 75 mm (3 inches) above the field. Infiltration already starts during flooding and stops when the water has disappeared from the field. Therefore, as shown in Figure 4, the increase in water content in the unsaturated zone is stronger in fields with high hydraulic conductivity than in fields with low hydraulic conductivity. The computation of increase of water content (M) in the unsaturated zone expressed in litres was made through the relation:

$$M = \int_{z_o}^{z_n} \Theta(z)\, dz$$

$\Theta$ = volumetric moisture content, Z = depth.

This increase corresponds at least to the amount of 75 mm of irrigation water per $m^2$; it is highest in the sandy field No. 4 and lowest in the loamy field No. 1 (Table III). Furthermore it can be seen from figure 4 and Table III that the penetration depth of irrigation water is lowest in field No. 1 and greater than 3.3 m in field No. 4.

Former studies in Pakistan (8) show that evapotranspiration reaches a depth of about 1-1.5 m below ground. From this it can be assumed that the irrigation water in the fields No. 1,2 & 3 might partly or totally be evaporated to the atmosphere. In field No. 4 a large amount of irrigation water stored up to lower depths will percolate to ground water.

The evaporation from near surface layers in these fields is favoured by shrinkage cracks generated in all the four fields with drying of the soil. These cracks reach a depth of about 50 cm below surface.

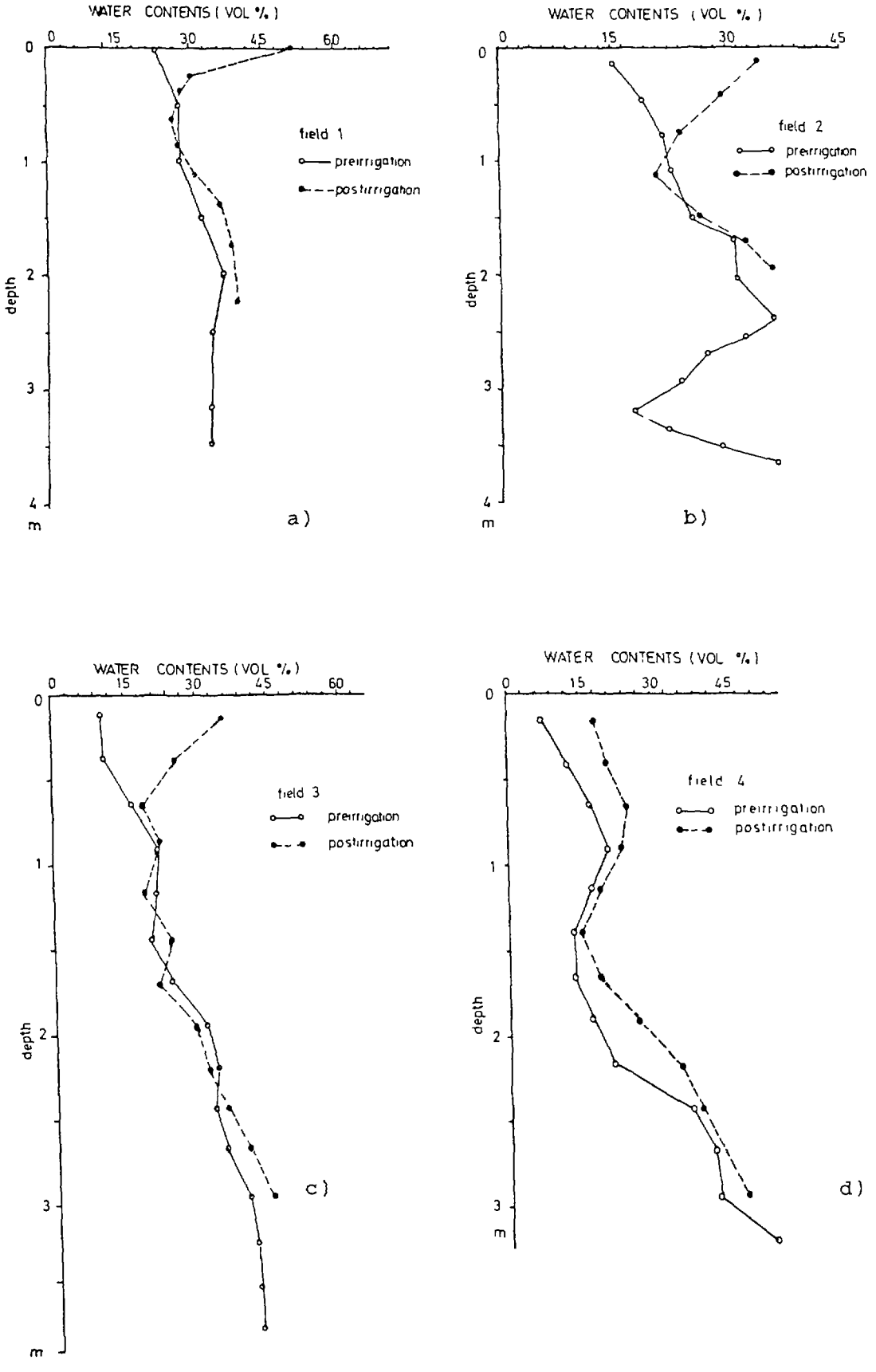


Figure 4: Variation of moisture with depth in fields 1,2,3,4.

Table III: Hydrogeological Properties of the Sediments in the Four Fields.

| Field No. | Clay and Silt content in % of accumulated grain size distribution | Water stored (Litres) upto depth as in col. 4 | Penetration depth (m) of irrigation water |
|---|---|---|---|
| 4 | 32.8 | 221 | 3.30 |
| 2 | 90.6 | 113 | 0.85 |
| 3 | 73.6 | 99 | 0.85 |
| 1 | - | 74 | 0.60 |

The hydraulic conductivity in fields 1,2 & 3 with post-irrigation water content of roughly 20 vol. % at 1 m depth is lower than $10^{-8}$ m/s; whereas in field 4, it is one order higher in magnitude. The calculated flow velocity ($v = k(\Theta)/\Theta$) for field 4 with a hydraulic conductivity of $10^{-7}$ m/s and a water content of 20 vol. % at a depth of 1 m is of the order of 16 m/a. This result is in fairly good agreement with the flow velocity determined by means of stable isotopes in the same field under post-irrigation conditions. During infiltration, the flow velocity must be in the order of a few meters a day; otherwise water could not percolate to the water table within 1-2 days. Calculating the flow velocity for fields 1,2 & 3 with hydraulic conductivity of less than $10^{-8}$ m/s at a water content of 20 vol. %, it is expected to be in the order of less than 1.6 m/a. Considering that fields 1,2 and 3 contain the prodominant sediments in the area, there is slow percolation and therefore weak contributions to the ground water recharge. This is in good agreement with former statements (9, 10).

## 5.2 Qualitative proof of hydraulic results

Tritium profiles in field No. 3 & 4 are depicted in figure 5.Sampling made in field 3 on 5.4.1981, has tritium peak at 250 cm depth with maximum concentration of 215 TU. The profile on 25.1.1983 has peak at 300 cm of concentration 170 TU. Dispersion due to molecular diffusion seems to be active during down-

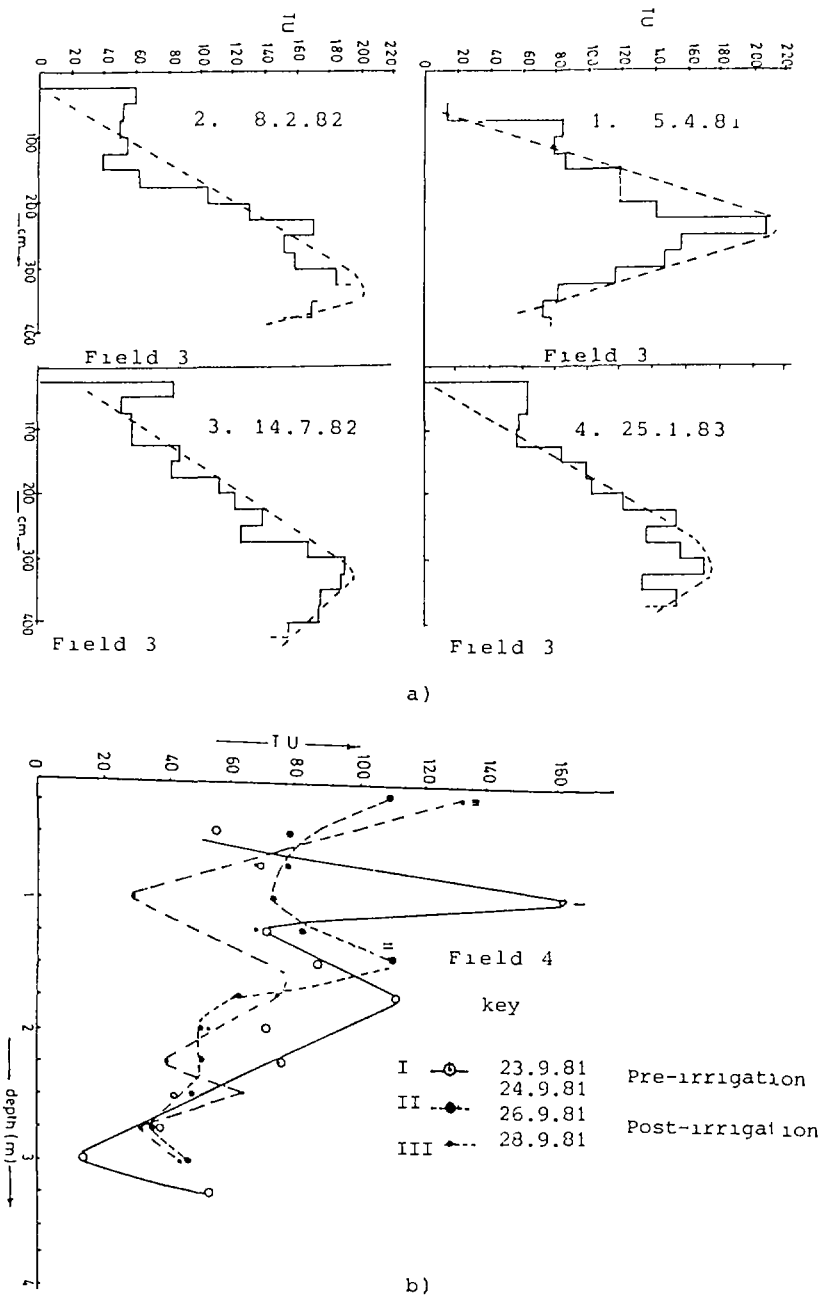


Figure 5: Variation tritium content with depth in field 3,2,4.

ward movement. Total rainfall between April, 1981 and january 1983 was about 1000 mm. Inspite of this rain, the downward movement at the depth of 250 cm in field 3 is very small i.e. even less than 0.5 m/a.

However, in field 4 (Fig. 5b) the downward displacement of the peak is quick i.e. about 1 m in only 4 days after 75 mm irrigation of the field. This weak percolation in field 3 and strong one in field 4 would result in different phenomenon of leaching

of salinity in the two fields. Figure 6a showing the variations of chloride ($Cl^-$) with depth indicates that strong percolation has leached out all salts near to water table. Whereas figure 6b (field 3) shows a peak at a depth of 75-80 cm.

Table IV: Rainfall Data of Monsoon 1981

| Date | Precipitation (mm) | $\delta^{18}O$ | $\delta D$ ‰ |
|---|---|---|---|
| 01.07.81 | 31 | -0.65 | +13.5 |
| 03.07.81 | 56 | -1.07 | + 4.6 |
| 06.07.81 | 30 | -8.08 | -55.1 |
| 10.07.81 | 69 | -0.62 | - 4.4 |
| 15.07.81 | 196 | -5.35 | -36.8 |
| 26.07.81 | 56 | -5.91 | -36.8 |
| 30.07.81* | 52 | -0.11 | -13.9 |

Total Rain: 490 mm
Weighted Average of $\delta^{18}O$ = - 3.57 ‰
$\delta D$ = -23.01 ‰

* All monsoons of 1981 were concentrated in the month of July.

## 5.3 Results of irrigation experiments

Results obtained from the irrigation experiments performed in Field No. 2 and 3 are as follows:

Field No. 2:
In the experiment many core samples were taken for analysis of $^{18}O/^{16}O$, D/H, Tritium, moisture and chloride determinations, and soil texture analysis. These results have been plotted in figures 7 and 8. The $\delta D$ - $\delta^{18}O$ plot of irrigation water standing in the field is depicted in figure 9a.

The moisture and isotopic data indicate that the penetration of irrigation water is approximately up to one meter depth for this particular soil.

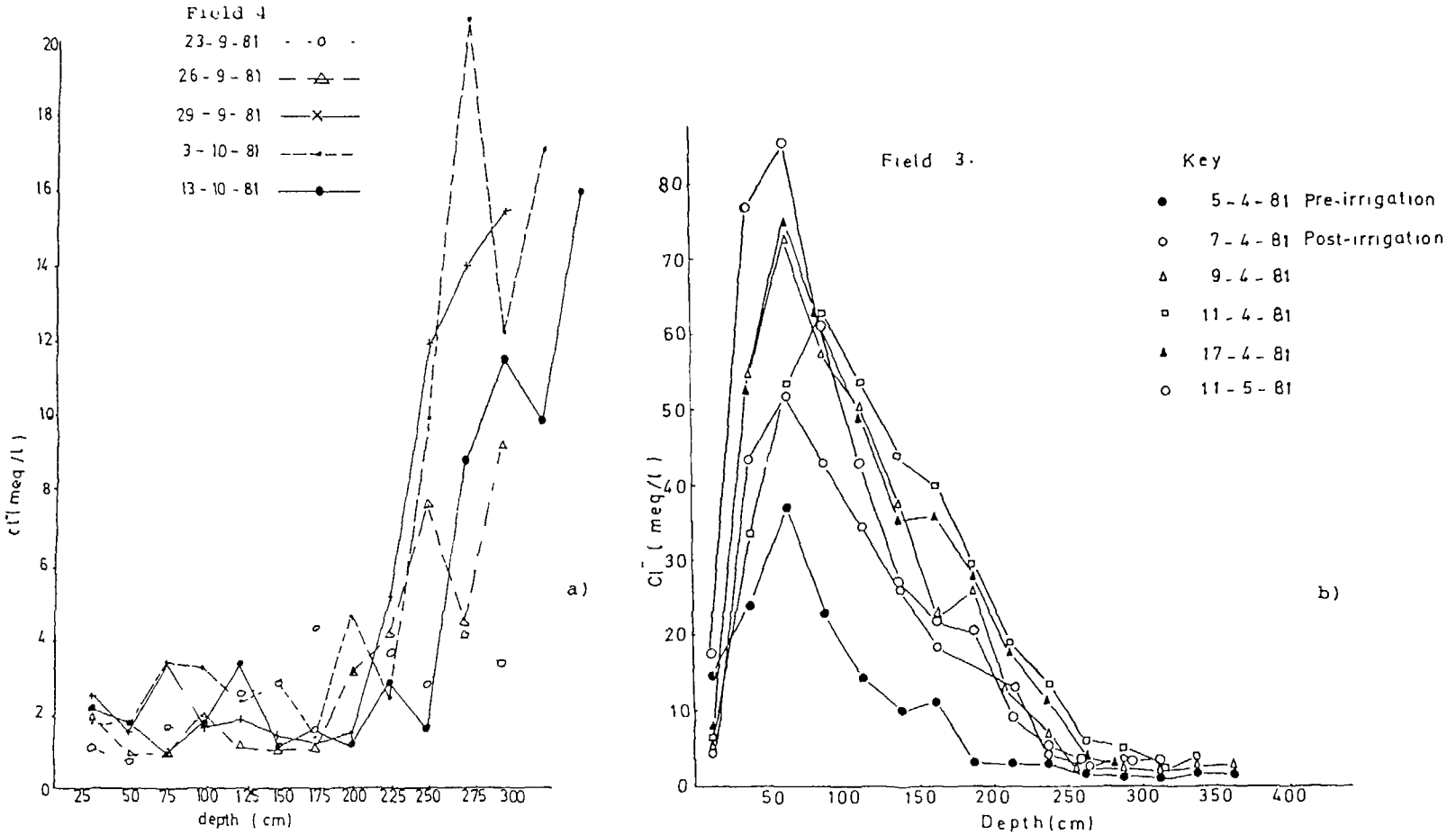


Figure 6: variation of $Cl^-$ with depth in field 3

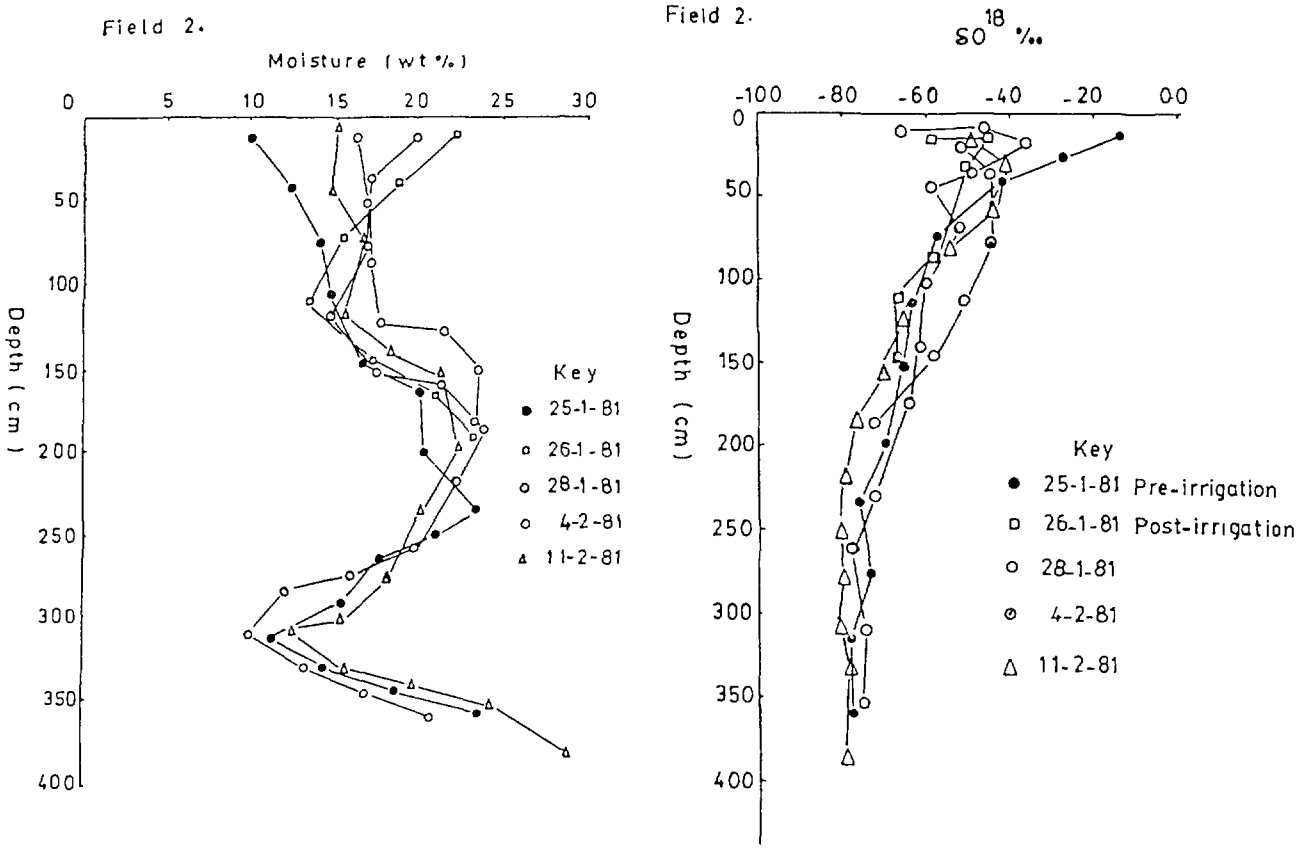


Figure 7: Variations of moisture and $\delta^{18}O$ with depth in field 2.

The variation of moisture and $^{18}O$ with depth indicates the influence of soil type on the movement and/or storage of soil moisture.

The pre-irrigation and post-irrigation $\delta^{18}O$ and $\delta D$ correlation for various sampling periods are: -

| | Date | Equation | Correlation Coefficient: $r^2$ |
|---|---|---|---|
| Pre-irrigation | 25.1.1981 | $\delta D = 4.63\ \delta^{18}O - 17.51$ | 0.95 |
| Post-irrigation | 26.1.1981 | $\delta D = 5.13\ \delta^{18}O - 13.24$ | 0.88 |
| | 28.1.1981 | $\delta D = 5.87\ \delta^{18}O - 8.15$ | 0.91 |
| | 4.2.1981 | $\delta D = 5.26\ \delta^{18}O - 9.25$ | 0.97 |

The slope for the pre-irrigation soil core is 4.63 which shows the evaporation effect in soil moisture up to 1,5 m depth.

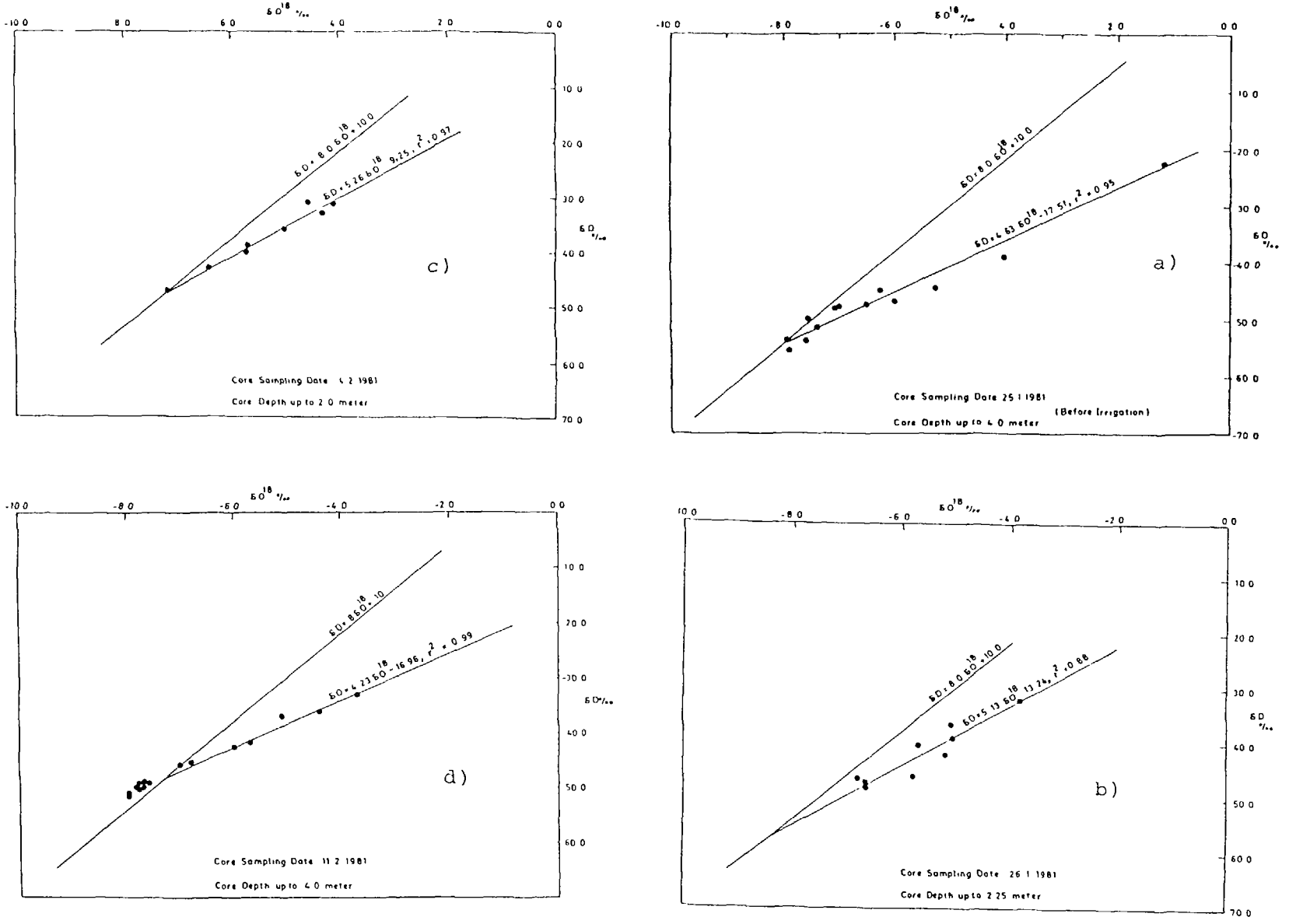


Figure 8: $\delta D$-$\delta^{18}O$ plot of Soil cores in field 2

During the process of infiltration, mixing of isotopically enriched soil moisture with the irrigation water occurs and shifts the isotopic composition towards that of irrigation water as it moves downward.

Later on,as the top layers dry out through the loss of water vapour to atmosphere, the soil moisture content is reduced below that of the field capacity and the rate of downward movement is drastically curtailed. Eventually this downward movement of water also ceases. Evaporation at the soil surface creates a region of high suction resulting in the upward movement of soil moisture through capillary action. During this process of evaporation, the soil moisture gets enriched isotopically.

This back and forth moisture movement is always operating in the soil after each irrigation. However, the depth of water penetration depends upon the type of soil, intensity of irrigation, atmospheric evaporation rates prevailing and other factors. Table III and Figure 4 demonstrate this fact clearly where the penetration depths for fields; 1,2 and 3 are within 1 m range and that for field 4 is three times more.

Field No. 3:
The soil texture of this field is slightly different from that of the previous one. The results of various experiments are shown in figures 9b to 12.

During this experiment, the irrigation water (70 mm) standing in the field, showed large enrichment in its isotopic composition with time - indicating higher evaporation rates (compare figure 9a & 9b) due to prevailing atmospheric conditions of less humidity and higher temperature.

$\delta D$ versus depth plot (Fig. 10a) indicates large deuterium distribution in the upper soil layers due to intense fluctuations in soil moisture. In lower layers the isotopic transport processes in the soil moisture smooth out the isotopic composition differences of water in different layers during the passage of time. In still deeper soil layers, these isotopic differences

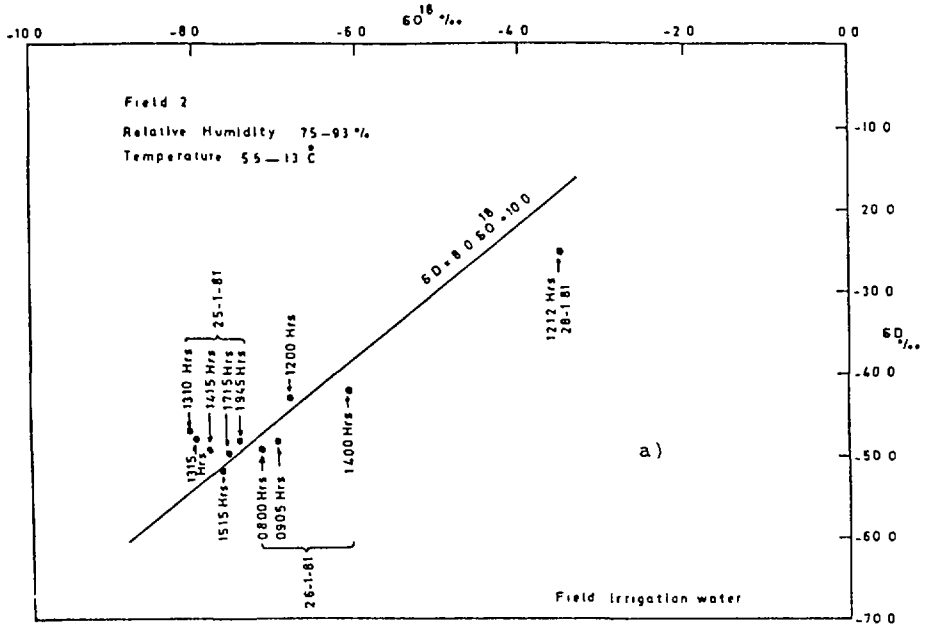


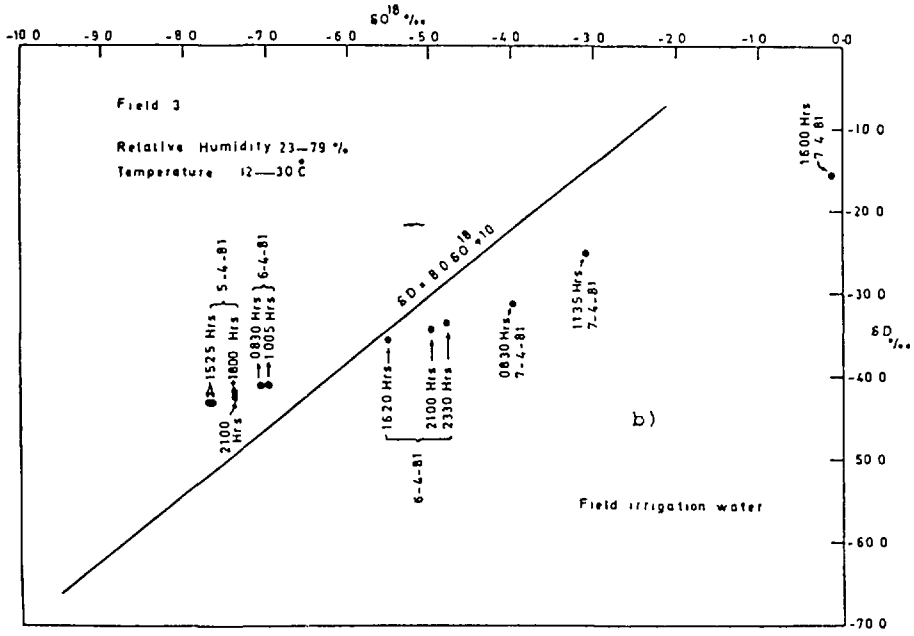


Figure 9: Enrichment in $\delta^{18}O/\delta D$ of standing water in fields 2 & 3.

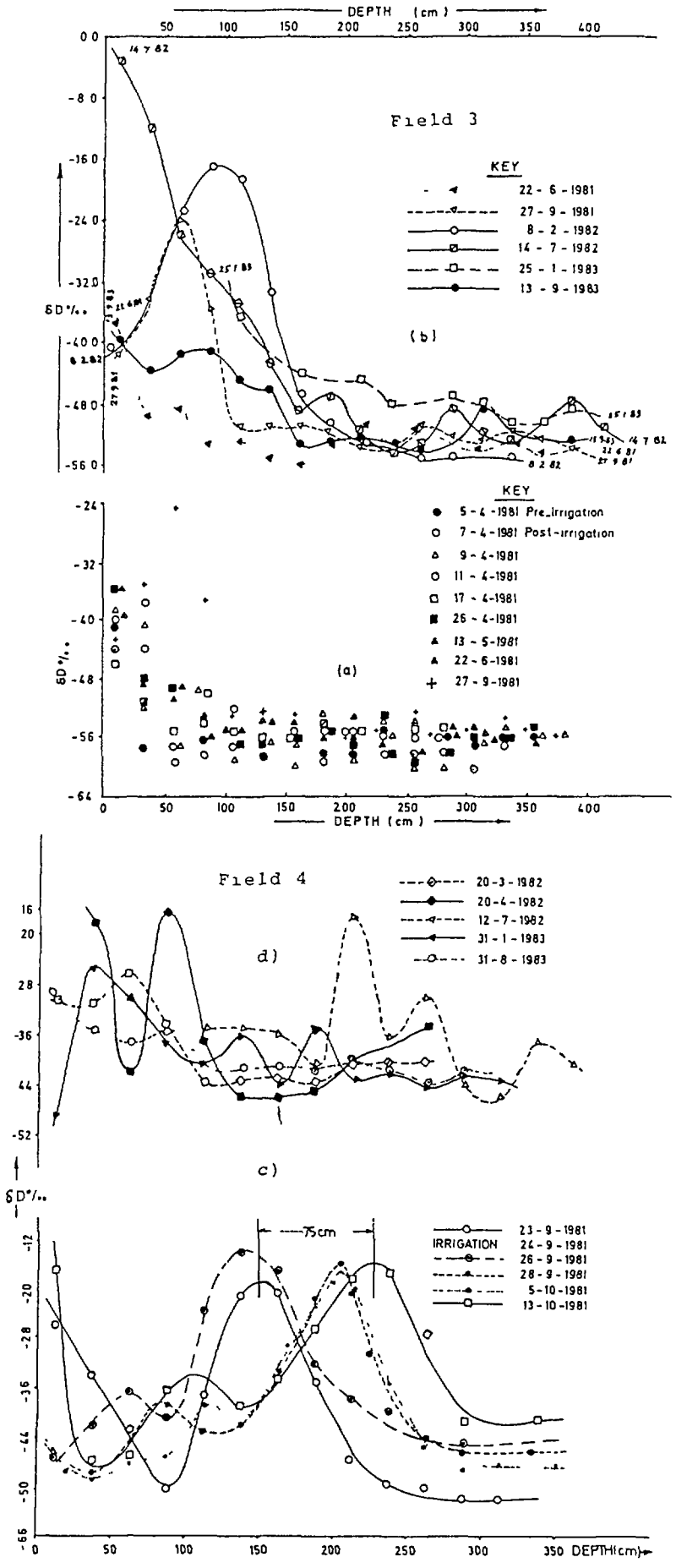


Figure 10: Deuterium profiles in field 3 & 4.

are not distinguishable. All these phases of smoothing are nicely demonstrated in figure 10a.

The $\delta D$-$\delta^{18}O$ relations of various soil cores (Figure 11) indicated that only a few points representing upper layers deviate from the general meteoric line.

$$\delta D = 8.0\ \delta^{18}O + 10.0$$

All other points group around this non-evaporated line showing least evaporation effect.

The chloride ion ($Cl^-$) measurements of the soil moisture in both fields (2&3) indicate that the accumulation of these ions is limited to the upper soil profile depth of 2.5 m. This is essentially due to prolonged irrigation of the soils, during each of which the soil salinity increases considerably depending upon the concentration of soil solution present and the chloride content of irrigation water. A typical case is presented in figure 6b where after the irrigation of the field, the chloride content increases from 37 meq/l to 85 meq/l during the period of about one month (5 April to 11 May, 81). Variations of electrolytical conductivity are shown in figure 12a.

Inspite of the high solubility of chloride in water and its ability to move faster through the soil than the average velocity of water molecule* available, the above figure shows a peak at a depth of 75-80 cm (its height increasing with time). This shows that the penetration of irrigation water was limited to the upper soil layers only. As the top soil dries up, the soil moisture starts moving upward carrying $Cl^-$ with it. Consequently the previously leached salt profiles shift upwards as indicated by the core sampling on 11.5.81 (Figure 6b).

---

* The apparent great average velocity of $Cl^-$ ions is due to the fact that they are excluded from the immediate vicinity of negatively charged soil particles where the water is relatively immobile and from narrow pores where solution velocities are slow (11).

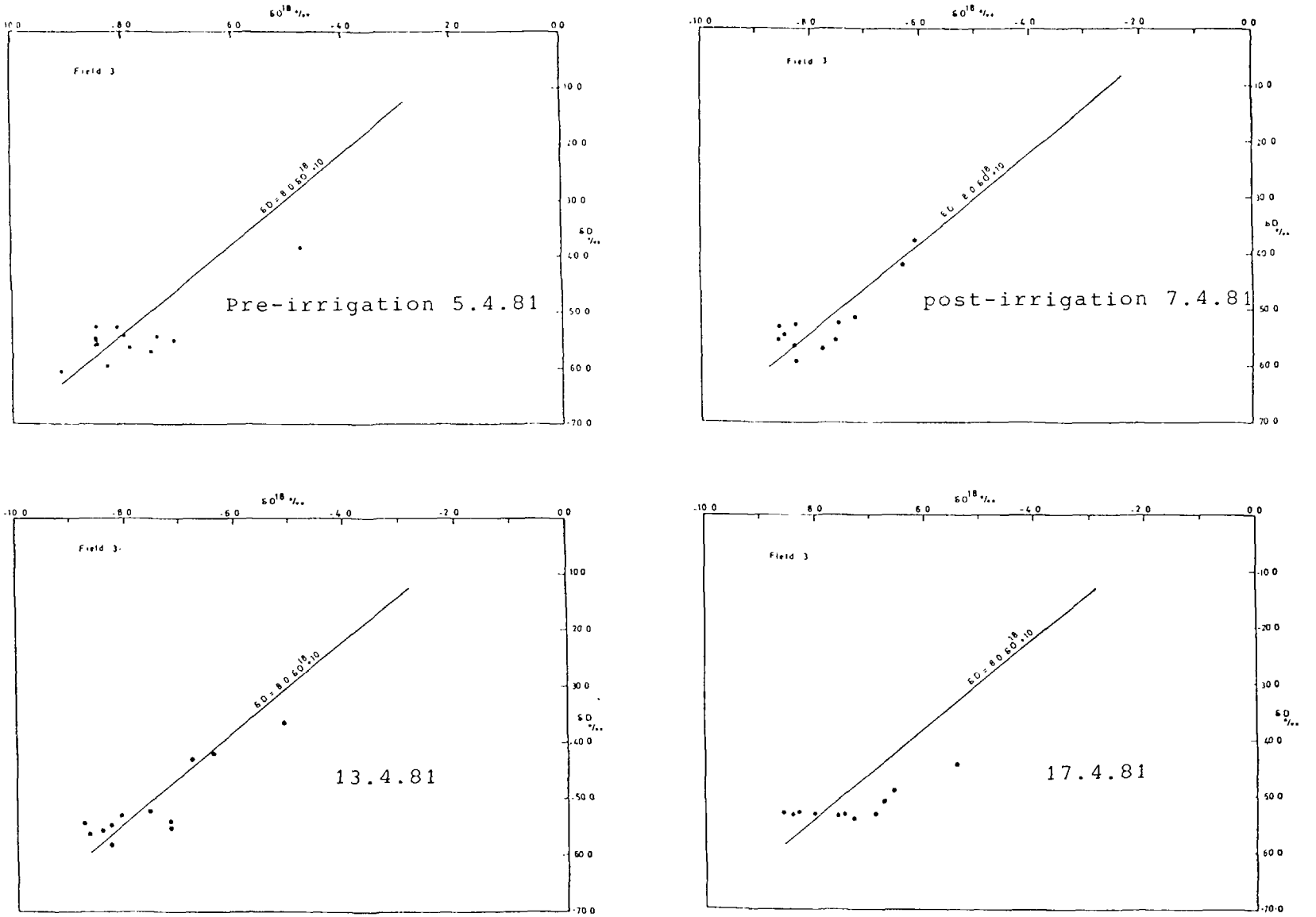


Figure 11 (a): $\delta D$-$\delta^{18}O$ plot of soil cores of field 3

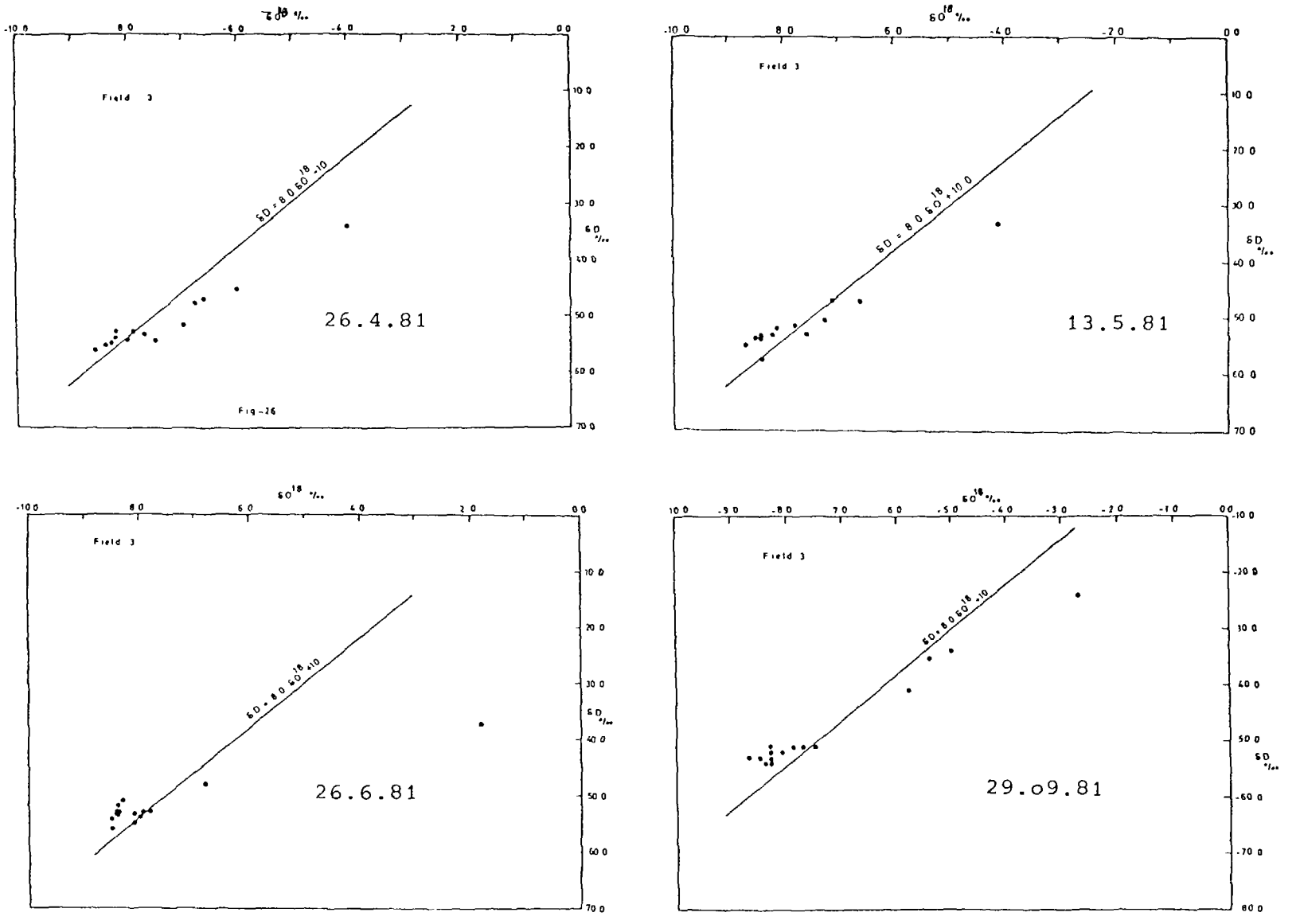


Figure 11 (b): $\delta D$-$\delta^{18}O$ plot of soil cores of field 3

The accumulation of salinity in soil can be diluted, to some extent by applying a higher amount of irrigation water or after heavy rains during which the soluble salts leach down to the greater depths.

The soil core samples taken on 27.9.1981, after monsoon rains, give an evidence that these rains have penetrated up to one meter depth by this time (Fig. 10a).

These irrigation experiments further demonstrate that the irrigation water (75 mm) keeps standing in fields 1,2 & 3 for hours as the percolation is slow there. During this process the field water encounters as much as 5 ‰ enrichment of $^{18}O$ in about 40 hrs indicating high evaporation rates. Whereas in field No. 4 all the water (13 cm) infiltrated within two hours. The mean values of $\delta^{18}O$ and $\delta D$ for four samples collected during this period from the field are $-8.23 \pm 0.04$ and $-46.6 \pm 0.4$ ‰ respectively. This indicates that any isotopic change due to evaporation is within analytical errors.

### 5.3.1 Percolation Velocities due to Normal Delta of Irrigation

When normal delta of irrigation water (75 mm) was applied to field 4, tritium peak at 80 cm was pushed to the depth of about 150 cm in 4 days (Fig. 5b) resulting in downward movement rate of 64 m/a. This irrigation water then hits a deuterium peak (due to rain) at depth of 150 cm which moves to 225 cm depth in 20 days (Figure 10c). The downward movement rate in this region is 14 m/a. This drop in flow rate is caused by the lateral propagation of water in the unsaturated zone which results in an increase of matrix suction in this region and the main driving force here are capillary forces only. Whereas in upper region (1 m), gravity forces are more pronounced than in greater depths. In field 3, the downward movement rate due to irrigation water is very slow and cannot be estimated accurately. Here most of irrigation water evaporates to the atmosphere and only small portion percolates.

## 5.4 Results of Rain Infiltration in Fields 3 & 4

### 5.4.1 Field No. 3

In $\delta D$ versus depth plot (Fig. 10a) of field 3 (April-June 1981), deuterium profile (on 27.9.1981) after monsoons shows a peak ($\delta D$ = -24.00) at 60 cm depth. This is essentially due to monsoon rains (490 mm) which have weighted averages as $\delta D$ = -23.01 ‰ (Table IV). As shown in Figure 10b this peak moves further down to 100 cm depth by 8.2.1982. Then, as the upper layers dry up, the soil moisture starts moving upward as is shown by profiles of later dates. Downward movement rate due to rains is less than 5 m/a.

### 5.4.2 Field No. 4

As compared to field 3, the monsoon rains ($\delta D$ = -23.01 ‰) penetrated upto a depth of 150 cm within the same duration resulting in downward movement rate of about 8 m/a (Figure 10c). This percolation rate is almost half than due to irrigation practices. This is essentially due to the fact that the field had previously no ridges around and most of the rain water disappeared as surface run off.

In figure 10d, the peak at depth of 100 cm moves down to 225 cm by mid July 1982 due to rains (75 mm) on 16/17th June 1982 with downward movement rate of 20 m/a. On later dates all isotopic differences disappear i.e. the isotopic peaks are washed out to water table due to monsoons of 1982 and 1983.

## 5.5 Prolonged Irrigation of Field 3 & 4

An experiment was set up to see percolation rates in the two fields when continuous irrigation maintaining a constant head of 100 mm was applied. The change of moisture content at various depths with time was monitored with a neutron probe.

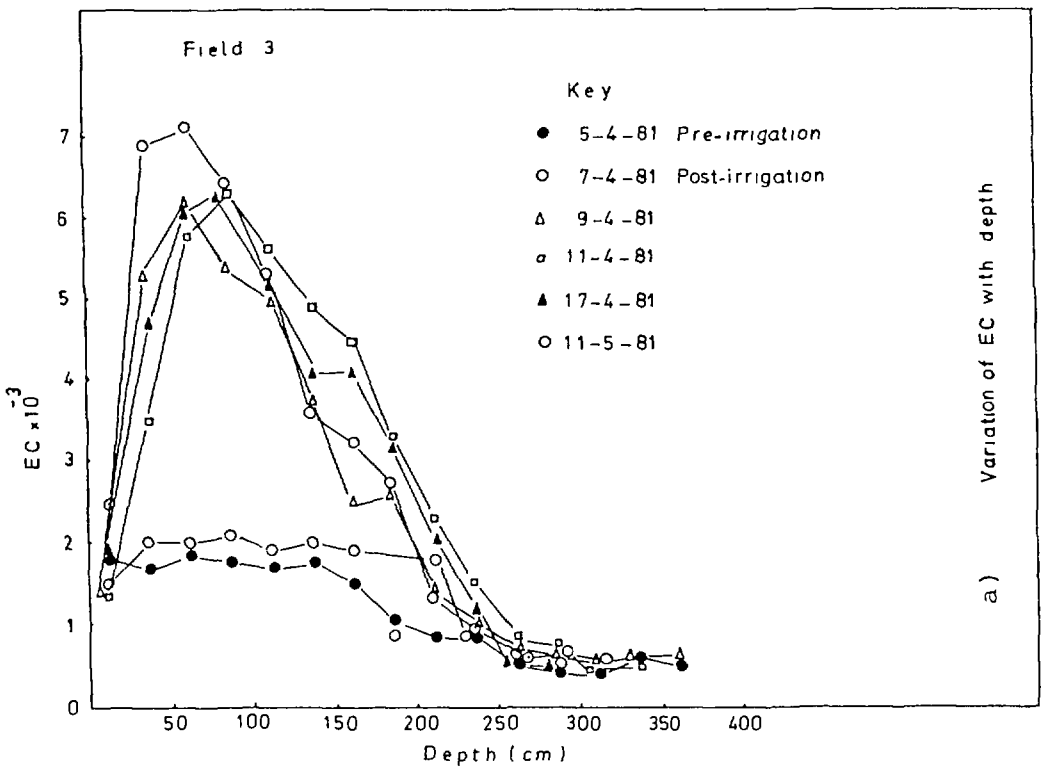


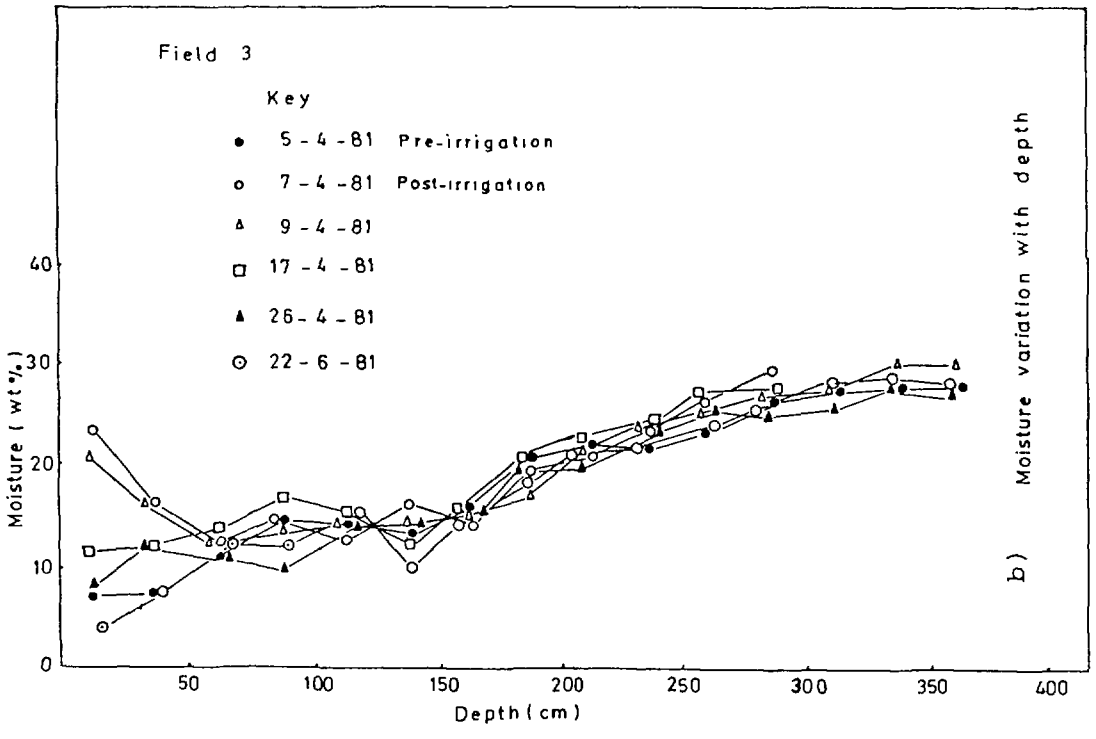


Figure 12: Variations of moisture and EC with depth in field 3

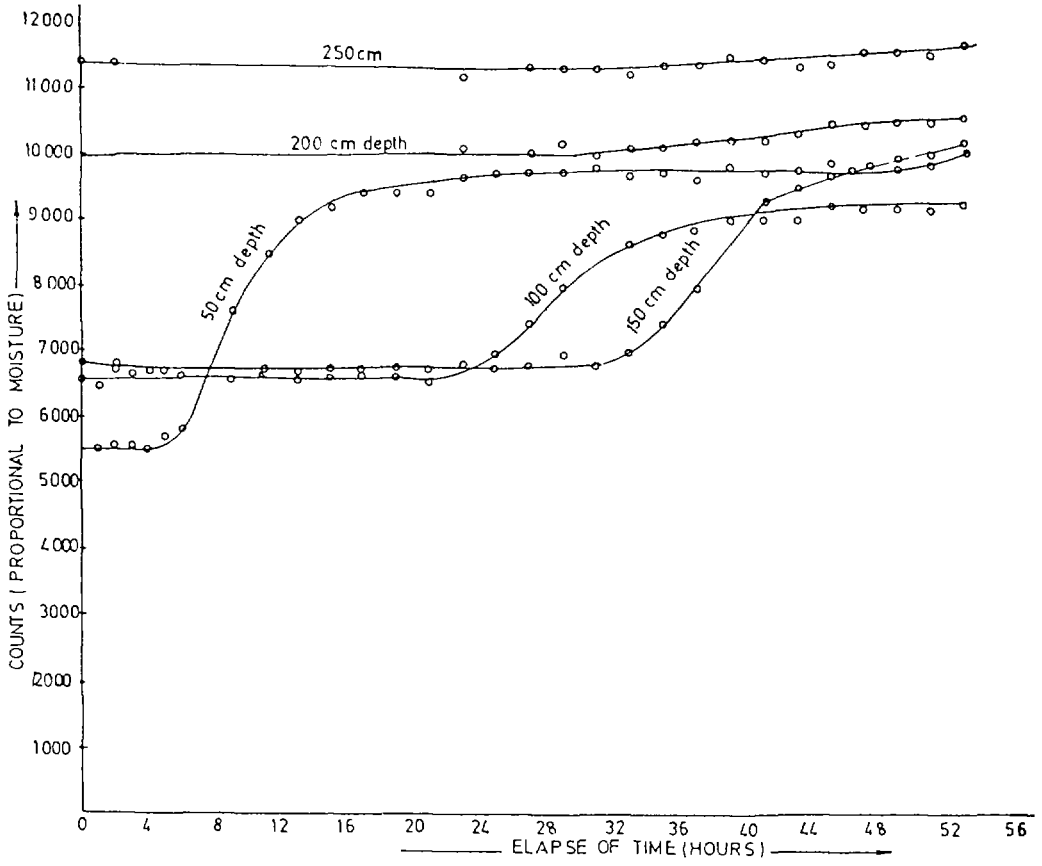


Fig.13 VARIATION OF MOISTURE WITH DEPTH DURING THE PROLONGED IRRIGATION OF FIELD 3

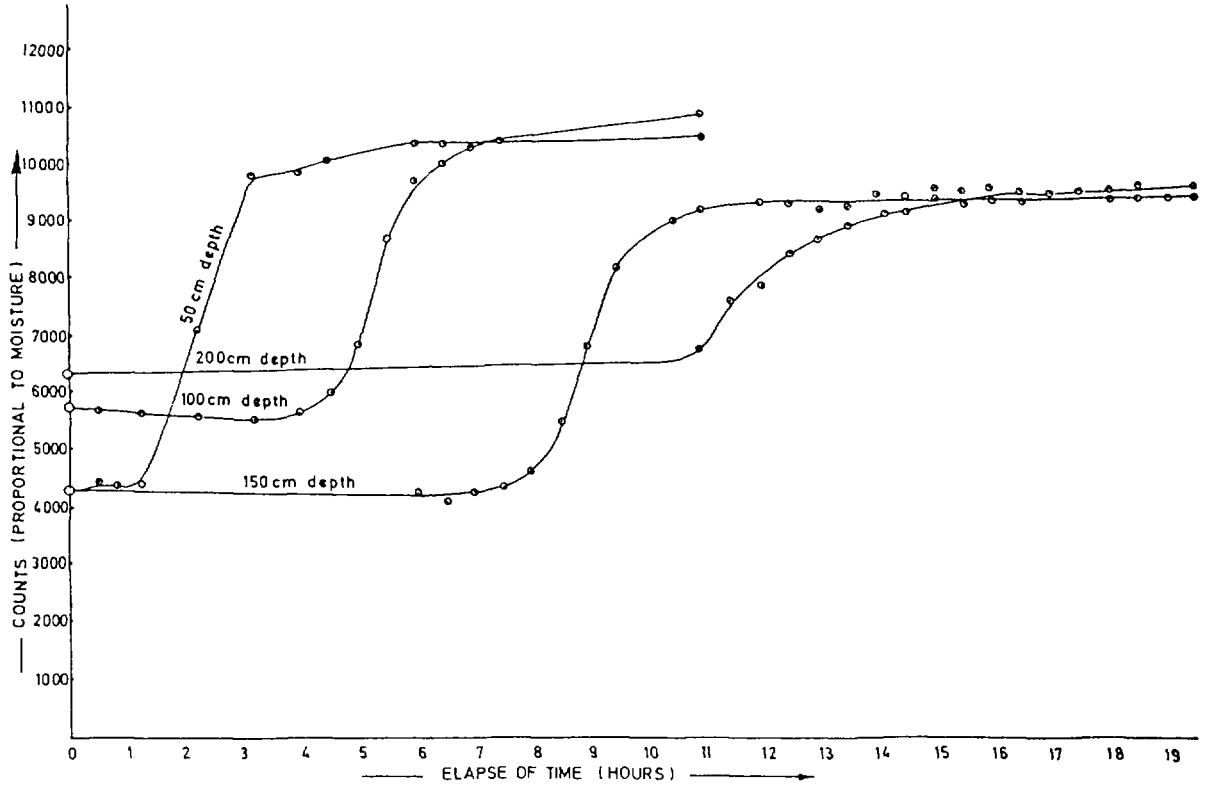


FIG - 14 VARIATION OF MOISTURE WITH DEPTH DURING THE CONTINUOUS IRRIGATION OF FIELD 4

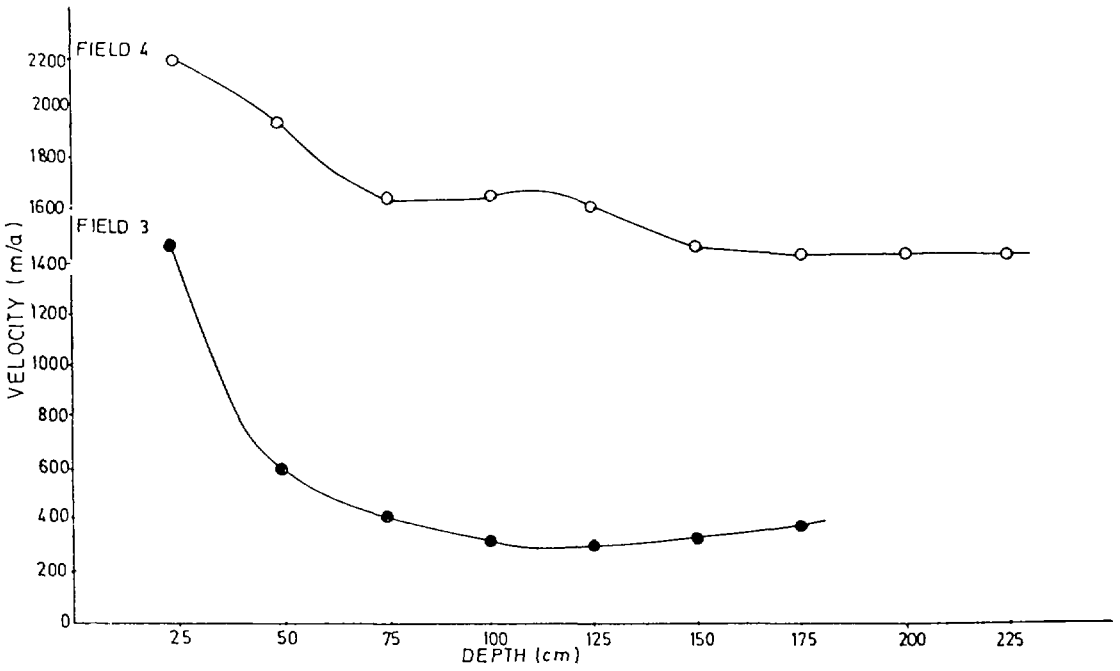


FIG 15 FLOW VELOCITIES IN FIELDS 3&4 DUE TO PROLONGED IRRIGATION ( 100mm)

The results of this experiment are given in figures 13 & 14. The calculated velocities at various depths in the two fields are depicted in Figure 15. Few important features of these curves are:

a) Velocities decrease with depth upto certain point and then become constant (Fig. 15).

b) Flow velocities in field 4 are 2 to 6 times higher than those in field 3.

c) Moisture profiles at various depths have different field capacities depending upon the soil type.

d) Upper layers due to higher silt %, have higher field capacities.

## 5.6 Contribution of Canal System to Groundwater

Isotopic and hydrochemical studies made by the authors (9) in the Faisalabad area resulted in the statement, that groundwater rise (water logging) is mainly due to the infiltration from the

canal system. The residence time of the groundwater above the pre-irrigation water table is in the order of some tens of years. Near canals there is a large amount of recent groundwater.

Figure 16 shows a histogram of the frequency distribution of $\delta O^{18}$ values of shallow and deep groundwater of the study area. In both cases, the distribution is highly skewed with the maximum frequency close to isotopic index (-8.6 ‰) of canal system estimated from actual canal samples. The range of isotopic variations of canal water is -5‰ to -11‰. The lower frequency occurs at delta values close to the isotopic index ( -4 ‰) estimated for recharge by infiltration of local precipitation , and that too only in shallow groundwater. Contribution from rains in deeper zone seems to be negligible. However, it is important that contribution from heavy rains (isotopically depleted) which can infiltrate rapidly through sandy soils as demonstrated by "prolonged irrigation experiment" cannot be determined while taking isotopic index as weighted average of all rains. Because of the possibility of such quick seepage, the contribution of rains is to be calculated for each single rainfall. Similarly, the contribution of irrigation water through

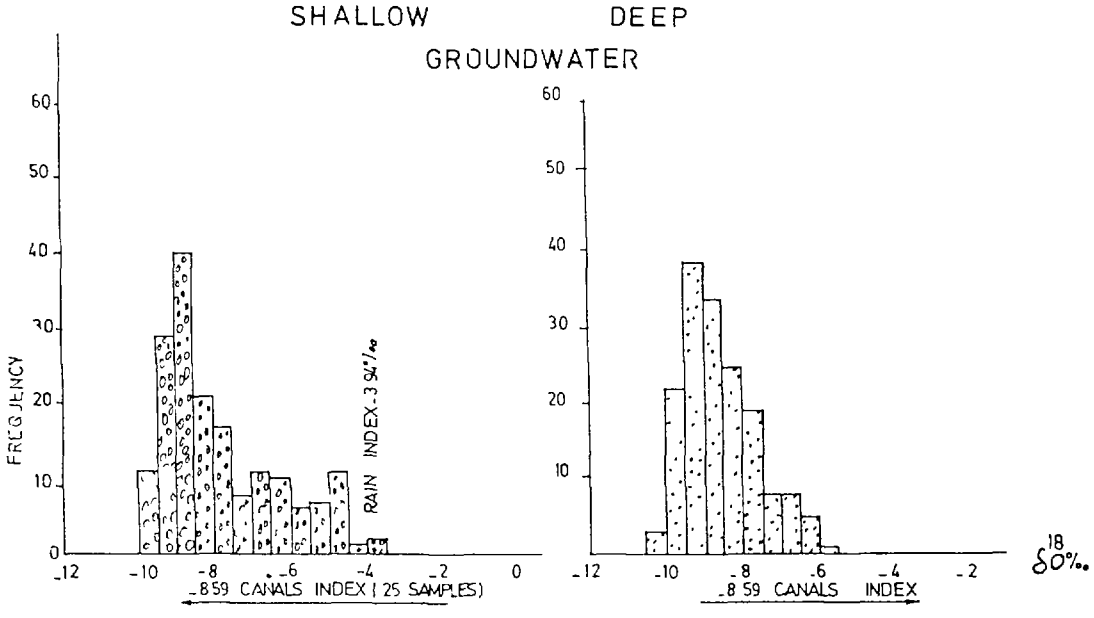


FIGURE-16 FREQUENCY DISTRIBUTION OF SHALLOW AND DEEP GROUNDWATER

sandy soils cannot be clearly distinguished from that of canal system as:

(a) it rapidly infiltrates down to the level at which it cannot be taken up and removed by evapotranspiration.

(b) the infiltrating irrigation water in sandy soils does not undergo any evaporation and its isotopic contents remain unchanged before infiltration (see section 5.3)

However, during the upward movement of soil moisture as a result of evaporation, the moisture of upper layers become enriched in heavy isotopes. At such a stage, the percentage of moisture of such dry layers is smaller as compared to post-irrigation conditions and mixing of this moisture with irrigation water does not shift the isotopic index of infiltrating water.

## 6. Conclusions

The results of this study indicate that in loamy soils the penetration of irrigation water is limited to a maximum of one meter depth and most of it remains stored in the upper layers of the soil whence it starts evaporating upward. In sandy soils this penetration is many times more and contribution of irrigation water to the underground reservoir becomes significant. Similar is the case of rains. Flow velocities (at 1 m depth and 20 vol. % moisture) are of the order of 16 m/a and less than 1.6 m/a for sandy and loamy soils respectively.

In the case of prolonged flooding of these fields - due to long duration rains or irrigation channels, the flow velocities are many times higher and decrease with depth.

Consequently the groundwater rise (water logging) is mainly due to the infiltration from canal system. The contribution from irrigated fields and rains to groundwater recharge is considered to be less than 30 %.

As remedial measures against water logging, the canal system passing through sandy soils be lined and irrigation practices in highly permeable soils be modified by reducing the delta of irrigation water.

Acknowledgement

Authors are grateful to the International Atomic Energy Agency, Vienna for providing technical assistance under the Project PAK/2734/GS, in the form of scientific supplies and expert services. Parts of the project were initiated in the frame of a german pakistan collaboration, sponsered by Kernforschungszentrum,Karlsruhe The local expenses were met by PINSTECH and NIAB. The keen interest taken by Directors of PINSTECH and NIAB is acknowledged with gratitude. Thanks are also due to many colleagues of both Institutes for their time to time help and cooperation. Special thanks are due to Mr. Riffat M. Qureshi for useful discussions on the text of the paper.

References

1. Krishnan, Geology of India & Burma.

2. Wadia, D.N. 1966, Geologiy of India.

3. Wynes, A.B. 1870, Records of Geological Survey of India.

4. Epstein, S., Mayeda, T.; Variations of the $O^{18}$ content of waters from natural sources. Geochim. Cosmochim. Acta 4 (1953) 213-224.

5. Gat, J.R.: Comments on the stable isotope method in Regional Groundwater investigations, Water Resources, Res. 1 (1971) 980-993.

6. IAEA, Guide book on nuclear techniques in hydrology (1968).

7. IAEA, Guide book on Nuclear Techniques in Hydrology (1983), Technical report series No. 91, IAEA, Vienna.

8. Ahmad, N. 1974: "Groundwater Resources of Pakistan" Ripon Printing Press, Lahore.

9. Seiler, K.P., Stichler, W., Hanif, M; Hussain, D., and Sajjad, I. "Isotopic and Hydrochemical studies at Faisalabad/Pakistan", Interamerican symposium on Isotope Hydrology; Bogota, Colombia, 18-22 August 1980.

10. HAQ, M.I.; SAJJAD, M.I; MALIK, K.A., Study of Downward Movement of Soil Water in Unsaturated Zone Using Isotopic Techniques, Proceedings of an International Symposium on "Isotope and Radiation Techniques in Soil Physics and Irrigation Studies" jointly organized by IAEA & FAO and held in AIX-EN-Provence, France, 18-22 April 1983, page: 375-388.

11. Thomas,G,W;and Swoboda,A,R. Anion exclusion effects of chloride movement in soils. Soil Science 110(1970)163-166.

# ETUDE ISOTOPIQUE ET GEOCHIMIQUE DES MOUVEMENTS ET DE L'EVOLUTION DES SOLUTIONS DE LA ZONE AEREE DES SOLS SOUS CLIMAT SEMI-ARIDE (SUD TUNISIEN)

K. ZOUARI*, J.F. ARANYOSSY**, A. MAMOU***, J.-Ch. FONTES*

* Laboratoire d'hydrologie et de géochimie isotopique, Université de Paris-Sud, Orsay, France

** Section d'hydrologie isotopique, Agence internationale de l'énergie atomique, Vienne

*** Direction des ressources en eau et en sol, Tunis, Tunisie

**Abstract**

Continuous core were obtained by dry coring through the unsaturated zone of the Djebel Dissa (Southern Tunisia). Segments of cores were distilled under vacuum. Oxygen 18 and deuterium analyses indicate a kinetic evaporation. The evaporating ressource was probably recharged through an exceptional rainy event or through a leakage of the deep confined aquifer.

The modelization, according to Barnes and Allison [22] gives an estimate of 1 mm $a^{-1}$ for the evaporation rate. The ionic balance is calculated after lixiviation of soil aliquotes. It shows an accumulation of salts above a depth of 7 m in the profile, in agreement with the isotope profile.

**Résumé**

Des carottes d'une vingtaine de mètres ont été réalisées à sec dans la zone non saturée de le région du Djebel Dissa (Sud Tunisien). Les tronçons de carottes ont été distillés sous vide. Les analyses de teneurs en $^{18}O$ et $^{2}H$ montrent que les solutions des profils subissent une évaporation cinétique à partir d'une recharge correspondant à une épisode de pluie exceptionnelle ou à une remontée de la nappe profonde captive. La modélisation du phénomène selon Barnes et Allison [22] conduit à une estimation de 1 mm $a^{-1}$ pour l'évaporation à travers le profil. Le bilan ionique obtenu par lixiviation montre une accumulation des sels au dessus de 7 m dans le profil ce qui est en accord avec l'évolution isotopique.

## I. INTRODUCTION

Dans les régions arides à semi-arides, les précipitations sont souvent irrégulières tant en intensité qu'en hauteur. L'évapotranspiration réelle est mal connue. Ainsi, l'évaluation du taux d'infiltration moyen à l'échelle du bassin versant, du sous bassin ou de la parcelle par estimation des différents termes du bilan hydrique est souvent entachée d'une forte incertitude. En particulier, les effets des fortes précipitations sur la recharge des nappes sont généralement mal appréhendés. De plus, les techniques hydrologiques classiques n'apportent pas suffisamment d'informations sur la migration des substances dissoutes dans la zone non saturée.

Donc, toute étude hydrogéologique en climat aride ou semi-aride, gagnera à être doublée d'une étude géochimique et isotopique qui permet d'examiner plus finement les mécanismes de l'infiltration et de l'évaporation.

Dans cette optique, l'étude réalisée au niveau du Djebel Dissa, dans le sud tunisien avait pour objectif:

- de mieux connaître les phénomènes qui accompagnent les mouvements de l'eau dans la zone non saturée,
- de mieux définir l'importance des évènements pluvieux exceptionnels sur la recharge des nappes,
- de préciser la migration des substances dissoutes dans la zone non saturée,
- d'estimer un taux d'évapotranspiration à travers les profils.

Ces différentes questions sont abordées par l'examen du traçage naturel par les isotopes de l'environnement ($^{18}O$, $^{2}H$), par les techniques géochimiques et par l'étude des paramètres hydrodynamiques de l'eau dans le sol sur des échantillons prélevés en carottage continu de profils de zone non saturée.

## II. CADRE GENERAL

### II.1 Choix du site

La cuvette du Djebel Dissa, situé à environ 15 km au NW de Gabès (33°55'N, 9°58E), est un petit bassin d'environ 45 $km^2$ de superficie qui collecte le

ruissellement des reliefs le long d'un petit cours d'eau temporaire: "l'Oued El Hebaji" dont le lit occupe longitudinalement le centre du bassin (fig. 1).

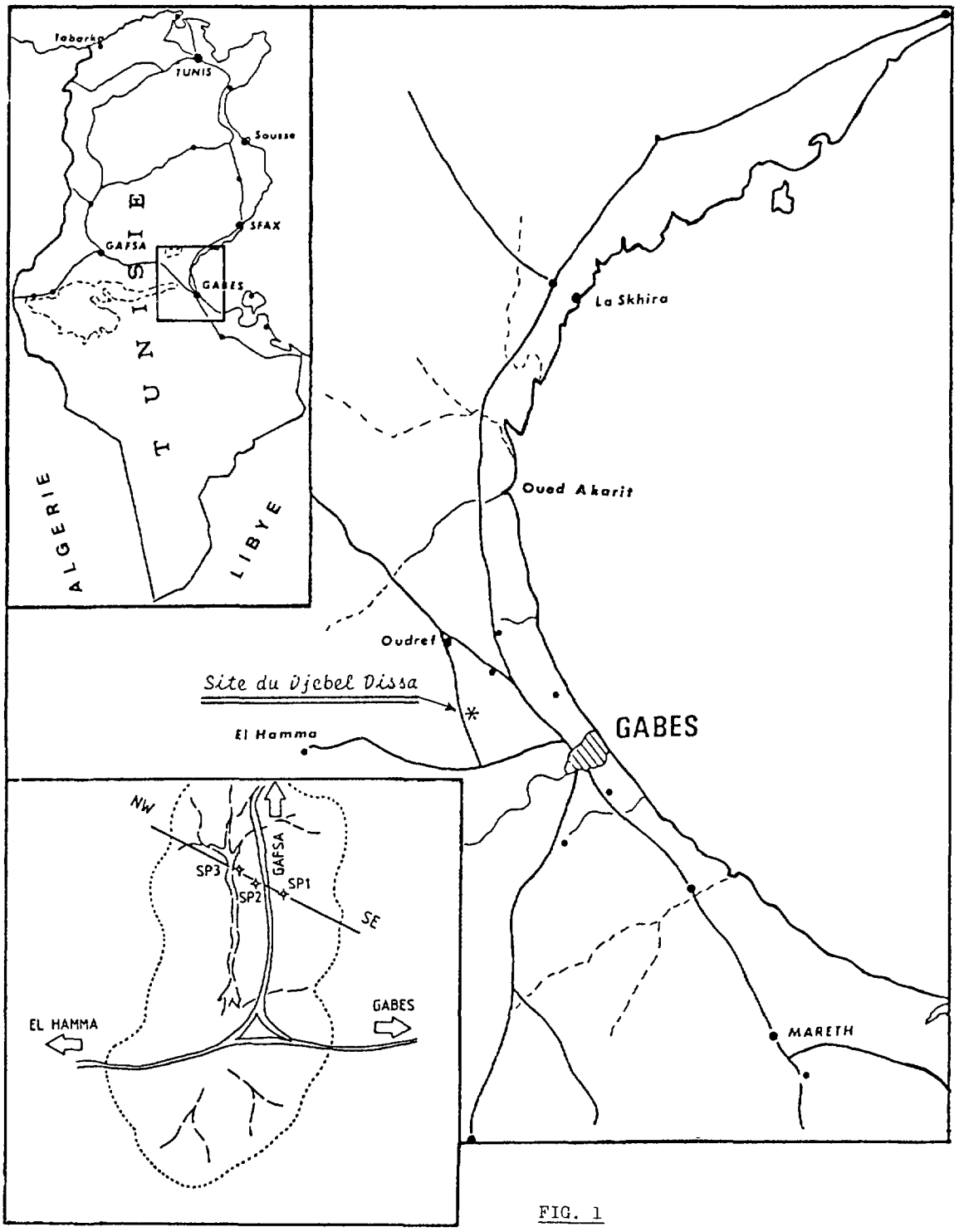


FIG. 1
Situation Géographique

Les raisons du choix de ce site furent:

- La disponibilité d'une série d'observations climatiques et hydropédologiques [1], ainsi que des résultats d'expériences de traçage isotopique et chimique [2] et des évaluations des paramètres hydrodynamiques de la zone non saturée [3].

- L'épaisseur locale de la zone non saturée, de l'ordre de 20 m, qui en fait un secteur favorable à l'étude de l'infiltration verticale.

- La pente topographique assez forte qui permet l'écoulement de surface ainsi que l'écoulement de la nappe phréatique vers le centre du bassin.

## II.2 Cadre géologique

La zone du Djebel Dissa est représentée par des dépôts alluviaux, colluviaux et éoliens du Quaternaire récent ou actuel, surmontant des dépôts silteux et argilo-gypseux du Plio-Quaternaire, le tout adossé à un relief calcaire et calcaro-marneux du Crétacé supérieur (Sénonien).

Les formations géologiques du site choisi se présentent de la façon suivante (fig. 2):

- Le Sénonien inférieur: Alternances de marnes jaunes ou blanches et de calcaires durs formant les flancs occidentaux de la colline. Les marnes sont souvent gypseuses et érodées.

- Le Sénonien supérieur: Calcaires blancs à roses qui constituent les reliefs du sommet du Djebel Dissa.

- Le Mio-Pliocène: Dépôts argilo-sableux à intercalations gypseuses avec sables et graviers à la base et croûte gypseuse à la partie sypérieure.

- Le quaternaire récent et actuel: Sédimentation continentale fine alluvionnaire, silto-limoneuse avec intercalation de gypse.

L'ensemble des dépôts quaternaires et mio-pliocènes est peu perméable [1, 3].

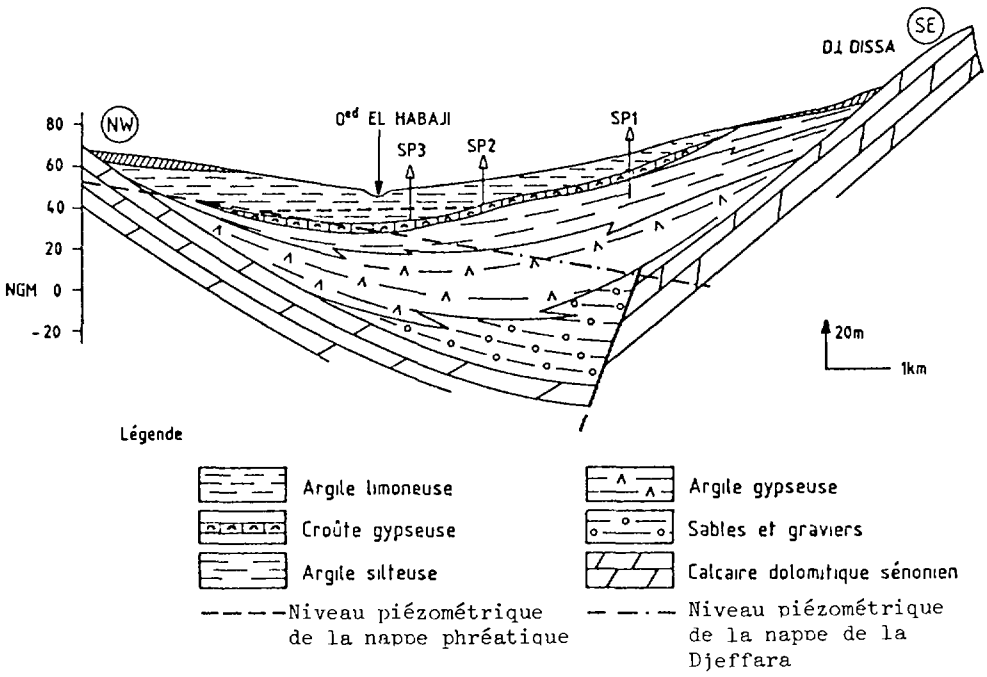


FIG 2 Corrélation lithostratigraphique a travers le BV. de DJ DISSA

## II.3 Cadre hydrogéologique

La nappe phréatique rencontrée au droit du site - à 7 m de profondeur à proximité de l'oued - correspond au niveau aquifère le plus superficiel d'un complexe multicouche logé dans les formations sénoniennes (calcaires), mio-pliocènes (sables et argiles) et quaternaires (alluvions).

Ce complexe aquifère porte le nom de "Nappe de la Djeffara", il reçoit la majeure partie de son alimentation par drainage de la nappe du "Continental Intercalaire" au niveau du seuil tectonique d'El Hamma situé 25 km plus à l'ouest [4, 5].

Les communications hydrauliques des niveaux aquifères de la nappe de la Djeffara au niveau du site ne sont pas bien connues. Cependant, la composition chimique de la nappe phréatique, similaire à celle des niveaux inférieurs de la nappe de la Djeffara suggère une drainance verticale à partir du niveau inférieur.

D'autre part, le suivi des fluctuations piézométriques de la nappe phréatique, montre une réponse très nette et rapide à la pluviométrie (fig. 3). Ceci démontre qu'au moins une partie des précipitations participe directement à l'alimentation de la nappe phréatique.

## II.4 Caractères climatiques

Le climat de la région de Djebel Dissa se caractérise par une pluviosité généralement faible, très variable et irrégulièrement répartie sur environ sept mois de l'année (de septembre à mars). La pluviosité annuelle moyenne est de l'ordre de 200 mm [2]. Cette pluviosité se caractérise par la présence d'événements exceptionnels; sécheresse prolongée et pluies de forte intensité (atteignant 150 $mm.h^{-1}$).

La température moyenne annuelle de la région est de l'ordre de 20°C, le mois le plus chaud est juillet (27°C) et le plus froid est janvier (10°C).

L'évaporation "piche" mesurée est très variable d'une année à l'autre, la moyenne est de l'ordre de 1800 mm. L'évapotranspiration calculée suivant la formule de Turc est de l'ordre de 1400 mm.

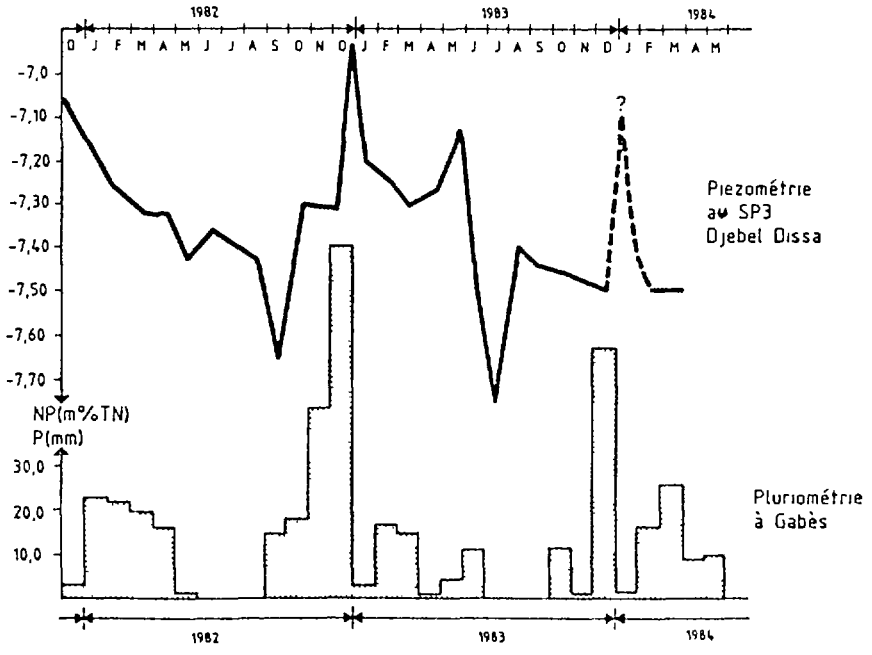


FIG 3 PIEZOMETRE DJ DISSA SP3

Le régime des vents saisonniers est le suivant:

- novembre à avril: les secteurs dominants sont W, NW, SW. Les vents sont alors violents et froids.

- mai à octobre: les vents de secteurs marins dominent (NE, E, SE), ils sont moins violents que les précédents et souvent chargés d'humidité.

- le sirocco: vent saharien, très chaud et sec, entraîne une brusque montée de température, un abaissement rapide de l'humidité relative de l'air et une forte évaporation.

## II.5 Caractéristiques isotopiques des précipitations

En l'absence de station de mesures des compositions isotopiques des précipitations dans le sud Tunisien, nous avons considéré les teneurs isotopiques des précipitations à Tunis-Carthage (station située au nord de la Tunisie: 36°83'N, 10°23'E et altitude 4 m), ceci malgré les sensibles différences climatiques entre les deux régions.

Les moyennes mensuelles pondérées des teneurs en oxygène-18 et en deutérium des précipitations pendant la période 1968-81 sont représentés sur les figures (4) et (5).

On peut distinguer:

a) Les mois pour lesquels la valeur mensuelle des précipitations est supérieure à 80 mm (fig. 4); ils se situent pour la plupart entre la droite des eaux météoriques en domaine océanique à l'échelle mondiale définie par CRAIG [6] et d'équation $\delta^2H = 8\ \delta^{18}O + 10$ d'une part, et celle des précipitations du bassin méditerranéan oriental définie par NIR [7] et GAT[8] pour laquelle l'excès en deutérium atteint +22 d'autre part. Les points *représentatifs de ces fortes précipitations à Tunis-Carthage s'alignent sur* une droite de régression: $\delta^2H = 7{,}99\ \delta^{18}O + 12{,}4$. Ils correspondent à des précipitations qui n'ont pas subi d'évaporation pendant la chute des gouttes d'eau. Leur teneurs moyennes en isotopes lourds est de -5‰ pour l'oxygène-18 et -30,2 pour le deutérium.

b) Les mois pour lequels la valeur mensuelle des précipitations est inférieure à 80 mm (fig. 5); la majeure partie de ces points se situe en dessous de la droite météorique à l'échelle mondiale. Ceci indique nettement que ces eaux météoriques ont subi une évaporation. Leur composition isotopique a donc été modifiée après condensation et ne reflète plus celle des masses d'airs humides dont elles sont issues. La moyenne est déplacée vers des valeurs enrichies en isotopes lourds ($\delta^{18}O = -3{,}81$, $\delta^2H = -21{,}97$‰/SMOW).

En conclusion, les précipitations supérieures à 80 mm, non évaporées, correspondent aux mois les plus froids et les plus humides. L'excès en

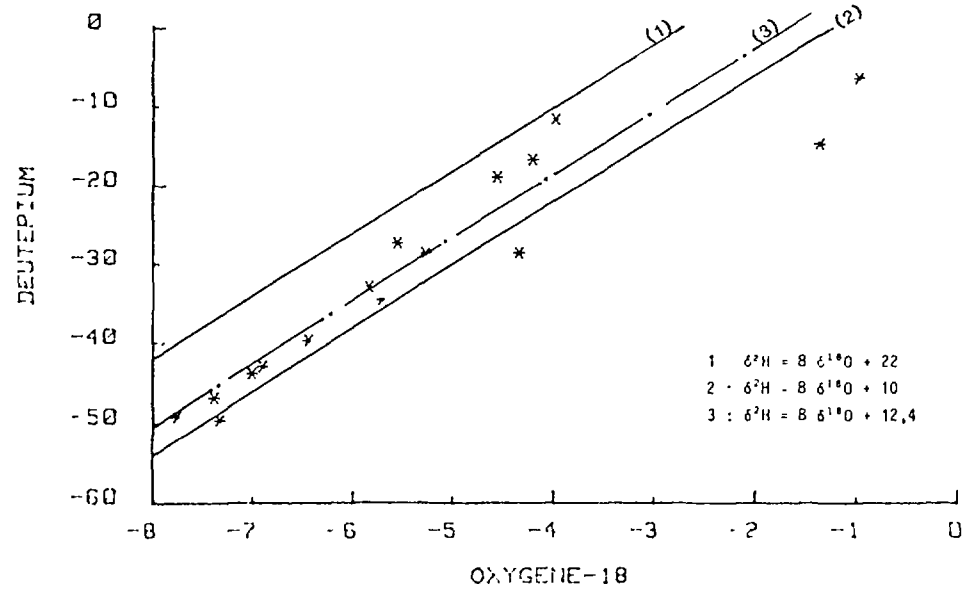


Fig 4 TUNIS - MOYENNES MENSUELLES > 80 mm

Période 1968-1981

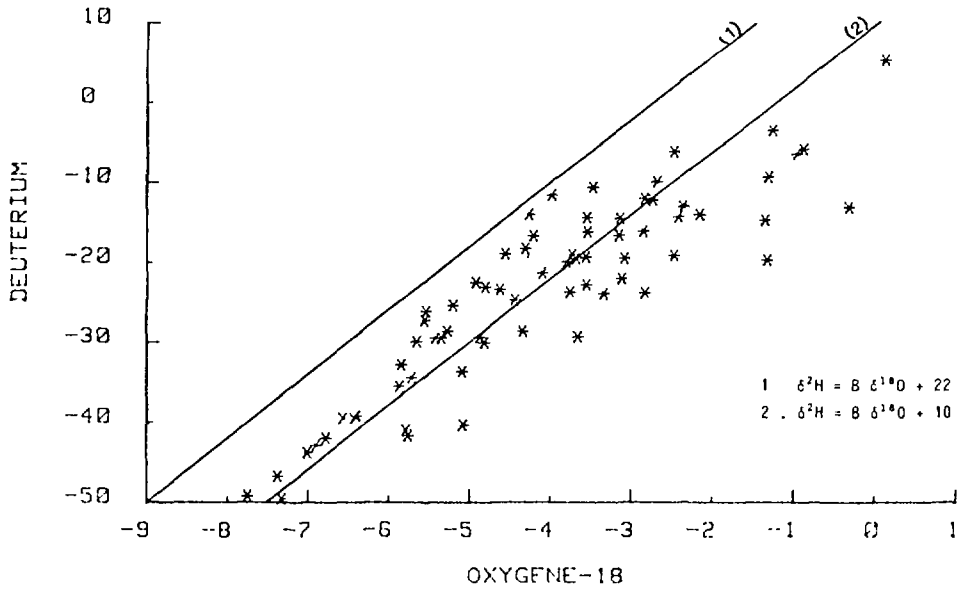


Fig 5 VALEURS MOYENNES MENSUELLES < 80mm

Tunis Carthage ( 1968-1981 )

d'après IAEA .

deutérium voisin de +12 traduit un mélange entre des vapeurs condensables d'origine océanique et méditerranéenne. Ainsi une recharge éventuelle pourra se produire pendant cette période où le bilan théorique en eau des sols est le plus favorable à l'infiltration. En revanche, les précipitations enrichies en isotopes lourds ont vraisemblablement subi une évaporation lors de la chute des gouttes d'eau dans un profil de l'atmosphère non saturée en vapeur d'eau. Elles correspondent aux mois chauds et de faible pluviosité.

## III. PLAN EXPERIMENTAL

### III.1 Travaux de terrain

Deux techniques ont été pratiquées pour les prélèvements d'échantillons :

- La méthode de la tarière manuelle qui peut atteindre, en rajoutant des éléments de rallonge au fur et à mesure de la progression du sondage, une profondeur de l'ordre de 10 m.

- La méthode "rotary" à sec (sans boue de forage), avec carottage pour extraction des échantillons dans les conditions les plus représentatives possibles.

  Trois carottages ont été réalisés pendant le mois d'avril 1981. Ces sondages ont été répartis de façon à représenter le mieux possible le bassin dans sa totalité (fig. 2). En amont, sondage SP1, profondeur 18,45 m, altitude 70 m. A 800 m de distance, à mi-pente, sondage SP2, profondeur 20,25 m, altitude 60 m. Au fond de la cuvette et à 500 m de distance de SP2, sondage SP3, profond de 19,8 m à 55 m d'altitude. La nappe a été rencontrée dans le sondage SP3 seulement, vers 7 m de profondeur (fig. 2).

Les sondages ont été entièrement carottés à sec afin de ne pas mélanger de l'eau de foration avec celle du profil. Les carottes ont été ensuite tronçonnées en échantillons de 10 à 20 cm de hauteur, conservées dans des boîtes de type "boîtes de pédologues" en aluminium dont l'étanchéïté était parachevée par la pose d'un ruban adhésif autour du couvercle.

Les profils lithologiques, établis sur le terrain, sont représentés sur la figure 6. Ils se caractérisent par des alternances de sables fins, sables gypseux, silteux et argileux.

### III.2 Opérations au laboratoire

a) Granulométrie

La granulométrie des éléments grossiers a été déterminée au laboratoire de l'ORSTOM à Gabès et les valeurs moyennes sont données par FERSI et al. [9].

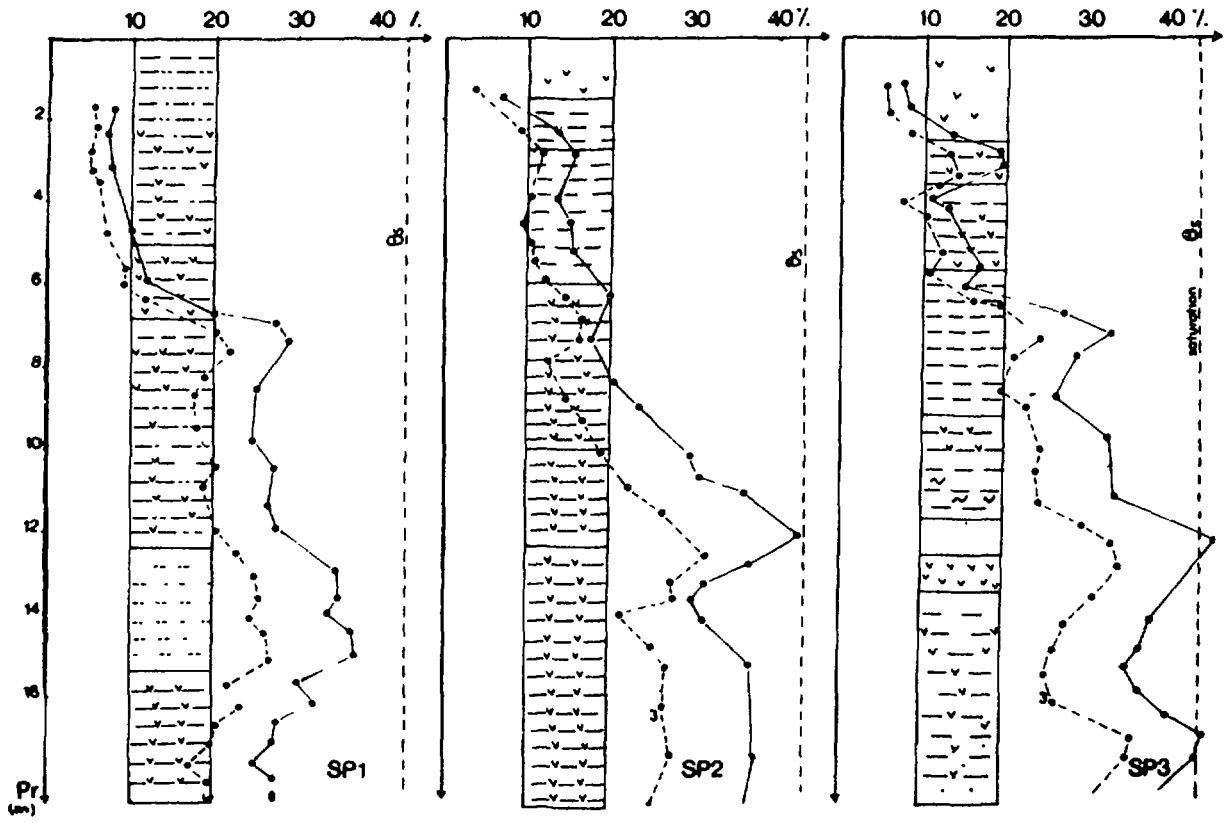


Figure 6 : PROFILS HYDRIQUES

Elle se présente de la manière suivante:

Particules < 2µm: 12%, limon fin; 2 à 20 µm: 12%, limon grossier; 20 à 50 µm: 7%, sable fin; 0,05 à 0,2 mm: 60%, sable grossier; 0,2 à 2 mm: 9%.

On note aussi la présence de matière organique, en moyenne 2%, ainsi que de gypse à la surface du sol ou dans les sédiments.

b) Minéralogie

Des mesures de diffraction de rayon x ont été réalisées sur des sédiments bruts. Les sédiments des sondages SP1 et SP3 présentent une minéralogie généralement homogène. Le quartz est le minéral qui domine dans ces deux profils. Il est présent à tous les niveaux et particulièrement dans les sept premiers mètres.

On trouve aussi du gypse le long des profils mais en faible quantité à partir de 6 m de profondeur. Certains minéraux argileux en faibles quantités ont été détectés (attapulgite) essentiellement dans les niveaux inférieurs des profils. Enfin, on note la présence de traces de calcite.

c) Teneurs en eaux des sédiments

L'extraction de l'eau des sédiments a été obtenue par distillation sous vide, afin d'éviter la contamination par la vapeur d'eau atmosphérique, suivant la technique déjà utilisée par SMITH [10], GONFIANTINI [11] et GOUVEA DA SILVA ROSA [12]. En se basant sur les définitions classiques [13], on a calculé les teneurs en eau pondérales dans les sédiments du sol, ainsi que les humidités volumiques correspondantes. Les résultats sont reportés sur le tableau 1. Les profils hydriques obtenus pour les trois sondages sont représentés sur la figure 6.

d) La technique d'élution

Les teneurs ioniques et la conductivité ont été mesurées sur des solutions d'élution des sédiments. La technique consiste à disposer une quantité précise de sédiment sec dans un volume d'eau déminéralisée et à agiter pendant environ 40 minutes, durée nécessaire à la dissolution des sels (déterminée par des mesures de conductivité faites tous les 3 minutes jusqu'à stabilisation).

En considérant:

$M_s$ = masse de l'échantillon de sol sec pris pour élution
$Q$ = quantité d'eau d'élution
$C_Q$ = concentration mesurée dans l'eau d'élution
$w$ = humidité pondérale mesurée

La concentration $C_i$ de la solution initiale du sol s'exprime par:

$$C_i = \frac{(Q \times C_Q)\ (1 - w)}{w\ M_s}$$

(en assimilant la volume d'eau Q à sa masse).

## IV. ANALYSES DES RESULTATS GEOCHIMIQUES ET ISOTOPIQUES

### IV.1 Chimie des eaux de la nappe

L'analyse chimique de l'eau de la nappe phréatique montre deux tendances dont la première prédomine:

- des eaux sulfatées calciques qui peuvent être expliquées par la dissolution du gypse, très répandu dans la région;

- des eaux chlorurées sodiques qui ont probablement comme origine le lessivage de NaCl apporté par voie atmosphérique sous forme d'embruns marins et accumulé dans les horizons supérieurs du sol sous l'effet de l'évaporation.

### IV.2 Variations de la salinité de l'eau dans la zone non saturée

a) Variations de la conductivité en fonction de la profondeur

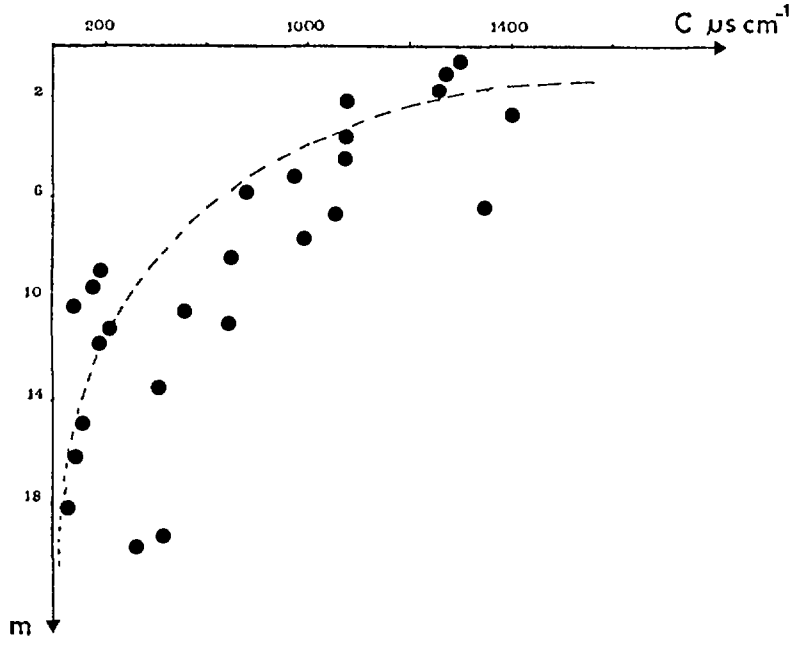


Fig 7 Relation: conductivité-profondeur SP3

Sur la figure 7 on constate que les teneurs totales en sels dissous des extraits aqueux, obtenus par élution des échantillons de sol, augmentent du bas des profils vers la surface. Les points représentatifs de cette évolution obéissent à une relation de type exponentiel dont le coefficient de corrélation est $r^2 = 0,68$.

Une autre relation établie entre les teneurs en sulfate et la profondeur (fig. 8) traduit la même évolution, ce qui montre l'importance de cet ion dans la salinité des solutions du sol. Toutefois, étant donnée la présence de gypse dans les profils il est probable qu'une partie de sulfate des solutions provienne de la matrice.

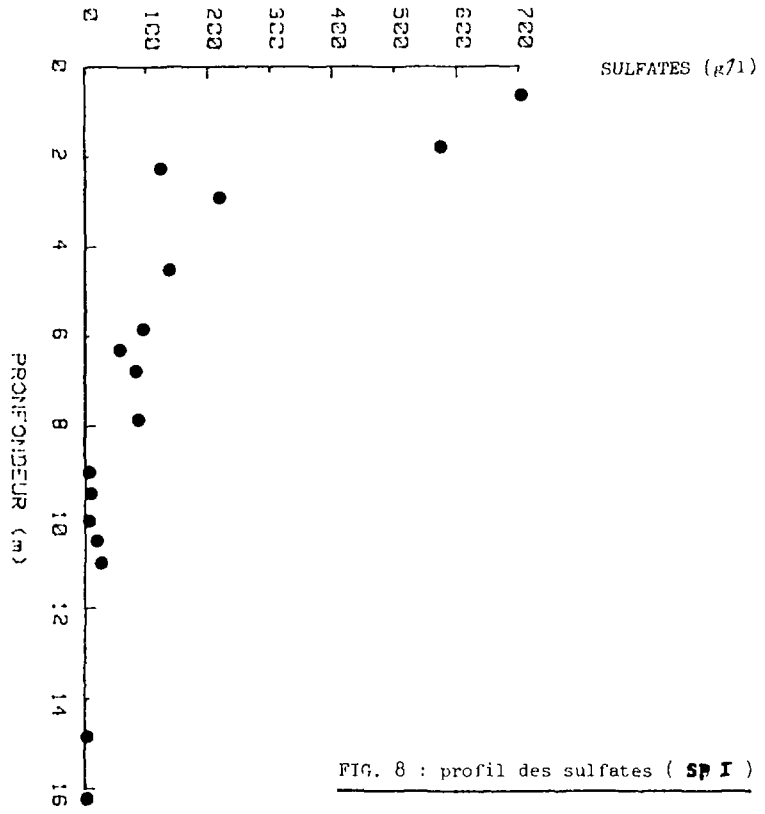


FIG. 8 : profil des sulfates ( SP I )

Cette évolution implique une concentration progressive en sels des solutions qui migrent par ascension capillaire sous l'effet de l'évaporation depuis les horizons inférieurs vers la surface. Ces observations sont en accord avec cells de TOOD et KEMPLER [14], EDMUNDS et WALTON [15], et GOUVEA DA SILVA ROSA [12].

b) Variations des teneurs en chlorures en fonction de la profondeur

L'évolution des teneurs en chlore des eaux interstitielles des profils avec la profondeur semble également traduire une concentration progressive vers la surface (fig. 9).

Toutefois, on observe, surtout dans les horizons supérieurs, des fluctuations comparables à celles qui ont été également mises en évidence dans les profils de ce type et qui sont probablement imputables aux variations de concentration dans les apports successifs des précipitations ainsi qu'aux effets de la ponction racinaire.

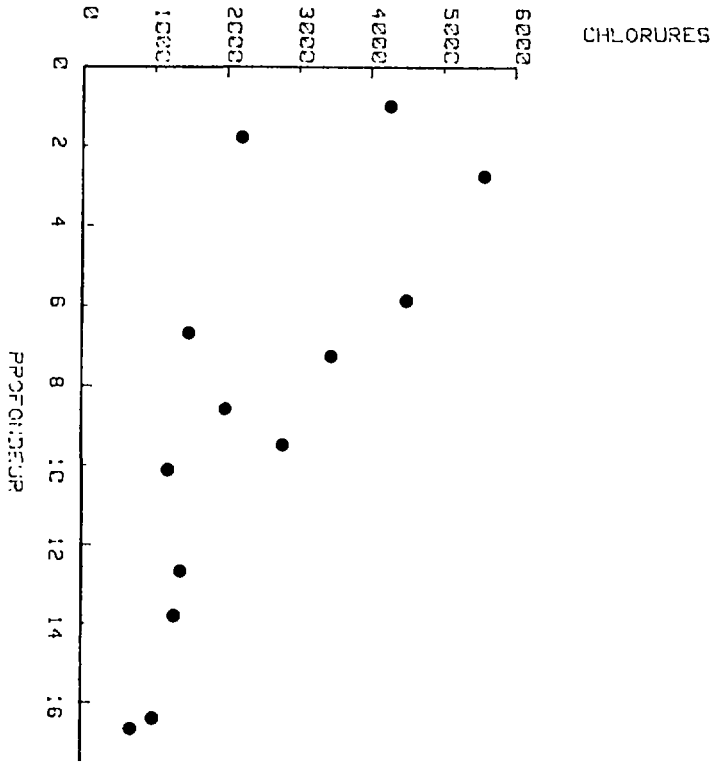


FIGURE 9 SONDAGE SP-1 Dj. DISSA

L'évaluation de l'évaporation réelle et de la recharge moyenne annuelle des nappes peut être théoriquement estimé par un bilan chimique des teneurs en chlorures. Cette méthode est souvent utilisée en climat aride ou semi-aride [15, 16].

On utilise la simple relation:

$$\frac{Q_v}{Q_I} = \frac{C_i}{C_p} - 1$$

avec $Q_v$ = quantité d'eau évaporée

$Q_i$ = quantité d'eau infiltrée

$C_i$ = concentration dans l'eau d'infiltration

$C_p$ = concentration dans l'eau de pluie

L'application de ce mode de calcul a permis d'estimer un rapport $Q_v/Q_i$ de l'ordre de 34 qui correspond à un taux moyen de recharge annuelle de l'ordre de 5 mm sur le site Dissa. Le calcul a été fait en considérant la valeur de 1600 mg/l comme concentration moyenne en chlorure de l'eau interstitielle.

## V. RESULTATS ISOTOPIQUES

### V.1 Présentation des résultats

Les variations des teneurs en isotopes lourds (oxygène-18 et deutérium) de l'eau du sol en fonction de la profondeur (fig. 10) pour les sondages SP1 et SP3 montrent:

- une zone superficielle (de 0 à 7 m de profondeur) où les variations de teneurs en oxygène-18 sont semblables. On y constate un enrichissement progressif depuis 7 m jusqu'à la surface.

- une zone profonde (au dessous de 7 m) où les teneurs en isotopes lourds ne varient pratiquement plus (SP3) ou très faiblement (SP1).

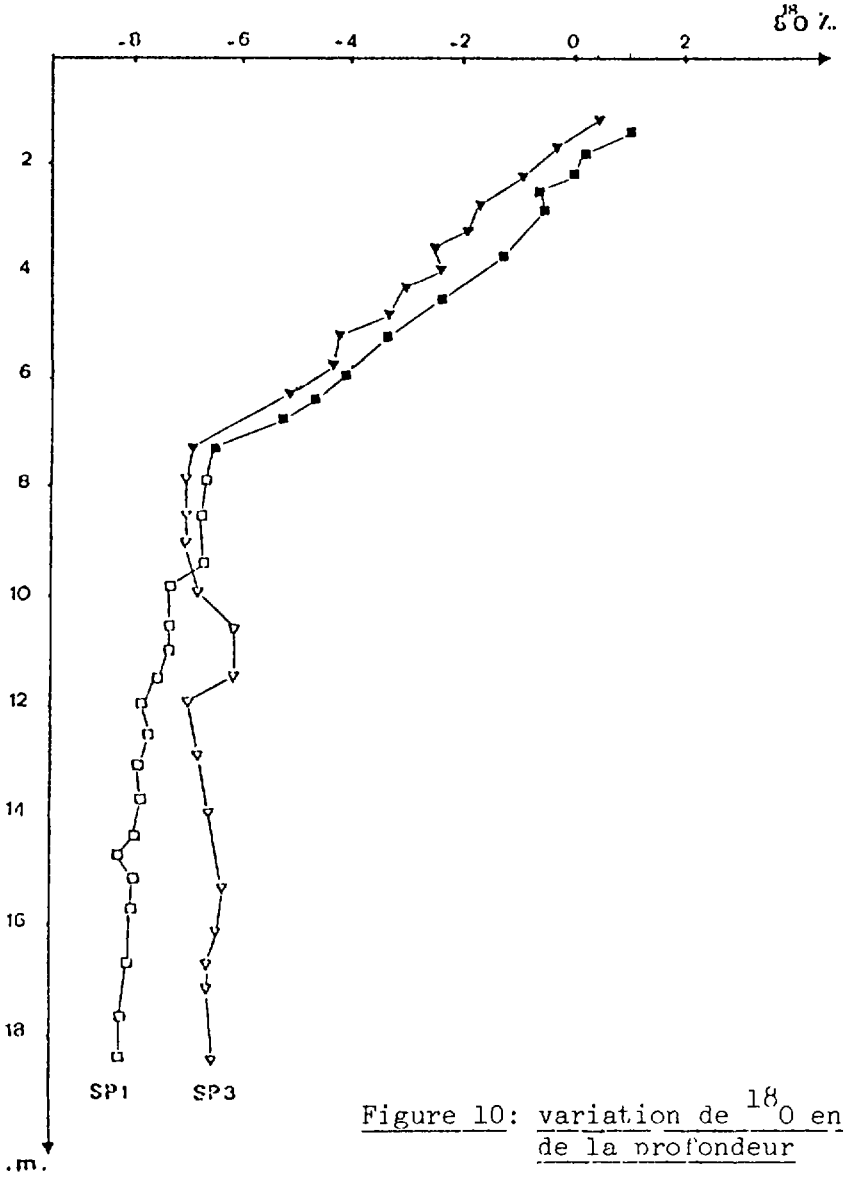


Figure 10: variation de $^{18}O$ en fonction de la profondeur

Dans un diagramme $\delta^2H$ en fonction de $\delta^{18}O$ (fig. 11), les points représentatifs des eaux de la zone superficielle (0-7 m), du sondage SP1 se disposent sur une droite d'évaporation d'équation: $\delta^2H = 3,86\ \delta^{18}O - 26,01$ ($r^2 = 0,6$).

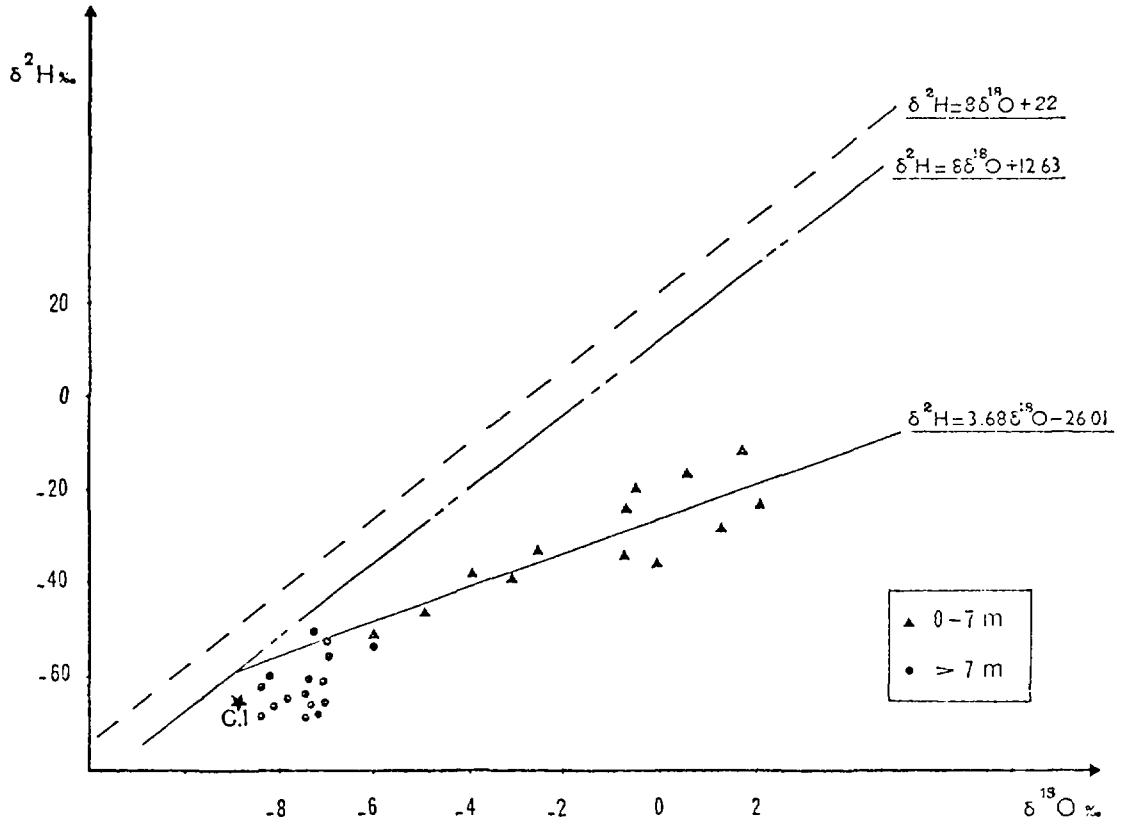


Figure 11 Relation: $^{18}O$ - $^{2}H$ (SP1)

L'examen du diagramme $^2H$ - $^{18}O$ des eaux du sol du sondage SP3 (fig. 12), montre tout d'abord l'importance de l'enrichissement isotopique dans la zone non-saturée située entre 7 m de profondeur et la surface.

Il est remarquable que la droite de régression passe à proximité du point représentatif de l'eau de la nappe du "Continental Intercalaire". Cela pourrait suggérer une alimentation per ascensum de la nappe phréatique par les eaux provenant du "Continental Intercalaire".

## V.2 Interprétation des résultats

### a) Relation $^{18}O$ - $^{2}H$

L'intersection de la droite d'évaporation, définie à partir des points représentatifs des eaux de la zone superficielle (0 à 7 m) du sondage SP1,

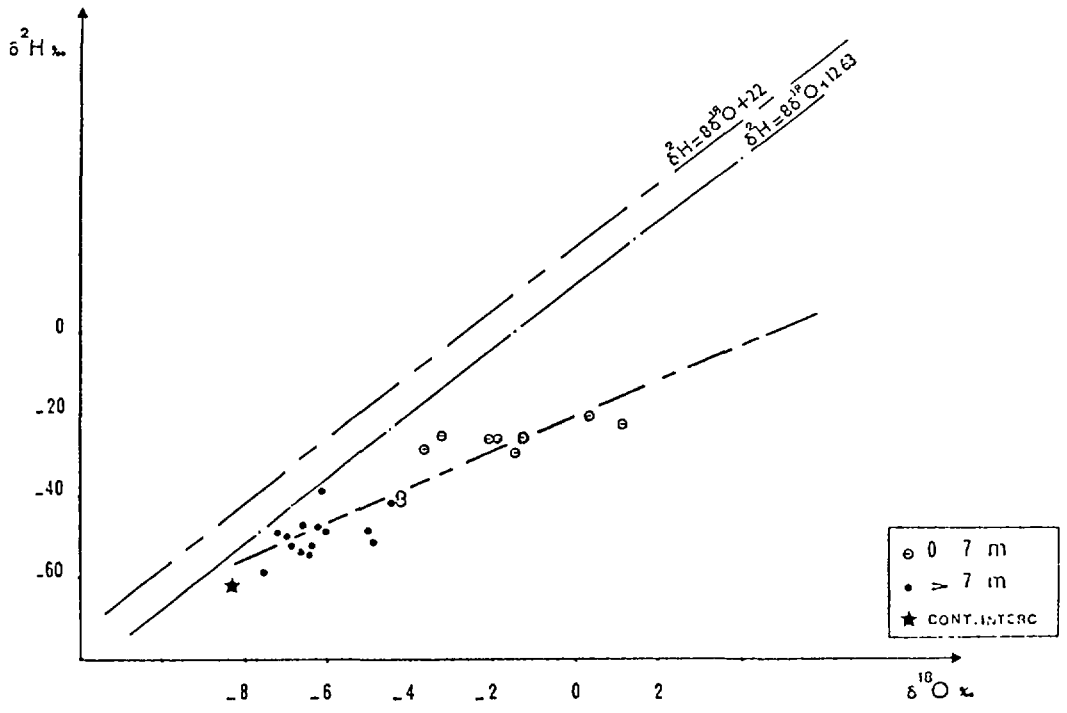


Figure: 12 Relation: $^{18}O$-$^{2}H$ (SP3)

avec la droite de pente 8, définie par les précipitations moyennes mensuelles supérieures à 80 mm à Tunis-Carthage ($\delta^2H = 8\ \delta^{18}O + 12,4$) permet d'évaluer une teneur en $^{18}O$ moyenne des précipitations infiltrées voisine de -8.8‰ ± 0.2‰. Il en est sensiblement de même pour SP3.

La teneur moyenne pondérée en oxygène-18 des pluies à Tunis-Carthage pendant les mois d'hiver (période favorable à une recharge éventuelle) étant de -5,5‰/SMOW (cf chap. II.5), il apparaît ainsi une différence significative entre la teneur moyenne en oxygène-18 des eaux de la nappe et de celle des eaux qui sont susceptibles de l'alimenter. Deux hypothèses pourraient permettre d'expliquer cette différence:

- Des chutes de pluies d'intensité assez forte saturent momentanément l'atmosphère en vapeur d'eau et arrivent au sol sans avoir subi d'évaporation notable. Ces pluies très appauvries en isotopes lourds s'infiltrent ensuite rapidement. Ce phénomène a été observé dans le Sahara occidental en Algérie par CONRAD et FONTES [17], à Béni-Abbès dans le désert algérien [18], en Libye par de nombreux auteurs [19, 20, 21]. Généralement, ces précipitations se produisent à haute altitude, à basse température et ne subissent guère qu'une rééquilibration avec leur propre vapeur.

- Le sol pourrait être en partie alimenté par un réservoir sous-jacent, c'est à dire par la nappe du "Complexe Terminal" ou du "Continental Intercalaire"

dont les valeurs en $^{18}O$ moyenne sont respectivement voisines de -7‰ à -8,4‰. En effet l'analyse isotopique des eaux souterraines de la région [4], a mis en évidence un apport ascendant de l'eau en provenance du "Continental Intercalaire" dans la région d'El Hamma à l'ouest de Gabès, à travers un système de failles qui favorise cet apport.

b) Variations des teneurs en oxygène 18 en fonction de la profondeur

Dans la zone superficielle (0 à 7 m), les variations en oxygène-18 présentent un enrichissement progressif, résultat d'une évaporation de type cinétique.

L'allure du profil du sondage SP1 dans la zone profonde (en dessous de 7 m) peut être expliquée par une diffusion en phase liquide vers le bas des isotopes lourds accumulés sous l'effet de l'évaporation. Ce processus rend compte du faible gradient décroissant de concentration en oxygène 18 entre la zone située vers 7 m de profondeur et la base du sondage.

A l'aide de l'application numérique de l'équation de diffusion sous sa forme la plus simple:

$$C(x,t) = C_o \exp - \frac{(x - x_o)^2}{4\ Dt}$$

C = concentration en $^{18}O$

D = coefficient de diffusion dans le milieu poreux

t = temps

x = distance au temps t

$x_o$ = distance au temps to

on peut tenter de quantifier le phénomène de diffusion qui serait engendré par le gradient de concentration isotopique observé.

Ce calcul indique toutefois que le transport par diffusion est faible et impliquerait un long temps d'évolution du profil.

Pour le sondage SP3, en dessous de 7 m, on est en présence d'un milieu saturé bien homogène puisque les valeurs en oxygène 18 n'évoluent plus en fonction de la profondeur. Néanmoins, la petite anomalie observée entre (10 - 12 m) serait due à une variation saisonnière du niveau piézométrique (battement de nappe).

c) Modèle d'évaporation

La tentative de modélisation se base sur l'équation proposée par Barnes et Allisson [22] pour décrire l'évolution des teneurs isotopiques dans la zone où le transfert liquide domine:

$$(\delta_i - \delta_{res}) = (\delta_{ef} - \delta_{res}) \exp [-f(z)/\hat{z}_i]$$

équation dans laquelle:

- $\delta_i$ = Composition isotopique à la distance z
- $\delta_{res}$ = Composition isotopique du réservoir
- $\delta_{ef}$ = Composition au maximum d'enrichissement isotopique
- f(z)= fonction de la distance définie par:

$$f(z) = \bar{\theta} \int_{zef}^{z} dz/\theta$$

- $Z_i$ = profondeur caractéristique liée au taux d'évaporation E, à la tortuosité $\tau$, à la teneur en eau volumique moyenne $\theta$ et à la diffusiuté $D_i$ des espèces en solution dans l'eau suivant la formule:

$$Z_i = \bar{\theta}\tau.D_i/E$$

Une représentation graphique de la fonction $\ln(\delta_i - \delta_{res})$ <u>versus</u> f(z) donne une droite de pente $-1/Z_i$ à partir de la quelle le taux d'evaporation peut être estimé.
L'application de cette équation aux profils obtenus à Dissa montre un accord satisfaisant entre les valeurs calculées et celles mesurées. (figure 13).

La relation graphique $\ln(\delta_i - \delta_{res})$ <u>versus</u> f(z) a permis de déterminer $\delta_{res}$ = -9.5‰. En appliquant les valeurs:

- $\delta_{ef}$ = +3,9‰,
- $Z_i$ = 8,0 mètres et
- $D_i$ = 1,45 . $10^{-9}$ $m^2.s^{-1}$ (Mills 1976 in [23])

on trouve:

$$E = \frac{\bar{\theta}\ \tau\ Di}{Z_i} \simeq 1mm/an$$

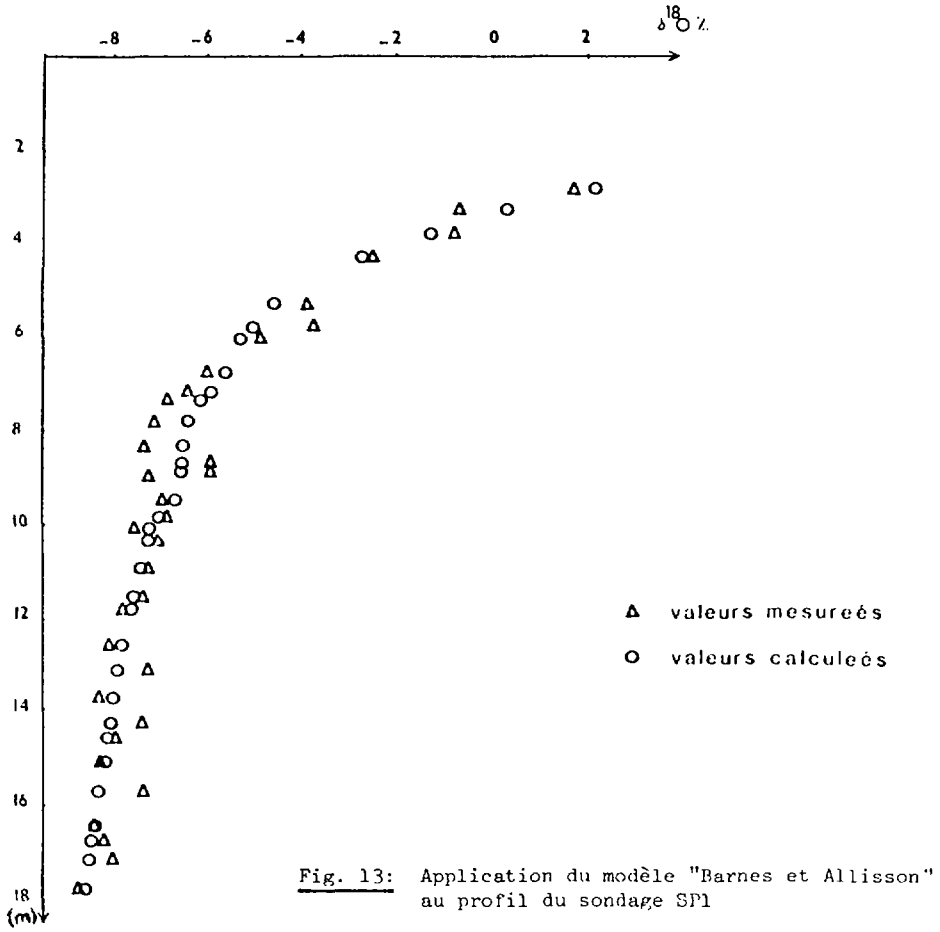


Fig. 13: Application du modèle "Barnes et Allisson" au profil du sondage SP1

## VI. CONCLUSION GENERALE

Cette étude de la zone non-saturée sous climat semi-aride à aride, à partir d'échantillons recueillis par carottage et distillation de profils de sol a permis de mieux définir les modalités du phénomène d'évaporation dans le milieu poreux non saturé:

1) L'évolution des teneurs en eaux pondérales et volumiques sur l'ensemble des profils montre qu'au dessus d'une profondeur d'environ 7 m, l'eau est reprise sous l'effet de l'évaporation.

2) Cette perte d'eau par évaporation est également mise en évidence par l'évolution des teneurs en isotopes lourds en fonction de la profondeur. En effet, les profils présentent, en général, un enrichissement en isotopes lourds dans la zone située entre 7 m de profondeur et la surface.

L'application du modèle d'évaporation de BARNES et ALLISON [22] montre un accord entre la courbe calculée et les données expérimentales. L'ajustement conduit à une valeur moyenne de 1 mm $a^{-1}$ pour le flux d'évaporation à travers le profil.

La comparaison des teneurs en oxygène-18 et en deutérium montre que les points représentatifs s'inscrivent dans le domaine des eaux évaporées dans des conditions cinétiques. De plus, les mesures des teneurs en isotopes stables ont permis de mettre en évidence une reprise évaporante à partir d'une réserve homogène correspondant à de fortes précipitations ou à une remontée de la nappe profonde.

3) L'étude du mouvement des sels montre qu'ils se comportent sensiblement comme les isotopes lourds, avec un enrichissement croissant des horizons inférieurs vers la surface sous l'effet de l'évaporation.

Par un bilan chimique portant sur les teneurs en chlorure, il a été possible d'estimer un taux de recharge efficace de l'ordre de 5 mm par an et un taux d'évapotranspiration réel de l'ordre de $Q_v/Q_i = 35$.

Références

[1] BOURGES, J., FLORET, C. et PONTANIER, R. (1973-75). Etude d'une toposéquence type du Sud Tunisien, Djebel Dissa. Publ. IES 89 et IES 93. ORSTOM, Tunisie.

[2] ARANYOSSY, J.F. (1978). Contribution à l'étude des transferts d'eau et de solutés dans la zone non saturée par traçage cationique et isotopique. Thèse, Paris. 132 p.

[3] VACHAUD, G., VAUCLIN, M. et COLOMBANI, J. (1981). Bilan hydrique dans le Sud Tunisien. Caractérisation expérimentale des transferts dans la zone non saturée. J. of Hydrology, 49, 31-52.

[4] ERESS (1972). Etude des ressources en eau du Sahara Septentrional Tunisie et Algerie. Rapport final. UNESCO, Paris.

[5] MAMOU, A. (1976). Contribution à l'étude hydrogéologique de la presqu'ile de Kebili. Thèse 3e Cycle. Paris VI.

[6] CRAIG, H. (1961). Isotopic variations in meteoric waters. Science, 133, 1702-1703.

[7] NIR, A. (1967). Development of Isotopes methods applied to groundwater hydrology. Am. Geophys. Union, Monograph. 11-109.

[8] GAT, J.R. (1970). Evolution of the isotopic composition of atmospheric water in the mediterranean sea area. Journal Geophys. Res. 75.

[9] FERSI, M. et ZANTE, P. (1981). Etude d'une toposéquence type du sud tunisien. Djebel Dissa. ES, 159. D.R.E.S., Tunisie.

[10] SMITH, D.B., WEAR, P.L., RICHARDS, M.J. et ROWE, P.C. (1970). Water movement in the unsaturated zone of high and low permeability strata by measuring natural tritium. In Isotope Hydrology Proc. Symp. IAEA. Vienna 73-87.

[11] GONFIANTINI, R. et FONTES, J.-Ch. (1963). Oxygen isotopic fractionation in the water of cristallization of gypsum. Nature, Vol. 200, No. 4907, pp. 644-646.

[12] GOUVEA DA SILVA ROSA, R.B. (1980). Migration des sels et des isotopes lourds à travers des colonnes de sédiment non saturé sous climat semi-aride. Thèse $3^{e}$ Cycle. Université Paris VI.

[13] HILLEL, D., KRENTOSV, D. et STILIANOU, Y. (1972). Procedure and test of an international drainage method for measuring soil hydraulic conductivity in situ. Soil. Sc, 114, 395-400.

[14] TOOD, R.M., KEMPLER, W.D. (1972). Salt dispersion coefficients wear and evaporating surface. Soil. Sc of Am. Proc. 36, 539-543.

[15] EDMUNDS, W.M., WALTON, N.R.G. (1980). A geochemical and isotopic approach to recharge evaluation in semi-arid zones. Past and present. Isot. tech. in groundwater hydrology. IAEA. Vienna.

[16] ERIKSSON, E. (1976). Interpretation of environmental isotope and hydrochemical data in groundwater hydrology. IAEA, 171, Vienna.

[17] CONRAD, G. et FONTES, J.-Ch. (1970). Hydrologie Isotopique du Sahara Nord occidental. In Isot. Hydr. Proced. Symp. IAEA. 405-419.

[18] FONTES, J.-Ch. (1976). Les isotopes du milieu dans les eaux naturelles. Houilles blanches, No. Special 3/4.

[19] EDMUNDS, W.M., WRIGHT, E.P. (1979). Groundwater recharge and paleoclimate in the Sirte and Kufra basins Libya. Journal of Hydrology, 40, 215-241.

[20] ZUPPI, G.M., GONFIANTINI, R., ARANYOSSY, J.F. et DRAY, M. (1982). The environmental in wadi Al Ahmar and wadi Al-Bab areas. Final report. IAEA.

[21] ALLEMOZ, M. et OLIVE, P.H. (1980). Recharge of groundwaters in arid areas : Case of the Djeffara plain in Tripolitania Libyan Arab Jamahiriya. IAEA. AG 158-13, pp. 181-192.

[22] BARNES, C.J. et ALLISON, G.B. (1983). The distribution of deuterium and oxygen-18 in dry soil. (I. Theory). Journ. of Hydrology 60, 141-156.

[23] ALLISON, G.B., BARNES, C.J. et HUGUES, M.W. (1983). The distribution of deuterium and oxygen-18 in dry soil (II. Experimental). Journ. of Hydrology 64, 377-397.

# LABORATORY AND FIELD EXPERIMENTS ON INFILTRATION AND EVAPORATION OF SOIL WATER BY MEANS OF DEUTERIUM AND OXYGEN-18

C. SONNTAG, D. CHRISTMANN, K.O. MÜNNICH
Institut für Umweltphysik,
Universität Heidelberg,
Heidelberg, Federal Republic of Germany

**Abstract**

Evaporation from bare soils causes an enrichment of deuterium and $^{18}O$ in the residual soil moisture, mainly at the evaporating front where soil water is transferred to water vapour diffusing through the upper soil layers already dry. Because of relatively small soil moisture contents in the vicinity of the evaporating front the maximum of "heavy isotope excess" there is not intense enough, that it could be used as a tracer mark for subsequent infiltration. Infiltration/ evaporation experiments with moist soil columns yielded uniform isotope profiles with a slight, non-peaked isotope excess. These profiles have a fairly low value for estimates of the local soil water balance. If soils, however, are evaporating only as being the case in some Saharian depression areas, where fossil groundwater evaporates by capillary rise and water vapour diffusion through the unsaturated zone, well developped isotope excess profiles are found, from which accurate numbers for the local groundwater evaporation rate can be derived as field work in the hyperarid Bir Tarfawi area (SW Egypt) has shown.

## 1) INTRODUCTION

The variation of deuterium and oxygen-18 in natural waters is due to isotope fractionation processes connected with evaporation and condensation in the global water cycle. The isotopically labelled water molecules HDO and $H_2^{18}O$, respectively, are favoured to remain in or be transferred to the liquid phase. The isotope fractionation between the phases is described by the fractionation factor $\alpha$ representing the quotient of the isotope ratio $R_{liq}$ in the liquid phase divided by the ratio $R_{vap}$ in the vapour, thus $\alpha=R_{liq}/R_{vap}>1$, where R stands for the isotope ratio D / H or $^{18}O$ / $^{16}O$, respectively /1,2/.

In a cloud the water droplets are considered to be in molecular equilibrium with the vapour. In this case equilibrium isotope fractionation is the only one existing. The equilibrium fractionation factor $\alpha_e=\alpha_e(T)$ depends on temperature only (see table 1). If the cloud water, being enriched in the heavy isotopic species by the factor $\alpha_e$, is removed by precipitation the residual moisture in the cloud becomes depleted in the heavy isotopes if compared to its previous composition. Precipitating air masses therefore become gradually depleted in D and $^{18}O$ /3,4/. Since the equilibrium isotope fractionation $\varepsilon_e=\alpha_e-1$ is 7 to 10 times larger for D than it is for $^{18}O$ (see table 1) the stable isotope data of precipitation fall on a straight line of slope 8 in the familiar $\delta D$ vs.

Table 1
Equilibrium Isotope Fractionation $\varepsilon_e(T)=\alpha_e-1$ with $\alpha_e=\alpha_e(T)$ calculated values between 0 and 30°C (Majoube 1971 /1/)

| Temperature /°C/ | 0 | 10 | 20 | 30 |
|---|---|---|---|---|
| $\alpha_e^D-1$ for HDO /‰/ | 112.6 | 97.9 | 85.2 | 74.2 |
| $\alpha_e^{18}-1$ for $H_2{}^{18}O$ /‰/ | 11.7 | 10.7 | 9.8 | 9.0 |
| $(\alpha_e^D-1)/(\alpha_e^{18}-1)$ | 9.6 | 9.1 | 8.7 | 8.2 |

$\delta^{18}O$ presentation /2,5/. This Meteoric Water Line $\delta D=8*\delta^{18}O+10$, however, does not go through the origin of the plot representing the composition of ocean water. It rather cuts the $\delta D$ axis at +10‰, which means that meteoric waters show a slight deuterium excess being attributed to kinetic isotope fractionation occurring with the vapour release from the ocean surface (evaporation) /6/. The vapour has to diffuse through a thin, quasi-stagnant air layer at the ocean surface (boundary air film) before it reaches the marine atmosphere above, and this causes an additional heavy isotope depletion of the marine vapour. Kinetic fractionation of water vapour molecules is always due to the fact that the heavy molecules are slightly less efficient in diffusing through an air layer. The kinetic fractionation factor $\alpha_k$ therefore is given by the ratio of the corresponding diffusion constants D and $D_i$ of the light (normal) and the heavy (isotopic) molecule species, resp., taken with the exponent $0.5<m<1$, i.e. $\alpha_k=(D/D_i)^m$. Evaporation from an open water body gives $.5<m<.68$, while diffusion through an air diaphragm of fixed thickness as being realized by a dry soil layer (see below) yields $m=1$. The corresponding kinetic fractionation is $\varepsilon_k=\alpha_k-1=(D/D_i)^m-1$, and this is approx. equal to $m*\varepsilon_D$ with $\varepsilon_D=(D-D_i)/D$ being the relative difference in the diffusion constants. For the water molecules HDO and $H_2{}^{18}O$ the kinetic fractionation $\varepsilon_D$ is about equal in magnitude, namely $\varepsilon_D{}^D=24.6‰$ and $\varepsilon_d{}^{18}=30.2‰$ /7/. Nevertheless, kinetic fractionation is (relatively) much more important in $^{18}O$ than it is in deuterium. This is due to the fact that the equilibrium fractionation for $^{18}O$ is so much smaller, and this has the consequence to shift all liquid water having undergone kinetic evaporation to the right hand side in the $D/^{18}O$ diagram.

The extent of kinetic fractionation in evaporation also depends significantly on the atmospheric moisture deficit $q_s(T)*(1-h)$ with $q_s$ being the saturation vapour pressure of the evaporating water and h being the actual vapour pressure in the atmosphere expressed in multiples of $q_s$. If the temperatures of the air and the liquid water are equal h is the relative humidity. If the air is totally dry (h=0) kinetic fractionation is largest, at h=1 (vapour saturation), however, fractionation is completely reduced to equilibrium fractionation.

## 2) INTENTION AND OUTCOME OF THE ARID ZONE SOIL MOISTURE STUDY

Soil water evaporation during the long dry season in (semi-)arid regions had been expected to produce isotopically enriched water below the evaporating front in sufficient quantity to be still noticeable after (layered) downward displacement by new infiltration in the next rainy season. At bare soil locations with positive water balance (annual rainfall > evapotranspiration) repetition of this yearly enrichment cycle should lead to a sequence of heavy isotope peaks individually enclosing a certain amount of water equivalent to the groundwater recharge of the corresponding year. With the idea of eventually assessing

the recharge contribution of individual years we have tried to simulate the generation of travelling heavy isotope enrichment peaks in laboratory soil columns. These experiments did, however, not yield the heavy isotope peaks expected, the amount of enriched soil water at the evaporating front being too small to produce a tracer peak persisting in a useful way during downward movement in the course of subsequent infiltration. Dispersion erases the localized peak, and causes the soil water to be slightly enriched as a whole. From this overall enrichment the local precipitation/evaporation balance can be estimated, but the accuracy of this estimate is rather poor. The idea of obtaining reliable groundwater recharge data from isotope analysis of soil cores taken on one single field trip did not work in this simple way. We were able to show in our 1980 Negev (Israel) soil moisture study that more detailed hydrometeorological data (air and soil temperature, humidity, precipitation) together with isotope data are needed for a good model estimate. Although reasonable numbers for groundwater recharge have been obtained in this study the necessary effort turned out to be rather high, and in particular continuous observation at the field spot seems indispensable. It looks more economic therefore to run an artificial tracer study (such as tritium soil tagging) instead.

More recently we started a systematic stable isotope study on soil moisture in a hyperarid region of the Eastern Sahara (Bir Tarfawi area, SW Egypt). There is practically no rainfall at all, but at some locations the groundwater comes close to the surface, in a few cases up to less than one meter. The unsaturated soil consequently reaches rather high moisture values despite the extremely hot and dry climate with more than 3 meters of potential evaporation. These moist depression areas must be considered to be natural discharge locations for the fossil Saharian groundwater. The evaporation occurs from bare (saline) soils. The actual evaporation rate, being expected to be orders of magnitude below potential evaporation, is controlled by soil moisture flow from the water table to the ground surface. It turned out that the well developped stable isotope profiles in the soil moisture allow estimating the groundwater evaporation rate rather precisely.

## 3) EVAPORATION ISOTOPE ENRICHMENT OF SOIL MOISTURE

Vertical moisture profiles of $\delta D$ and $\delta^{18}O$ in evaporating soils show significant enrichment at the evaporating front /8,9,10/. The situation becomes particularly simple where water is being supplied by capillary rise from below since this leads to an approximate steady state in moisture content and isotopic composition, the evaporating front (dry/wet interface) remaining at a more or less fixed position below the soil surface. At this interface liquid water is converted into vapour, and all fractionation is located there. In addition to the equilibrium fractionation the fixed thickness dry soil layer causes kinetic fractionation (m=1), and all parameters controlling the evaporation process can be estimated easily, and solely based on data (moisture content and isotope profile) drawn from the spot observation.

Steady state evaporation means that the amount of water per unit soil surface and time being supplied to the evaporating front from below is equal to the amount passing the dry soil layer above by diffusion and thus being evaporated into the atmosphere. The latter quantity $Q_{vap}$ depends on the moisture deficit of the atmosphere $q_s(T)*(1-h)$ (for simplicity we shall assume equal temperature T for soil water and atmosphere, resp.) and on the thickness $Z_0$ of the dry soil diffusion diaphragm. Thus the continuity of soil moisture mass flow reads

$$Q_{liq} = Q_{vap} = p*D_{vap}*(q_s(T)*(1-h))/Z_0 = W*(1-h)$$

(p=soil porosity, $D_{vap}$= eff. diffusion constant of water vapour in the soil matrix)

Steady state moisture flow further implies flow continuity of the isotopically labelled water molecules as well, i.e. the water vapour released to the atmosphere must have the same heavy isotope content as has the original soil water supplied from below. This makes it necessary that the soil water at the evaporating front be isotopically heavier to the extent of the total (equilibrium and kinetic) fractionation between the liquid and the vapour phase. With the liquid at the evaporating front becoming heavy the preferential removal of the light species by evaporation provides the compensation needed for the situation to become steady in the distribution of moisture and of isotopic composition. Allowing arbitrary isotopic composition $R_a$ of the atmospheric vapour the steady state isotope balance at the evaporating front reads

$$R_p*W*(1-h) - (1/\alpha_e)*(1/\alpha_k)*R_f*W*1 + (1/\alpha_k)*R_a*W*h = 0$$

($R_p$, $R_f$, $R_a$ = isotope ratio of the local precipitation or groundwater, of the evaporating front moisture, and of the atmospheric vapour, respectively)

Note that the atmospheric vapour reaching the evaporating front by downward diffusion through the dry soil is also depleted by kinetic fractionation. Eliminating $R_f$ yields

$$R_f = \alpha_e*\alpha_k*R_p*(1-h) + \alpha_e*R_a*h$$

If the original soil water were in isotopic equilibrium with the atmospheric vapour - a situation expected to be realized in an approximative sense - $\alpha_e R_a$ were to be replaced by $R_p$. Isotope records of atmospheric moisture show, however, considerable e.g. seasonal variation corresponding to the one familiar with local precipitation, and therefore this simplification usually is not appropriate. Before discussing our result obtained for the isotopic composition $R_f$ of the evaporating front any further it is helpful to add and subtract $R_p h$ to obtain

$$R_f = \alpha_e\alpha_k R_p(1-h) + P_p h + (\alpha_e R_a - R_p)*h$$

This makes it possible to treat the influence of time variations in atmospheric isotope composition as a perturbation of the standard case $R_a=R_p/\alpha_e$. With the approximation $\alpha_e\alpha_k=1+\varepsilon_e+\varepsilon_k$ we obtain

$$R_f = R_p*(1+(\varepsilon_e+\varepsilon_k)*(1-h)) + R_p*((1+\varepsilon_e)*(R_a/R_p)-1)*h$$

Neglecting the scaling factor $(1+\delta_p)^{-1}$, i.e. using $R_p$ as a local isotope reference standard (instead of SMOW), this equation reads in the commonly used approximate $\delta$-notation

$$\delta_f = \delta_p + (\varepsilon_e+\varepsilon_k)(1-h) + \Delta*h$$
where $\Delta=\delta_{ca}-\delta_p$ with $1+\delta_{ca}=\alpha_e*R_a$ (liquid in equilibrium with the actual atmospheric moisture)

This relation describes the composition of the evaporating front in reasonably good approximation. It should be mentioned, however, that transformation to the usual $\delta D/\delta^{18}O$ diagram (origin=SMOW) causes significant distortion due to the fact that for each isotope this transformation correctly involves multiplication with a quotient of two isotope ratios, namely of the old and the new standard, respectively. At least for deuterium, however, these isotope ratios are often sufficiently different from each other to produce a significant error if one just shifts the scale by their percentage difference. Fig. 1 therefore shows both the correct (heavy) line together with the (dotted) line obtained by simple $\delta$-translation. - P on the MWL (Meteoric Water Line) represents the effective average of local precipitation and thus the soil moisture supply water. Equilibrium plus kinetic fractionation $\varepsilon_e+\varepsilon_k$ for both isotopes involved leads to point A on the far right, representing the soil moisture of an evaporating front in contact with a completely dry atmo-

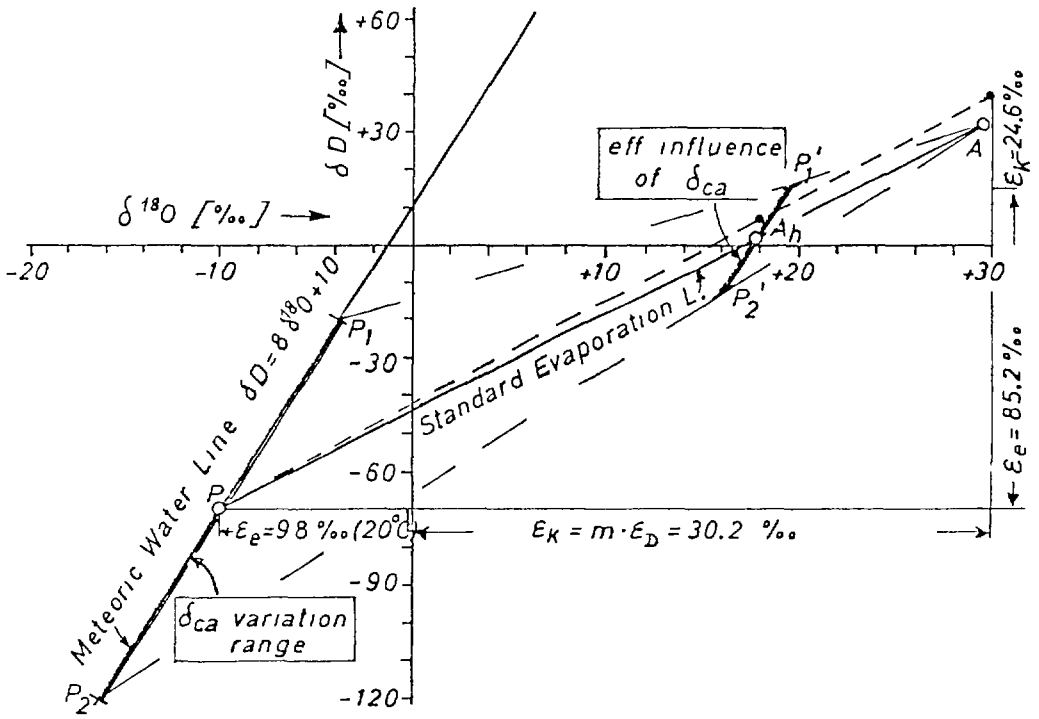


Fig. 1
Steady state isotopic composition $A_h$ of a soil moisture sample from the evaporating front, presented in the $\delta D$ vs. $\delta^{18}O$ diagram.
For the Standard Evaporation Line shown (solid line PA) the isotopic composition of the supply water P is identical with the fictitious equilibrium condensate from the atmospheric water vapour involved. If the atmospheric vapour composition (at the same humidity h) varies as indicated by the variation range of the fictitious equilibrium condensate $\delta_a$ the soil moisture composition may vary between $P_1'$ and $P_2'$. Note that the point A is shifted somewhat (filled dot, broken line) if one uses the simple, but strictly incorrect procedure to present fractionation by just adding $\varepsilon$ instead of multiplying with $\alpha=1+\varepsilon$ (s e text).

sphere (h=0). For an atmospheric humidity 0<h<1, and for the specific case that the isotopic composition of the soil supply water $R_p$ and of the atmospheric vapour is such as if they were in isotopic equilibrium with each other, i.e. $R_p=\alpha_a R_a$ or $\Delta=0$, the composition of the evaporating front falls on the straight line between P and A. Its distance from P is simply multiplied with (1-h). Note that the slope of the line PA is independent of h, it just depends on temperature (the slope shown in the figure is for 20°C with $\Delta\delta D/\Delta\delta^{18}O=2.58$).

In the general case the composition of the atmospheric vapour may vary considerably as mentioned before. Correspondingly, the variation range may also be expressed by an equivalent variation of $\delta_{ca}$, the isotopic composition of its fictitious condensate, i.e. of liquid water in equilibrium with the atmospheric vapour in question. The observed range of $\delta_{ca}$ is denoted in the figure by the points $P_1$ and $P_2$ on the MWL. Quite analogueously to the reasoning used before it becomes evident that the (steady state) isotopic composition of the evaporating front soil moisture now lies on the line of slope 8 from $P_1'$ to $A_h$ and $P_2'$ in figure 1. Thus the influence of varying isotopic composition in the atmospheric vapour is reduced by the factor h. Moreover, the considerable relaxation time involved in the development of this isotopic soil moisture profile tends to further reduce this range of variation, and the composition of the evaporating front will presumably be found not too far away from the evaporation line PA.

## 4) LABORATORY EXPERIMENTS

The present arid zones soil moisture study started with laboratory experiments on isotopic enrichment in soil columns evaporating under controlled hydrometeorological conditions. Moist sand columns of different grain size with known initial soil water and isotope content are connected with their open end to a simple climate chamber being flushed continuously with air of controlled relative humidity and isotopic composition (Fig.2). In the various evaporation experiment runs the rel. humidity in the chamber was held at a fixed value between 10 and 90 %. After the evaporation run the columns are cut into layers of about 15 millimeters thickness. The water contained in these samples is extracted quantitatively for isotope analysis by vacuum distillation. The sample moisture content is obtained gravimetrically /10/.

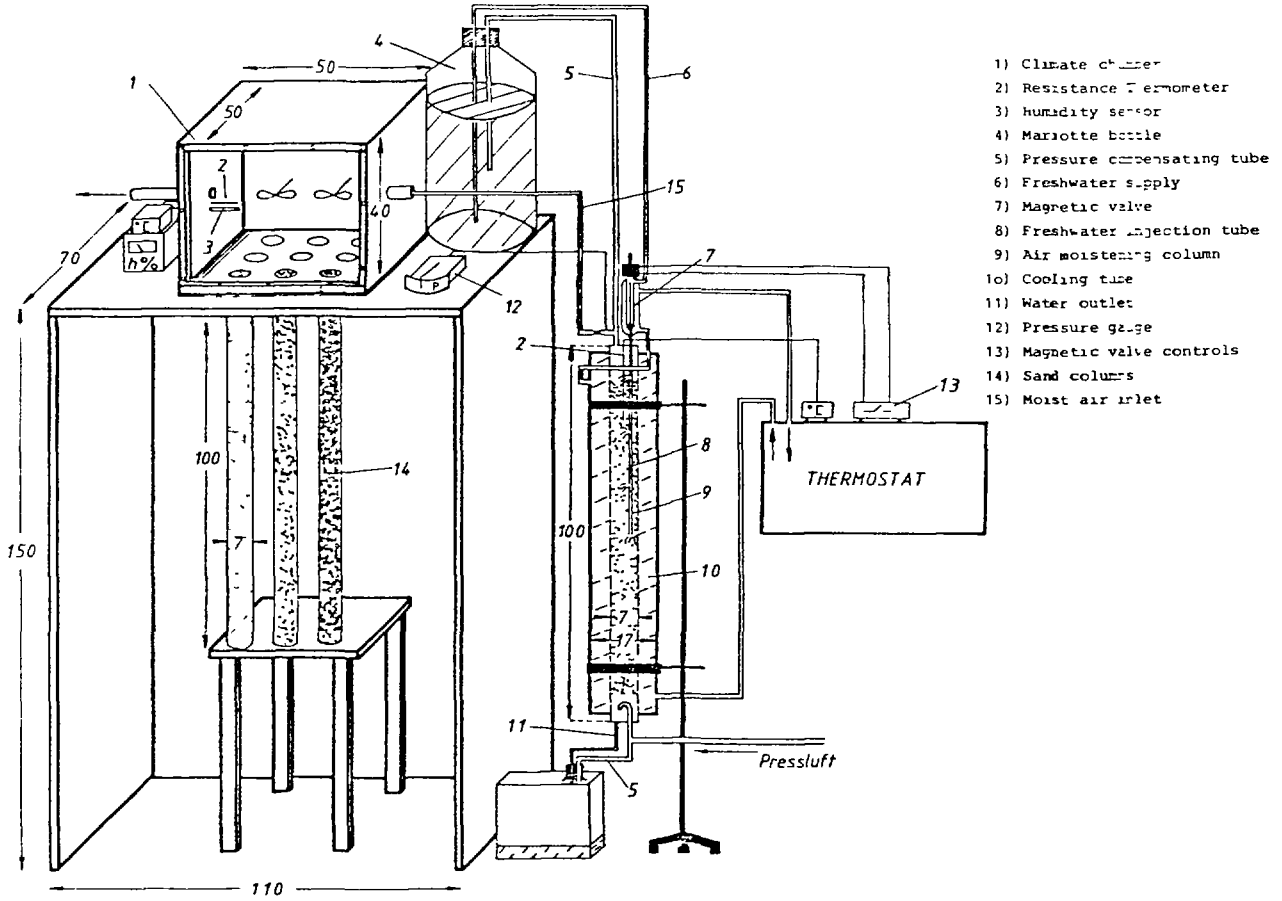


Fig. 2
Experimental set-up for moist snd columns evaporating into an atmosphere of constant relative humidity and known isotopic composition.

The moisture profiles obtained in these experiments show very dry sand on top and, with a transition zone, wet sand underneath. In the transition zone water vapour is released from the liquid and diffuses through the dry soil diaphragm into the climate chamber. At the upper end (evaporating front) of the transition zone the vapour pressure over the liquid (or adsorbed) moisture begins to drop significantly. Beyond this level we have a linear vapour pressure gradient through the top sand layers towards the "atmosphere". The thickness of this sand layer and thus the vapour gradient controls the evaporation rate. With ongoing evaporation and growing thickness of the dry layer (increasing depth of the evaporating front) the evaporation rate therefore decreases. The isotopic profiles (Fig. 3) show the heavy isotope enrichment expected on the basis

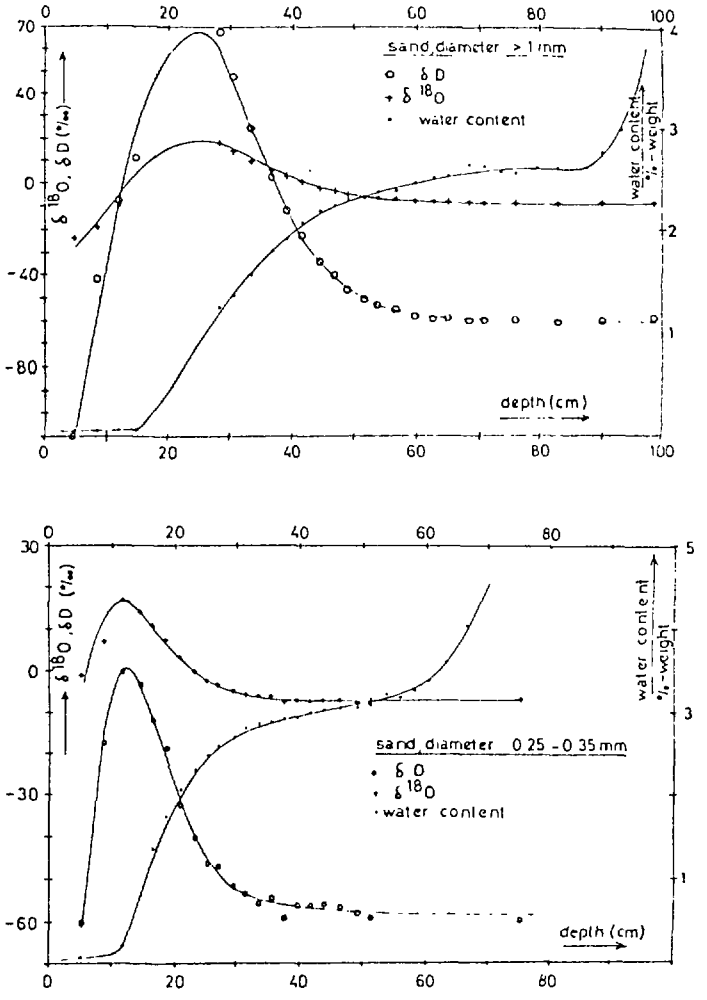


Fig. 3
Moisture and isotope profiles obtained from sand column experiments.

Columns of fine (a) and coarse (b) sand after 43 days of evaporation in an absolutely dry atmosphere. The wet/dry boundary shows strong enrichment of the heavy isotopes.

of the theoretical treatment in section 3.). The heavy isotope excess is due to equilibrium and to kinetic fractionation as well, and depends primarily on the vapour pressure difference $q_a(1-h)$ across the dry soil layer, i.e. on the humidity of the atmosphere referred to the saturation pressure (temperature) at the evaporating front. Figure 4 shows $\delta D$ vs. $\delta^{18}O$ diagrams of various evaporation experiments. The data points fall on straight lines with a slope between 2 and 3, cutting the MWL at the original sand moisture (Heidelberg tap water). These "Soil Evaporation Lines" reflect the influence of vapour diffusion kinetic fractionation shifting the residual liquid away from the MWL to comparatively high $^{18}O$ values. For sand of fine and medium grain size, and for other fine pore soils the slope of the experimental evaporation lines is close to the theoretical one (section 3.). In contrast with the theoretical estimate, however, the slope slightly increases with increasing humidity in the climate chamber. This effect is not yet understood. Experiments with coarse sand yield higher slope, presumably due to convection in the dry soil diaphragm. In this sand layer dry air is underlaid by air of higher humidity and thus lower density, and this results in unstable stratification. Only in a rather fine pore matrix the resulting convection is being damped sufficiently by molecular friction.

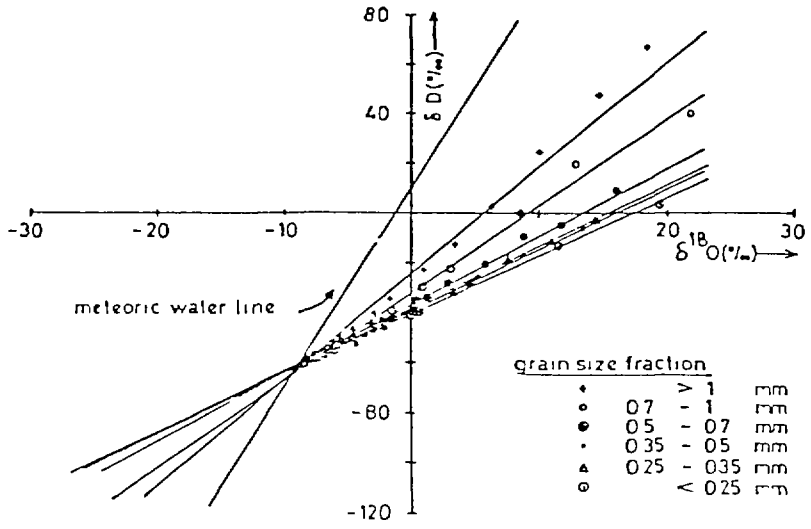


Fig. 4
Evaporation lines for sand of different grain size evaporating into dry air.

At a grain size above about 1 mm the evaporation slope is already close to the one observed for open water bodies, and the additional convection transport of course also increases the evaporation rate.

In the specific case of steady state evaporation, i.e. with a fixed thickness dry soil diaphragm (fixed depth evaporating front, constant evaporation rate) the heavy isotope enrichment exactly at the evaporating front is given by $R_f$ as derived in section 3., and decreases downward with $\exp(-z/z_*)$, where z is the distance from the evaporating front. This is true if the moisture content is constant over the depth range (about $2z_*$) influenced by downward mixing of enriched water. The steady state exponential profile of the heavy isotope excess is produced by downward molecular diffusion of heavy isotope tagged water molecules "produced" at the evaporating front by preferential removal of the light isotope species and by counteradvection of "standard" water from below. The mean penetration depth $z_*$ of the tagged water is given by the downward diffusion constant divided by the upward flow velocity both quantities taken in the moist part of the soil. If the moist soil were completely saturated we would have to use the molecular diffusion constant of liquid water. In reality, however, the water-filled fraction $\theta$ of the total porosity p may be so low that vapour diffusion makes the major contribution. In this case we have to use a combined diffusion constant (the values introduced for $D_{vap}$, $D_{liq}$, and Dare eff. values, reduced by about 30% to include bottleneck resistance /8,10/ or "tortuosity")

$$D = D_{liq}*(1+L*((1-\theta)/\theta)*(D_{vap}/D_{liq}))$$

with $D_{vap}=0.2$ cm²/sec, $D_{liq}=1.2*10^{-5}$ cm²/sec, and the density ratio $L=2*10^{-5}$ of water vapour and liquid water at room temperature. Inserting these numerical values we obtain $D=D_{liq}*(1+.4*(1-\theta)/\theta)$. This means that D is about five times larger than $D_{liq}$ if e.g. only 10% of the pore space is filled with water.

The drying process of a soil after rainfall is a transient problem. In this case evaporation exceeds water supply from below, and the evaporating front moves downward. This in turn means thickening of the dry soil diaphragm and leads to a continuous slowing down of the evapo-

ration rate /10/. Our soil experiments show in agreement with theoretical considerations that this further leads to a penetration depth $z_*$ increasing with time, and also to a lower enrichment at the evaporating front. Consequently, the vertically integrated isotope excess allows an estimate of the time passed after the last rain event.

Infiltration/evaporation experiments with columns in the laboratory have been made to simulate the situation in semi-arid regions, with a long dry season. The intention was to use enrichment peaks as tracer marks for the subsequent infiltration. Artificial rainfall was produced by controlled water flow through stainless steel capillary bundles. This in fact yields sufficiently homogeneous irrigation of the soil surface. Various evaporation/irrigation experiments with different soil columns and automatically controlled irrigation intervals did not yield the expected heavy isotope peaks suitably pronounced to allow balancing in the soil moisture system (see also sections 2. and 6.)

## 5) SOIL MOISTURE STUDY AT SDE BOQER, NEGEV/ISRAEL

From November 1979 until May 1980 (in cooperation with Prof. A. Issar (Sde Boker) and Prof. J. Gat (Weizmann Institute, Rehovot) an isotope soil moisture study was carried out at a dune sand- and at a loess/loam-location near Sde Boker, Negev/Israel. In this long-term field study, which has covered the whole winter-rain season, soil cores have been regularly collected for D- and $^{18}O$-analysis of soil water samples. Since a positive water balance between rainfall and evaporation was to be expected, also tritium tracer experiments have been done, in order to measure the downward displacement of soil moisture. The main effort, however, was directed to the stable isotope investigation. For the interpretation of the observed time variation of the soil moisture isotope data the local hydrometeorological data is needed. These daily weather data has been collected from the meteorological station of Sde Boker. Moreover, the local atmospheric water vapour has been sampled daily for isotope analysis and, of course, all precipitation events, which yielded 120 mm total rainfall over this half-year's period. With this hydrometeorological data in hand we have tried to simulate the observed time variation in the soil moisture and stable isotope profiles, the results being shown in figures 5 and 6. In the middle part of these figures the moisture and isotope profiles of various sampling dates are presented. The upper part shows the time variation of the daily potential evaporation (evaporation pan data), the precipitation and the actual evaporation obtained from our soil water model estimates. In the lower part of the figures the daily soil water percolation rate at 1 meter depth is presented. These deep infiltration rates have been obtained from our model estimates of the daily soil water and isotope balances, which are based on the local hydrometeorological data. At barren soil condition the soil moisture at this depth is save against evaporation loss up to a one-year's period, i.e. these percolation rates sum up to the groundwater recharge of this particular year: about 30 mm for the dune sand of Revivim and 6 mm for the loess/loam of Sde Boker. These numbers are for a total rainfall of 120 mm being considerably higher than for normal years (about 80 mm).

Figures 5 and 6:
Infiltration and evaporation for the semi-arid climate of the Negev (Israel) estimated by a hydrological model based to a major extent on stable isotope data.

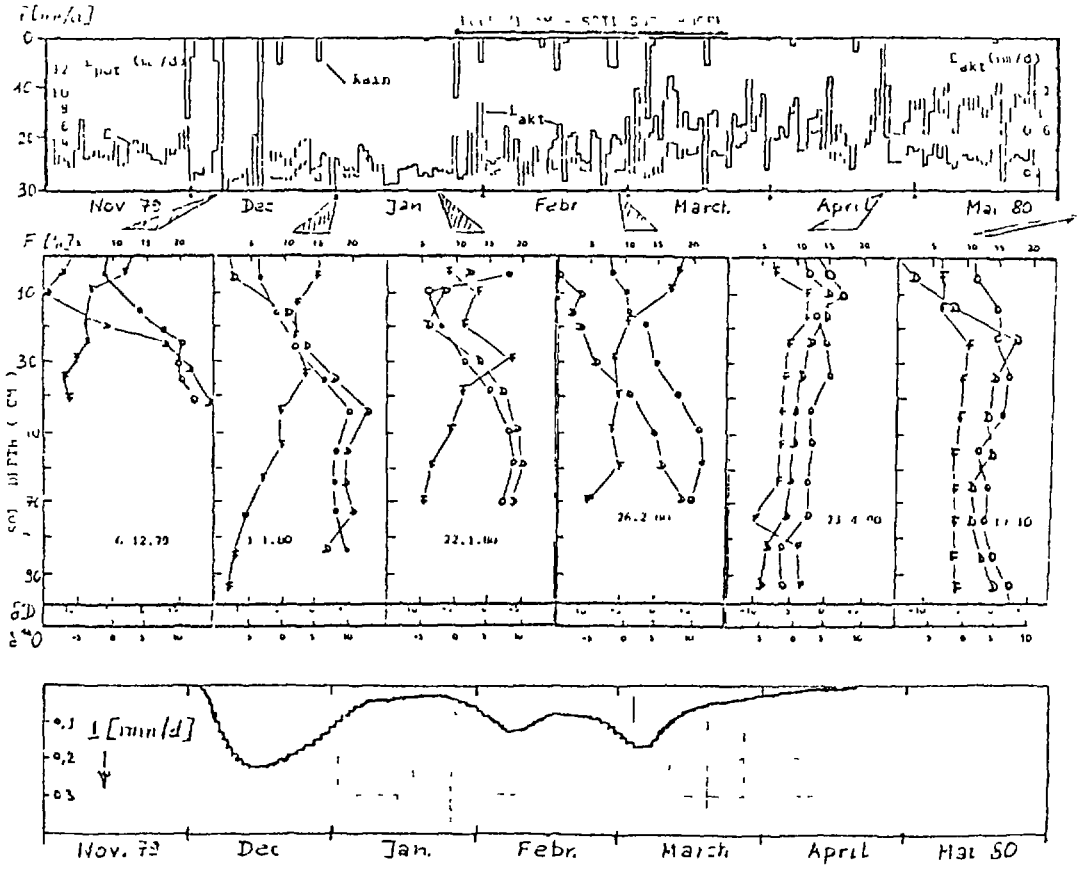


Fig. 5 presents

(a) precipitation (measured), potential evaporation (calculated from pan A data), and actual evaporation given by the model)
(b) measured soil profiles of moisture (F), deuterium (D), and oxygen-18
(c) model predicted recharge, being in good agreement with the measured data

The study covers the period November 1979 to May 1980 for a loess soil at Sde Boquer.

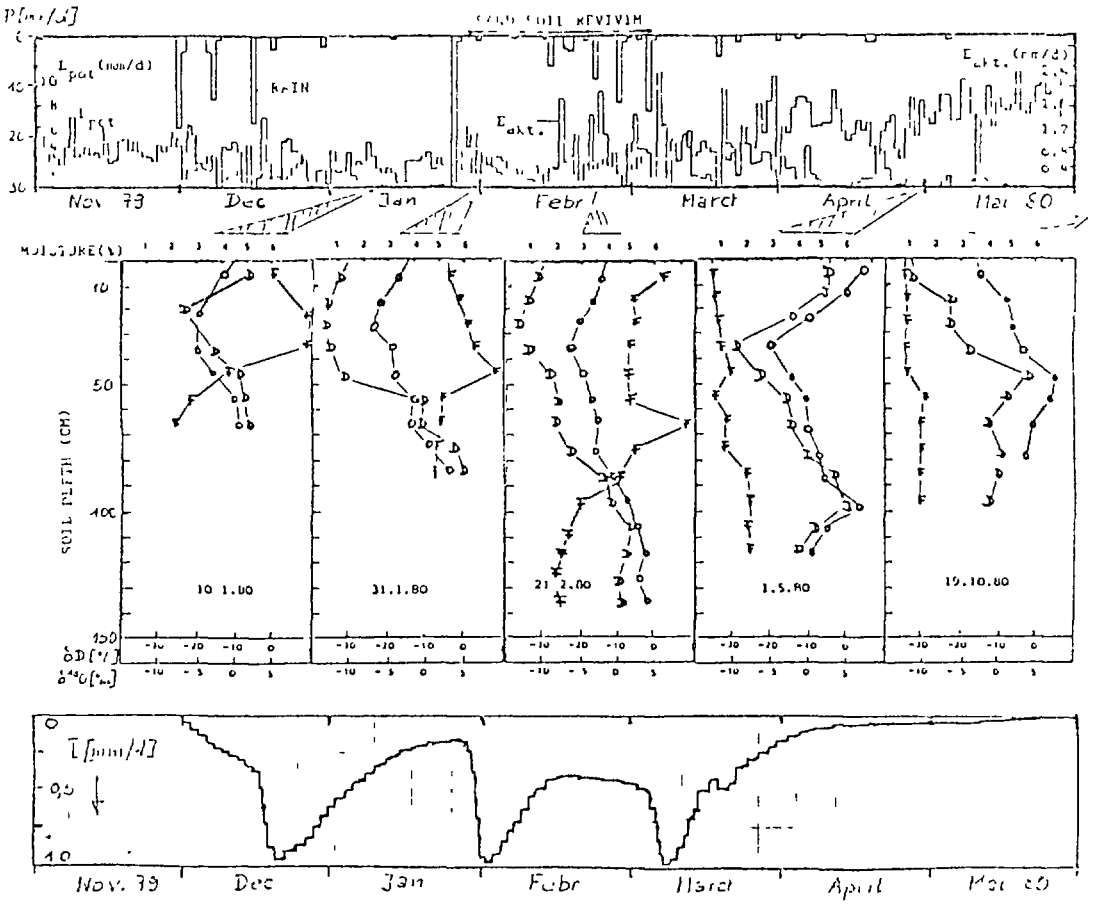


Fig. 6 presents corresponding data in the same way and for the same time period as does figure 5 above, but for a sand at Revivim, about 20 km away from Sde Boquer

## 6) STABLE ISOTOPE STUDY ON THE EVAPORATION FROM SAHARIAN DEPRESSION AREAS - NATURAL DISCHARGE OF FOSSIL GROUNDWATER

In many Saharian depression areas, even in hyperarid regions of the Central Sahara with practically no rainfall at all, groundwater is found close to the soil surface, at some locations at less than one meter depth. Under a surface layer of some 10 centimeters thickness there exists a rather moist unsaturated zone. Under these conditions considerable groundwater evaporation is to be expected. The groundwater loss in these depression areas seems to be compensated by radial subsurface inflow from the surrounding higher elevation desert area. In this (quasi-)steady state situation we should expect a well developped heavy isotope excess profile in the soil moisture with the maximum at the evaporating front and an exponential decrease underneath as discussed in section 4.

During two field campaigns (November/December 1983 and February/March 1984) 14 soil cores have been collected from various locations around Bir Tarfawi in SW Egypt close to the Sudanese border.

Figure 7 shows the D and $^{18}O$ profiles from the first expedition together with the gravimetric soil moisture profiles. Since the isotopic soil moisture data points in the $\delta D$ vs. $\delta^{18}O$ diagram (see figure 1) should fall on the evaporation line of slope $\cong 2.5$ we have the $\delta D$ scale in the figures 7a,b compressed by this factor. This makes the

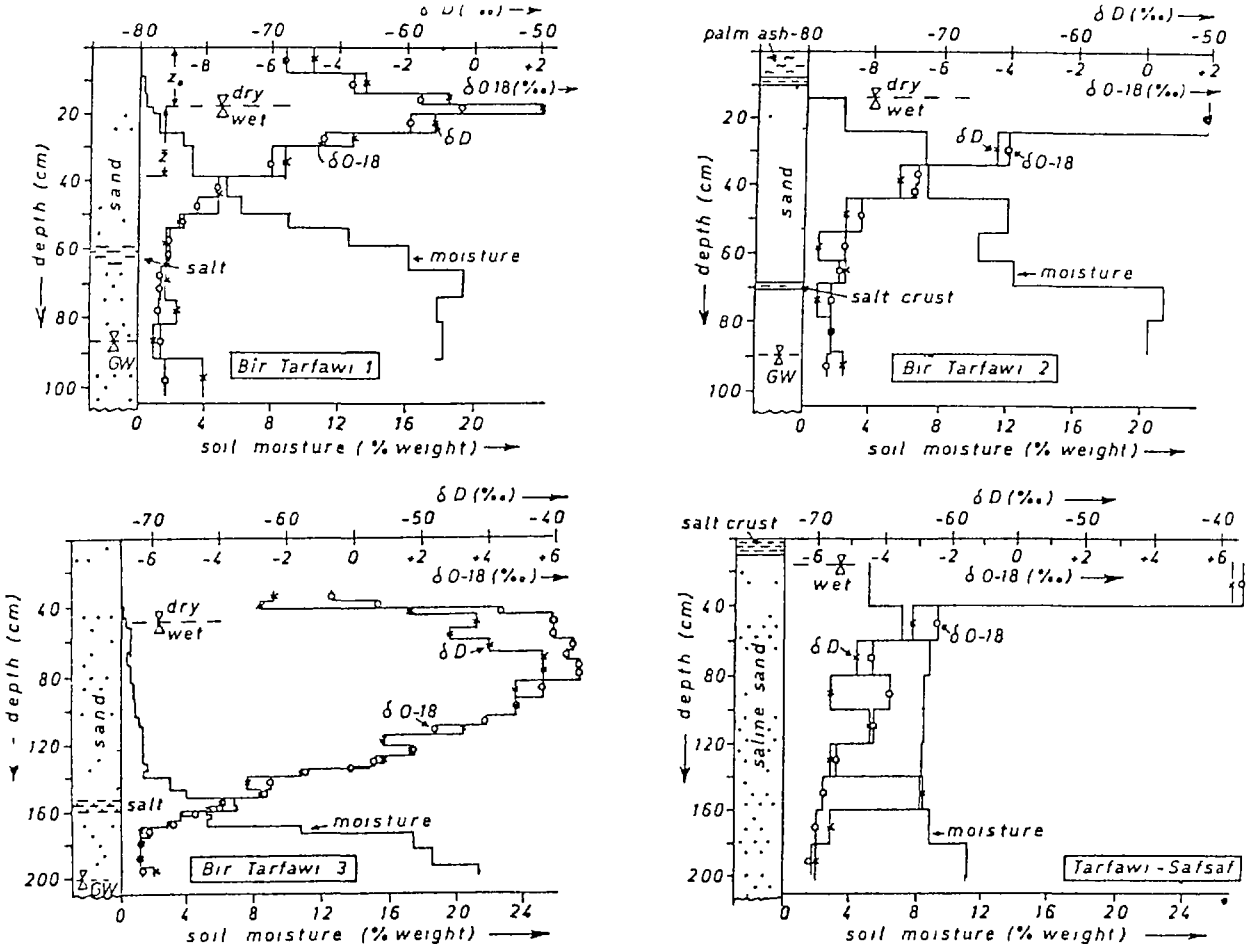


Fig. 7a

Soil moisture and stable isotope profiles in sand cores from the Bir Tarfawi area, SW Egypt. The δD and $\delta^{18}O$ scales have been adjusted to each other in such a way that, theoretically, they are predicted to coincide (see text).
The Bir Tarfawi 1 to 3 samples have been taken with a sand auger specially designed at the institute, while the Tarfawi-Safsaf samples were taken by a normal Purckhauer auger.

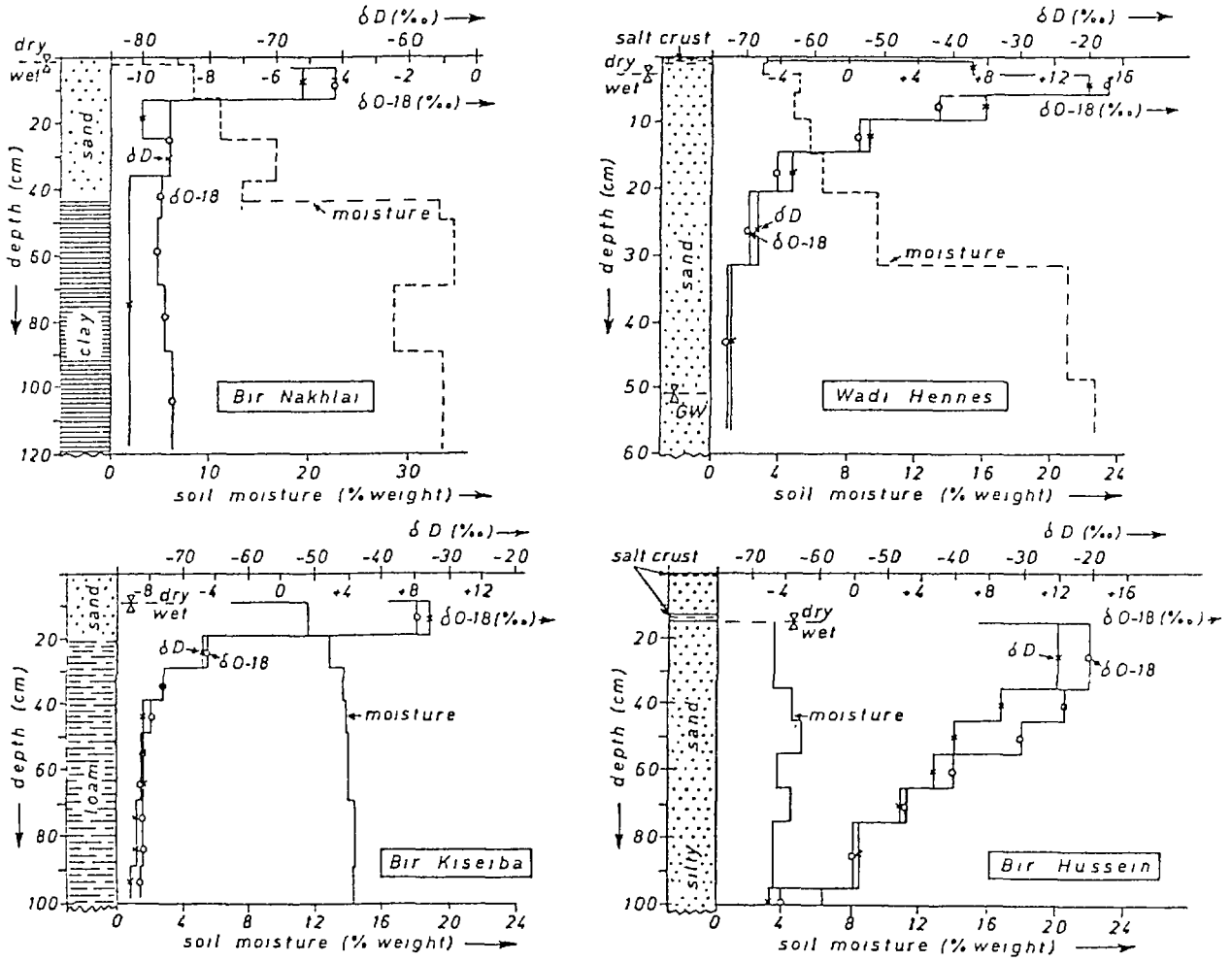


Fig. 7b

Profiles as in fig. 7a, but from Nakhlei, Kisheba, and Hussein, small depression areas with high groundwater level, located 100 km east of Bir Tarfawi, and also from Wadi Hennes, south of Bahariya.

depth profiles of the two isotopes practically coincident if the isotope scales are shifted in such a way that the data points for the supply water
fall upon each other. This procedure in fact makes the profiles coincide in the figures shown. The enrichment peaks define the position of the evaporating front, and we know therefore the thickness $z_0$ of the water vapour diffusion diaphragm. With local temperature and soil porosity data we have estimated the mean annual vapour flow rates $E_{z1}$. They are presented in table 2 (converted to evaporation in millimeters per year) together with numbers for the annual soil water supply from below $E_{z_0}$ having been obtained independently from the observed heavy isotope excess penetration depth $Z_0$ with help of the effective moisture diffusion constant (see section 4.), the latter depends on the liquid moisture content and therefore varies with depth. The two independent estimates of the groundwater evaporation are in fairly good agreement. They

Table 2
Actual evaporation from sand profile data:
$E_{z_m}$ (based on the measured heavy isotope penetration depth $Z_m$)
$E_{z_1}$ (based on the calculated vapour flux density j through the dry sand diaphragm of thickness L on top of the profile, i.e. $j=p*D/L$, where p and D are estimated values for porosity and vapour diffusion constant)

These values are compared with $E_{th}$, the theoretical evaporation as calculated from capillary rise data with parameters estimated after Eagleson /11/.

| location | actual evaporation (mm/year) | | |
|---|---|---|---|
| | $E_{zm}$ | $E_{z1}$ | $E_{theor}$ |
| Bir Tarfawi 1 | 70 | 20 | 200 |
| Bir Tarfawi 2 | 30 | 20 | 150 |
| Bir Tarfawi 3 | 54 | 58 | 05-20 |
| Tarfawi-Safsaf | 40 | 20 | |
| Bir Kiseiba | 140 | 30 | |
| Bir Nakhlai | 200 | 200 | 200 |
| Bir Hussein | 84 | 20 | |
| Wadi Hennes | 76 | 100 | 800 |

are for some cases, however, in considerable disagreement with the solely theoretical prediction based on soil moisture rise from the water table and subsequent vapour diffusion. Theoretical evaporation data of this kind appear to be much higher than the experimental ones in many cases. This may be due to soil moisture permeability data selected wrongly. In addition, high salt content in these desert soils (in some horizons even salt crusts have been observed) may have partly blocked the bottlenecks in the pore space.

The groundwater evaporation rates measured we consider important data, inparticular for the assessment of the total groundwater release from the various Saharian depressions. These natural groundwater discharge data are urgently needed for a reliable regional groundwater balance.

REFERENCES:


/1/ MAJOUBE, M. (1971): Fractionnement en Oxygene-18 et en Deuterium entre l'eau et sa vapeur, J.Chim.Phys. 68, 1423-1436

/2/ GAT, J.R., GONFIANTINI, R. (1981): Stable Isotope Hydrology, Technical Reports Series No.210, IAEA Vienna

/3/ SONNTAG, C. (1978): Palaklimatische Information im Isotopengehalt $^{14}C$ datierter Saharawasser: Kontinentaleffekt in D und $^{18}O$, Geol.Rundschau 67, 413-423

/4/ SONNTAG, C. et al. (1983): Variations of Deuterium and Oxygen-18 in Continental Precipitation and Groundwater, and their Causes, in: A. Street-Perrott et al. (eds.), Variations in the Global Water Budget, Reidel Dordrecht, 107-124

/5/ CRAIG, H. (1961): Isotopic Variations in Meteoric Waters, Science 133, 1702-1703

/6/ MUNNICH, K.O. (1979): Report on Gas Exchange and Evaporation Studies, in: "Isotopes in Lake Studies", Panel Proc. Ser., IAEA Vienna, pp. 233-244

/7/ MERLIVAT, L. (1978): Molecular Diffusivities of $H_2{}^{16}O$, $HD^{16}O$ and $H_2{}^{18}O$ in Gases, J.Chem.Phys. 69, 2864-2871

/8/ ZIMMERMANN, U. ET AL. (1967): Soil Water Movement and evapotranspiration: Changes in the Isotopic Composition of the Water, in: Isotopes in Hydrology, IAEA Vienna, 567-585

/9/ ALLISON, G.B. et al. (1983): Effect of Climate and Vegetation on Oxygen-18 and Deuterium Profiles in Soils, in: Isotope Hydrology 1983, 105-123

/10/ MUNNICH, K.O. et al (1980): Isotope Fractionation due to Evaporation from Sand Dunes, Z.Mitt.Zentralinst.Isot.Strahlenforsch. (Leipzig) 29, 319-332

/11/ EAGLESON, P.S. (1978): Climate, Soil and Vegetation, Water Res. Research, 14, 722-730

# ETUDE ISOTOPIQUE DES MOUVEMENTS DE L'EAU EN ZONE NON SATUREE SOUS CLIMAT ARIDE (ALGERIE)

M. YOUSFI*, J.F. ARANYOSSY**,
B. DJERMOUNI***, J.-Ch. FONTES*

* Laboratoire d'hydrologie et de géochimie isotopique,
Université de Paris-Sud,
Orsay, France

** Section d'hydrologie isotopique,
Agence internationale de l'énergie atomique,
Vienne

*** Commissariat aux énergies nouvelles,
Alger, Algérie

**Abstract**

Modelling of isotopic profiles ($^{18}O$, $^{2}H$) in the unsaturated zone located in a discharge area with an arid climate (north western Sahara), leads to the evaluation of effective evaporation in the order of 1 mm/year through a soil thickness of about ten meters.

**Résumé**

La modélisation des profils isotopiques (oxygène-18, deutérium) dans la zone non saturée en zone de décharge sous climat aride (Sahara Nord occidental) conduit à une évaluation de l'évaporation nette de l'ordre de 1 mm/an à travers un couvert de sol d'environ une dizaine de mètres.

## I. APERCU CLIMATOLOGIQUE

Le secteur d'études a été établi dans la vallée de l'Oued Saoura à proximité de Béni-Abbès dans le N.W. Saharien (Fig. 1).

La région est affectée d'un climat aride (Dubief, 1959, 1963; Dervieux, 1956):

### Evaporation

(bac Colorado, 4 ans): 3,2 m $a^{-1}$
(piche, 25 ans): 4,8 m $a^{-1}$

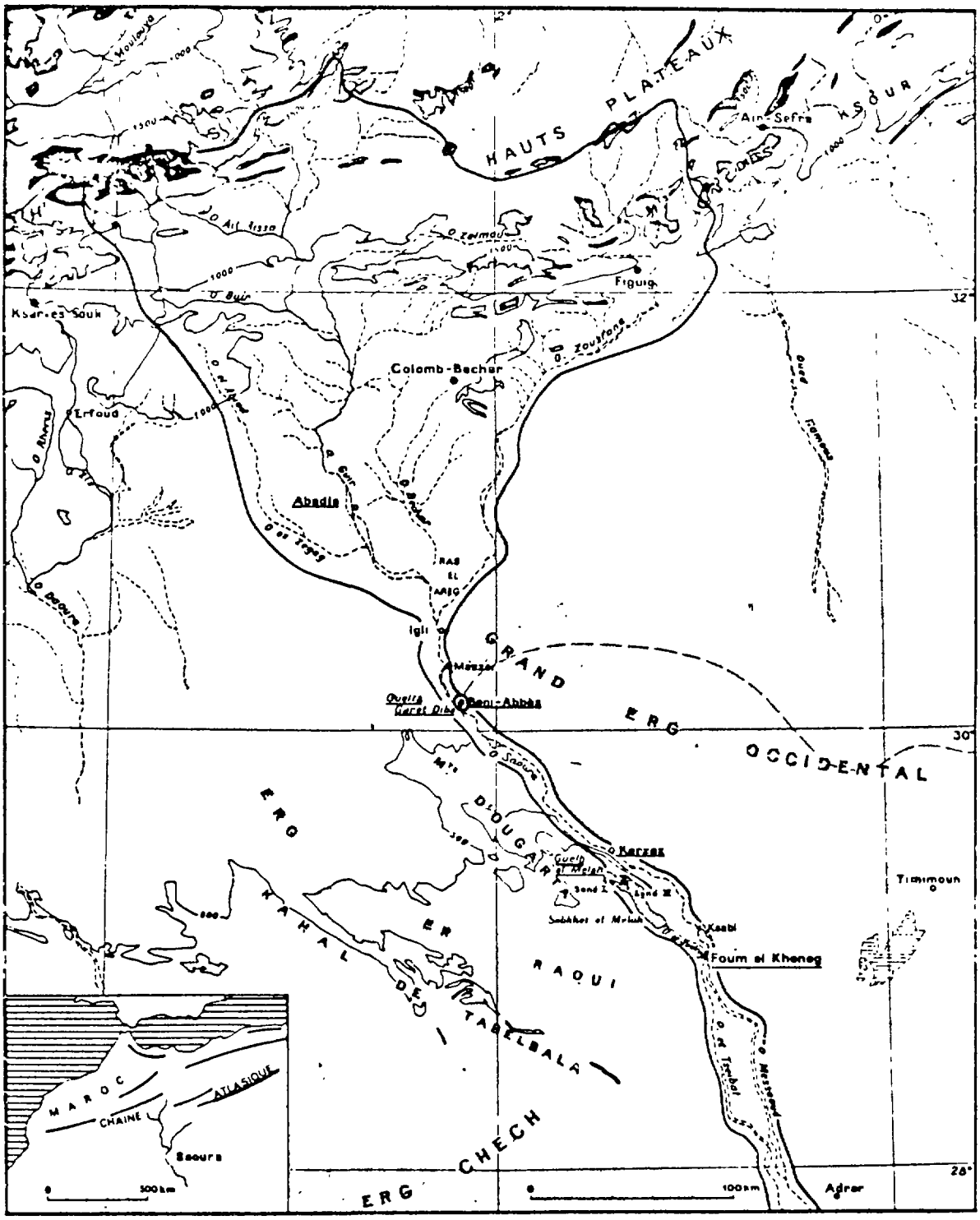


FIGURE 1
Bassin de l'oued Saoura (Sahara nord-occidental).
Conrad. G. 1974

Humidité relative moyenne annuelle

$07^H$ : 49%
$13^H$ : 32%  moyenne 36%
$18^H$ : 26%

Température

moyenne annuelle (25 ans) : 22,8°C
amplitude journalière moyenne : 14,6°C
amplitude max. sur moyennes mensuelles : 24°C

Précipitation

annuelle moyenne (34 ans) : 40,7mm
fréquence retour 50 ans : 89 mm
fréquence retour 100 ans : 101 mm
maximum journalier observé en 38 ans : 56 mm
durée maximale sans pluie > 5 mm (34 ans) : 3 a 8 m
durée maximale sans pluie > 10 mm (34 ans) : 6 a 10 m

## II. TERRAINS SUPERFICIELS

Dans la vallée de l'Oued Saoura, les sables dunaires du Grant Erg Occidental sont relayés par des alluvions quaternaires ordonnées en terrasses imbriquées et partiellement couvertes de colluvions. L'ensemble est adossé aux faciès indurés de la "dalle hamadienne" mio-pliocène dans laquelle est entaillée la vallée (fig. 2).

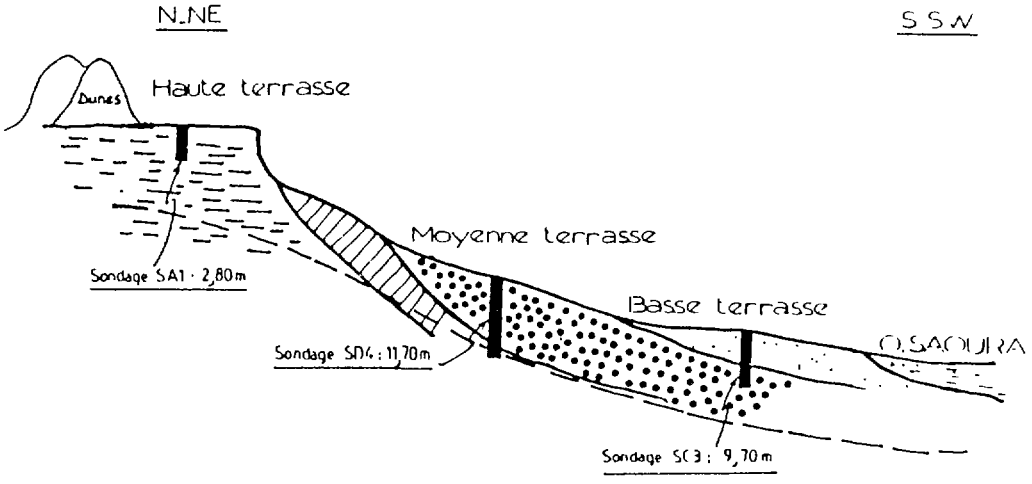


Fig 2. Coupe schématique des sites de sondages

## III. METHODES

Le principe de l'étude consiste à carotter "à sec" et de façon continue les horizons superficiels. Trois sites ont été primitivement implantés:

- Hassi Rokna (sondage SAI) dans la dalle de dépôts travertineux pliocènes souvent silicifiés qui frange la vallée. Ce carottage entrepris dans des niveaux horizontaux en position haute, était destiné à l'étude de l'infiltration verticale des précipitations. Il dut, malheureusement, être abandonné à la profondeur de 2,8 m par suite de la présence d'une induration siliceuse qui endommagea l'outil.

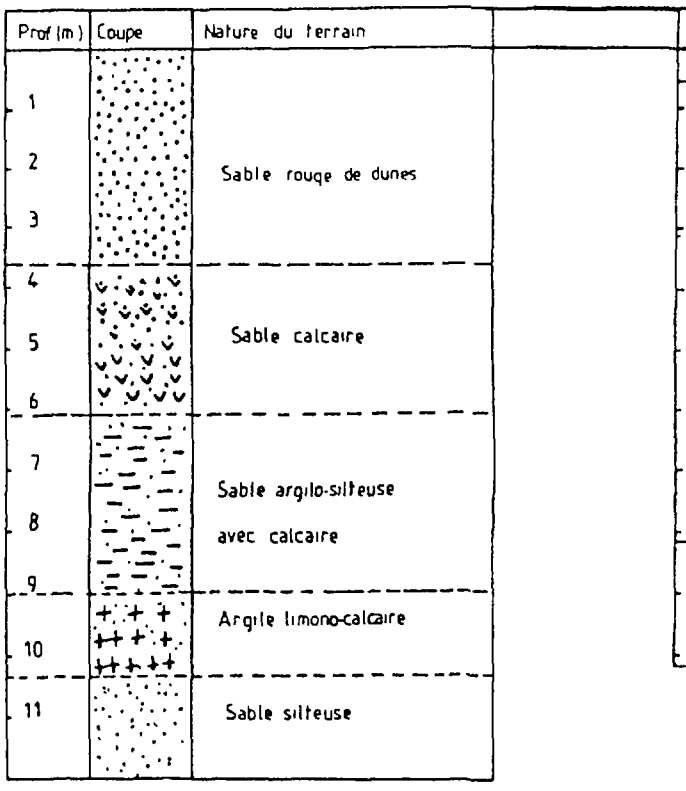


Fig 3a: coupe lithologique (sondage SD4)

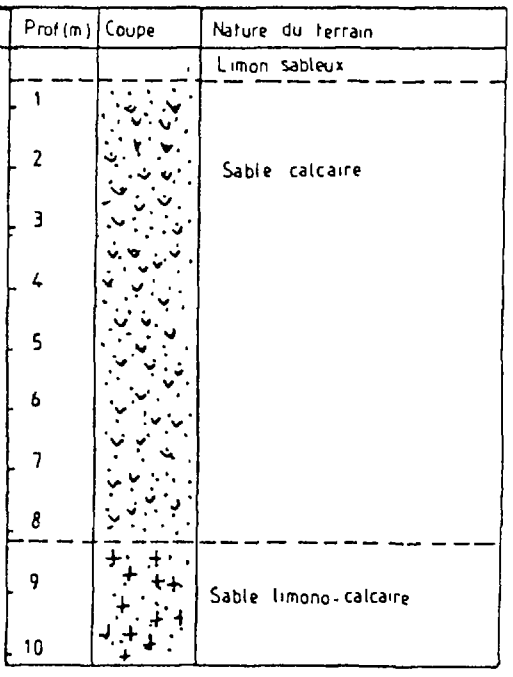


Fig 3b: coupe lithologique (sondage SC3)

- Hassi Juiffa (sondage SD4) sur la terrasse moyenne de la Saouara faite de sables d'argiles et de dépôts parfois grossiers correspondant à un alluvionnement ancien de l'oued qu'elle domine de 15 m environ en ce secteur. Le carottage a traversé environ 10 m de dépôts fins (fig. 3a) non saturés et a atteint la nappe de la terrasse moyenne (exploitée à environ - 12 m par rapport au niveau du sol dans le puits d'Hassi Juiffa).

- Site SC3 sur la basse terrasse de la Saoura en aval de Hassi Juiffa, à quelques centaines de mètres de l'axe de l'oued, mais au-dessus du lit majeur des crues des vingt dernières années. La rencontre d'un niveau de dépôts très grossiers dans les alluvions sableuses et limoneuses (fig. 3b) a contraint à interrompre l'ouvrage à une profondeur de 9,7 m sans rencontrer la nappe d'inféroflux.

Les carottes sont tronconnées sur le terrain en éléments de 20 cm dont le coeur est conditionné dans un récipient de 350 ml hermétiquement scellé selon la méthode par ailleurs exposée (Zouari et al., ce volume).

Sur ce matériel les mesures suivantes sont réalisées au laboratoire:

- teneur en eau pondérale
- granulométrie et minéralogie de la matrice
- analyse chimique des extraits aqueux de sédiment sec.
- analyse isotopique ($^{2}H$, $^{18}O$, $^{3}H$) des eaux extraites des sols par distillations sous vide.

## IV. CONTEXTE ISOTOPIQUE REGIONAL

Les précipitations à Béni-Abbès (épisodes isolées) ont été étudiées par Conrad et Fontes (1970) et Yousfi (1984). Il apparaît une grossière tendance inverse entre la hauteur d'eau précipitée et la composition isotopique (Fig. 4a). Les valeurs extrêmes de teneur en $^{18}O$ des précipitations sont + 13.6 et - 9.7 ‰. Les fortes averses ( > 10 mm par 24h) susceptibles de recharger les nappes ont des teneurs < - 7‰. Les teneurs comparées en deutérium et oxygène 18 montrent que les précipitations ne sont pas fortement évaporées (Fig. 4b). La nappe d'eau souterraine la plus importante de la région est celle du Grand Erg Occidental. Sa teneur en oxygène 18 est de l'ordre de - 5‰ (Conrad et Fontes, 1970; Gonfiantini et al., 1974). La nappe d'inféroflux de la Saoura correspond à un mélange en proportions variables entre l'eau de la nappe de l'Erg qui se décharge dans la vallée et les eaux de crue de l'Oued infiltrées dans les hautes berges.

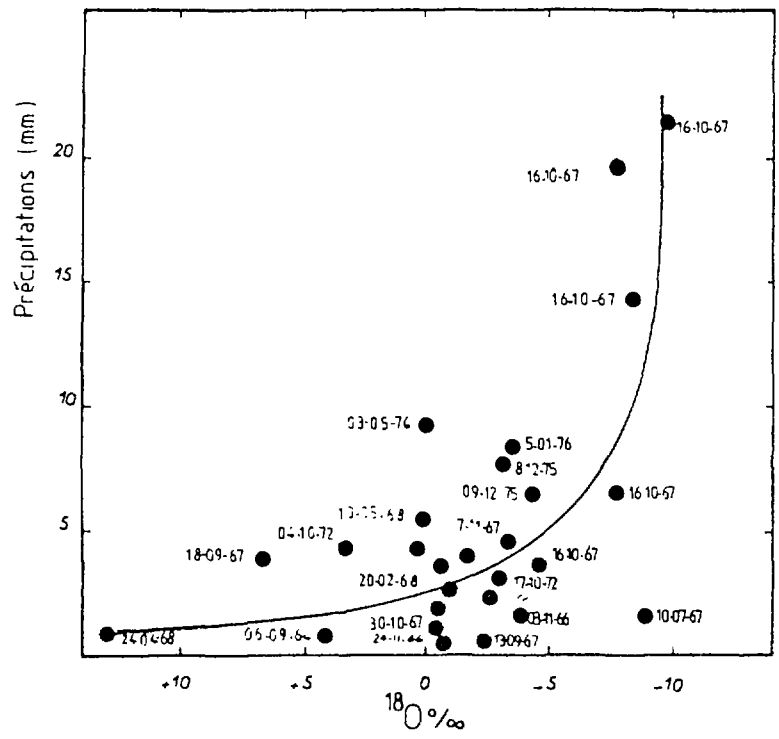


Fig 4a Variations de la Composition Isotopique en Fonction de la Hauteur des Précipitations à Beni-Abbès

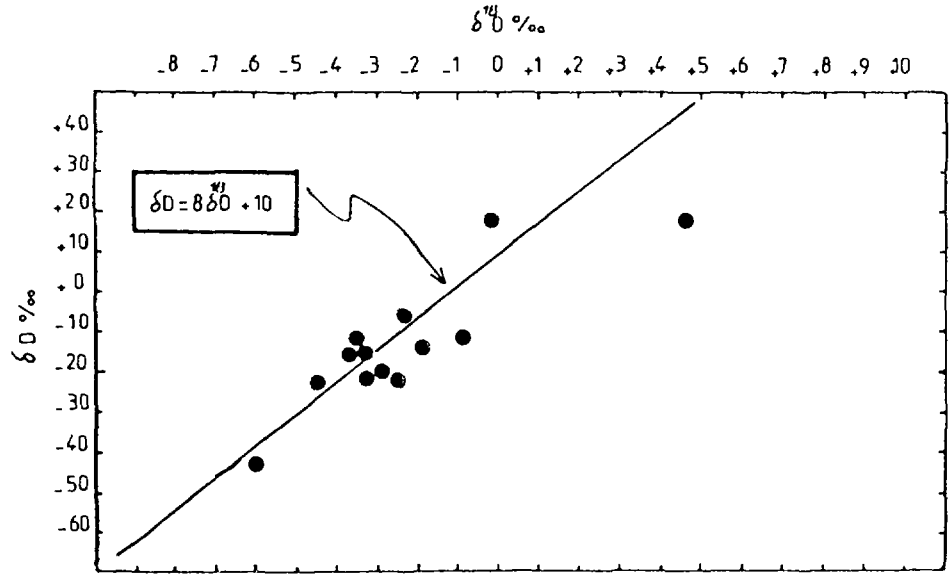


Fig 4b: relation $\delta^{18}O - \delta D$ dans les eaux de pluie : Béni Abbès (précipitations mensuelles 1969-1976)

## V. CARACTERISTIQUES PHYSIQUES DES PROFILS

Les fractions fines < 50 µm varient de 5 à 50% pondéraux en SC3 et peuvent atteindre 90% en SD4. Les teneurs pondérales en eau (Fig. 5a et 5b) sont inférieures à 5% jusque vers 3m de profondeur et augmentent ensuite vers la base des profils pour atteindre environ 14% à la base de SC3 et 18% à la base de SC3 et SD4 respectivement. Les teneurs totales en sels des solutions du sol sont reflétées par la conductivité électrique mesurées au cours des expériences de lixiviation selon la méthode de Gouvea da Silva Rosa (1980).

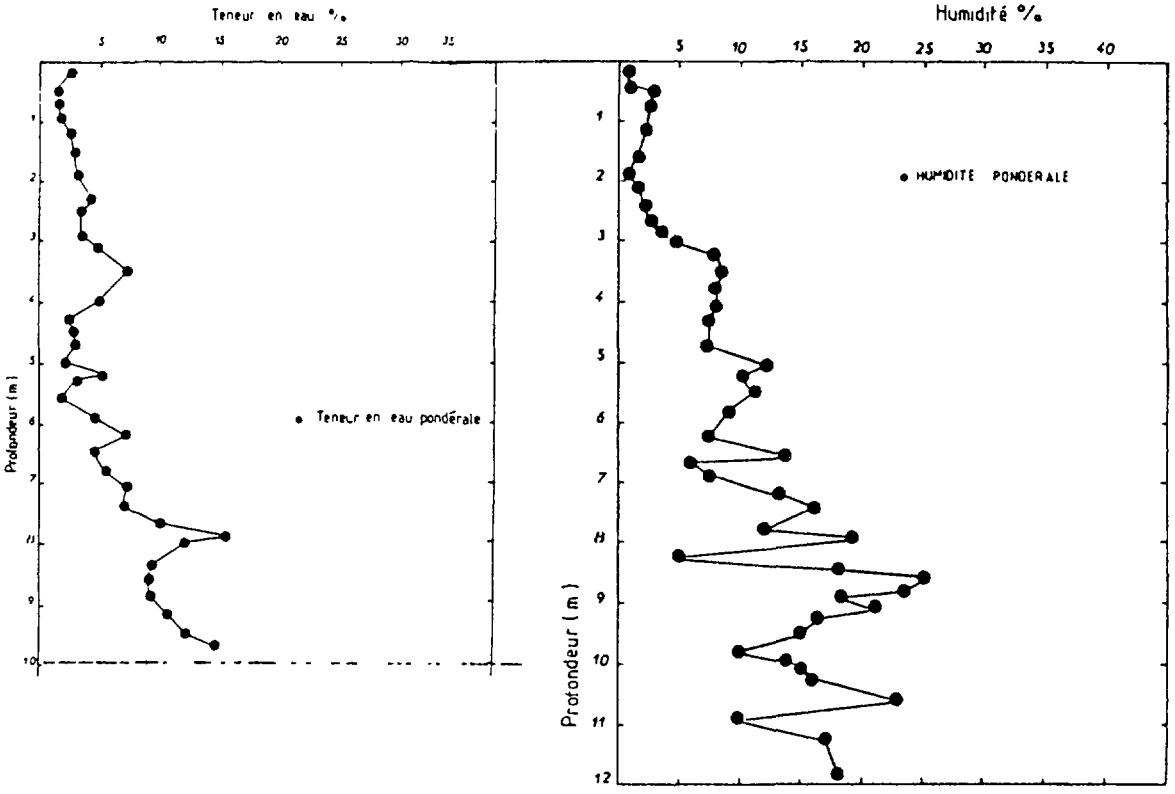


Fig 5a: Profils des teneurs en eau : SC3

Fig 5b: Profil Hydrique ( Sondage SD4 )

Bien entendu, l'attribution de la salinité ainsi obtenue aux solutions interstitielles présuppose que la totalité du la charge saline soit restée dissoute et ne puisse provenir de la mise en solution de la matrice des profils. Ceci n'est vrai que pour les chlorures qui n'atteignent pas le seuil de saturation de la halite (sauf au sommet de SC3). Il est clair, en revanche, qu'une large part des ions $SO^{2-}$ et $Ca^{2+}$ proviennent de la mise en solution du gypse, en particulier dans le sondage SD4. Seules les teneurs en chlorures seront considérées comme un indice de concentration évaporatoire des solutions du sol. Les figures 6a et 6b montrent une évolution assez

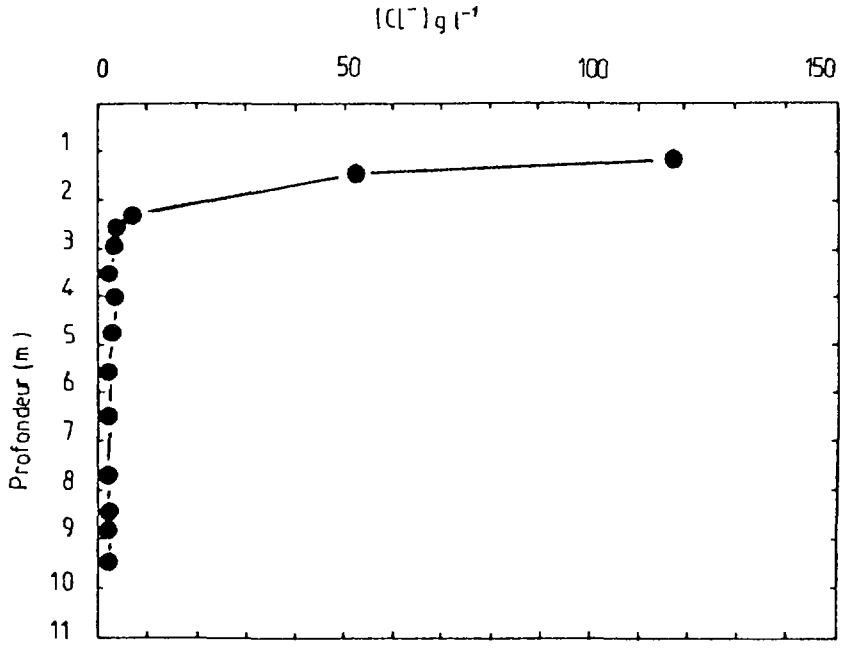


Fig 6a variations de $Cl^-$ en fonction de la profondeur: sondage SC3

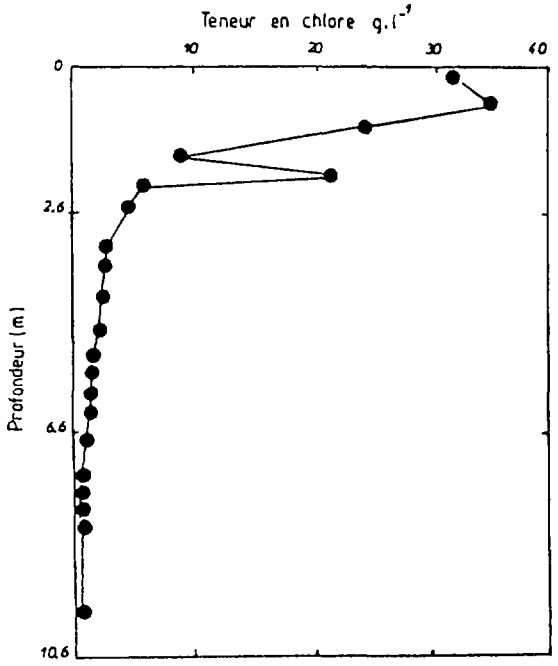


Fig 6b: Variation de la Teneur en Chlore avec la Profondeur Sondage SD4

semblable. On distingue une partie basale du profil où les teneurs augmentent faiblement et progressivement jusque vers 2 m de profondeur en SC3 et 2.6 m en SD4. Au-dessus vient une augmentation brutale qui porte les teneurs en $Cl^-$ des solutions interstitielles jusqu'à environ 35 $gl^{-1}$ vers 45 cm en SD4 et 290 $gl^{-1}$ à la partie supérieure de SC3. Compte-tenu des erreurs inhérentes à la méthode de détermination (l'incertitude est multipliée par le facteur de dilution entre la masse de solution réellement contenue à l'origine dans la prise d'essai de sol et la quantité d'eau distillée utilisée pour l'obtention

de l'éluat) on peut proposer l'interprétation suivante du profil de sels solubles. Les sels se concentrent à la partie haute de la zone non saturée sous l'effet de l'évapo-transpiration. Cette accumulation est très forte à partir de la profondeur où le transit en phase vapeur est le mécanisme dominant du mouvement ascendant de l'eau du sol. Plus bas, dans la zone où domine le transit liquide, la faible salinisation des solutions reflète soit la fraction d'eau qui est vaporisée, soit la diffusion verticale descendante en phase liquide des ions, accumulés à la partie supérieure. Selon toute probabilité, c'est ce second mécanisme qui est prédominant, voire exclusif. Dans chaque cas, les profils de teneurs ioniques des solutions du sol se raccordent vers le bas à des valeurs de concentrations proches de celles des eaux de la nappe, aux puits de Hassi Juiffa et en aval de celui-ci. Ceci suggère que l'évaporation de la nappe est la source essentielle de sels du profil.

## VI. TENEURS EN ISOTOPES LOURDS DES SOLUTIONS DU SOL

Le transit de l'eau dans le sol sous l'effet de l'évaporation s'accompagne de trois phénomènes qui modifient la composition isotopique (Zimmermann et al., 1967 a et b; Dincer et Zimmermann, 1974; Münnich et al., 1980 : Sonntag et al., 1978; Allison, 1982; Allison et al., 1982; Allison et Hughes, 1983; Barnes et Allison, 1983).

- un enrichissement isotopique gouverné par les paramètres bien connus pour les bassins à niveaux constants (Craig et Gordon, 1963; Fontes et Gonfiantini, 1967) : température, humidité relative de l'atmosphère libre au-dessus du sol, composition isotopique de la vapeur atmosphérique et composition isotopique de l'eau qui alimente le système;

- une diffusion de la vapeur atmosphérique dans la partie supérieure du profil où se produit essentiellement un transit gazeux;

- une distribution par diffusion, en phase liquide et vers le bas, des isotopes lourds qui ont une tendance à se concentrer préférentiellement à la partie supérieure de la zone où le transit en phase liquide est dominant.

La conjugaison des trois phénomènes donne lieu à l'établissement d'un profil caractéristique (Sonntag et al., 1980; Barnes et Allison, 1983) de l'évaporation à travers un sol soumis à des conditions arides c'est-à-dire pour lequel le phénomène de recharge est en moyenne négligeable par rapport à

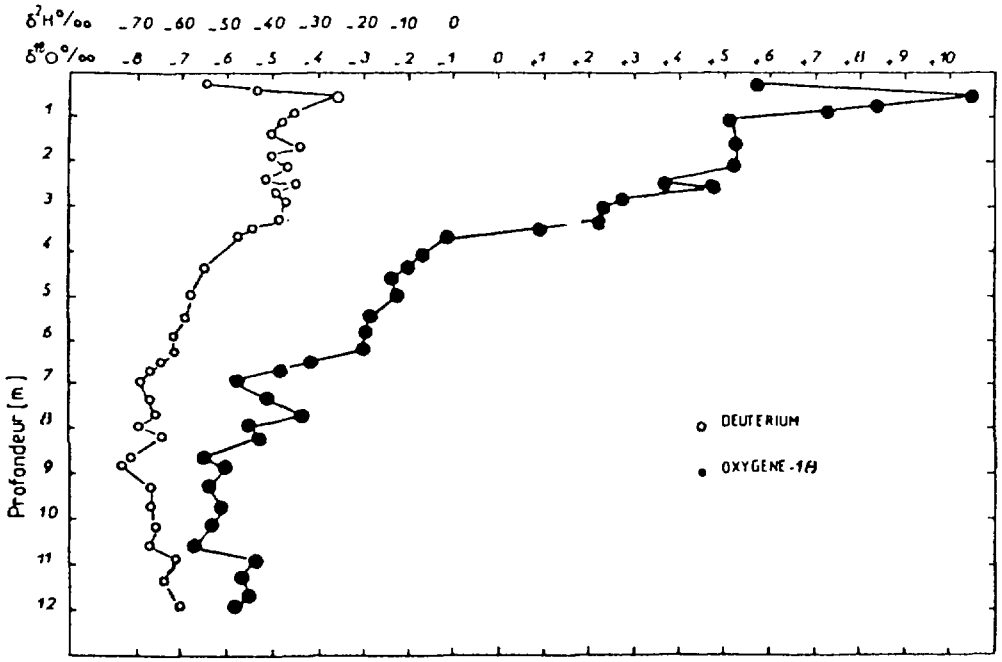


Fig 7a : Variations Des Teneurs En Deutérium Et En Oxygène-18 Avec La Profondeur (Sondage SD4)

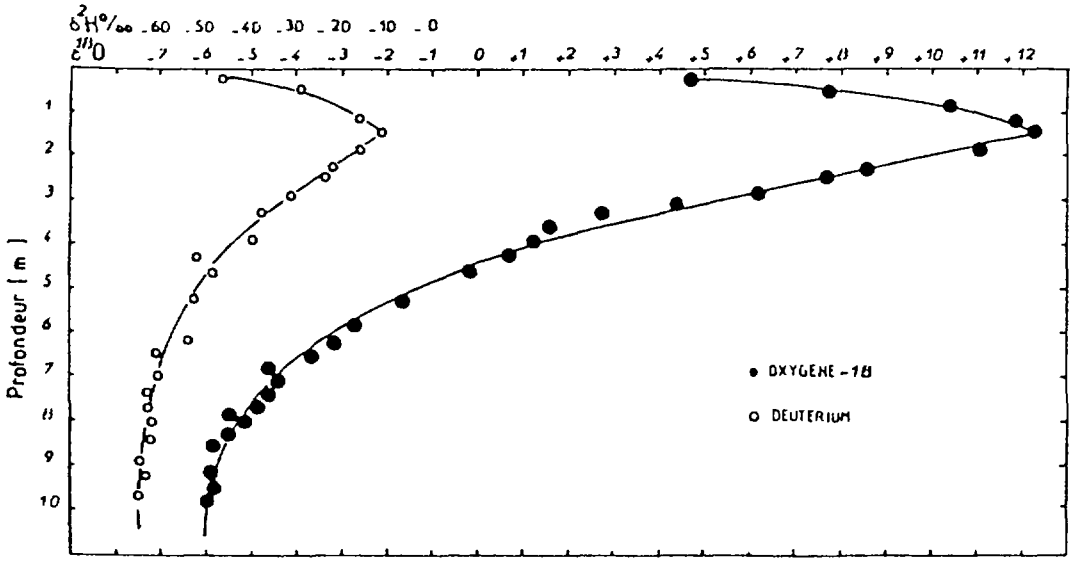


Fig 7b : Variations Des Teneurs En Oxygène-18 Et En Deutérium Avec La Profondeur (Sondage SC3)

la décharge par évaporation. Ce sont de tels profils isotopiques que l'on obtient en SD4 et, encore plus proche de l'allure théorique, en SC3, aussi bien pour l'évolution des teneurs en deutérium qu'en oxygène 18 (Fig. 7a et 7b). Les enrichissements maximums qui définissent la zone de transition entre la montée capillaire et le flux de vaporisation, s'inscrivent à environ 0,50 m en SD4 et 1,5 m en SC3. Les pics de teneurs en isotopes lourds atteignent alors respectivement:

| | $^{18}O$ | $^{2}H$ |
|---|---|---|
| SD4 | + 10.45 | - 25.0 |
| SC3 | + 12.30 | - 10.3 |

Au bas des profils, les compositions isotopiques sont assez proches de celles de la nappe, sans toutefois être identiques.

Dans le diagramme deutérium-oxygène 18, les points se répartissent en chaque site sur une droite dont coefficient angulaire et ordonnée à l'origine sont très comparables (Fig. 8a et 8b) :

$$SD4 : \delta^2H : (2,66 \pm 0,13)\ \delta^{18}O - (50,6 \pm 0,64) \quad (r^2 = 0,96)$$
$$SC3 : \delta^2H : (2,79 \pm 0,06)\ \delta^{18}O - (47,1 \pm 0,43) \quad (r^2 = 0,0995)$$

Cette excellente similitude était prévisible dans la mesure où les caractéristiques des droites d'évaporation ne dépendent que :

- des paramètres climatiques moyens du lieu que l'on peut considérer comme uniques en SD4 et SC3 étant donné la faible distance (environ 800 m) entre les deux ouvrages;

- de la teneur en isotopes lourds de l'eau au début du processus d'évaporation (la nappe) que l'on peut également considérer comme identique pour les deux profils.

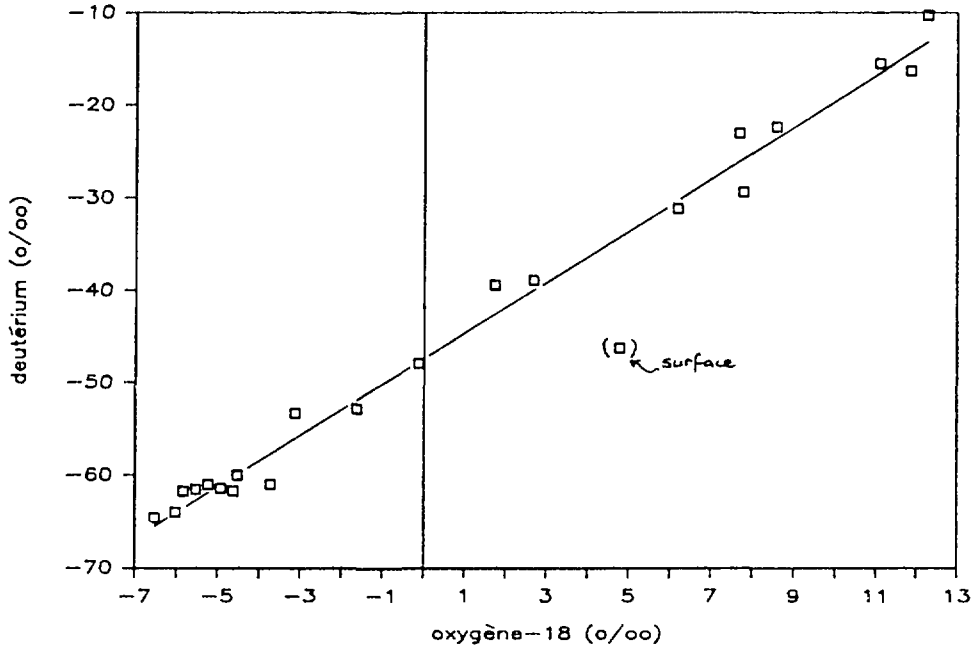


Fig. 8a - Corrélation $^{2}H/^{18}O$ pour le sondage SC3 :
$\delta^2H = 2,79\ \delta^{18}O - 47,1$ (point entre parenthèses exclu)

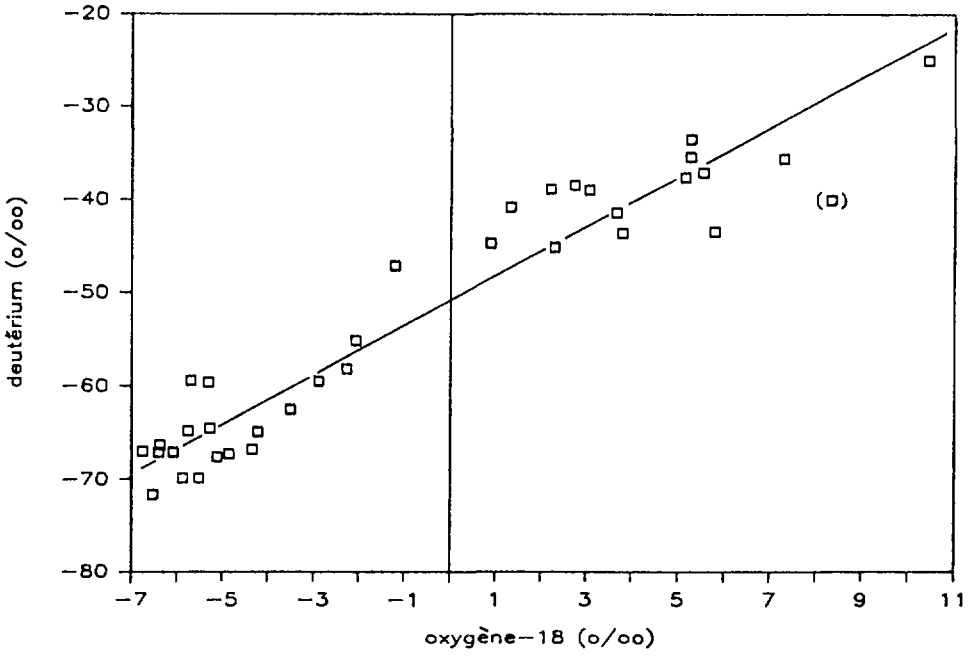


Fig. 8b - Corrélation $^{2}H/^{18}O$ pour le sondage SD4 :
$\delta^{2}H = 2,66\ \delta^{18}O - 50,6$ (point entre parenthèses exclu)

La comparaison des teneurs en sels et en isotopes lourds est rendue délicate par l'incertitude sur les teneurs en sels et sur l'origine de certains ions (cf. V). Elle permet toutefois de distinguer une partie du profil où l'enrichissement en sels et en isotopes lourds se produit sous l'effet de la diffusion vers le bas. A la partie supérieure, la présence de sels accumulés dans la zone où le transport en phase vapeur domine peut être due à l'évaporation des eaux météoriques et/ou aux déplacements de la zone de transit de vapeur dans l'épaisseur du profil.

## VII. MODELISATION DE L'EVAPORATION

### VII.1 Les éléments de la modélisation

#### VII.1.1 Transit de vapeur

Dans la zone où le flux dominant est celui de la phase vapeur, Barnes et Allison (1983) établissent l'équation de bilan suivante:

$$\delta_i = (\alpha_i^*)^{-1}\ \delta_i^a + \varepsilon_i^* + \eta_i\ (1 + \delta_i^{res}) + (\delta_i^{res} - \delta_i^a)\ \frac{z}{z + h_a z} \qquad \text{(éq. 1)}$$

dans laquelle:

i est l'isotope considéré $^{2}H$ ou $^{18}O$,

$\alpha^*$ est le facteur de fractionnement à l'équilibre entre l'eau vapeur et l'eau liquide,

$\varepsilon^* = 1 - \alpha^*$,

$\delta^a$ est la teneur en isotopes lourds de la vapeur d'eau atmosphérique,

$\delta^{res}$ est la teneur en isotopes lourds de l'eau qui alimente le flux ascendant à la base du profil,

$\delta$ est la composition isotopique de l'eau de profil à la profondeur z,

$\eta$ rend compte de "l'effet cinétique" dû à la diffusion plus ou moins rapide des espèces isotopique en fonction de la quantité de molécules de vapeur d'eau présente dans l'atmosphère avec

$$\eta_i = \left( \frac{D^v}{D_i^v} \right)^n - 1 \qquad \text{(éq. 2)}$$

$D^v$ est le coefficient de diffusion de la vapeur d'eau légère,

$D_i^v$ est le coefficient de diffusion de la molécule comportant l'isotope i,

n est l'exposant de diffusivité qui rend compte de la turbulence de l'air au niveau de la surface évaporante ($n \simeq 1$ pour un air immobile),

$h_a$ est l'humidité relative moyenne de l'atmosphère

$$h_a = 1 - \frac{z^{ef}}{\bar{z}} \qquad \text{(éq. 3)}$$

$z^{ef}$ est la profondeur où s'observe le maximum d'enrichissement isotopique,

$\bar{z}$ est la profondeur de pénétration ("pénétration depth") telle que

$$\bar{z} = N_{sat}\, D^{v*}/\rho E \qquad \text{(éq. 4)}$$

$N_{sat}$ désigne la masse volumique de la vapeur d'eau saturante à la température donnée,

$\rho$ est la masse volumique de l'eau liquide,

$D^{v*}$ est la diffusivité réelle de la vapeur dans le profil qui est liée à la diffusivité de la vapeur dans l'air par

$$D^{v*} = (p - \theta)\, \tau D^v \qquad \text{(éq. 5)}$$

p est la porosité totale,

$\theta$ est la teneur en eau volumique,

$\tau$ est la tortuosité du profil,

E est le flux d'évaporation,

Dans ces relations les termes $\delta$ sont exprimées en fraction décimale ou parts pour un.

VII.1.2 Transit de liquide

Dans la zone où domine le transit liquide, l'équation de bilan isotopique s'écrit:

$$\delta_i - \delta_i^{res} = (\delta_i^{ef} - \delta_i^{res}) \exp [-f(z)/\hat{z}_i] \qquad \text{(éq. 6)}$$

dans laquelle les symboles les mêmes que précédemment et où f(z) est une fonction dite de distance qui intègre les variations de teneur en eau en fonction de la profondeur

$$f(z) = \bar{\theta} \int_{z^{ef}}^{z} dz/\theta \qquad \text{(éq. 7)}$$

$\hat{z}_i$ est une profondeur caractéristique pour le système considérée; elle est liée au taux d'évaporation E, à la tortuosité $\tau$, à la teneur en eau volumique $\bar{\theta}$ et à la diffusivité des espèces moléculaires dans l'eau liquide $D_i^l$

$$\hat{z}_i = \bar{\theta}\tau D_i/E \qquad \text{(éq. 8)}$$

La détermination de $z_i$ peut être faite graphiquement puisque l'équation ( 6) montre que, la fonction

$$\ln[(\delta_i - \delta_i^{res})/(\delta_i^{ef} - \delta_i^{res})] \text{ vs } f(z) \qquad \text{(éq. 9)}$$

doit être linéaire avec une pente égale à $-1/\hat{z}_i$. Cela fait donc trois méthodes numériquement indépendantes pour estimer le flux d'évaporation à travers un profil.

## VII.2 Application numérique

Cela a été fait pour le sondage SC3 dont l'allure est conforme à celle des modèles théoriques.

VII.2.1 Valeurs adoptées pour variables et paramètres

- température = 22.8°C (moyenne annuelle),
- tortuosité, $\tau$ = 0.66 (Penman, 1940),
- porosité, p = 0.35 (mesurée),
- diffusivité $D^v$ = 26.5 x $10^{-6}$ $m^2$ $s^{-1}$ (De Vries et Kruger, 1967),
- teneur en eau volumique moyenne, $\bar{\theta}$ = 0,082,
- masse volumique de l'eau, p = 1000kgm$^{-3}$,
- teneur en eau de l'atmosphère à saturation, $N_{sat}$ = 0.02058 k gm$^{-3}$ à 22.8°C,
- teneur en oxygène 18 de l'eau d'alimentation $\delta^{res}$ = -0.0065,
- facteur d'enrichissement isotopique à l'équilibre entre la vapeur et l'eau liquide à 22.8°C, $\varepsilon^*_{18}$ = 0.00928,
- facteur de fractionnement isotopique à l'équilibre entre la vapeur et l'eau liquide à 22.8°C, $\alpha^*_{18}$ = 0.9907 (Bottinga et Craig, 1961),
- effet de diffusion cinétique, $\eta_{18}$ = 0.02848 (Merlivat, 1978).

L'ajustement ne porte alors que sur la teneur en $^{18}O$ de la vapeur d'eau de l'atmosphère libre et éventuellement sur son humidité relative qui varie à Béni-Abbès entre 0.10 et 0.70 pour une valeur moyenne de 0.36 à la température moyenne de 22.8°C.

VII.2.2 Résultats

Concernant le transfert au phase vapeur, le meilleur ajustement à la courbe expérimentale est réalisé en adoptant les valeurs 0,65 pour l'humidité relative et -0,005 pour la composition en oxygène-18 ($\delta^{18}O$ = -5‰) de la vapeur d'eau atmosphérique (Yousfi, 1984). Le taux d'évaporation correspondant à ces valeurs est de 1.4 mm/an. Cependant, des mesures ultérieures de la teneur en oxygene-18 de la vapeur atmosphérique dans la région de Béni-Abbès ont donné des valeurs bien plus négatives que celles considerées ($\delta_i$ = -19‰). Par ailleurs, la valeur l'humidité relative est, dans ce cas, sans aucun doute surévaluée.

En adoptant une valeur de 35% pour l'humidité relative et -19‰ pour la composition isotopique de la vapeur atmosphérique l'ajustement (cf. tableau I) montre des valeurs beaucoup plus basses en surface et une valeur de pic légèrement plus élevée. Il faut cependant rappeler que d'une part l'échantillonnage dans la partie la plus superficielle du sol est très délicate surtout quand l'humidité volumique est très faible, que d'autre part les valeurs obtenues sur le terrain représentent une moyenne intégrée sur

20 cm d'épaisseur de profil tandis que le modèle donne des valeurs ponctuelles à différents niveaux. Les valeurs très basses calculées dans la partie la plus superficielle du sol où l'humidité est très faible interviennent donc moins dans cette moyenne. Il semble donc en définitive que l'ajustement proposé est vraisemblable. Par ailleurs, le taux d'évaporation calculé sur ces nouvelles basses donne une valeur de 1,2 mm/an finalement très proche de celle obtenue précédemment.

Tableau I: Essai d'ajustement de la courbe expérimentale.

| Profondeur | $\delta^{18}O$‰ mesurées | $\delta^{18}O$‰ calculées Yousfi (1984) | $\delta^{18}O$‰ calculées Aranyossy (1985) |
|---|---|---|---|
| 0,0 - 0,20 | + 4,84 | + 4,83 | - 1,64 |
| 0,3 - 0.50 | + 7,80 | + 7,43 | - 3,83 |
| 0,7 - 0.90 | + 10,38 | + 9,80 | + 10,68 |
| 1,10 - 1,20 | + 11,90 | + 11,70 | + 13,93 |
| 1,30 - 1,50 | + 12,30 | + 12,85 | + 16,30 |

. Yousfi (1984): $\delta^{a\ 18}O = -0,005$ ; $ha = 0,65$

. Aranyossy (1985): $\delta^{a\ 18}O = -0,019$ ; $ha = 0,35$

VII.3 Calcul graphique (éq. 6, 8 et 9)

Les valeurs expérimentales conduisent à la relation numérique:

$$\ln \frac{\delta_{18} - \delta_{18}^{res}}{\delta_{18}^{ef} - \delta_{18}^{res}} = - 0.40\ f(z) + 0.067 \quad (r = 0.98)$$

soit $1/\hat{z}_i = 0.40$ et $\hat{z}_i = 2.50m$

en utilisant comme valeur de la diffusivité

$D_{18} = 1.45 \times 10^{-9}\ m^2\ s^{-1}$ (Mills, 1976 in Barnes et Allison, 1983)

il vient

$$E = \frac{\bar{\theta}\tau D_i^1}{\hat{z}_i} \simeq \frac{0.082 \times 0.66 \times 1.45 \times 10^{-9}}{2.5}$$

soit $E \simeq 3{,}14 \times 10^{-11}$ m $s^{-1} \simeq$ 1mm $a^{-1}$

Cette estimation expérimentale est très inférieure (de plusieurs ordres de grandeur) aux chiffres obtenus par Zunker (1930) pour le flux de vapeur qui peut transiter à travers un sol limoneux sous le simple effet de la diffusion.

## VIII. CONCLUSIONS

Les estimations des flux d'évaporation à travers un profil de sédiment fin montrent une bonne concordance autour de 1mm par an avec deux méthodes isotopiques semi-indépendantes.

La technique des profils isotopiques naturels dans la zone non saturée a prouvé son efficacité pour la détermination des taux d'évaporation. Elle est donc particulièrement adaptée à l'étude des zones de décharge des nappes par évaporation.

Cette technique pourrait même être perfectionnée par la réalisation de prélèvements de vapeur à différentes profondeurs dans la zone non-saturée ce qui allègerait la contrainte des carottage "à sec" si la preuve pouvait être apportée que la vapeur des sols est en équilibre isotopique avec l'eau liquide des profils. Cette tentative est en cours sur le site de Béni-Abbès.

## REFERENCES


[1] ALLISON, G.B. (1982). The relationship between $^{18}O$ and $^{2}H$ in water sand columns undergoing evaporation. J. of Hydrology, 55: 163-169.

[2] ALLISON, G.B., HUGHES, M.W. (1983). The use of natural tracers as indicators of soil-water movement in a temperate semi-arid region. J. of Hydrology, 60: 157-173.

[3] BARNES, C.J., ALLISON, G.B. (1983). The distribution of deuterium and oxygen-18 in dry soils (1, Theory), J. of Hydrology, 60: 141-156.

[4] BOTTINGA, Y., CRAIG, H. (1969). Oxygen isotope fractionation between CO and water and the isotopic composition of marine atmosphere. Earth Planetary Sci. Letters, 5: 282-295.

[5] CONRAD, G., FONTES, J.Ch. (1970). Hydrologie isotopique du Sahara occidental. IAEA SM 129/24, 405-419.

[6] CRAIG, H., GORDON, L.I. (1963). Isotopic exchange effects in the evaporation of water. J. of Geophysical Res. 68: 5079-5087.

[7] DERVIEUX, F. (1956). La nappe phréatique du Souf (Algérie). Etude du renouvellement de la nappe. Contribution à l'étude des phénomènes capillaires dans un milieu pulvérulent. Terres et Eaux, 29: 5-39.

[8] DE VRIES, D.A., KRUGER, A.J. (1967). On the value of the diffusion coefficient of water vapour in air (In Phénomènes de transport avec changement de phase dans les milieux poreux ou colloïdes). Colloques internationaux CNRS Symp., Paris, 61-72. DINCER, T., PAYNE, B.R. (1971). An environmental isotope study of the South western karst region of Turkey. J. of Hydrology, 14: 233-258.

[9] DINCER, T., ZIMMERMANN, U. (1974). Study of the infiltration and recharge through the sand dunes in arid zones with special reference to the stable isotopes and thermonuclear tritium. J. of Hydrology, 23: 79-109.

[10] DUBIEF, J. (1959, 1963). Le climat du Sahara. Institut de Recherches Sahariennes, Algérie, mémoire hors série, tome 1: 312 p., tome 2: 275 p.

[11] FONTES, J.Ch., GONFIANTINI, R. (1970). Composition isotopique et origine de la vapeur d'eau atmosphérique dans la région du lac Léman. Earth Planet. Sc. Lett., 7: 325-329.

[12] GONFIANTINI, R., CONRAD, G., FONTES, J.Ch. (1974). Etude isotopique de la nappe du Continental Intercalaire et ses relations avec les autres nappes du Sahara Septentrional. Isotope Techn. in Groundwater Hydrology, Vol. I: 227-241.

[13] GOUVEA DA SILVA ROSA B. (1980). Migration des sels et des isotopes lourds à travers des colonnes de sédiments non saturés sous climat semi-aride. Thèse 3$^{e}$ cycle, Paris VI.

[14] MERLIVAT, L. (1978). Molecular diffusivities of $H_2\,{}^{16}O$, HDO and $H^{18}O$ in gases. J. Chem. Phys., 69(6): 2864-2871.

[15] MUNNICH, K.O., SONNTAG, C., CHRISTMANN, D., THOMA, G. (1980). Isotope fractionation due to evaporation from sand dunes. Z. Mitt. Zentralist. Isotop. Strahlenforsh, 29, 319 pages.

[16] SONNTAG, C., KLITZSCH, E., LOEHNERT, E.P., EL SHAZLY, E.M, MUENNICH, K.O., JUNGHAUS, Cl., THORVEHIE, V., WEISTROFFER, K., SWAILEM, F.M. (1978). Paleoclimatic information from deuterium and oxygen-18 in carbon-14-dated north Saharian groundwaters: Groundwater formation in the past, In: Isotope Hydrology 1978, 2: 569-581, IAEA, Vienna.

[17] YOUSFI, M. (1984). Etude géochimique et isotopique de l'évaporation et de l'infiltration en zone non saturée sous climat aride: Beni Abbès, Algerie. Thèse. Université de Paris-Sud, Orsay, France.

[18] ZIMMERMANN, U., MUNNICH, K.O., ROETER, W. (1967). Downward movement of soil moisture traced by means of hydrogen isotopes. Geophys. Monog., 11: 28-36.

# CONCLUSIONS AND RECOMMENDATIONS ON THE USEFULNESS OF STUDIES OF THE ISOTOPES $^{18}O$, $^{2}H$ AND $^{3}H$ IN WATER IN THE UNSATURATED ZONE

G. ALLISON,
Commonwealth Scientific and Industrial
Research Organization,
Division of Soils,
Glen Osmond, Australia

J.-Ch. FONTES
Laboratoire d'hydrologie et de géochimie isotopique,
Université de Paris-Sud,
Orsay, France

C. SONNTAG
Institut für Umweltphysik,
Universität Heidelberg,
Heidelberg, Federal Republic of Germany

## Evaluation of local recharge

For estimation of local recharge environmental tritium has been used extensively in temperate climates. The method has been shown to give quantitative estimates of recharge when the annual recharge flux is approximately superior to 10 mm $a^{-1}$.

Although the time elapsed since the fallout peak is now such that this peak will often have moved from the unsaturated to the saturated zone, tritium profiles taken through the unsaturated zone (and the saturated zone where necessary) should still provide reliable estimates of local recharge using the tritium inventory of the profile. If rainfall is uniformly distributed the peak location method may still be used, provided the peak falls within the unsaturated zone.

In arid regions $^{3}H$ may be helpful for obtaining semi-quantitative estimates of local recharge. However, the high variability of both rainfall amount and its tritium concentration make the input function very difficult to evaluate.

When soils are suspected of transmitting only low water fluxes (either net discharge or recharge) tritium profiles must be treated with caution as diffusion of atmospheric water vapour of relatively high tritium concentration may distort the tritium budget.

Labelling of soil water with artificial tritium has also been used extensively under temperate and semi-arid conditions for successfully estimating local recharge. However, it only gives information on recharge in the time interval between injection and sampling. This technique also appears to be a promising tool for evaluating soil water flow parameters and other terms in the water balance equation, and can give, for example, useful estimates of evapotranspiration in irrigated lands.

For low rates of local recharge (< approx. 10 mm $a^{-1}$) measurements of the displacement of $^{18}O$ and $^{2}H$ delta values of soil water from the local meteoric line may give semi-quantitative information on recharge rates. Profiles of the chloride concentration of soil water may also be used to estimate low rates of recharge, provided an estimate of the net accession of $Cl^-$ at the soil surface can be made.

It is not considered promising to estimate relatively high rates of recharge from stable isotope profiles in soil water, either by identifying a seasonal enrichment peak in the profile or by identifying changes in concentration associated with seasons or single events.

Groundwater discharge

$^{18}O$ and $^{2}H$ profiles appear to be promising tools for quantitative estimation of groundwater discharge when this occurs through the unsaturated zone. However, some further work needs to be done to develop the technique fully.

Problems in measuring and interpreting stable isotope profiles in the unsaturated zone

(i) Sampling and sample handling must be carried out by experienced personnel. Small evaporative losses render a sample useless. Heating of samples during sampling of consolidated or cemented materials may be a problem.

(ii) Specific data requirements are influenced strongly by the characteristic time for development of the isotope profile. For example at a site where groundwater discharge is occurring at a low rate, the characteristic time may be many years. In this case mean annual values of most parameters may suffice (isotopic composition of atmospheric water vapour,

temperature, atmospheric vapour mixing ratio). When characteristic times become shorter than one year, interpretation may become more difficult and more detailed data collection necessitated.

(iii) Some parameters are of crucial importance and special attention needs to be given to them. These are:

- Tortuosity, especially in the liquid phase
- Pore size distribution
- Mineralogy, with special reference to the presence or otherwise of gypsum
- Density

Future work

Multiple sampling at single locations where recharge is occurring has shown that stable isotope profiles at a single site show only small differences between each other. Similar consistency is expected in areas of net groundwater discharge. In this case a relationship should exist between discharge rates deduced from these profiles, groundwater depth and soil characteristics. Sampling at a range of groundwater depths and in a range of soil textural classes should allow extrapolation to enable estimates of discharge on a regional scale to be made. Remote sensing techniques show promise in mapping of shallow groundwater depths.

It is recommended that profiles of the concentration of chloride in soil water are always measured in conjunction with stable isotope profiles (measurement of conductivity will usually suffice). Under some conditions such profiles can be interpreted in terms of evaporation rate and so provide confirmation of values obtained from stable isotopes.

Stable isotopes represent a possible means of partitioning liquid and vapour fluxes in soils and to study diffusion phenomena under natural conditions. Such basic soil physical parameters may give insight to the movement of contaminants in soils.

# LIST OF PARTICIPANTS


| | |
|---|---|
| Allison, G. | CSIRO, Division of Soils<br>Private Bag No. 2<br>Glen Osmond<br>South Australia 5064<br>Australia |
| Fontes, J.-Ch. | Université de Paris-Sud<br>Laboratoire d'hydrologie et de géochimie isotopique<br>F-91405 Orsay<br>France |
| Moser, H. | Institut für Radiohydrometrie<br>Gesellschaft für Strahlen- und Umweltforschung mbH<br>D-8042 Oberschleissheim<br>Federal Republic of Germany |
| Munnich, K.O. | Universität Heidelberg<br>Institut für Umweltphysik<br>Im Neuenheimer Feld 366<br>D-69 Heidelberg<br>Federal Republic of Germany |
| Seiler, K.P. | Institut für Radiohydrometrie<br>Gesellschaft für Strahlen- und Umweltforschung mbH<br>D-8042 Oberschleissheim<br>Federal Republic of Germany |
| Sonntag, Ch. | Universität Heidelberg<br>Institut für Umweltphysik<br>Im Neuenheimer Feld 366<br>D-69 Heidelberg<br>Federal Republic of Germany |
| Kumar, B. | National Geophysical Research Institute<br>Hyderabad 500 077<br>India |
| Sharma, P. | Physical Research Laboratory<br>Navrangpura<br>Ahmedabad 380 009<br>India |
| Issar, A. | Ben-Gurion University of the Negev<br>P.O. Box 653<br>Beer Sheva 84120<br>Israel |

Sajjad, M.I.
Pakistan Institute of Nuclear Science and Technology
Post Office Nilore
Islamabad
Pakistan

Mamou, A.
Direction des Ressources en Eau et en Sol
DRES-CRDA
6029 Gabès
Tunisia

Zouari, K.
c/o Laboratoire d'hydrologie et de géochimie isotopique
Université de Paris-Sud
F-91405 Orsay
France

SECRETARIAT

| | | |
|---|---|---|
| Scientific Secretary: | J.F. Aranyossy | Isotope Hydrology Section |
| | T.T. Akiti | Isotope Hydrology Section |
| | C. Atkins | Joint FAO/IAEA Division of Isotope and Radiation Applications of Atomic Energy for Food and Agricultural Development |
| | M. Gomez Martos | Isotope Hydrology Section |
| | R. Gonfiantini | Isotope Hydrology Section |
| | B.R. Payne | Isotope Hydrology Section |
| | Y. Yurtsever | Isotope Hydrology Section |

85-05871